

Methods in Molecular Biology™

VOLUME 128

NMDA Receptor Protocols

Edited by
Min Li



HUMANA PRESS

NMDA Receptor Protocols

METHODS IN MOLECULAR BIOLOGY™

John M. Walker, SERIES EDITOR

134. **T Cell Protocols: Development and Activation**, edited by Kelly P. Kearse, 2000
133. **Gene Targeting Protocols**, edited by Eric B. Kmieciak, 1999
132. **Bioinformatics Methods and Protocols**, edited by Stephen Misener and Stephen A. Krawetz, 1999
131. **Flavoprotein Protocols**, edited by S. K. Chapman and G. A. Reid, 1999
130. **Transcription Factor Protocols**, edited by Martin J. Tymms, 1999
129. **Integrin Protocols**, edited by Anthony Howlett, 1999
128. **NMDA Protocols**, edited by Min Li, 1999
127. **Molecular Methods in Developmental Biology: Xenopus and Zebrafish**, edited by Matt Guille, 1999
126. **Developmental Biology Protocols, Volume II**, edited by Rocky S. Tuan and Cecilia W. Lo, 1999
125. **Developmental Biology Protocols, Volume I**, edited by Rocky S. Tuan and Cecilia W. Lo, 1999
124. **Protein Kinase Protocols**, edited by Alastair Reith, 1999
123. **In Situ Hybridization Protocols (2nd ed.)**, edited by Ian A. Darby, 1999
122. **Confocal Microscopy Methods and Protocols**, edited by Stephen W. Paddock, 1999
121. **Natural Killer Cell Protocols: Cellular and Molecular Methods**, edited by Kerry S. Campbell and Marco Colonna, 1999
120. **Eicosanoid Protocols**, edited by Elias A. Lianos, 1999
119. **Chromatin Protocols**, edited by Peter B. Becker, 1999
118. **RNA-Protein Interaction Protocols**, edited by Susan R. Haynes, 1999
117. **Electron Microscopy Methods and Protocols**, edited by M. A. Nasser Hajibagheri, 1999
116. **Protein Lipidation Protocols**, edited by Michael H. Gelb, 1999
115. **Immunocytochemical Methods and Protocols (2nd ed.)**, edited by Lorette C. Javois, 1999
114. **Calcium Signaling Protocols**, edited by David G. Lambert, 1999
113. **DNA Repair Protocols: Eukaryotic Systems**, edited by Daryl S. Henderson, 1999
112. **2-D Proteome Analysis Protocols**, edited by Andrew J. Link, 1999
111. **Plant Cell Culture Protocols**, edited by Robert D. Hall, 1999
110. **Lipoprotein Protocols**, edited by Jose M. Ordovas, 1998
109. **Lipase and Phospholipase Protocols**, edited by Mark H. Doolittle and Karen Reue, 1999
108. **Free Radical and Antioxidant Protocols**, edited by Donald Armstrong, 1998
107. **Cytochrome P450 Protocols**, edited by Ian R. Phillips and Elizabeth A. Shephard, 1998
106. **Receptor Binding Techniques**, edited by Mary Keen, 1999
105. **Phospholipid Signaling Protocols**, edited by Ian M. Bird, 1998
104. **Mycoplasma Protocols**, edited by Roger J. Miles and Robin A. J. Nicholas, 1998
103. **Pichia Protocols**, edited by David R. Higgins and James M. Cregg, 1998
102. **Bioluminescence Methods and Protocols**, edited by Robert A. LaRossa, 1998
101. **Mycobacteria Protocols**, edited by Tanya Parish and Neil G. Stoker, 1998
100. **Nitric Oxide Protocols**, edited by Michael A. Titheradge, 1998
99. **Human Cytokines and Cytokine Receptors**, edited by Reno Debets and Huub Savekoul, 1999
98. **Forensic DNA Profiling Protocols**, edited by Patrick J. Lincoln and James M. Thomson, 1998
97. **Molecular Embryology: Methods and Protocols**, edited by Paul T. Sharpe and Ivor Mason, 1999
96. **Adhesion Protein Protocols**, edited by Elisabetta Dejana and Monica Corada, 1999
95. **DNA Topoisomerases Protocols, Volume II: Enzymology and Drugs**, edited by Mary-Ann Bjornsti and Neil Osheroff, 1999
94. **DNA Topoisomerases Protocols, Volume I: DNA Topology and Enzymes**, edited by Mary-Ann Bjornsti and Neil Osheroff, 1999
93. **Protein Phosphatase Protocols**, edited by John W. Ludlow, 1998
92. **PCR in Bioanalysis**, edited by Stephen J. Meltzer, 1998
91. **Flow Cytometry Protocols**, edited by Mark J. Jaroszeski, Richard Heller, and Richard Gilbert, 1998
90. **Drug-DNA Interaction Protocols**, edited by Keith R. Fox, 1998
89. **Retinoid Protocols**, edited by Christopher Redfern, 1998
88. **Protein Targeting Protocols**, edited by Roger A. Clegg, 1998
87. **Combinatorial Peptide Library Protocols**, edited by Shmuel Cabilly, 1998
86. **RNA Isolation and Characterization Protocols**, edited by Ralph Rapley and David L. Manning, 1998
85. **Differential Display Methods and Protocols**, edited by Peng Liang and Arthur B. Pardee, 1997
84. **Transmembrane Signaling Protocols**, edited by Dafna Barsagi, 1998
83. **Receptor Signal Transduction Protocols**, edited by R. A. John Challiss, 1997
82. **Arabidopsis Protocols**, edited by José M Martínez-Zapater and Julio Salinas, 1998
81. **Plant Virology Protocols: From Virus Isolation to Transgenic Resistance**, edited by Gary D. Foster and Sally Taylor, 1998
80. **Immunochemical Protocols (2nd ed.)**, edited by John Pound, 1998
79. **Polyamine Protocols**, edited by David M. L. Morgan, 1998
78. **Antibacterial Peptide Protocols**, edited by William M. Shafer, 1997
77. **Protein Synthesis: Methods and Protocols**, edited by Robin Martin, 1998
76. **Glycoanalysis Protocols (2nd ed.)**, edited by Elizabeth F. Hounsell, 1998
75. **Basic Cell Culture Protocols (2nd ed.)**, edited by Jeffrey W. Poillard and John M. Walker, 1997
74. **Ribozyme Protocols**, edited by Philip C. Turner, 1997
73. **Neuropeptide Protocols**, edited by G. Brent Irvine and Carvell H. Williams, 1997
72. **Neurotransmitter Methods**, edited by Richard C. Rayne, 1997
71. **PRINS and In Situ PCR Protocols**, edited by John R. Gosden, 1996
70. **Sequence Data Analysis Guidebook**, edited by Simon R. Swindell, 1997
69. **cDNA Library Protocols**, edited by Ian G. Cowell and Caroline A. Austin, 1997
68. **Gene Isolation and Mapping Protocols**, edited by Jacqueline

METHODS IN MOLECULAR BIOLOGY™

NMDA Receptor Protocols

Edited by

Min Li


Johns Hopkins School of Medicine, Baltimore, MD

Humana Press  Totowa, New Jersey

© 1999 Humana Press Inc.
999 Riverview Drive, Suite 208
Totowa, New Jersey 07512

All rights reserved. No part of this book may be reproduced, stored in a retrieval system, or transmitted in any form or by any means, electronic, mechanical, photocopying, microfilming, recording, or otherwise without written permission from the Publisher. Methods in Molecular Biology™ is a trademark of The Humana Press Inc.

All authored papers, comments, opinions, conclusions, or recommendations are those of the author(s), and do not necessarily reflect the views of the publisher.

This publication is printed on acid-free paper. 
ANSI Z39.48-1984 (American Standards Institute) Permanence of Paper for Printed Library Materials.

Cover design by Patricia F. Cleary.

For additional copies, pricing for bulk purchases, and/or information about other Humana titles, contact Humana at the above address or at any of the following numbers: Tel.: 973-256-1699; Fax: 973-256-8341; E-mail: humana@humanapr.com; Website: <http://humanapress.com>

Photocopy Authorization Policy:

Authorization to photocopy items for internal or personal use, or the internal or personal use of specific clients, is granted by Humana Press Inc., provided that the base fee of US \$10.00 per copy, plus US \$00.25 per page, is paid directly to the Copyright Clearance Center at 222 Rosewood Drive, Danvers, MA 01923. For those organizations that have been granted a photocopy license from the CCC, a separate system of payment has been arranged and is acceptable to Humana Press Inc. The fee code for users of the Transactional Reporting Service is: E0-89603-580-8/99 \$10.00 + \$00.25].

Printed in the United States of America. 10 9 8 7 6 5 4 3 2 1

Library of Congress Cataloging in Publication Data

Main entry under title:

Methods in molecular biology™.

NMDA receptor protocols / edited by Min Li

p. cm. -- (Methods in molecular biology ; 128)

Includes index.

ISBN 0-89603-713-4 (alk. paper).

1. Methyl aspartate—Receptors—Laboratory manuals. I. Li, Min, 1962—

II. Series: Methods in molecular biology (Totowa, NJ); 128.

[DNLM: 1. Receptors, N-Methyl-D-Aspartate—genetics. 2. Receptors, N-Methyl-D-

Aspartate—analysis. W1 ME9616J v. 128 1999 / WL 102.8 N7384 1999]

QP 364.7N635 1999

572.8—dc21

DNLM/DLC

for Library of Congress

98-53445

CIP

Preface

Ligand-gated ion channels in the brain are a family of membrane receptor molecules critical to the chemistry of synaptic transmission. Since the synthesis of *N*-methyl-D-aspartate by J. C. Watkins in the 1960s, and subsequent pharmacological studies by a number of groups, NMDA receptors have emerged as key molecules involved in neuronal excitation and toxicity. The molecular studies of NMDA receptors began in the late 1980s, thanks to molecular cloning of the genes encoding various receptor subunits. The ability to express, purify, and analyze various forms of recombinant NMDA receptor proteins in a variety of heterologous systems has offered us enormous opportunities for both basic research of the NMDA receptor structure and function, as well as for clinical investigation and high-throughput drug screens for bioactive compounds.

Ion channels have been studied extensively using pharmacological and electrophysiological approaches. *NMDA Receptor Protocols* differs from other books covering various aspects of techniques involved in conducting those experiments in that it details experimental protocols for studying NMDA receptors, with a strong emphasis on state-of-the-art molecular techniques. The wide range of topics includes molecular cloning of NMDA receptor subunits, expression and functional characterization of cloned genes, investigation of NMDA receptor properties using *in vivo* and *in vitro* preparations, and design and construction of expression systems suitable for special purposes, such as high-throughput drug screens. Although *NMDA Receptor Protocols* does focus on NMDA receptors, the described methods are applicable to related ligand-gated ion channels. With some modifications, one may extend the techniques to other membrane receptors or signaling systems.

I want to thank many who have contributed to this book. I am particularly grateful to Stephen Desiderio, Jeremy Nathans, Lily Jan, and Yuh Nung Jan, who have played a profound role in shaping my view and approaches to science. William Dower at Affymax Research Institute was instrumental in this project. John Walker has read through every chapter and provided helpful editorial comments. Many thanks also go to Ms. Robyne Butzner for her secretarial participation in all stages of this project. Last, I thank Lu for her continuing encouragement and support.

Min Li

Contents

Preface	v
Contributors	ix
1 Isolation of Receptor Clones by Expression Screening in <i>Xenopus</i> Oocytes Fumio Nakamura, Yoshio Goshima, Stephen M. Strittmatter, and Susumu Kawamoto	1
2 Expression of NMDA Receptor Channel Subunit Proteins Using Baculovirus and Herpesvirus Vectors Susumu Kawamoto, Satoshi Hattori, Shigeo Uchino Masayoshi Mishina, and Kenji Okuda	19
3 Transient Expression of Functional NMDA Receptors in Mammalian Cells Paul L. Chazot, Miroslav Cik, and F. Anne Stephenson	33
4 Stable Expression of Human NMDA Receptors in Cultured Mammalian Cells Mark A. Varney, Fen-Fen Lin, Christine Jachec, Sara P. Rao, Stephen D. Hess, Edwin C. Johnson, and Gönül Veliçelibi	43
5 Expression of Extracellular N-Terminal Domain of NMDA Receptor in Mammalian Cells Erik A. Whitehorn, William J. Dower, and Min Li	61
6 Immunocytochemistry of NMDA Receptors Ronald S. Petralia and Robert J. Wenthold	73
7 The Use of Ligand Binding in Assays of NMDA Receptor Function Ian J. Reynolds and Terre A. Sharma	93
8 Calmodulin Modification of NMDA Receptors Su Zhang and Richard L. Huganir	103
9 Detergent Solubilization and Immunoprecipitation of Native NMDA Receptors Robert J. Wenthold, Jaroslav Blahos II, Kyung-Hye Huh, and Ronald S. Petralia	113
10 Redox Sensitivity of NMDA Receptors Stuart A. Lipton	121

11	In Vitro Selection of Peptides Acting on NMDA Receptors Steven E. Cwirla, William J. Dower, and Min Li	131
12	NMDA Receptor Pharmacology and Analysis of Patch-Clamp Receptors Jerry M. Wright and Robert W. Peoples	143
13	Determination of Membrane Topology of Glutamate Receptors Hendrika M. A. VanDongen and Antoius M. J. VanDongen	155
14	Engineering the NMDA Receptor Channel Lining Antonio V. Ferrer-Montiel and Mauricio Montal	167
15	High-Throughput Functional Detection of NMDA Receptor Activity Martin Donal Dunningham and Sara Mary Cunningham	179
	Index	189

Contributors

JAROSLAV BLAHOS II • *Laboratory of Neurochemistry, National Institutes of Health, Bethesda MD.*

PAUL L. CHAZOT • *School of Pharmacy, University of London, London, UK.*

MIROSLAV CIK • *School of Pharmacy, University of London, London, UK.*

SARA MARY CUNNINGHAM • *Clontech Laboratories Inc., Palo Alto, CA.*

MARTIN CUNNINGHAM • *Shakefork Sable Consulting, Los Gatos, CA.*

STEVEN E. CWIRLA • *Department of Molecular Biology, Affymax Research Institute, Palo Alto, CA.*

WILLIAM DOWER • *Department of Molecular Biology, Affymax Research Institute, Palo Alto, CA.*

ANTONIO V. FERRER-MONTIEL • *Biology Department, University of California, San Diego, CA.*

YOSHIO GOSHIMA • *Department of Pharmacology, Yokohama City University School of Medicine, Yokohama, Japan.*

SATOSHI HATTORI • *Department of Bacteriology, Yokohama City University School of Medicine, Yokohama, Japan.*

STEPHEN D. HESS • *SIBIA Neurosciences Inc., La Jolla, CA.*

KYUNG-HYE HUH • *Laboratory of Neurochemistry, National Institutes of Health, Bethesda MD.*

FEN-FEN LIN • *SIBIA Neurosciences Inc., La Jolla, CA.*

CHRISTINE JACHEC • *SIBIA Neurosciences Inc., La Jolla, CA.*

EDWIN C. JOHNSON • *SIBIA Neurosciences Inc., La Jolla, CA.*

SUSUMU KAWAMOTO • *Department of Bacteriology, Yokohama City University School of Medicine, Yokohama, Japan.*

MIN LI • *Department of Physiology, Johns Hopkins University School of Medicine, Baltimore, MD.*

STUART LIPTON • *CNS Research Institute, Brigham and Women's Hospital, Harvard Medical School, Boston, MA.*

MASAYOSHI MISHINA • *Department of Molecular Neurobiology and Pharmacology, School of Medicine, University of Tokyo, Tokyo, Japan.*

MAURICIO MONTAL • *Biology Department, University of California, La Jolla, CA.*

- FUMIO NAKAMURA • *Department of Neurology, Yale University School of Medicine, New Haven, CT.*
- KENJI OKUDA • *Department of Bacteriology, Yokohama City University School of Medicine, Yokohama, Japan.*
- RONALD S. PETRALIA • *Laboratory of Neurochemistry, National Institutes of Health, Bethesda, MD.*
- ROBERT W. PEOPLES • *Laboratory of Molecular and Cellular Neurobiology, National Institutes of Health, Bethesda, MD.*
- SARA P. RAO • *SIBIA Neurosciences Inc., La Jolla, CA.*
- IAN REYNOLDS • *Department of Pharmacology, University of Pittsburgh, Pittsburgh, PA.*
- TERRE A. SHARMA • *Department of Cell Biology, Scripps Institute, La Jolla, CA.*
- F. ANNE STEPHENSON • *School of Pharmacy, University of London, London, UK.*
- STEPHEN M. STRITTMATTER • *Department of Neurobiology, Yale University School of Medicine, New Haven, CT.*
- SHIGEO UCHINO • *Molecular Medicine Laboratory, Yokohama Research Center, Yokohama, Japan.*
- ANTONIUS M. J. VANDONGEN • *Duke University Medical Center, Durham, NC.*
- HENDRIKA M. A. VANDONGEN • *Duke University Medical Center, Durham, NC.*
- GÖNÜL VELİÇELİBİ • *MitoKor, San Diego, CA .*
- MARK A. VARNEY • *SIBIA Neurosciences Inc., La Jolla, CA.*
- JERRY M. WRIGHT • *Department of Physiology, Johns Hopkins University School of Medicine, Baltimore, MD.*
- SU ZHANG • *Department of Neuroscience, Johns Hopkins University School of Medicine, Baltimore, MD.*

Isolation of Receptor Clones by Expression Screening in *Xenopus* Oocytes

Fumio Nakamura, Yoshio Goshima,
Stephen M. Strittmatter, and Susumu Kawamoto

1. Introduction

Xenopus laevis oocytes have contributed greatly to the study of glutamate receptors. The isolation of the first cDNA clone for a glutamate receptor channel, GluR1, was achieved by utilizing an oocyte expression cloning system (1). In 1991–1992, three groups reported the isolation of cDNA clones encoding of *N*-methyl-D-aspartate (NMDA) receptor channel subunit (2–4). Two of the three groups employed the oocyte system to isolate NMDA receptor clones (2,3). Furthermore, a metabotropic glutamate receptor (mGluR) clone was also identified with the oocyte system (5).

This technique was pioneered by Nakanishi's group to identify a G-protein-coupled substance-K receptor (6). It combines transient protein expression in oocytes with highly sensitive electrophysiological analysis. *Xenopus* oocyte possesses an efficient machinery to translate protein from RNA. Its large size (~1 mm) allows injection of RNA and two-electrode voltage clamp with relative ease. The voltage-clamp method can detect trace concentrations of channel proteins in cellular membranes. Since the oocyte itself is a living cell, it has a set of intracellular signal cascades. For example, the phosphatidylinositol (PI) turnover initiated by G-protein-coupled receptors activates Ca²⁺-sensitive Cl⁻ channels in the oocyte membrane, producing a large inward current (6–8). The combination of these features has facilitated the isolation of dozens of cDNA clones from voltage-dependent ion channels, to ligand-gated ion channels, to G-protein-coupled receptors, to transporters. A further advantage of this system is that prior to creating cDNA libraries, poly(A)+ RNA from various tissues can be screened in entire or in fractionated states (9).

However, this system has several disadvantages in common with other transient expression methods. First, the represented character of a target molecule in the oocyte may be attributed by endogenous components. Second, during an incubation period sufficient for protein expression, the target molecule may chronically activate signal cascades and cause desensitization. This often becomes a serious limitation in the analysis of constitutively active mutant forms of signaling molecules (10). Third, compared to utilizing cDNA transfection or viral infection methods, the oocyte system requires an RNase-free technique and a greater number of manipulations.

Many excellent reviews of its methodology have appeared (8,9,11). Here we include the most useful approaches selected from our own work and from recently published reports. This chapter will deal with the preparation of suitable mRNA, construction of a cDNA library, sibling selection of cDNA clones, in vitro transcription, injection of RNA into oocytes, and voltage-clamp analysis of oocytes. At the end, we discuss our experience in applying this system to the study of G-protein-coupled receptors from chick dorsal root ganglion cells (12,13).

2. Materials

2.1. Reagents for RNA Preparation, cDNA Library Construction, and In Vitro Transcription

To obtain good preparations of RNA, avoiding RNase contamination is important. Always wear powder-free plastic gloves when handling RNA. Reagents for RNA are strictly discriminated from other laboratory stocks. H₂O for RNA experiments is supplemented with 0.1% diethyl pyrocarbonate (DEPC), heated at 50°C for 2 h, and then autoclaved twice. All glassware and metals should be heat-treated at 200°C for 18 h to inactivate RNase. Removing RNase on heat-resistant plasticware is accomplished by immersing 0.1% DEPC water for 30 min and then autoclaving. Unopened, sterilized plasticware can be used as RNase-free. Heat-labile plasticwares (such as electrophoresis apparatus) are immersed 0.1% DEPC water or 0.1% H₂O₂ for 30 min, and then rinsed thoroughly with DEPC-treated H₂O.

Both plasmids and λ phages can be used as vectors for expression cloning. Suitable vectors contain specific RNA polymerase promoters flanking the cloning site. This allows the synthesis of cRNA by in vitro transcription to be used for oocyte injection. The choice of the cDNA synthesis method is critical to the success of expression cloning. cDNA libraries should be unidirectional to ensure that only sense cRNA is obtained during in vitro transcription of clones. The SuperScript plasmid system for cDNA cloning is one of the most useful systems currently available.

2.1.1. Reagents for RNA Preparation

- 1 M Tris HCl, pH 7.4: Dissolve 60.6 g Tris base in 400 mL DEPC-treated H₂O. Adjust pH 7.4 with 5 N HCl. Adjust the volume to 500 mL, and then autoclave. Do not use DEPC, because it reacts with Tris.
- 1 M HEPES NaOH, pH 7.5: Dissolve 119 g HEPES in 400 mL H₂O. Adjust pH 7.5 with 5 N NaOH, and then adjust the volume to 500 mL. Add 500 μ L DEPC, mix vigorously, and then autoclave.
- 0.5 M EDTA, pH 8.0: Add 18.6 g EDTA disodium salt in 80 mL DEPC-treated H₂O. Stir vigorously on a magnetic stirrer. Adjust pH 8.0 with ~2 g of NaOH pellets. The EDTA disodium salt will not dissolve until the pH is adjusted to approx 8.0. Adjust the volume to 100 mL, and then autoclave.
- 60% (w/v) Sucrose: Dissolve 300 g sucrose in DEPC-treated H₂O. Adjust the volume to 500 mL. Add 500 μ L DEPC, shake vigorously, and then autoclave.
- 10% Lithium dodecyl sulfate: Dissolve 1 g lithium dodecyl sulfate in 10 mL DEPC-treated H₂O. Do not autoclave.
- TE (10 mM Tris HCl, pH 7.4, 1 mM EDTA): Add 5 mL 1 M Tris HCl, pH 7.4, and 1 mL 0.5 M EDTA in a 500-mL RNase-free bottle. Adjust the volume to 500 mL, and then autoclave. Do not use DEPC.
- Sucrose gradient buffers: Prepare 5 and 30% sucrose buffers supplemented with 10 mM HEPES NaOH, pH 7.5, 1 mM EDTA, and 0.1% lithium dodecyl sulfate. Add 0.5 mL 1 M HEPES NaOH, pH 7.5, 100 μ L 0.5 M EDTA, 0.5 mL lithium dodecyl sulfate, and either 4.1 mL (final 5%) or 25 mL (final 30%) 60% sucrose in a 50-mL RNase-free tube. Adjust the volume to 50 mL with DEPC-treated H₂O. Then make a linear (5–30% w/v) sucrose gradient (**Note 1**).
- H₂O-saturated phenol: Thaw highest-quality phenol in warm water bath, and add equal volume of DEPC-treated H₂O. Mix vigorously, let stand at 4°C overnight, and then remove the H₂O. Repeat twice with fresh RNase-free H₂O. Cover the phenol with RNase-free H₂O, and store at 4°C (up to 3 mo).
- Phenol/chloroform: Mix equal volume of saturated phenol and chloroform. Cover with RNase-free H₂O, and store at 4°C (up to 3 mo).
- H₂O-saturated diethyl ether: Mix vigorously an equal volume of diethyl ether and DEPC-treated H₂O. Store at 20°C. When using diethyl ether, strictly avoid flame.

2.1.2. cDNA Synthesis Kit

This kit is for SuperScript Plasmid System, Gibco-BRL No. 18248-013, Gibco-BRL 8717 Grovemont Circle, Gaithersburg, MD 20884-9980, tel: 800-858-6686, 301-840-4027, fax: 301-258-8238 <http://www.lifetech.com>.

2.1.3. In Vitro T7 RNA Transcription Kit

This kit is the MEGAscript T7 kit, Ambion no. #1334, Cap analog (m⁷G[5']ppp [5']G), Ambion no. #8050, Ambion Inc., 2130 Woodward St., Suite 200, Austin TX, 78744, tel: 800-888-8804, 512-651-0201, fax: 512-445-7139 <http://www.ambion.com>

2.2. Vendors of Egg-Laying Female *Xenopus* Frogs and Frog Brittle

Frogs are supplied from the following vendors in the US. Frog brittle is also purchased from the same vendors:

Nasco, 901 Janesville Ave, Fort Atkinson, WI 53538-0901, tel: 1-800-558-9595.
Xenopus-1, 716 Northside, Ann Arbor, MI 48105, tel: 313-426-2083.

2.3. Surgery Apparatus

Two sets of fine forceps, DUMONT INOX No. 5 for biology.
Hemostatic forceps, 10 cm.
Microspring scissors, straight S/S, 10 cm, or razor blade.
Microdissecting scissors.
GUT chromic C6.

2.4. Buffers for Oocytes

The original ND96 buffer contains final 1.8 mM MgCl₂. However, following ND96 perfusion, buffer omits MgCl₂, because the inward current of NMDA receptor is blocked by Mg²⁺ (2). The contents of perfusion should be determined by the subjected molecule.

2.4.1. ND96 Oocyte Culture Solution

ND96 final concentration is 5 mM HEPES NaOH, pH 7.6, 96 mM NaCl, and 2 mM KCl. Depending on the purpose, MgCl₂, CaCl₂, sodium pyruvate, and antibiotics are supplemented.

X10 ND96 stock solution: Dissolve 56.1 g NaCl, 1.49 g KCl, and 11.9 g HEPES in 800 mL H₂O. Adjust to pH 7.6 with 5 N NaOH, adjust volume to 1 L, and sterilize with autoclave. Store at 4°C (up to 1 yr).

NDE96 (oocyte culture medium): Final 2.5 mM Na pyruvate, 1.8 mM MgCl₂, 1.8 mM CaCl₂, 50 U/mL penicillin, 0.05 mg/mL streptomycin, and 0.125 µg/mL amphotericin B are supplemented.

Mix 50 mL X10 ND96 concentrate, 0.9 mL 1 M MgCl₂ (sterilize by autoclaving, and store at 4°C), 0.9 mL 1 M CaCl₂ (1 M CaCl₂; sterilize by 0.22-µm filtration, and store at 4°C), 1.25 mL 1 M Na pyruvate (1 M Na pyruvate; sterilize by 0.22-µm filtration, and store at 4°C), and 2.5 mL ×100 antibiotic antimycotic solution (Sigma Chemical Co., St. Louis, MO: A-9909).

Adjust the volume to 500 mL with autoclaved H₂O. Store at 18°C, and use within 2 wk.

ND96 for perfusion (for NMDA receptor study): Final 0.3 mM CaCl₂ is supplemented. Dilute 50 mL X10 ND96 10-fold, and then add 150 µL 1 M CaCl₂. Sterilization is not required, but use immediately. The original ND-96 contains final 1.8 mM MgCl₂.

2.4.2. OR-2 (Oocyte Dissection and Washing Medium)

OR-2 final concentration is 5 mM HEPES NaOH, pH 7.6, 82.5 mM NaCl, 2.5 mM KCl, 1 mM MgCl₂.

X10 OR-2 stock solution: Dissolve 48.2 g NaCl, 1.87 g KCl, 11.9 g HEPES, and 2.03 g MgCl₂ 6H₂O in 800 mL H₂O. Adjust pH 7.6 with 5 N NaOH, adjust volume to 1 L, and sterilize with autoclave. Store at 4°C.

X1 OR-2: Dilute X10 concentrate 10-fold with autoclaved H₂O. Store at 18°C, and use within 2 wk.

2.4.3. Collagenase Solution

Dissolve 15–20 mg Collagenase (Gibco-BRL: no. 17018-029) in 8–10 mL X1 OR-2. Use immediately.

2.5. Electrophysiology Apparatus Vendors in US

A simple configuration of monitoring electrophysiological response in oocytes is shown in **Fig. 1**. The system is mounted on a settled bench and kept from strong vibration. Each oocyte is placed in a small chamber and clamped with two electrodes under an inverted microscope. The response is amplified by a TEV-200 clamp system, then monitored, and recorded on a Macintosh computer. The analog data are digitized at 10 Hz (10 points/s).

2.5.1. Two-Electrode Voltage-Clamp System Configuration

Detector and Amplifier: Dagan Corp's CA-1a is an oocyte clamp system. The following items are included: amplifier (TEV-200), three headstages for channel 1 (TEV-201), channel 2 (TEV-202), and virtual current monitor/bath clamp (VCM/BC-203), and perfusion chamber (Micro Bath CCP-2D), Dagan Corp., 2855 Park Ave. Minneapolis, MN 55407, tel: 612-827-5959, fax: 612-827-6535 <http://www.dagan.com>

2.5.2. Table and Electrode Supporters

Table XI Super Invar (60 × 60 cm), XI-22-4.

Multiaxis stage XYZ (X 2), 461XYZ-LH-M.

Folder (X 2), MPH-3.

Posts (X 4), MSP-3.

Adapters (X 2), MCA-2.

Perfusion chamber base stage TSX-1D (this item is not essential).

Newport Corp., 1791 Deere Ave., Irvine, CA 92606, tel: 800-222-3144, 949-863-3144, fax: 714-253-1680, <http://www.newport.com>

2.5.3. Data Monitoring and Recording

Apple Macintosh Quadra 800 8M RAM/250M HD, Apple Computer, Inc., 1 Infinite Loop, Cupertino, CA 95014, tel: 408-996-1010, fax: 1-800-505-0171, <http://www.apple.com>

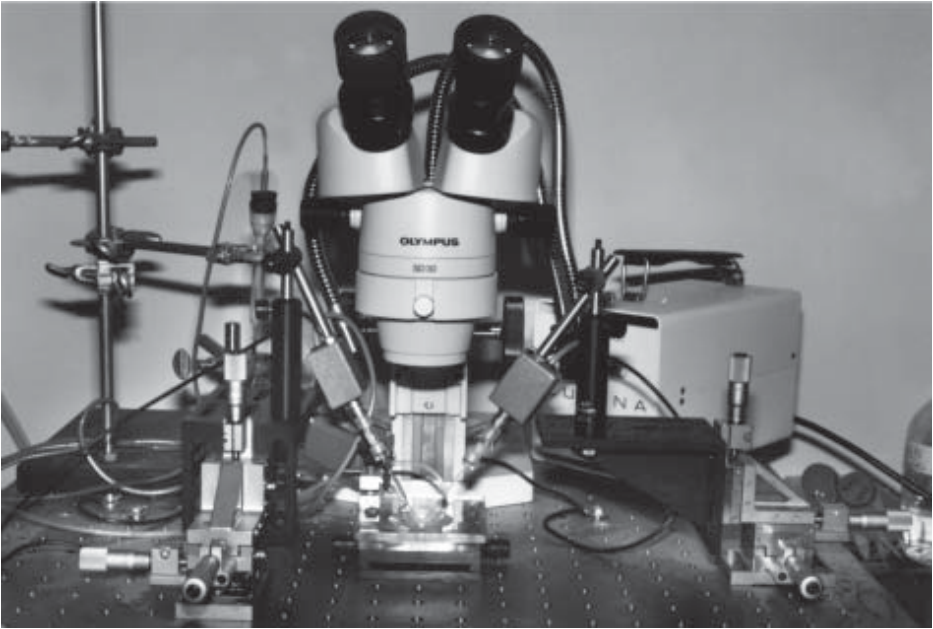


Fig. 1. Typical configuration of a two-electrode voltage-clamp system is shown. A dissecting microscope, an oocyte chamber, and two XYZ stages are mounted on an Invar table. The chamber is placed under the microscope and illuminated by a flexible lamp. Two detectors are mounted on the XYZ stages via supporters. Each supporter is configured with a folder, two rod-shaped posts, and an adapter. The adapter connects two posts and allows flexible movements of the distal post. Glass electrodes are attached to the headstages. A bath clamp detector is located behind the left detector. Two electrodes of the bath clamp are immersed in the perfusion.

Data interface 16-bit A/D converter and driver software.

ITC-16 Mac computer interface.

Instrutech Corp., 20 Vanderventer Ave., Suite 101E, Port Washington, NY 11050-3752, tel: 516-883-1300, fax: 516-883-1558, <http://www.instrutech.com>

2.5.4. Data Monitoring Software for Macintosh

This consists of Axodata Ver 1.1 (latest version is Axograph 3.5).

Axon Instruments Inc., 1101 Chess Dr., Foster City, CA 94404, tel: 650-571-9400, fax: 650-571-9500 <http://www.axonet.com>

2.5.5. Micropipet and Glass Electrode

Narishige Micropipet Puller PB-7.

Narishige USA Inc., 404 Glen Cove Ave., Sea Cliff, NY 11579, tel: 800-445-7914.

Microinjector: Nanoliter Injector A203XVY.

Glass pipet for RNA injection: RNase-free 3.5-in. glass capillaries no. 4878, World Precision Instruments, Inc., 175 Sarasota Center Blvd., Sarasota, FL 34240-9258, tel: 941-371-1003, fax: 941-377-5428 <http://www.wpiinc.com>
Electrodes: Borosilicate glass 100- μ L disposable micropipets (Fisher: no. 21-164-2H) and 3M KCl (Electrode fillings). Sterilize with 0.22- μ m filtration, and store at 20°C.

2.5.6. Other Required Instruments

Invert stereo microscope (10–30 \times).
Flexible lamp (150 W).
Peristaltic pump (for perfusion).

3. Method

General protocols for messenger RNA isolation and cDNA library construction have been described (9,11,14). In this chapter, we will focus on the sibling selection of cDNA clones, in vitro transcription reaction, and the manipulation of *Xenopus* oocytes.

3.1. RNA Isolation and cDNA Library Construction

Compared to other expression cloning methods, an advantage of oocyte expression cloning is that positive RNA pools can be characterized and concentrated prior to creating a cDNA library. If entire poly(A)+ RNA elicits a weak or absent response, size fractionation may provide a positive fraction. A minimum of 10 μ g of mRNA are required for characterization in oocytes and synthesis of a cDNA library.

3.1.1. RNA Size Fractionation

Tissue-derived poly(A)+ RNA may be subjected to size fractionation prior to oocyte expression (9,14). We generally use the nondenaturing sucrose gradient protocol.

1. Prepare 11.5 mL of sucrose gradient (5–30% w/v) containing 10 mM HEPES NaOH, pH 7.5, 1 mM EDTA, and 0.1% lithium dodecyl sulfate in a RNase-free ultracentrifugation tube (Beckman SW41 or equivalents) (Note 1).
2. The poly(A)+ RNA (~100 μ g) is dissolved in 100 μ L TE, heated to 65°C for 5 min, chilled on ice, and then layered on the gradient.
3. The tube is centrifuged at 100,000g for 15 h at 4°C in an SW 41 rotor.
4. By using a micropipet, fractions of approx 450 μ L each can be successively collected into 1.5-mL tubes. The fractionation can be assayed by monitoring the UV absorbance of 18S and 28S ribosomal bands, which are always present in sufficient quantity to be detectable.
5. The fractions should be ethanol-precipitated twice and resuspended in 10 μ L DEPC-treated H₂O.

3.1.2. cDNA Library Synthesis

Oligo d(T) primer has been used for the primer of reverse transcription. Recently, lock-docking primer that anneals the junction site of mRNA and poly(A)⁺ tail provides more efficient reverse transcription (15). The following example is a construction of a unidirectional cDNA library in a plasmid vector.

1. Five micrograms of chick dorsal root ganglion mRNA are reverse-transcribed with SuperScript (Gibco-BRL: no. 18248-013).
2. After synthesis of the second strand, an asymmetric *Bst*XI adapter is ligated.
3. The product is digested with *Not*I, which site is introduced in the 3'-primer.
4. The cDNA is electrophoresed through agarose gel, and the fractions of appropriate molecular weight are collected.
5. The cDNA is extracted from the gel with silica gel column trapping method (Qiagen column).
6. The cDNA is ligated to a vector digested with *Bst*XI and *Not*I, and dephosphorylated at the 5'-end. The vector should contain RNA priming sequences (T7, T3, or SP6). If several different expression cloning methods are planned, use a multipurpose expression vector, such as pcDNA1, pcDNA3.1 (Invitrogen), and pCI-neo (Promega). These vectors contain RNA transcription primers as well as eukaryotic promoters.
7. The ligated sample is transformed to highly competent *Escherichia coli* cells.
8. The bacteria are cultured overnight at 37°C, supplemented with 10% glycerol, then rapidly frozen in liquid nitrogen, and stored -80°C.

3.2. Library Sibling Selection and In Vitro Transcription

3.2.1. Library Sibling Selection

1. The screening is initiated with pools of 1000–5000 single clones. Thaw 5–10 µL of frozen cDNA library-transformed *E. coli*, suspend into 200 µL LB, and store at 4°C.
2. An aliquot of the LB suspension is sequentially diluted from 10³- to 10⁸-fold. Each dilution (100 µL) is plated on a 10-cm diameter LB plate containing appropriate selection antibiotics (for pcDNA1, ampicillin and tetracycline). The plate is incubated for 12–16 h at 37°C. Calculate the titer of suspension from the number of colonies on the plate. If 100 µL of 10⁵ dilution gives 120 colonies, original suspension contains $120 \times 10^5/100 = 120,000$ clones in 1-µL aliquots (**Note 2**).
3. Plate 200 µL of freshly made dilution (500–1000 colonies/100 µL) in one 15-cm diameter LB plate. Dry the plate for 10–15 min until wet spots completely evaporate. Incubate the plate for 12–16 h at 37°C.
4. Add 5 mL of LB medium, scrape the colonies, and collect in a 15-mL tube. An aliquot (500 µL) is supplemented with 10% glycerol and then stored -80°C.
5. Purify plasmid DNA samples from the *E. coli* suspension by conventional method or by column-based purification kits (Qiagen, Promega). The latter is relatively expensive, but minimizes RNase contamination. Store the plasmids at -20°C.

6. If one of the pools provides a positive response in the oocyte assay, it can be divided and rescreened in the same manner until a single clone is isolated.

3.2.2. cDNA Template Preparation

1. Plasmid DNA (5 μg) is linearized by digestion with a restriction enzyme that cleaves distal to the cDNA insert. It is preferable to use an enzyme that cleaves DNA to produce either a 5' overhang or a blunt end. *NotI* is used for the digestion of a unidirectional expression library in pcDNA1.
2. After the digestion, 2 μg of proteinase K (Sigma: P2308) is added, and the incubation is continued for 30 min at 37°C to eliminate RNase.
3. The template is extracted with an equal volume of phenol/chloroform two times, rinsed with 3 vol of diethyl ether two times, and ethanol-precipitated.
4. The DNA precipitate is washed with 70% ethanol once, briefly dried, and then dissolved in 5–10 μL RNase-free TE.
5. Inspect 1- μL aliquot by agarose-gel electrophoresis. The sample is stored at -20°C.

3.2.3. In Vitro Transcription

Transcription kits are commercially available from several vendors. The following example utilizes the Ambion T7 kit, which supplies 10 \times concentrated reaction buffer, nucleotide (ATP, GTP, CTP, and UTP) solutions, T7 RNA polymerase, and 7.5 M LiCl/50 mM EDTA solution. In vitro transcripts that are to be injected into oocytes should have a 5' 7-methyl guanosine residue (m⁷G[5']ppp[5']G) or cap structure. It functions in the protein synthesis initiation process and protects the RNA from degradation. Capped in vitro transcripts can be synthesized by the addition of the cap analog to the reaction mixture. Normally, a 2–10 molar ratio/of the cap analog to GTP is included.

1. Prepare reaction mixture in one tube following order:
 - 5.5 μL RNase-free H₂O
 - 2 μL 75 mM ATP (final 7.5 mM)
 - 2 μL 75 mM CTP (final 7.5 mM)
 - 2 μL 75 mM UTP (final 7.5 mM)
 - 0.5 μL 75 mM GTP (final 1.88 mM)
 - 2 μL 40 mM Cap analog (m⁷G[5']ppp[5']G)(final 4 mM; Cap analog:GTP is 2.1:1)
 - 2 μL 10 \times T7 transcription buffer
 - 1 μL Linearized cDNA template (1 $\mu\text{g}/\mu\text{L}$)
 - 2 μL T7 RNA polymerase mixture (containing RNase inhibitor).For transcription of multiple samples, the reaction mixture can be premixed, divided, and then supplemented with templates and the enzymes.
2. Incubate the tube for 2–3 h at 37°C.
3. The reaction is terminated by the addition of 30 μL RNase-free H₂O and 25 μL 7.5 M LiCl/50 mM EDTA solution. Mix briefly, chill for 30 min at -20°C, and

then centrifuge at 12,000g for 15 min at 4°C. Rinse the pellet with 600 μ L 70% ethanol.

4. Dissolve precipitated RNA in 100 μ L RNase-free H₂O.
5. To remove proteins, the solution is extracted with equal volume of phenol/chloroform two times, and then rinsed with 3 vol of water-saturated diethyl ether three times.
6. Add 4 μ L 3 M sodium acetate and 250 μ L ethanol, mix briefly, chill for 30 min at -20°C, and then centrifuge at 12,000g for 15 min at 4°C. The ethanol-precipitated RNA is rinsed with 600 μ L 70% ethanol two times, and dissolved in 20–30 μ L RNase-free H₂O.
7. Inspect the product by gel electrophoresis, and determine the concentration (OD₂₆₀) and OD₂₆₀/OD₂₈₀ ratio (should be more than 1.5) by spectrophotometer. The yield of RNA is generally 15–30 μ g. RNA is stored -80°C until use.

3.3. Oocyte Preparation and RNA Injection

3.3.1. Maintenance of Frogs

Five to 10 female frogs are maintained in a 30 × 30 × 60 cm tank with 18–22°C water to a depth of 10 cm. Higher water temperature tends to increase bacterial and/or fungus infection and to lower the translation level in oocytes. The tank should be placed in a silent room with a constant light and dark (12/12 h) cycle. Feed brittle (3 g/frog), and change water twice a week.

3.3.2. Frog Anesthesia and Excision of Ovary

1. Sterilize surgical apparatus by immersing in 70% ethanol.
2. Frogs are anesthetized by immersing in ice water for 15–30 min, and then placed on crushed ice.
3. Make a diagonal incision (0.75–1.5 cm) on one side of lower abdomen with surgical small scissors or razor blade. Cut skin and muscle layer.
4. Pull up several lobes of ovary with large forceps. One lobe contains roughly 100 oocytes.
5. Cut a sufficient number of lobes, and place in 3 mL OR-2 medium in a 6-cm culture dish (Falcon: 3002).
6. Close the incision with 6/0 chromic gut. Close the muscle and skin in one layer. To strengthen suture, rapid coagulation glue (super glue, and so forth) may be placed on the skin suture. Operated frogs are placed on ice for 1 h and then returned to a water tank.

3.3.3. Separation of Oocytes

1. Tear to open an ovarian lobe with small forceps, remove excess OR-2 medium with Kimwipes, and transfer to 10 mL of collagenase solution in a 50-mL tube.
2. Gently rock the tube on a shaker at 60 rpm for 90–100 min at 18–22°C. When oocytes begin to separate, place the lobes on the 6-cm culture dish.

3. Remove the collagenase solution with a plastic pipet, and wash the oocytes with OR-2 twice in the same dish. Oocytes can be dissociated from the ovary by gentle pipeting or by dissection with fine forceps under the microscope.
4. Transfer the separated oocytes to fresh OR-2 in culture dish. Rinse the oocytes with OR-2 six times. Extensive washing is essential to keep oocytes healthy. The *Xenopus* oocyte is two-toned in color: the animal pole is gray to dark-colored, whereas vegetal pole is light-colored. Mature oocytes have a large diameter (1–1.2 mm) and no patch in the animal pole, a fine surface, and a sharp edge between animal and vegetal poles (stage V) or a transitional zone between both hemispheres (stage VI). A layer of follicle cells surrounds each oocyte. Collagenase treatment loosens and removes this layer. Separated yet folliculated oocytes often accompany small blood vessels that are visualized under the microscope.
5. Collect mature oocytes (stages V and VI) in the NDE96 medium in a 6-cm culture dish. At this stage, both folliculated and defolliculated oocytes are collected. Incubate the oocytes at 18°C overnight.
6. Before RNA injection, collect healthy and defolliculated oocytes. Manual defolliculation may be performed at this stage. The follicle layer can be removed with small forceps under the microscope.

3.3.4. RNA Injection

1. RNase-free 3.5-in. glass capillary is used for an RNA injection pipet. Fine tapers are pulled with a two-step micropipet puller.
2. Break the tips with a razor blade under a microscope to achieve the desired tip diameter. The outer diameter should be 10–40 μm . A blunt end is preferred.
3. The pipet is filled with low-viscosity silicon oil (Sigma: dimethylpolysiloxane, DMPS-V, 5cs, no. 9016-00-6) from the open end.
4. Attach the pipet to a microinjector.
5. Place 20–30 oocytes in an OR-2-filled, roughly scratched 6-cm culture dish.
6. Place 1–3 μL of RNA solution on an RNase-free surface (a screw cap of Eppendorf tube or Parafilm) under a dissection microscope.
7. Suck the drop into the pipet.
8. Perform a sham injection several times to confirm the ejection of RNA solution from the pipet.
9. Insert the pipet tip to an oocyte, and inject 50–100 nL of RNA. During the injection, the oocyte will visibly expand. Then inject RNA to the next oocyte. Some oocytes may release yolk after the injection. If the outflow is sustained, the needle diameter may be too large.
10. The injected oocytes are transferred to the NDE96 medium. A six-well culture dish (Falcon: 3046) is convenient for culturing different samples. One well can contain 40 oocytes.
11. The oocytes are incubated for 1–5 d at 18°C. Inspect daily, and change medium every other day. Damaged or dead oocytes should be removed immediately (**Note 3**).

3.4. Electrophysiological Detection of Oocyte Response

3.4.1. Making Glass Electrodes

Glass electrodes are created by two-step pulling. The tip pore size can be estimated by the following procedures.

1. Connect the open end to a syringe containing 10 mL of air via small tube.
2. Immerse the tip in 100% methanol.
3. Press the syringe until air bubbles appear in the methanol.
4. Read the scale on the syringe. An appropriate pipet is obtained when compression of the air to 6 mL elicits the bubbles.
5. The open end of the pipet is connected to an empty syringe, and then the tip is immersed in 3 M KCl. With suction, the tip's narrow cavity is filled with KCl solution.
6. The remainder of the pipet is filled with 3 M KCl from the open end with an Eppendorf microloader (Eppendorf: 5242 956.003).
7. Air bubbles in the pipet are removed by gentle tapping.

3.4.2. Preparation of Electrodes and Perfusion

1. The surface of silver wire contacting to solutions should be coated with AgCl. A silver wire is immersed in the sodium hypochlorite- (5%) based bleach solution (Clorox) for 10 min. The coating guarantees equilibrium between electrode and solutions.
2. Virtual current monitor/bath clamp electrodes are placed in the downstream of an oocyte chamber. Embedding the electrodes in ND96/agarose may reduce the ionized silver toxicity to the oocyte. However, it is not necessary as long as the perfusion flows continuously. ND96 is perfused at 2–3 mL/min.
3. Attach two glass pipets to the channel 1 and channel 2 detectors, and immerse the tips in the perfusion solution.
4. Measure the resistance of electrodes. (For the TEV-200, activate the Z test.) The resistance should be between 3 and 10 M Ω . If the resistance is out of this range or if obvious KCl leakage occurs, then change the glass electrode.

3.4.3. Two-Electrode Voltage Clamp of Xenopus Oocytes

1. Place an oocyte in the center of a chamber, and visualize animal pole.
2. Move the electrodes, and gently touch to the oocyte.
3. Adjust the electrode voltage offset to 0 mV.
4. Gently tap the end of electrode supporter, and then monitor the voltage. If the tip penetrates the membrane, the voltage drops down to –40 to –50 mV. Insert the other side of electrode in the same manner.
5. Start voltage clamp at –60 mV. Voltage clamp of a healthy oocyte will require an inward current between –10 and –100 nA.
6. Apply a ligand solution to the oocytes, and detect responses (**Notes 3 and 4**).

3.4.4. Analysis of NMDA-Type Glutamate Receptor

The *Xenopus* oocyte expression system has contributed greatly to our understanding of glutamate receptors. Heinemann and his colleagues successfully isolated the first glutamate receptor clone, GluR1, with this assay (1,16). The cDNA clone for an NMDA receptor subunit, NMDAR1(ζ 1-NR1), was also identified with this system (2,3). Moriyoshi's group (2) cloned the NMDAR1 cDNA from a rat forebrain cDNA library constructed from size-selected poly (A)+ RNA of 3–5 kbp. Initial pools consisted of 3000 cDNA clones. The isolated clone showed the expected features of an NMDA receptor: responsiveness to NMDA receptor agonists, response enhancement by glycine, competitive inhibition by d-APV, and voltage dependency of Mg^{2+} block (2,3). Four additional homologs, NMDAR2A(ϵ 1-NR2A)–NMDAR2D (ϵ 4-NR2D), have been identified by low-stringency screening of cDNA libraries or by polymerase chain reaction (16).

Although the oocyte system allowed isolation of the ζ 1-NR1 subunit, the properties of the receptor exhibited in oocyte experiments must be carefully interpreted. Native NMDA receptors in brain are probably a heterogeneous combination of different subunits. Recent studies have suggested that ζ 1-NR1 subunit has a high-affinity binding site for glycine, but not for NMDA or the competitive glutamate antagonist [3H]CGP-39653 (17,18). The glutamate binding site of native NMDA receptors seems to be located on the ϵ -NR2 subunits (19,20). The NMDA response of ζ 1-NR1 expressing oocyte may be attributed by endogenous ϵ -NR2-like subunits that bind to NMDA (21). Even if the coexpression of different NMDA receptor subunits is attempted in oocytes, the expression level of each subunit may be drastically different. Several groups have reported that ϵ 4-NR2D clones could not be expressed in *Xenopus* oocytes, possibly because of the high GC content of ϵ 4-NR2D mRNA, particularly around and downstream of the translation initiation site (22,23). Therefore, the precise characteristics of recombinant NMDA receptors must be assessed by a combination of the experiments from oocyte and other expression systems.

3.4.5. Analysis of G-Protein-Coupled Receptors in Oocytes

The oocyte expression system is also used for the analysis of G-protein-coupled receptor signal cascade. Several types of G-protein-coupled receptors, such as serotonin 5HT_{1c} receptor (7) and metabotropic glutamate receptor 1 (5), activate PI cascade via G_q and/or G_i proteins. Inositol 1,4,5-trisphosphate binds to its receptor on intracellular Ca²⁺ store and then induces the elevation of cytoplasmic Ca²⁺ concentration. One unique feature of *Xenopus* oocyte is that the cell possesses Ca²⁺-sensitive Cl⁻ channels in its plasma membrane. The activation of PI turnover leads a large Cl⁻ current in oocytes (7,8). Since

the reversal potential of Cl^- current is around -20 mV, an inward current is observed when the oocyte is clamped near the resting potential (-60 mV). Dozens of G-protein-coupled receptors have been cloned using this in vivo signal amplification cascade. We have cloned a cytosolic protein CRMP-62 that is involved in growth cone guidance (12) and P2Y_1 ATP receptor as a touch sense receptor (13) from a chick dorsal root ganglion cDNA library using the oocyte expression system.

The sensitivity of this system largely depends on the extent to which receptors activate PI turnover in oocytes. Gi/Go- and Gs-coupled receptors are ineffective or less effective in activating PI turnover and, therefore, can be more difficult to isolate in the oocyte system. To circumvent this problem, several approaches have been proposed. One approach is coexpression of an appropriate downstream effector in oocytes. The cystic fibrosis transmembrane conductance regulator (CFTR) was recently used for the isolation of Gs-coupled receptors (24,25). Inwardly rectifying potassium channels (26) or phospholipase C $\beta 2$ has been used for characterization of Gi/Go-coupled receptors.

An alternative approach is coexpression of chimeric Gq/Gi and/or Gq/Go proteins that interact with Gi/Go-coupled receptors and with endogenous phospholipase C. It has been shown that the carboxyl-terminus of G-protein α -subunit specifies receptor coupling. The substitution of the last three amino acid residues of Gq with the corresponding residues of Gi renders the chimera protein to interacting with Gi/Go-coupled receptor and activating PI turnover in HEK-293 cells (27). Based on this finding, we have tested Gq/Gi chimeric protein in oocytes. When the cRNAs of Gq/Gi chimera is introduced with the cRNA of Gi-coupled muscarinic m2 receptor, oocytes become roughly 200-fold more sensitive to acetylcholine stimulation (Fig. 2). Thus, the chimeras of Gq with other G-proteins may provide new tools for the isolation of a broad range of G-protein-coupled receptors. A similar approach, introducing G_{15} or G_{16} proteins in cultured mammalian cells, has been proposed (28,29).

4. Notes

1. For convenience, the sucrose step gradient can be used. Prepare 5, 11, 18, 24, and 30% (w/v) sucrose buffers containing 10 mM HEPES NaOH, pH 7.5, 1 mM EDTA, and 0.1% lithium dodecyl sulfate. Place 2.3 mL of 30% sucrose buffer in the bottom of tubes, and then gently overlay each 2.3 mL with 24–5% sucrose buffer in descending order. Stand the tube at 20°C for 4–6 h.
2. The titer of *E. coli* in LB suspension is rapidly decreased. We usually estimate the actual titer of overnight samples at 70%.
3. Make positive and negative controls of injected oocytes to evaluate the oocyte expression system quality. As a positive control, a small amount (50 μg) of cloned receptor cRNA, such as $5\text{HT}_{1\text{C}}$ cRNA (7), is injected. As a negative control, H_2O is injected.

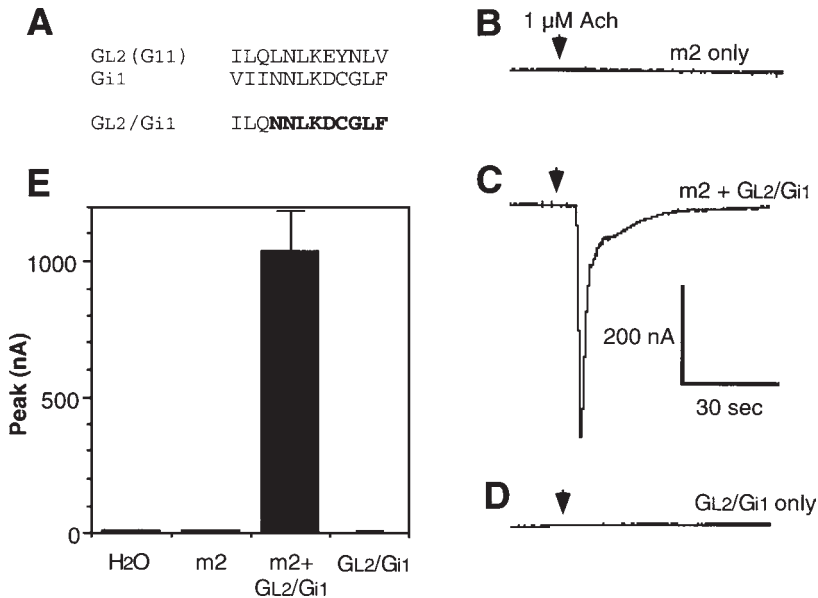


Fig. 2. Gq/Gi chimera enhances of Gi-coupled receptor-mediated response in oocyte. (A) Schematic representation of G_{L₂/Gi1} chimera. G_{L₂/Gi1} is a member of Gq class G-proteins. The amino acid sequences of carboxyl-terminus of G_{L₂} and Gi1 are shown. In G_{L₂/Gi1} chimera, the last nine amino acid residues of Gq protein are substituted with those of Gi1. (B–D) Typical traces of acetylcholine stimulation on muscarinic m2 receptor (B), m2 receptor and G_{L₂/Gi1} chimera (C), and G_{L₂/Gi1} chimera (D) expressing oocytes. Muscarinic m2 receptor cRNA (50 pg) injected to the oocytes in (B) and (C). The cRNA of G_{L₂/Gi1} chimera (200 pg) was coinjected in (C). The same amount of chimeric G-protein cRNA was injected in (D). All oocytes were clamped at –60 mV. The resting currents were around –40 nA. No or weak response was observed to 1 μ M acetylcholine stimulation on (B) or (D). In m2- and G_{L₂/Gi1}-injected oocytes (C), transient, large inward Cl[–] current (–500 nA) was observed within 10 s after the acetylcholine stimulation. The response is similar to the activation of the Gq coupled receptor. (E) The average \pm SEM of peak current is shown. Each column is the average of the peak currents from five to seven oocytes of the individual treatments. Similar results were obtained from three different experiments.

- If both injected and noninjected oocytes are dead or sick, the preparation of oocytes may be inadequate or NDE96 medium may be old. Prepare new solutions.
- If the injected oocytes are dead or sick, the diameter of injection pipet may be too large or the pipet may be too deeply inserted.
- If the oocyte-injected RNA sample is sick, but not positive or negative controls, the preparation of RNA may be inadequate.

- d. If the oocyte-injected cloned receptor cRNA does not respond to its ligand, the expression or signal amplification in the oocytes may be poor.
 - e. If some of the H₂O-injected or noninjected oocytes respond to the ligand for screening, the batch of oocytes has background response. Record the oocyte character and its identity. Keep the frogs laying high-expression and low-background oocytes.
 - f. Each batch of oocyte has different properties. Positive response for screening ligand should be confirmed with several batches of oocytes from different frogs.
4. Ligand solution can be applied either by switching the perfusion to the ligand-containing buffer or by the addition of concentrated ligand into the oocyte chamber. Since a low concentration of hydrophobic ligands in ND96 tends to be absorbed to plasticwares, highly purified bovine serum albumin (BSA) (USB: no. 10857 Albumin, Fraction V) solution may be used as carrier of the ligands. Prepare 0.1% BSA in ND96. Mix concentrated ligand solution (mM range) with BSA/ND96, and then dilute it with BSA/ND96 to obtain desired concentration. Conventionally prepared BSA should not be used, because it contains lysophosphatidic acid (LPA), which activates Cl⁻ current in oocytes (30).

Acknowledgments

F. N. and S. M. S. are supported by grant from Spinal Cord Research Foundation of the Paralyzed Veterans of America. S. M. S. is supported from the National Institute of Health. S. M. S. is a John Merck Scholar in the Biology of Developmental Disorders in Children. Y. G. is supported by CREST of Japan Science and Technology Corporation (JST). We thank Dr. Shigetada Nakanishi (Kyoto University) for providing us with the opportunity to present this chapter.

References

1. Hollmann, M., O'Shea-Greenfield, A., Rogers, S. W., and Heinemann, S. (1989) Cloning by functional expression of a member of the glutamate receptor family. *Nature* **342**, 643–648.
2. Moriyoshi, K., Masu, M., Ishii, T., Shigemoto, R., Mizuno, N., and Nakanishi, S. (1991) Molecular cloning and characterization of the rat NMDA receptor. *Nature* **354**, 31–37.
3. Nakanishi, N., Axel, R., and Shneider, N. A. (1992) Alternative splicing generates functionally distinct N-methyl-D-aspartate receptors. *Proc. Natl. Acad. Sci. USA* **89**, 8552–8556.
4. Yamazaki, M., Mori, H., Araki, K., Mori, K. J., and Mishina, M. (1992) Cloning, expression and modulation of a mouse NMDA receptor subunit. *FEBS Lett.* **300**, 39–45.
5. Masu, M., Tanabe, Y., Tsuchida, K., Shigemoto, R., and Nakanishi, S. (1991) Sequence and expression of a metabotropic glutamate receptor. *Nature* **349**, 760–765.
6. Masu, Y., Nakayama, K., Tamaki, H., Harada, Y., Kuno, M., and Nakanishi, S. (1987) cDNA cloning of bovine substance-K receptor through oocyte expression system. *Nature* **329**, 836–838.

7. Julius, D., MacDermott, A. B., Axel, R., and Jessell, T. M. (1988) Molecular characterization of a functional cDNA encoding the serotonin 1c receptor. *Science* **241**, 558–564.
8. Moriarty, T. M. and Landau, E. M. (1990) *Xenopus* oocyte as model system to study receptor coupling to phospholipase C, in *G Proteins* (Iyengar, R. and Birnbaumer, L., eds.), Academic, New York, pp. 479–501.
9. Romero, M. F., Kanai, Y., Gunshin, H., and Hediger, M. A. (1998) Expression cloning using *Xenopus laevis* oocytes. *Methods Enzymol.* **296**, 17–52.
10. Honda, Z., Takano, T., Hirose, N., Suzuki, T., Muto, A., Kume, S., et al. (1995) Gq pathway desensitizes chemotactic receptor-induced calcium signaling via inositol trisphosphate receptor down-regulation. *J. Biol. Chem.* **270**, 4840–4844.
11. Dascal, N. and Lotan, I. (1992) Expression of exogenous ion channels and neurotransmitter receptors in RNA-injected *Xenopus* oocytes. *Methods Mol. Biol.* **13**, 205–225.
12. Goshima, Y., Nakamura, F., Strittmatter, P., and Strittmatter, S. M. (1995) Collapsin-induced growth cone collapse mediated by an intracellular protein related to UNC-33. *Nature* **376**, 509–514.
13. Nakamura, F. and Strittmatter, S. M. (1996) P2Y₁ purinergic receptors in sensory neurons: contribution to touch-induced impulse generation. *Proc. Natl. Acad. Sci. USA* **93**, 10,465–10,470.
14. Sambrook, J., Fritsch, E. F., and Maniatis, T. (1989) *Molecular Cloning: A Laboratory Manual*, 2nd ed. Cold Spring Harbor Laboratory Press, Cold Spring Harbor, NY.
15. Borson, N. D., Salo, W. L., and Drewes, L. R. (1992) A lock-docking oligo(dT) primer for 5' and 3' RACE PCR. *PCR Methods Appl.* **2**, 144–148.
16. Hollmann, M. and Heinemann, S. (1994) Cloned glutamate receptors. *Annu. Rev. Neurosci.* **17**, 31–108.
17. Kawamoto, S., Uchino, S., Hattori, S., Hamajima, K., Mishina, M., Nakajima-Iijima, S., et al. (1995) Expression and characterization of the ζ 1 subunit of the *N*-methyl-D-aspartate (NMDA) receptor channel in a baculovirus system. *Mol. Brain Res.* **30**, 137–148.
18. Uchino, S., Nakajima-Iijima, S., Okuda, K., Mishina, M., and Kawamoto, S. (1997) Analysis of the glycine binding domain of the NMDA receptor channel ζ 1 subunit. *Neuroreport* **8**, 445–449.
19. Kendrick, S. J., Lynch, D. R., and Pritchett, D. B. (1996) Characterization of glutamate binding sites in receptors assembled from transfected NMDA receptor subunits. *J. Neurochem.* **67**, 608–616.
20. Laube, B., Hirai, H., Sturgess, M., Betz, H., and Kuhse, J. (1997) Molecular determinants of agonist discrimination by NMDA receptor subtypes: Analysis of the glutamate binding site on the NR2B subunit. *Neuron* **18**, 493–503.
21. Soloviev, M. M. and Barnard, E. A. (1997) *Xenopus* oocytes express a unitary glutamate receptor endogenously. *J. Mol. Biol.* **273**, 14–18.
22. Ishii, T., Moriyoshi, K., Sugihara, H., Sakurada, K., Kadotani, H., Yokoi, M., et al. (1993) Molecular characterization of the family of the *N*-methyl-D-aspartate receptor subunits. *J. Biol. Chem.* **268**, 2836–2843.

23. Monyer, H., Burnashev, N., Laurie, D. J., Sakmann, B., and Seeburg, P. H. (1994) Developmental and regional expression in the rat brain and functional properties of four NMDA receptors. *Neuron* **12**, 529–540.
24. Luebke, A. E., Dahl, G. P., Roos, B. A., and Dickerson, I. M. (1996) Identification of a protein that confers calcitonin gene-related peptide responsiveness to oocytes by using a cystic fibrosis transmembrane conductance regulator assay. *Proc. Natl. Acad. Sci. USA* **93**, 3455–3460.
25. Uezono, Y., Bradley, J., Min, C., McCarty, N. A., Quick, M., Riordan, J. R., et al. (1993) Receptors that couple to 2 classes of G proteins increase cAMP and activate CFTR expressed in *Xenopus* oocytes. *Receptors Channels* **1**, 233–241.
26. Krapivinsky, G., Gordon, E. A., Wickman, K., Velimirovic, B., Krapivinsky, L., and Clapham, D. E. (1995) The G-protein-gated atrial K⁺ channel I_{KACH} is a heteromultimer of two inwardly rectifying K⁺-channel proteins. *Nature* **374**, 135–141.
27. Conklin, B. R., Farfel, Z., Lustig, K. D., Julius, D., and Bourne, H. R. (1993) Substitution of three amino acids switches receptor specificity of Gq α to that of Gi α . *Nature* **363**, 274–276.
28. Milligan, G., Marshall, F., and Rees, S. (1996) G₁₆ as a universal G protein adapter: implications for agonist screening strategies. *Trends Pharmacol. Sci.* **17**, 235–237.
29. Offermanns, S. and Simon, M. I. (1995) G α_{15} and G α_{16} couple a wide variety of receptors to phospholipase C. *J. Biol. Chem.* **270**, 15,175–15,180.
30. Tigyí, G. and Miledi, R. (1992) Lysophosphatidates bound to serum albumin activate membrane currents in *Xenopus* oocytes and neurite retraction in PC12 pheochromocytoma cells. *J. Biol. Chem.* **267**, 21,360–21,367.

Expression of NMDA Receptor Channel Subunit Proteins Using Baculovirus and Herpesvirus Vectors

Susumu Kawamoto, Satoshi Hattori,
Shigeo Uchino, Masayoshi Mishina, and Kenji Okuda

1. Introduction

Foreign gene transfer and expression in the cells are among the most important techniques for determining the characteristics and function of cloned genes. Glutamate receptor genes have been expressed by RNA injection of *Xenopus* oocytes or transfection of mammalian cells, such as HEK, CHO, and COS cells, and bacterial *Escherichia coli* cells. Viral vectors, such as baculovirus (*Autographa californica* nuclear polyhedrosis virus, AcNPV) or herpesvirus (herpes simplex virus-1, HSV-1), have been also used because of high efficiency of gene transfer. Existing viral clones expressing recombinant glutamate receptor proteins (1–25) are summarized in **Table 1**.

Although the baculovirus system is useful for some molecular and functional studies, the system is limited to insect cells and mammalian liver cells (26–28). **Figure 1** illustrates a general construction scheme for baculovirus expression vectors. Since the baculovirus DNA (130 kb) is too long to be manipulated by using standard genetic engineering techniques, a so-called transfer vector is used to insert a foreign gene into the virus, replacing the polyhedrin gene. The recombinant transfer vector containing glutamate receptor (GluR) cDNA is transfected into the insect cell, together with wild-type baculovirus DNA. Since the two DNA molecules have common sequences flanking the genes of interest, a recombinant baculovirus is obtained by homologous recombination. Wild-type baculovirus produces the polyhedrin protein, whereas the recombinant baculovirus produces the foreign gene product under the control of very strong polyhedrin promoter.

Table 1
Summary of Viral Vectors
Expressing Glutamate Receptor Proteins

Viral vector, mouseGluR/ratGluR	Reference
Baculovirus vector	
$\alpha 1$	1–5
$\alpha 2$ /GluRB	3,6–9
($\alpha 4$)/GluRD	9–11
($\beta 2$)/GluR6	12–14
$\zeta 1$ /NMDAR1	15–17
$\epsilon 1$	(18 and this study)
$\epsilon 2$	(18 and this study)
$\delta 2$	(18 and this study)
mGluR1 (rat)	13
Herpesvirus vector	
($\alpha 1$)/GluR1	19
($\beta 2$)/GluR6	20–22
$\zeta 1$	This study
Adenovirus vector	
($\alpha 1$)/GluR1	23
($\alpha 2$)/GluR2	23
($\zeta 1$)/NMDAR1 (antisense)	24
Adenoassociated virus vector	
($\zeta 1$)/NMDAR1 (antisense)	25

Here we have used the transfer vectors pJVP10Z and pBlueBacIII. Since the vectors contain the *lacZ* gene, selection of recombinant virus clones was performed by β -galactosidase assay with X-gal as a substrate. The cDNA of interest is inserted downstream from the polyhedrin promoter in the transfer vectors. The recombinant baculovirus produced *in vivo* by homologous recombination was plaque-purified by screening using both β -galactosidase assay and polyhedra-negative morphology as criteria. Dot-blot hybridization analysis of DNA produced in insect cells infected with the purified recombinant virus revealed the presence of foreign gene, GluR subunit cDNA.

Molecular neurobiological approaches by which foreign genes can be transferred to or expressed in cultured neurons and in brain would greatly facilitate research and therapeutics. Viral vectors, such as herpesvirus, adenovirus, or adeno-associated virus, but not retrovirus, are good candidates, because they can transfer or express genes in the nondividing neurons. Recent reviews (29–30) have focused on the characteristics of these three viral vectors for gene expression in neurons. The wide host range of HSV-1, both *in vivo* and *in vitro*, and the

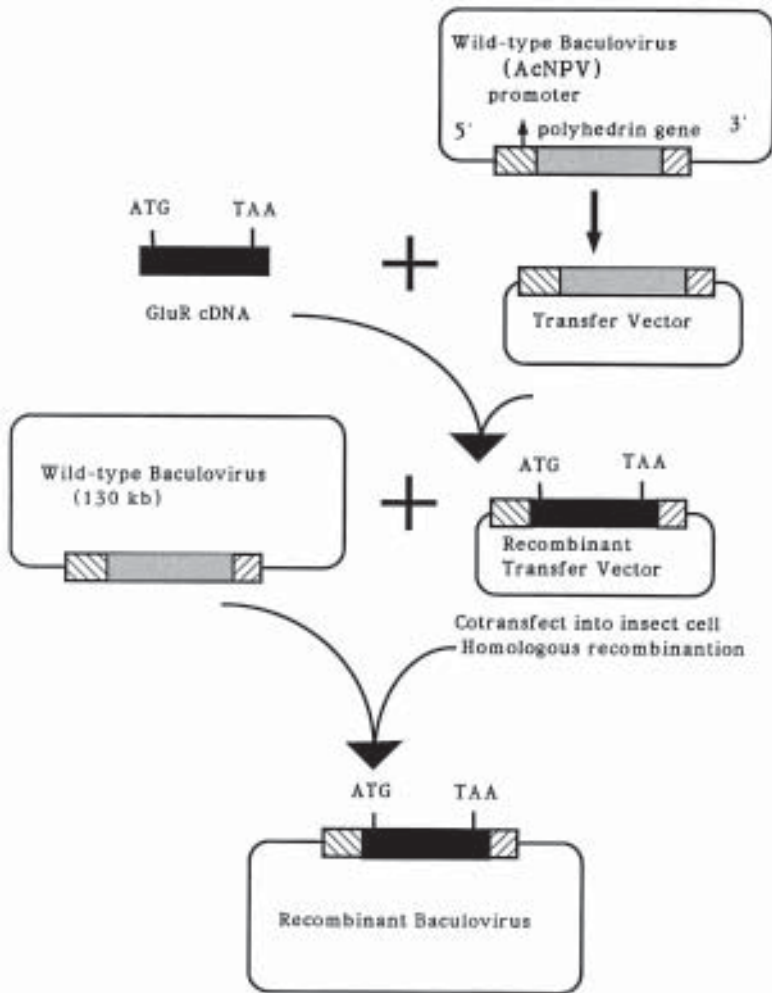


Fig. 1. General construction scheme for baculovirus expression vector. See details in the text.

relative ease of its genetic manipulation have made it an attractive candidate as a tool for gene transfer. In particular, the natural propensity of the virus to infect and establish lifelong latent infection in postmitotic neurons has prompted much recent effort in developed HSV-1 vectors.

Two different types of HSV-1 vectors have been developed. For the first type, the recombinant virus vector, the gene of interest is inserted into the backbone of the viral genome by genetic recombination. The second type of HSV-1 vector is “ampicon”-based and has been termed a “defective” virus vector

because of its inability to replicate in the absence of the parental virus as helper. The amplicon plasmid includes prokaryotic sequences that allow propagation and drug selection in bacteria, an origin of replication and packaging signal from HSV-1, and a transcriptional unit for expressing the gene of interest. The latter type of HSV-1 vector has been used in our laboratory, and the protocols about that have been described here.

We (1–7,15,17,18) have characterized or would like to characterize glutamate receptor proteins by using the baculovirus vector system in vitro, and their function in vitro and in vivo with a herpesvirus vector system. This chapter describes the detailed protocols to isolate these viruses. Several protocols for baculovirus (31–33) or herpesvirus (34,35) expression systems have already been published (see Notes 1 and 2).

2. Materials

2.1. Baculovirus Vector System

1. *Spodoptera frugiperda* insect Sf9 (Sf21) cells: Sf cells can be maintained at 27°C without CO₂ (see Note 1).
2. TNM-FH insect medium (Sigma #T-1032) (Sigma Chemical Co., St. Louis, MO) or EX-CELL 400 serum-free medium (JRH Biosciences [Lenexa, KS] #14400), containing 50 µg/mL gentamicin sulfate.
3. AcNPV DNA (circular or linear) from Invitrogen (San Diego, CA).
4. Transfer vector (see Note 2): the pJVP10Z vector was provided by Palmer Taylor (University of California, San Diego), and pBlueBacIII was purchased from Invitrogen. They contain β-galactosidase gene, and color selection can be done for virus purification or virus titer check.
5. Lipofectin reagent (Gibco-BRL #18292) (Gibco-BRL, Gaithersburg, MD).
6. Fetal bovine serum (FBS).
7. SeaPlaque agarose (FMC Bioproducts [Rockland, ME] #50101) was dissolved in water (3% [w/v]) and autoclaved.
8. X-gal stock solution (20 mg/mL dimethylsulfoxide).
9. TE: 10 mM Tris-HCl, pH 8.0, and 0.1 mM EDTA.

2.2. Herpesvirus Vector System

1. Rabbit skin cells provided from Michael G. Kaplitt (Cornell University Medical College and The Rockefeller University).
2. Vero cells.
3. DMEM medium (Gibco-BRL #12800-017).
4. MEM medium (Nissui #05901, Nissui Pharmaceutical Co., Tokyo, Japan).
5. Opti-MEM medium (Gibco-BRL #31985-021).
6. FBS.
7. Trypsin-EDTA solution (Sigma #T-3924).
8. Phosphate-buffered saline (PBS) (Dulbecco's PBS [-] "Nissui," Nissui #05913).

9. TE: 10 mM Tris-HCl, pH 8.0, and 0.1 mM EDTA.
10. 0.1 N Na₂CO₃.
11. Suspension buffer A: 20 mM Tris HCl, pH 7.5, and 150 mM NaCl.
12. Suspension buffer B: 50 mM Tris-HCl, pH 7.4, 0.3 mM EDTA, 1 mM dithiothreitol, and 1 mM phenylmethylsulfonyl fluoride.

3. Methods

3.1. Expression System Using Baculovirus Vectors

3.1.1. Cloning of NMDA Receptor Channel Subunit cDNAs into the Transfer Vectors

The NMDA receptor channels contain two classes of subunits in hetero-oligomeric association, the core ζ 1 (NMDAR1, NR1) subunit, and the regulatory ϵ 1- ϵ 4 (NMDAR2A-2D, NR2A-2D) subunits.

1. The 3020-bp *Nru*I-*Nae*I fragment, containing 53 bp of 5'-untranslated region (see **Note 3**), the complete coding region (2814 bp), and 153 bp of 3'-untranslated region, was prepared from the mouse NMDA receptor channel ζ 1 subunit cDNA (**36**). The fragment was inserted into the unique *Nhe*I site downstream of the polyhedrin promoter in the transfer vector pJVP10Z using blunt-end ligation.
2. The cDNAs encoding the mouse NMDA receptor channel ϵ 1- and ϵ 2-subunits were inserted into the unique *Nhe*I site downstream of the polyhedrin promoter in the transfer vectors pBlueBacIII (Invitrogen) (for GluR ϵ 1 cDNA) or pJVP10Z (for GluR ϵ 2 cDNA) as follows. For the ϵ 1-subunit, the 4395-bp fragment, containing the complete coding region, was subcloned to the *Nco*I site of pBlueBacIII. For the ϵ 2-subunit, the 4855-bp fragment, containing 10 bp of 5'-untranslated region (see **Note 3**), the complete coding region (4446 bp) and 399 bp of 3'-untranslated region, was subcloned to the unique *Nhe*I site of pJVP10Z.
3. Recombinant plasmids, pJVP10Z/GluR ζ 1, pBlueBacIII/GluR ϵ 1, and pJVP10Z/GluR ϵ 2, carrying the respective inserts in the correct orientation were identified by DNA sequencing using an automatic DNA sequencer 373A (Applied Biosystems).

3.1.2. Cotransfection of Viral and Transfer Vector DNAs Using Lipofectin

1. Seed six-well dishes with 2.5×10^6 Sf9 (or Sf21) cells/well. Incubate at 27°C for 1 h to allow the cells to attach.
2. Wash the cells twice with 1 mL of serum-free TNM-FH insect medium.
3. Add 1 mL of serum-free TNM-FH insect medium.
4. Mix 1.0 μ g recombinant transfer vector and 0.2 μ g AcNPV DNA in 6 μ L TE, and 4 μ g lipofectin in a polystyrene tube (total 12 μ L). Incubate at room temperature for 15 min.
5. Add the lipofectin/DNA mixture to the cells.

6. Incubate for 24 h at 27°C.
7. Add 1 mL serum-supplemented (10% [v/v] FBS) TNM-FH insect medium.
8. Incubate for 48 h at 27°C. Transfer the medium to the tube, centrifuge at 1000g for 15 min at 4°C. Store the supernatant (recombinant virus solution) at 4°C.

3.1.3. Purification of Recombinant Virus by Plaque Assay

1. Seed 10-cm dishes with 4×10^6 Sf cells per dish, and incubate at 27°C for 1 h to allow the cells to attach.
2. Dilute the recombinant virus solution to 10^3 - to 10^4 -fold.
3. Remove media, and add 1.6 mL diluted virus solution to each plate.
4. Incubate plates for 1 h at 27°C.
5. Incubate 2 mL serum-supplemented TNM-FH insect medium and 2 mL 3% (w/v) SeaPlaque agarose at 42°C in polypropylene tubes.
6. Add 60 μ L X-gal stock solution and 4 mL TNM-FH insect medium.
7. At the end of the 1-h incubation period, remove all inoculum by using Pasteur pipets. Slowly add 8 mL of overlay. Leave the overlay to solidify for 1 h.
8. Seal the plates with Parafilm.
9. Incubate plates for several days at 27°C.
10. To pick a blue plaque, place the top of a sterilized Pasteur pipet directly onto the plaque. Carefully apply gentle suction until a small plug of agarose is drawn into the pipet.
11. Place the agarose plug in 1 mL medium. Vortex well, and store at 4°C.
12. Several rounds of plaque purification are necessary to isolate recombinant viruses.

3.1.4. Amplification of Recombinant Virus

1. Seed 75-cm² flask with 9×10^6 Sf cells/flask. Incubate at 27°C for 1 h to allow the cells to attach.
2. The medium is removed, and the cells are inoculated with recombinant AcNPV at a multiplicity of infection (MOI) of 0.01 in a volume of 2 mL.
3. After incubation for 1 h at 27°C, add 8 mL TNM-FH insect medium supplemental with 10% (v/v) FBS.
4. After incubation for 5–7 d, the medium is harvested. Transfer the medium to the tube, and centrifuge at 1000g for 15 min at 4°C. Store the supernatant (recombinant virus solution) at 4°C (see **Note 4**).

3.1.5. Expression of NMDA Receptor Channel Subunit Proteins Using Recombinant Baculovirus

Both monolayer culture and suspension culture can be used for expression of recombinant NMDA receptor channel proteins. Multiwell plates, dishes, or flasks can be used for monolayer culture and spinners for suspension culture.

Sf21 cells were infected with recombinant baculovirus at an MOI of 5–10. Several (usually three) days postinfection, the sufficient expression level of the recombinant proteins can be obtained (see **Fig. 2** and **Note 5**). Character-

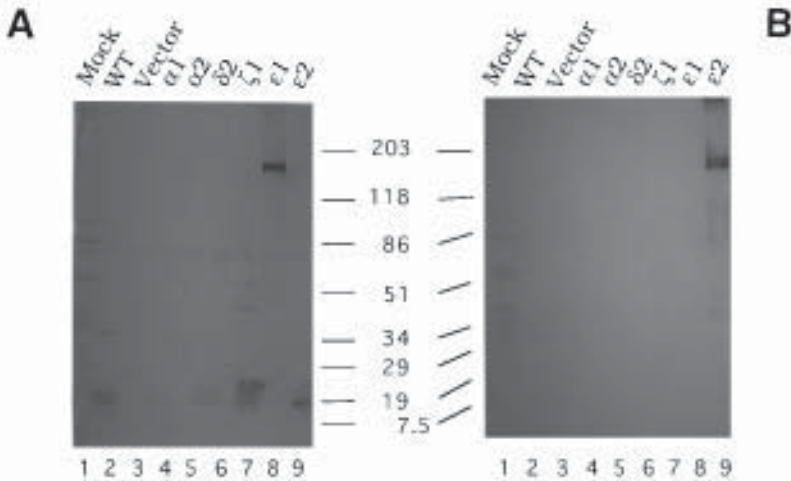


Fig. 2. Western blotting of baculovirus-infected Sf21 cells. Sf21 cells were placed in 12-well dishes and infected with AcNPV (lane 2), AcNPV/pJVP10Z (A) (or AcNPV/pBlueBacIII) (B) (vector only; without GluR cDNA insert) (lane 3), AcNPV/GluR α 1 (lane 4), AcNPV/GluR α 2 (lane 5), AcNPV/GluR δ 2 (lane 6), AcNPV/GluR ζ 1 (lane 7), AcNPV/GluR ϵ 1 (lane 8), AcNPV/GluR ϵ 2 (lane 9), or mock-infected (lane 1). At 3 d postinfection, the particulate fractions (12,000g pellet; 2.6 μ g of protein) of cell lysates were analyzed on a continuous 4–20% gradient SDS-PAGE gel and subjected to immunodetection using anti-GluR ϵ 1 (A) or anti-GluR ϵ 2 (B) antibodies. The positions of molecular-size markers (kDa) are indicated. Our experiments using tunicamycin or peptide: *N*-glycosidase F (EC 3.5.1.52) indicate that the large- and small-sized bands are glycosylated and non-*N*-glycosylated species, respectively (data not shown).

ization of the baculovirus-expressed mouse ζ 1-subunit has been already described in detail (15–17), and that of ϵ 1- and ϵ 2-subunits will be described elsewhere in detail.

3.2. Expression System Using Herpesvirus Vectors

In order to obtain HSV-1 vector, amplicon plasmid (Fig. 3) is first transfected to the Vero cells or rabbit skin cells, and superinfected with helper virus for packaging to recombinant defective virus.

3.2.1. Construction of Plasmid pHCMV/GluR ζ 1

The amplicon plasmid, which is a vector for producing defective HSV-1 vector, essentially contains a eukaryotic transcription unit and *cis*-acting HSV sequences, encoding an origin of DNA replication and a cleavage/package signal (37). The plasmid pHCL contains the bacterial *lacZ* gene under the control of the human cytomegalovirus (CMV) immediate early promoter (38).

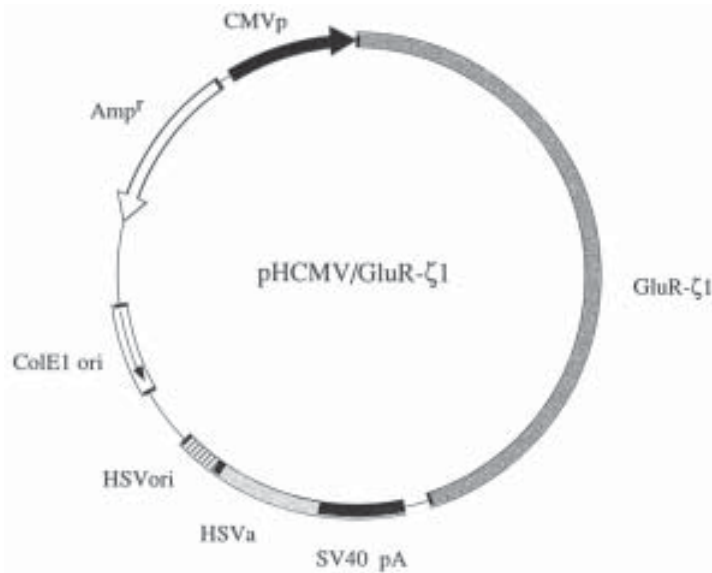


Fig. 3. Construction of HSV amplicon plasmid. The mouse NMDA receptor GluR ζ 1 subunit cDNA was inserted into the multiple cloning site of the vector. Key elements of the vector for packaging and expression of recombinant genes in eukaryotic cells are the HSV-1 cleavage/packaging signal “a” sequence (HSV α), the HSV-2 Oris origin of replication (HSVori), the CMV immediate early gene 1 promoter, and the simian virus 40 (SV40) polyadenylation signal.

The amplicon pHCMV/GluR ζ 1 was generated as follows. pHCL was digested with *Hind*III and *Sal*I to remove the bacterial *lacZ* gene and ligated to simian virus 40 polyadenylation signal, which was released from pRep4 (Invitrogen) digested with *Hind*III and *Xho*I. The resultant plasmid, pHCMV-pA, has several cloning sites for expression of a foreign gene. A 3.3-kb *Nru*I-*Nsi*I fragment from the pBSK ζ 1 (36) was inserted into *Hind*III site downstream from the CMV promoter by using blunt-end ligation.

3.2.2. Transfection

1. Seed 75-cm² flask with 5×10^6 rabbit skin cells/flask.
2. After 24–48 h (70–90% confluency), cells were detached by trypsin-EDTA solution and washed twice with PBS.
3. Resuspend the cells with Opti-MEM (1×10^7 cells/400 μ L), add amplicon plasmid (30 μ g/30 μ L TE), mix well by pipeting, and transfer to a cuvet.
4. By using Gene Pulser (Bio-Rad) charge the pulse (960 μ F, 220 V).
5. Leave at room temperature for 5 min, then resuspend the cells with 12 mL 10% FBS-DMEM, and mix well by pipeting.

6. Aliquot 4 mL each to three filter-capped 25-cm² flasks.
7. Incubate overnight at 37°C in 5% CO₂ incubator.

3.2.3. Superinfection

1. Wash the cells once with 4 mL 1% FBS-PBS.
2. Inoculate with 200 µL helper virus (tsK strain) (*see Note 6*) solution (1% FBS-PBS) at an MOI of 0.1.
3. Rock at room temperature for 5 min.
4. Leave at 31°C for 1 h in 5% CO₂ incubator.
5. Add 4 mL 1% FBS-DMEM, and incubate at 31°C in 5% CO₂ incubator.
6. When most cells are infected, harvest the virus solution (2–4 d).

3.2.4. Preparation of Stocks

1. Peel off the infected cells by cell scraper, and transfer to 15-mL centrifuge tube.
2. Freeze/thaw three times in liquid N₂ or dry ice/ethanol.
3. Centrifuge at 800g for 8 min at 4°C.
4. Use the supernatant as the virus solution (P0).

3.2.5. Amplification of Recombinant Defective HSV-1 Vector

1. Seed 25-cm² filter-capped flasks with Vero cells, and incubate the cells to 90–100% confluency.
2. Wash the cells with 4 mL of 1% FBS-PBS.
3. Add 1 mL of P0 virus solution.
4. Rock at room temperature for 5 min.
5. Leave at 31°C for 1 h in 5% CO₂ incubator.
6. Remove the virus solution.
7. Add 4 mL of 1% FBS-DMEM, and incubate at 31°C in 5% CO₂ incubator.
8. When all the cells are infected (24–48 h), recover the virus solution (P1).

3.2.6. Preparation of Defective HSV-1 Vector Solution for Experiments

1. Inoculate with the virus solution at the optimal (usually the highest) ratio of defective/helper virus.
2. Freeze/thaw three times.
3. Centrifuge at 800g for 8 min at 4°C to remove cell debris.
4. Transfer the supernatant to the tube, and centrifuge at 14,500g for 1 h at 4°C.
5. Remove supernatant.
6. Resuspend the pellet in suspension buffer A, aliquot, and store at –70°C.

3.2.7. Expression of NMDA Receptor Channel Subunit Protein Using Defective HSV-1 Vector

Defective HSV-1- or mock-infected Vero cells were lysed in 0.1 N Na₂CO₃ and then pelleted by centrifugation at 12,000g for 30 min. The pellets were

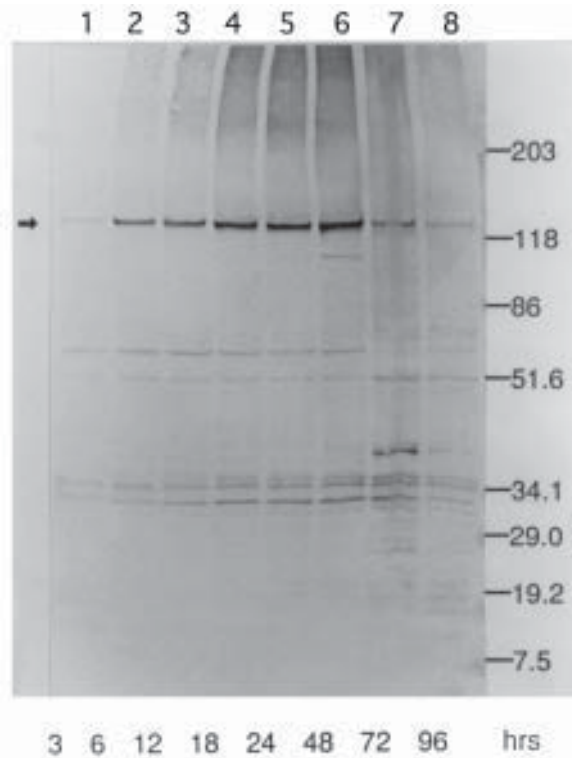


Fig. 4. Time-course of NMDA receptor channel GluR ζ 1-subunit expression in dvGluR ζ 1-infected Vero cells. At 3, 6, 12, 18, 24, 72, and 96 h postinfection, the particulate fractions (12,000g pellet; 2.6 μ g of protein) of cell lysates were subjected to Western analysis using anti-GluR ζ 1 antibody as in **Fig. 2**. The positions of molecular-size markers (kDa) and recombinant GluR ζ 1 protein (arrow) are indicated.

suspended in suspension buffer B. In the experiment with immunoblotting, proteins were separated by SDS-PAGE gel and transferred onto polyvinylidene difluoride membrane (Millipore). To detect GluR ζ 1 protein, incubation was done sequentially with the rabbit anti-GluR ζ 1 antibody and goat anti-rabbit IgG conjugated to horseradish peroxidase with 3,3'-diaminobenzidine as substrate.

In the initial characterization of GluR ζ 1 expressed in mammalian cells, the total particulate fraction of the cell lysate was analyzed by immunoblotting using rabbit anti-GluR ζ 1 antibody. As shown in **Fig. 4**, a predominant band was observed in Vero cells infected with defective HSV vector containing GluR ζ 1 cDNA (dvGluR ζ 1). No predominant band was present in the cells mock-infected or infected with *LacZ* recombinant defective HSV-1.

Time-course analysis of GluR ζ 1 expression in Vero cells was performed. Vero cells were infected with dvGluR ζ 1 at an MOI of 1. **Figure 4** shows the time-course of immunodetected proteins expressed in dvGluR ζ 1-infected Vero cells. The size of the recombinant GluR ζ 1 protein expressed in dvGluR ζ 1-infected cells is ca. 120 kDa and is slightly greater than the calculated value (M_r of 103,477 after the removal of an amino-terminal signal peptide), suggesting that the apparent size difference may be owing to *N*-glycosylation of the protein, as is the case with AcNPV/GluR ζ 1-infected Sf21 cells (15–17). Expressed GluR ζ 1 was detectable 3 h postinfection and reached a maximum between 6 and 48 h post-infection (lanes 2–6).

4. Notes

1. Conventional manipulations of insect cells and baculoviruses were described in **refs. 31–33**.
2. Convenient kits for baculovirus expression system are available from Invitrogen, Pharmingen, Clontech, Novagen, or Gibco-BRL.
3. It is believed that 5'-untranslated region should be <100 bp for efficient expression.
4. It is believed that expression efficiency of recombinant viruses after several generations often decreases possibly because of the appearance of mutant viruses.
5. Our attempts to express the ϵ 4-subunit of the NMDA receptor channel with the baculovirus system were unsuccessful. The reason for this is unknown at present. Failure to express this subunit in *Xenopus* oocyte was also reported (39,40), and a likely reason, as Monyer et al. (40) suggested, may be the high GC content of ϵ 4 mRNA, particularly around and downstream of the translation initiation site.
6. We use temperature-sensitive tsK strain for helper virus to generate recombinant defective HSV-1 vector. The strain can amplify at 31°C, but not at 37°C. Therefore, when experiments are done at over 37°C, the effects of helper virus amplification can be neglected. Infection of cells by the tsK strain can be detected as the cytopathic effects (CPE) of cell rounding and cell fusion. Most of the tsK strains remain within the cells. Plaque assay of the resulting stock at a non-permissive temperature (37°C) demonstrated that the reversion of the temperature-sensitive helper virus tsK to wild-type virus was at a rate of <10⁻⁷/mL, consistent with previous observations. Defective virus titer was estimated from the ratio of amplicon/helper virus DNA.

Acknowledgments

The authors are grateful to Shigetada Nakanishi (Kyoto University) for providing them with the opportunity to present this chapter, Stephen M. Strittmatter (Yale University) for comments on the manuscript, and to Tomoko Ito for secretarial assistance. This work is supported by Grants-in-Aid from Ministry of Education, Science, Sports, and Culture of Japan.

References

1. Kawamoto, S., Onishi, H., Hattori, S., Miyagi, Y., Amaya, Y., Mishina, M., et al. (1991) Functional expression of the $\alpha 1$ subunit of the AMPA-selective glutamate receptor channel, using a baculovirus system. *Biochem. Biophys. Res. Commun.* **181**, 756–763.
2. Kawamoto, S. (1992) Functional expression of glutamate receptor (GluR) using the baculovirus gene expression system. *Yokohama Med. Bull.* **43**, 157–163.
3. Kawamoto, S., Hattori, S., Oiji, I., Ueda, A., Fukushima, J., Sakimura, K., et al. (1993) Expression of the $\alpha 1$ and $\alpha 2$ subunits of the AMPA-selective glutamate receptor channel in insect cells using a baculovirus vector. *Ann. NY Acad. Sci.* **707**, 460–462.
4. Kawamoto, S., Hattori, S., Oiji, I., Hamajima, K., Mishina, M., and Okuda, K. (1994) Ligand-binding properties and *N*-glycosylation of $\alpha 1$ subunit of the α -amino-3-hydroxy-5-methyl-4-isoxazole-propionate (AMPA)-selective glutamate receptor channel expressed in a baculovirus system. *Eur. J. Biochem.* **223**, 665–673.
5. Kawamoto, S., Uchino, S., Xin, K.-Q., Hattori, S., Hamajima, K., Fukushima, J., et al. (1997) Arginine-481 mutation abolishes ligand-binding of the AMPA-selective glutamate receptor channel $\alpha 1$ -subunit. *Mol. Brain Res.* **47**, 339–344.
6. Hattori, S., Okuda, K., Hamajima, K., Sakimura, K., Mishina, M., and Kawamoto, S. (1994) Expression and characterization of the $\alpha 2$ subunit of the α -amino-3-hydroxy-5-methyl-4-isoxazole propionate (AMPA)-selective glutamate receptor channel in a baculovirus system. *Brain Res.* **666**, 43–52.
7. Kawamoto, S., Hattori, S., Sakimura, K., Mishina, M., and Okuda, K. (1995) *N*-Linked glycosylation of the α -amino-3-hydroxy-5-methylisoxazole-4-propionate (AMPA)-selective glutamate receptor channel $\alpha 2$ subunit is essential for the acquisition of ligand-binding activity. *J. Neurochem.* **64**, 1258–1266.
8. Keinänen, K., Köhr, G., Seeburg, P. H., Laukkanen, M.-L., and Oker-Blom, C. (1994) High-level expression of functional glutamate receptor channels in insect cells. *Biotechnology* **12**, 802–806.
9. Kuusinen, A., Arvola, M., Oker-Blom, C., and Keinänen, K. (1995) Purification of recombinant GluR-D glutamate receptor produced in Sf21 insect cells. *Eur. J. Biochem.* **233**, 720–726.
10. Kuusinen, A., Arvola, M., and Keinänen, K. (1995) Molecular dissection of the agonist binding site of an AMPA receptor. *EMBO J.* **14**, 6327–6332.
11. Keinänen, K., Arvola, M., Kuusinen, A., and Johnson, M. (1997) Ligand recognition in glutamate receptors: Insights from mutagenesis of the soluble AMPA-binding domain of GluR-D. *Biochem. Soc. Trans.* **25**, 835–838.
12. Pickering, D. S., Taverna, F. A., Salter, M. W., and Hampson, D. R. (1995) Palmitoylation of the GluR6 kainate receptor. *Proc. Natl. Acad. Sci. USA* **92**, 12,090–12,094.
13. Ross, S. M., Taverna, F. A., Pickering, D. S., Wang, L.-Y., MacDonald, J. F., Pennefather, P. S., et al. (1994) Expression of functional metabotropic and ionotropic glutamate receptors in baculovirus-infected insect cells. *Neurosci. Lett.* **173**, 139–142.

14. Taverna, F. A. and Hampson, D. R. (1994) Properties of a recombinant kainate receptor expressed in baculovirus-infected insect cells. *Eur. J. Pharmacol.* **266**, 181–186.
15. Kawamoto, S., Uchino, S., Hattori, S., Hamajima, K., Mishina, M., Nakajima-Iijima, S., et al. (1995) Expression and characterization of the $\zeta 1$ subunit of the *N*-methyl-D-aspartate (NMDA) receptor channel in a baculovirus system. *Mol. Brain Res.* **30**, 137–148.
16. Sydow, S., Köpke, A. K. E., Blank, T., and Spiess, J. (1996) Overexpression of a functional NMDA receptor subunit (NMDAR1) in baculovirus-infected *Trichoplusia ni* insect cells. *Mol. Brain Res.* **41**, 228–240.
17. Uchino, S., Nakajima-Iijima, S., Okuda, K., Mishina, M., and Kawamoto, S. (1997) Analysis of the glycine binding domain of the NMDA receptor channel $\zeta 1$ subunit. *Nuroreport* **8**, 445–449.
18. Kawamoto, S., Hattori, S., Xin, K.-Q., Uchino, S., Fukushima, J., Hamajima, K., et al. (1996) Molecular and functional analyses of the glutamate receptor channel subunits expressed in baculovirus and herpesvirus vector systems. *Biochem. Soc. Trans.* **24(4)**, 567S.
19. Neve, R. L., Howe, J. R., Hong, S., and Kalb, R. G. (1997) Introduction of the glutamate receptor subunit 1 into motor neurons in vitro and in vivo using a recombinant herpes simplex virus. *Neuroscience* **79**, 435–447.
20. Bergold, P. J., Casaccia-Bonnetfil, P., Xiu-Liu, Z., and Federoff, H. J. (1993) Transsynaptic neuronal loss induced in hippocampal slice cultures by a herpes simplex virus vector expressing the GluR6 subunit of the kainate receptor. *Proc. Natl. Acad. Sci. USA* **90**, 6165–6169.
21. Casaccia-Bonnetfil, P., Stelzer, A., Federoff, H. J., and Bergold, P. J. (1995) A role for mossy fiber activation in the loss of CA3 and hilar neurons induced by transduction of the GluR6 kainate receptor subunit. *Neurosci. Lett.* **191**, 67–70.
22. During, M. J. (1995) HSV vectors in the mammalian brain: molecular analysis of neuronal physiology, generation of genetic models, and gene therapy of neurological disorders, in *Viral Vectors: Gene Therapy and Neuroscience Applications* (Kaplit, M. G. and Loewy, A. D., eds.), Academic, San Diego, pp. 89–107.
23. Sudo, M., Tsuzuki, K., Okado, H., Miwa, A., and Ozawa, S. (1997) Adenovirus-mediated expression of AMPA-type glutamate receptor channels in PC12 cells. *Mol. Brain Res.* **50**, 91–99.
24. Kammesheidt, A., Kato, K., Ito, K.-I., and Sumikawa, K. (1997) Adenovirus-mediated NMDA receptor knockouts in the rat hippocampal CA1 region. *Neuroreport* **8**, 635–638.
25. Shafron, D. R., Simpkins, C. E., Jebelli, B., Day, A. L., and Meyer, E. M. (1998) Reduced MK801 binding in neocortical neurons after AAV-mediated transfections with NMDA-R1 antisense cDNA. *Brain Res.* **784**, 325–328.
26. Hofmann, C., Sandig, V., Jennings, G., Rudolph, M., Schlag, P., and Strauss, M. (1995) Efficient gene transfer into human hepatocytes by baculovirus vectors. *Proc. Natl. Acad. Sci. USA* **92**, 10,099–10,103.

27. Sandig, V., Hofmann, C., Steinert, S., Jennings, G., Schlag, P., and Strauss, M. (1996) Gene transfer into hepatocytes and human liver tissue by baculovirus vectors. *Hum. Gene Ther.* **7**, 1937–1945.
28. Boyce, F. M. and Bucher, N. L. R. (1996) Baculovirus-mediated gene transfer into mammalian cells. *Proc. Natl. Acad. Sci. USA* **93**, 2348–2352.
29. Karpati, G., Lochmüller, H., Nalbantoglu, J., and Durham, H. (1996) The principles of gene therapy for the nervous system. *TINS* **19**, 49–54.
30. Slack, R. S. and Miller, F. D. (1996) Viral vectors for modulating gene expression in neurons. *Curr. Opinion Neurobiol.* **6**, 576–583.
31. Summers, M. D. and Smith, G. E. (1988) *A Manual of Methods for Baculovirus Vectors and Insect Cell Culture Procedures*, Texas Agricultural Experiment Station Bulletin No. 1555.
32. O'Reilly, D. R., Miller, L. K., and Luckow, V. A. (eds.) (1992) *Baculovirus Expression Vector, A Laboratory Manual*, W. H. Freeman and Company, New York.
33. Richardson, C. D. (ed.) (1995) *Baculovirus Expression Protocols, Methods in Molecular Biology*, vol. 39, Humana Press, Totowa, NJ.
34. Ho, D. Y. (1994) Amplicon-based herpes simplex virus vectors. *Methods Cell Biol.* **43**, 191–230.
35. Kaplitt, M. G. and Loewy, A. D. (eds.) (1995) *Viral Vectors: Gene Therapy and Neuroscience Applications*, Academic, San Diego.
36. Yamazaki, M., Mori, H., Araki, K., Mori, K. J., and Mishina, M. (1992) Cloning, expression and modulation of a mouse NMDA receptor subunit. *FEBS Lett.* **300**, 39–45.
37. Spaete, R. R. and Frenkel, N. (1982) The herpes simplex virus amplicon: A new eucaryotic defective-virus cloning amplifying vector. *Cell* **30**, 295–304.
38. Kaplitt, M. G., Pfaus, J. G., Kleopoulous, S. P., Hanlon, B. A., Rabkin, S. D., and Pfaff, D. W. (1991) Expression of a functional foreign gene in adult mammalian brain following *in vivo* transfer via a herpes simplex virus type 1 defective viral vector. *Mol. Cell. Neurosci.* **2**, 320–330.
39. Ishii, T., Moriyoshi, K., Sugihara, H., Sakurada, K., Kadotani, H., Yokoi, M., et al. (1993) Molecular characterization of the family of the *N*-methyl-D-aspartate receptor subunits. *J. Biol. Chem.* **268**, 2836–2843.
40. Monyer, H., Burnashev, N., Laurie, D. J., Sakmann, B., and Seeburg, P. H. (1994) Developmental and regional expression in the rat brain and functional properties of four NMDA receptors. *Neuron* **12**, 529–540.

Transient Expression of Functional NMDA Receptors in Mammalian Cells

Paul L. Chazot, Miroslav Cik, and F. Anne Stephenson

1. Introduction

The NMDA subtype of excitatory glutamate receptor is a multisubunit, fast-acting, ligand-gated cation channel with a high permeability for Ca^{2+} . NMDA receptors have been shown to be of importance in physiological processes, such as long-term potentiation, and also in pathophysiological conditions, including chronic neuronal degeneration and acute excitotoxicity (**1**). Molecular cloning has identified five genes encoding two types of NMDA receptor subunits, the NR1 and NR2A-D subunits. Additionally, the NR1 subunit gene undergoes alternative splicing to yield eight variant forms, thus providing further heterogeneity. The quaternary structures of NMDA receptors are not known, but most are believed to be heteromeric complexes comprising multiple copies of both NR1 and NR2 subunits in as-yet unknown stoichiometries (summarized in **1**). Since the absolute polypeptide compositions of native NMDA receptors are unknown, a convenient model system in which to study the properties of defined cloned NMDA receptor subtypes and thus to compare them with their *in vivo* counterparts is their expression in mammalian cells. This permits the pharmacological, functional and biochemical characterization of either a single type of NMDA receptor subunit or coexpression of combinations of NR1 and NR2 subunit genes (e.g., **2–4**). Furthermore, mutant NMDA receptors, created by site-directed mutagenesis, can be expressed in mammalian cells, and the properties of the wild-type and mutant receptors compared, thus yielding information relating to the importance of particular subunit amino acid residues to receptor structure and function, e.g., receptor subunit stoichiometry (**5**); receptor subcellular targeting (**6**); the importance of Ca^{2+} ion

permeability for cytotoxicity (7); the glutamate binding site (8); the glycine binding site (9); the voltage-dependent Mg^{2+} block site (10).

2. Materials

1. NMDA receptor cDNAs were subcloned in the mammalian expression vector, pCIS, a gift from Genentech, San Francisco, CA. Large-scale DNA plasmid preparations were then carried out using the Qiagen MAXI kit to give a final stock concentration of 1 mg DNA/mL.
2. 250-mL sterile flasks/ CO_2 incubator/sterile hood.
3. The growth media for human embryonic kidney (HEK) 293 cells is Dulbecco's Minimal Essential Media (DMEM)/F12 1:1 mixture supplemented with 10% (v/v) fetal calf serum (FCS), 500 IU/mL penicillin, 50 μ g/mL streptomycin, 3.0 g/L sodium hydrogen carbonate, pH 7.6, and glutamine. Following transfection, HEK 293 cells are grown in the same media, but importantly without glutamine.
4. For subculturing, use standard Hank's buffered salt solution (HBSS), containing sodium carbonate, but without calcium chloride and magnesium sulfate, and trypsin-EDTA, which is 0.5% (w/v) trypsin and 0.2% (w/v) EDTA in HBSS. Both reagents are from Sigma, Poole, Dorset, UK.
5. 10 mM Tris EDTA (TE buffer), pH 8.0, diluted 1:10 with H_2O (1:10 TE).
6. 2X *N*-2-hydroxyethylpiperazine-*N'*-2-ethane sulfonic acid (HEPES) buffered saline (2X HBS), which is: 50 mM HEPES, pH 7.12, 280 mM NaCl, 1.1 mM sodium hydrogen phosphate.
7. 2.5 M Calcium chloride in sterile water.
8. Phosphate-buffered saline (PBS): 4 mM disodium hydrogen phosphate, 1.7 mM potassium dihydrogen phosphate, pH 7.4, 137 mM NaCl, 107 mM KCl.
9. 15% (v/v) Glycerol in PBS.
10. 50 mM Tris, pH 7.4, 5 mM EDTA, 5 mM EGTA.
11. Routinely, HEK 293 cells are grown in DME/F12 media containing glutamine in 250-mL flasks in a sterile incubator at 37°C with a CO_2 content of 5%. They are subcultured every 2–3 d with each 250-mL flask divided into four fresh 250-mL flasks.

3. Methods

All procedures are performed in a sterile hood.

1. On the day before transfection, HEK 293 cells grown to 90% confluence should be removed from 1 \times 250 mL flask and subcultured in 4 \times 250 mL flasks. Remove media from flask, and superficially wash the cells with HBSS buffer, preheated to 37°C. Apply 2 mL trypsin-EDTA, also preheated to 37°C, and incubate for 1 min at 37°C. Dilute with 10 mL DME/F12 containing glutamine media, and re-suspend the cells carefully in a pipet until a suspension of single cells is achieved. Apply 3 mL of this suspension to a fresh 250-mL flask, supplement with 9 mL DME/F12-containing glutamine cell-culture media, and incubate at 37°C in 5% CO_2 . On the day of transfection, the cells should then be approx 50% confluent.

- Three hours before transfection, change the cell-culture media to fresh DME/F12 minus glutamine (10 mL/flask), and increase the CO₂ to 7.5%. This latter step is important, and it ensures that the media is pH 7.3–7.4 at the moment of transfection.
2. Thirty minutes prior to transfection, prepare the following in Eppendorf tubes.
 - a. Sample 1: For single NMDA receptor subunit expression, 440 μ L 1:10 TE buffer + 10 μ L plasmid DNA (10 μ g). For the coexpression of two NMDA receptor subunits with a DNA ratio of 1:3, 440 μ L 1:10 TE buffer + 2.5 μ L plasmid DNA 1 + 7.5 μ L plasmid DNA 2 (10 μ g total), or for a DNA ratio 1:10, 430 μ L 1:10 TE buffer + 2 μ L plasmid DNA 1 + 18 μ L plasmid DNA 2 (20 μ g total). For the coexpression of three NMDA receptor subunits with a DNA ratio of 1:3:3, 432.5 μ L 1:10 TE buffer + 2.5 μ L plasmid DNA 1 + 7.5 μ L plasmid DNA 2 + 7.5 μ L plasmid DNA 3 (17.5 μ g total).
 - b. Sample 2: 500 μ L 2 \times HBS. Pre-warm the sterile 2.5 M CaCl₂ solution to 37°C.
 3. To commence the transfection, add 50 μ L CaCl₂ dropwise into tube 1, shake vigorously by hand for 15 s, and then apply dropwise (1 drop/5 s) with a 2-mL sterile pipet to tube 2. When all the liquid has been added, mix with a sterile pipet, and apply evenly to the surface of a flask of subcultured HEK 293 cells. Gently swirl the flask, and observe under a microscope. A fine precipitate should be visible almost immediately, and it will continue to develop more clearly within 1 h. Return the flask to the incubator for 3 h and maintain the level of CO₂ at 7.5%.
 4. Carry out a glycerol shock of the HEK 293 cells being transfected to increase the efficiency of transfection. Prewarm the glycerol/PBS solution and DME/F12 minus glutamine cell-culture media to 37°C. Remove the cell-culture media from the flask containing the transfected cells by aspiration with a sterile pipet. Carefully add 1.5 mL glycerol/PBS to the cells with swirling for 30 s. Remove the glycerol by aspiration, and superficially rinse the cells with 5 mL DME/F12 minus glutamine cell-culture media. Then, add 10 mL fresh DME/F12 minus glutamine media, containing if required 1 mM ketamine (*see Note 4*). Examine the cells under the microscope to ensure that they are still attached to the flask. Return to the incubator, now adjusted to 5% CO₂, and leave the transfected cells to grow for 24 h.
 5. To harvest the transfected cells, scrape them from the surface of the flask, and centrifuge at 1000g for 5 min. Decant the supernatant and homogenize the cell pellet with a dounce glass/glass homogenizer (at least 10 strokes) on ice in 50 mM Tris-HCl, pH 7.4, containing 5 mM EDTA and 5 mM EGTA (50 mL/flask). Centrifuge the homogenate at 50,000g for 30 min at 4°C. Repeat this washing procedure, and resuspend the final pellet in 2 mL homogenization buffer/flask. The yield of protein is approx 1 mg/flask. The washed cell homogenate can now be assayed for radioligand binding activities, including the effect of allosteric effectors thereon. Radioligands that have been used include: for the glutamate binding site, [³H] CGP 39653 (**3**), for the channel gating site, [³H] MK801 (**4**), and for the glycine binding site, [³H] glycine, [³H] L 689,560 (**11**), [³H] 5,7 dichlorokynurenic acid (DKA; **12**), and [³H] MDL 105,519 radioligand binding activities (**13**).

6. For the measurement of cell cytotoxicity following transfection, 24 h post-transfection, remove 50 μL of cell-culture supernatant from a flask containing transfected cells, dilute 1:10 with media, transfer to a 96-well enzyme-linked immunoadsorbent assay (ELISA) plate, and assay for lactate dehydrogenase (LDH) activity using the Promega Cytotox 96™ kit (7). Cell cytotoxicity is expressed as the percentage of LDH activity found in the supernatant with respect to the total LDH activity. Total LDH activity is measured by freeze/thaw lysing the transfected cells, collecting the resultant media, and assaying for LDH activity using the Promega Cytotox 96™ kit as above. Corrections for spontaneous LDH release, phenol red, and endogenous LDH in the cell culture media were made by the measurement of LDH activity in media taken from a flask of untransfected cells.

4. Notes

1. The method described is that which is in routine use in our laboratory using HEK 293 cells, the mammalian expression vector pCIS, which utilizes the cytomegalovirus promoter, and cell transfection using the calcium phosphate method. HEK 293 cells are the mammalian cell line of choice for both the transient and stable expression of many ligand-gated ion channels. This is because they are both fast-growing with a doubling time of 24 h in DME/F12 plus glutamine media (but note that cell growth is reduced following transfection and culturing in DME/F12 minus glutamine), and they form gap junctions, which is advantageous for electrophysiological characterization. It should be noted that other cell lines and transfection methods have been used for both transient and stable expression of functional NMDA receptors and include, e.g., lipofectamine and electroporation methods in CHO and Ltk-cells, respectively (14,15). The pCIS mammalian expression vector was used owing to its compatibility with HEK 293 cells, but others are appropriate and available commercially. If possible, the subcloning strategy should excise as much as feasible of the 5'- and 3'-noncoding DNA of the NMDA receptor subunit clones. It has been shown that the untranslated 5'- and 3'-ends of the NMDA receptor clones can inhibit the levels of subunit expression (16). The quality of the plasmid DNAs used for the transfections is important. Plasmid preparations should have an optical density ratio $\text{OD}_{\lambda=260\text{nm}}/\text{OD}_{\lambda=280\text{nm}} = 1.8\text{--}2.0$.
2. When using two or more clones for transfection, we have found that optimal expression is dependent on the ratios of the plasmid DNAs used for transfection. Thus, for one or two subunit clones, maximal expression is achieved with 10 μg DNA with a 1:3 ratio for pCISNR1-1a:pCISNR2A yielding the highest level of [^3H] MK801 radioligand binding activity (17). Other ratios that we routinely use are 1:3 for pCISNR1-1a:pCISNR2B, 1:10 for pCISNR1-1a:pCISNR2C, and for the three subunit combination pCISNR1-1a:pCISNR2A:pCISNR2C, 1:3:3, the latter using a total DNA of 17.5 μg .
3. A high efficiency of transfection is critically dependent on both the care with which the CaCl_2/DNA solution is applied to the 2X HBS solution for the forma-

tion of a fine precipitate and the glycerol shock, which must be performed carefully since the cells can easily detach from the flasks in this step.

4. In early studies, we used 400 μM DL-2-amino-5-phosphonopentanoic acid (DL-AP5) to protect from receptor-mediated cell cytotoxicity post-transfection. However, now, we routinely use 1 mM ketamine. This is preferred because of ready solubility, ease of removal prior to radioligand binding assays, and low cost. Alternative effective protective conditions include a combination of 400 μM DL-AP5/400 μM DKA or 1 μM MK801.
5. Because of cytotoxicity problems following the expression of NMDA receptors in HEK 293 cells, it was necessary to establish the earliest time-point at which receptor expression was maximal. These results are shown in **Fig. 1**. It was found that 24 h post-transfection was the optimal time-point for the expression of functional NMDA receptors. Beyond this, the appearance of unprocessed, i.e., non-N-glycosylated, NR1-subunit is evident. [^3H] MK801 binding activity starts to decrease from maximal levels 62 h posttransfection (**17**).
6. We found that the expression of certain NMDA receptor subunit combinations, i.e., NR1-1a/NR2A, NR1-1a/NR2B, and NR1-1a/NR2A/NR2C, but not NR1-1a/NR2C, results in cell death. This was thought to be caused by an increase in intracellular Ca^{2+} following activation of the cloned NMDA receptors expressed in the HEK 293 cells by L-glutamate and glycine present in the cell-culture media. Cell death post-transfection can be prevented by the inclusion of various NMDA receptor antagonists in the cell-culture media. We have developed the use of the cytotoxicity assay to assess the functional expression of different NMDA receptor subtypes, to demonstrate that cell death is owing in part to an influx of extracellular Ca^{2+} by the inclusion of EGTA in the cell-culture media and also to assess the efficacy of different classes of NMDA receptor antagonists. Some of these results are summarized in **Fig. 2**.
7. The calcium phosphate transfection method described here gave transfection efficiencies in the range of 20–30%. Transfection efficiency was determined initially by cotransfection of NMDA receptor clones with pSV β -galactisidase (Promega Ltd., Southampton, UK). The percentage cell death following the coexpression of NR1-1a and NR2A clones was equal to the transfection efficiency. Thus percentage cytotoxicity can also be used as a measure of transfection efficiency. Alternatively, cotransfection with a plasmid containing the green fluorescent protein (GFP) cDNA may be used. The latter is particularly useful for electrophysiological studies where, in contrast to staining for β -galactisidase activity where cells must first be fixed, viable transfected cells can be identified.
8. The method described here has concentrated on the transfection of HEK 293 cells in 250-mL flasks for subsequent characterization by radioligand binding, cytotoxicity, and immunochemical assays. When the functional properties of the cloned receptors are to be studied by either electrophysiological methods or Ca^{2+} -flux assays using fura-2, fewer cells are required. Transfections are then carried out exactly as above, except that after the glycerol shock stage, the cells

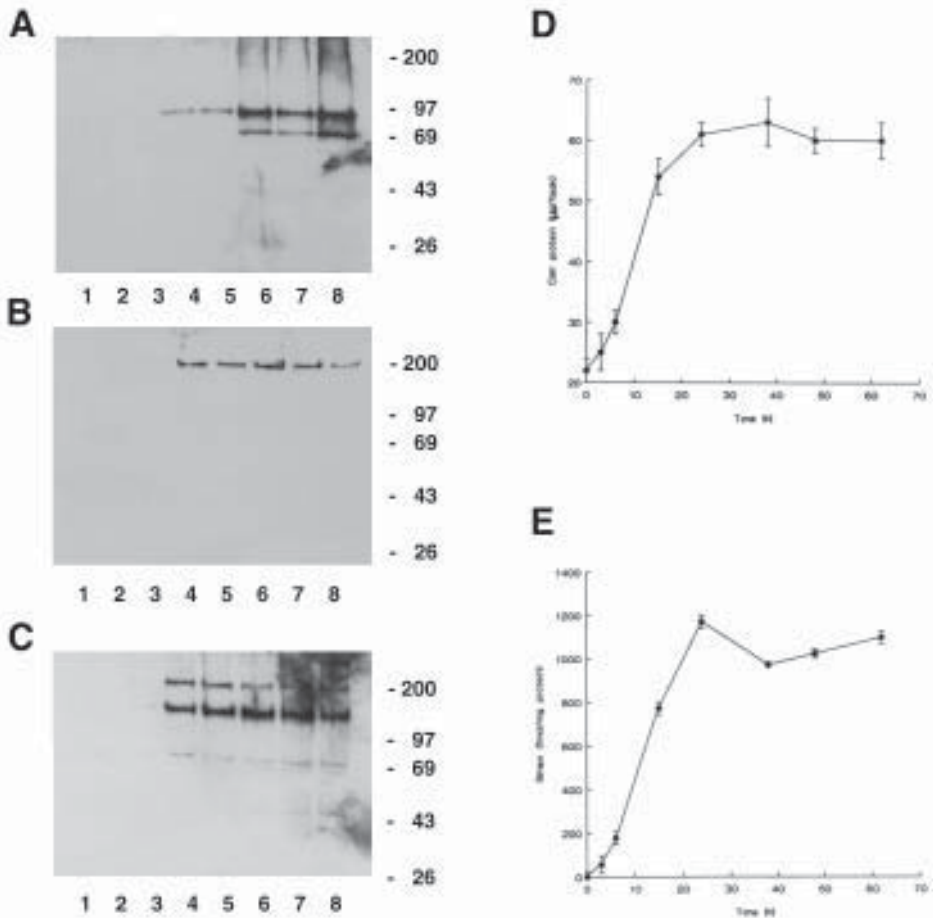


Fig. 1. The time-course for the expression of NMDA receptor subunit clones following their transfection in HEK 293 cells. HEK 293 cells were transfected with NMDA receptor subunit clones by the calcium phosphate method and cultured in the presence of AP5. Transfected cells were harvested at 0, 3, 6, 15, 24, 38, 48, and 62 h, and analyzed by immunoblotting, for total protein and for [³H] MK801 radioligand binding activity. **A–C** are immunoblots where **A** is transfection with pCISNR1-1a alone; **B** is transfection with pCISNR2A, and **C** is for cells transfected with pCISNR1-1a and pCISNR2A combined. **D** shows the time-course for cell protein concentration post-transfection, and **E**, [³H] MK801 radioligand binding activity post-transfection where **D** and **E** are transfections with both pCISNR1-1a and pCISNR2A.

are trypsinized as described (Methods 1) and then transferred onto poly-D-lysine-coated CELLOctate cover slips. These are then incubated in 90-mm Petri dishes overlaid with cell-culture media at 37°C in 5% CO₂ (18).

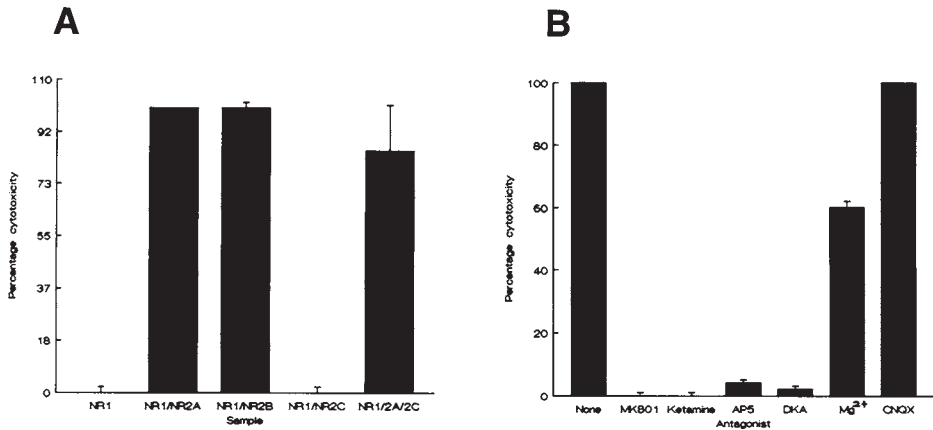


Fig. 2. Cell cytotoxicity, a novel assay for the expression of functional NMDA receptors. **(A)** The effect of the expression of different NMDA receptor subtypes on cytotoxicity post-transfection. HEK 293 cells were transfected with different combinations of NMDA receptor subunit clones as shown. Cells were harvested 20 h post-transfection and the percentage cell death determined by the measurement of LDH activity using the Promega Cytotox 96™ kit (Promega, Madison, WI). The results are expressed with respect to the expression of the NR1/NR2A, which results in 100% death of transfected cells, and they are the means \pm SD for three separate transfection experiments. Note that the expression of the respective NMDA receptor subunits was verified by immunoblotting using the appropriate specificity antibodies. **(B)** A comparison of the protection of NMDA receptor-mediated cytotoxicity post-transfection by different classes of NMDA receptor antagonist. HEK 293 cells were transfected with pCISNR1-1a and pCISNR2A, and then cultured in the absence and presence of the NMDA receptor antagonists, MK801 (1 μ M), ketamine (1 mM), DL-AP5 (1 mM), 5,7 DKA (1 mM), magnesium chloride (20 mM), and the non-NMDA receptor antagonist 6-cyano-7-nitroquinoxaline-2,3-dione (CNQX) (200 μ M). Cells were collected 20 h post-transfection and the percentage cytotoxicity measured as before. Results are expressed as the percentage cell death compared to NR1-1a/NR2A, which is 100%, and they are the means \pm SD for three separate transfections.

- Work in our laboratory has concentrated on the radioligand binding and biochemical properties of the cloned NMDA receptors expressed transiently in HEK 293 cells. With a transfection efficiency of 20–30%, 1 pmol [³H] MK801 specific binding sites/mg protein was expressed, which corresponds to 200,000 binding sites/transfected cell. The expression of the NMDA receptor subunits is monitored by immunoblotting using the appropriate specificity antibodies (e.g., 4,19). The coassembly of the expressed subunits can be demonstrated by quantitative immunoprecipitation again using the appropriate antibodies (e.g., 4). Note that NMDA receptors expressed in HEK 293 cells are more readily solubilized under

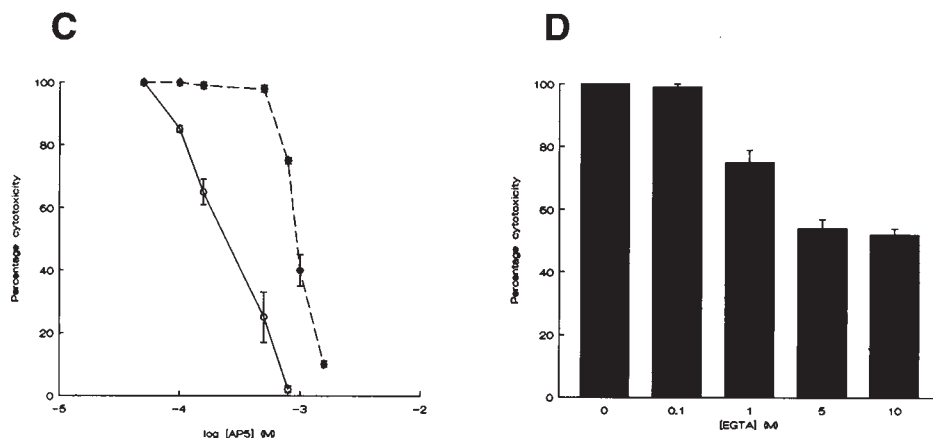


Fig. 2. (continued) **(C)** Comparison of the concentration dependence of DL-AP5 for the protection against cytotoxicity post-transfection following expression of NR1-1a/NR2A and NR1-1a/NR2B receptor subtypes. HEK 293 cells were transfected with pCISNR1-1a/pCISNR2A and pCISNR1-1a/pCISNR2B clones and then cultured in the presence of increasing concentrations of DL-AP5. Transfected cells were collected 20 h post-transfection, and the percentage cell death was determined by measurement of LDH release as before. The results show the dose dependencies for the protection against cell death for NR1-1a/NR2A (o) and NR1-1a/NR2B (•) with the EC_{50} values determined as 200 ± 50 and $900 \pm 100 \mu M$, respectively. This 4.5-fold difference in efficacy between the subtypes is in agreement with their threefold difference in affinity for DL-AP5 as determined by radioligand binding assays. **(D)** Demonstration that NMDA receptor-mediated cytotoxicity post-transfection is owing in part to influx of extracellular Ca^{2+} . HEK 293 cells were cotransfected with pCISNR1-1a and pCISNR2A, and subsequently cultured in the presence of increasing concentrations of the calcium chelator, EGTA, before cell harvesting at 20 h post-transfection. Cytotoxicity was measured as before, and the results are expressed as the percentage cell death compared to NR1-1a/NR2A, which was defined as 100%. A maximal protection against cytotoxicity posttransfection of 50% was achieved by 10 mM EGTA, thus demonstrating that the cytotoxicity is owing in part to influx of extracellular Ca^{2+} .

nondenaturing conditions than NMDA receptors expressed in neuronal tissue, since the NMDA receptor-associated proteins, such as PSD-95, are not expressed in these cells. The molecular size of the expressed receptors can be determined by gel filtration (20).

- Cell-surface expression can be demonstrated by immunocytochemistry using N- and C-terminal-directed anti-NR1 antibodies, under permeabilizing and non-permeabilizing conditions (21). The importance of *N*-glycosylation can be investigated by growing the transfected cells in the presence of tunicamycin (0.5 $\mu g/mL$ media). Using such an approach, we have shown that *N*-glycosylation

is not required for cell-surface expression, but it is important for the correct assembly of functional NMDA receptors (21).

Acknowledgments

The authors would like to thank Drs. S. Nakanishi and M. Mishina for generously supplying the NMDA receptor subunit cDNAs. We also thank Sarah Coleman for her contribution to the experiments described herein. The work described in this chapter was funded by the BBSRC (UK).

References

1. Sucher, N., Awobuluyi, M., Choi, Y-B., and Lipton, S. A. (1996) NMDA receptors: from genes to channels. *TIPS* **17**, 348–355.
2. Buller, A. L., Larson, H. H., Schneider, B. E., Beaton, J. A., Morrisett, R. A., and Monaghan, D. T. (1994) The molecular basis of NMDA receptor subtypes: native receptor diversity is predicted by subunit composition. *J. Neurosci.* **14**, 5471–5484.
3. Laurie, D. J. and Seeburg, P. H. (1994) Ligand binding affinities at recombinant *N*-methyl-D-aspartate receptors depend on subunit composition. *Eur. J. Pharmacol.* **268**, 335–345.
4. Chazot, P. L., Coleman, S. K., Cik, M., and Stephenson, F. A. (1994) Molecular characterisation of *N*-methyl-D-aspartate receptors expressed in mammalian cells yields evidence for the coexistence of three subunit types within a discrete receptor molecule. *J. Biol. Chem.* **269**, 24,403–24,409.
5. Behe, P., Stern, P., Wyllie, D. J., Nassar, M., Schoepfer, R., and Colquhoun, D. (1995) Determination of NMDA R1 subunit copy number in recombinant NMDA receptors. *Proc. R. Soc. Lond. B.* **262**, 205–213.
6. Ehlers, M. D., Tingley, W. G., and Haganir, R. L. (1995) Regulated subcellular distribution of the NR1 subunit of the NMDA receptor. *Science* **269**, 1734–1737.
7. Cik, M., Chazot, P. L., and Stephenson, F. A. (1994) Expression of NMDAR1-1A (N598Q)/NMDAR2A receptors results in decreased cell mortality. *Eur. J. Pharmacol.* **266**, R1–R3.
8. Laube, B., Hirai, H., Sturgess, M., Betz, H., and Kuhse, J. (1997) Molecular determinants of agonist discrimination by NMDA receptor subunits. *Neuron* **18**, 493–503.
9. Kuryatov, A., Laube, B., Betz, H., and Kuhse, J. (1994) Mutational analysis of the glycine-binding site of the NMDA receptor. *Neuron* **12**, 1291–1300.
10. Mori, H. H., Masaki, T., Yamakura, T., and Mishina, M. (1992) Identification by mutagenesis of a Mg²⁺-block site of the NMDA receptor channel. *Nature* **358**, 673–675.
11. Grimwood, S., LeBourdelle, B., and Whiting, P. J. (1995) Recombinant human NMDA homomeric NR1 receptors expressed in mammalian cells form a high-affinity glycine antagonist binding site. *J. Neurochem.* **64**, 525–530.
12. Lynch, D. R., Anegawa, N. J., Verdoorn, T., and Pritchett, D. B. (1994). *N*-Methyl-D-aspartate receptors: Different subunit requirements for binding of glutamate

- antagonists, glycine antagonists, and channel-blocking agents. *Mol. Pharmacol.* **45**, 540–545.
13. Chazot, P. L., Reiss, C., and Stephenson, F. A. (1997) [³H] MDL 105,519, a novel antagonist for the glycine site of the NMDA receptor *Br. J. Pharmacol.* (Suppl.) **119**, C39.
 14. Brimecombe, J. C., Boeckman, F. A., and Aizenman, E. (1997) Functional consequences of NR2 subunit composition in single recombinant *N*-methyl-D-aspartate receptors. *Proc. Natl. Acad. Sci. USA* **94**, 11,019–11,024.
 15. Varney, M. A., Jahec, C., Deal, C., Hess, S. D., Daggett, R., Skvoretz, R., et al. (1996) Stable expression and characterisation of recombinant human heteromeric *N*-methyl-D-aspartate receptor subtypes NMDAR1A/2A and NMDAR1A/2B in mammalian cells. *J. Pharm. Exp. Ther.* **279**, 367–378.
 16. Wood, M. W., VanDongen, H. M. A., and Vandongen, A. M. J. (1996) The 5'-untranslated region of the *N*-methyl-D-aspartate receptor NR2A subunit controls efficiency of translation. *J. Biol. Chem.* **271**, 8115–8120.
 17. Cik, M., Chazot, P. L., and Stephenson, F. A. (1993) Optimal expression of cloned NMDAR1/NMDAR2A heteromeric glutamate receptors: a biochemical characterisation. *Biochem. J.* **296**, 877–883.
 18. Stern, P., Cik, M., Colquhoun, D., and Stephenson, F. A. (1994) Single-channel properties of cloned NMDA receptors in a human cell line: comparison with results from *Xenopus* oocytes. *J. Physiol.* **476**, 391–397.
 19. Chazot, P. L., Cik, M., and Stephenson, F. A. (1992) Immunological detection of the NMDAR1 glutamate receptor expressed in human embryonic kidney 293 cells and in rat brain. *J. Neurochem.* **59**, 1176–1178.
 20. Chazot, P. L. and Stephenson, F. A. (1997) Biochemical evidence for the existence of a pool of unassembled C2 exon-containing NR1 subunits of the mammalian fore-brain NMDA receptor. *J. Neurochem.* **68**, 507–516.
 21. Chazot, P. L., Cik, M., and Stephenson, F. A. (1995) An investigation into the role of *N*-glycosylation in the functional expression of a recombinant heteromeric NMDA receptor. *Mol. Membr. Biol.* **12**, 331–337.

Stable Expression of Human NMDA Receptors in Cultured Mammalian Cells

Mark A. Varney, Fen-Fen Lin, Christine Jachec, Sara P. Rao, Stephen D. Hess, Edwin C. Johnson, and Gönül Veliçelebi

1. Introduction

NMDA receptors are ligand-gated cation channels that are activated by glutamate and glycine. They are distributed throughout the mammalian CNS, and play an important role in normal development and plasticity of the CNS, and likely in such specialized functions as memory and learning. Prolonged activation of these channels has been implicated in several pathophysiological conditions, such as stroke and epilepsy. Therefore, NMDA receptors represent relevant molecular targets for therapeutic agents in the treatment of stroke, epilepsy, head trauma, and pain (1–3).

There is mounting evidence that NMDA receptors are heteromeric complexes composed of NMDAR1 and NMDAR2 (A, B, C, or D) subunits (4). Each of the mRNAs encoding these subunits has a distinct anatomical distribution (5), and coexpression of different combinations of these subunits results in channels with unique biophysical and pharmacological properties (6). Subtype-selective agonists, antagonists, and modulators of NMDA receptors can be valuable pharmacological tools in understanding the physiological roles of specific NMDA receptor subtypes. These pharmacological agents can also be used to elucidate the involvement of the specific subtypes in the development of particular pathophysiological conditions and can be further developed as therapeutic agents.

One method of discovering compounds selectively acting on specific NMDA receptor subtypes is random screening of compound libraries for functional activity on cell lines expressing recombinant NMDA receptor subunits in different combinations. To this end, we cloned cDNAs encoding human NMDA receptor 1A (hNMDAR1A), 2A (hNMDAR2A), 2B (hNMDAR2B),

2C (hNMDAR2C), and 2D (hNMDAR2D) subunits (7–10), and confirmed transient expression of hNMDAR1A/2A, hNMDAR1A/2B, hNMDAR1A/2C, and hNMDAR1A/2D receptor complexes in both *Xenopus* oocytes and HEK293 cells by demonstration of agonist-induced inward currents. Subsequently, we established stable expression of the hNMDAR1A/2A and hNMDAR1A/2B complexes in L(tk⁻) (11) and HEK293 cells, and demonstrated a functional response to glutamate and glycine by measurement of agonist-induced elevation in cytosolic free calcium ([Ca²⁺]_i). Next, we validated the pharmacological properties of the agonist-induced [Ca²⁺]_i signal in the stable clonal cell lines using reference agonists and antagonists. Finally, we established these cell lines as stable targets to screen compounds for their ability to activate directly the NMDA receptors, or inhibit or potentiate glutamate/glycine-induced activation of the NMDA receptors.

We demonstrated stable expression of hNMDAR1A/2A and hNMDAR1A/2B receptors in two different host cells using two different expression vectors: (1) mouse L(tk⁻) fibroblasts using an inducible expression vector with a glucocorticoid-inducible promoter (pMMTV), and (2) HEK293 cells using an expression vector with a constitutive promoter (pCMV). The complete functional and pharmacological characterization of the L(tk⁻)-derived L238-491-26 cells expressing hNMDAR1A/2A and L334-12-17 cells expressing hNMDAR1A/2B has recently been described in detail (11). Therefore, we will focus here on the detailed description of the experimental methods involved in the establishment of stable expression of human NMDAR1A/2A and NMDAR1A/2B receptors in HEK293 cells.

2. Materials

2.1. Reagents and Supplies Used in Tissue Culture

1. Human embryonic kidney (HEK293) cells were obtained from G. Wahl, The Salk Institute (La Jolla, CA). This cell line is also available from American Type Culture Collection (Manassas, VA, cat. no. ATCC CRL 1573).
2. Stock poly-D-lysine solution: Suspend 25 mg of 30,000–70,000 mol wt poly-D-lysine (Fluka, Ronkonkoma, NY, cat. no. 81358) in 250 mL of autoclaved deionized H₂O (dH₂O) to give a final concentration of 0.1 mg/mL. The poly-D-lysine solution may be stored at -20°C for up to 1 month.
3. Tissue-culture dishes (10 cm²) were purchased from Nalgene Nunc (Rochester, NY, cat. no. 150350) and coated with poly-D-lysine as follows: Dilute stock poly-D-lysine solution fourfold, pipet 5 mL into each plate, and swirl to cover the entire bottom of the dish. Incubate for 30–60 min at room temperature. Remove the poly-D-lysine solution completely by aspiration, and wash twice with 5 mL sterile dH₂O. Remove the dH₂O, and dry the plates in a hood. Coated plastic plates can be stored at 4°C for up to 3 wk.
4. Twenty-four-well cell-culture clusters (Costar, Cambridge, MA, cat. no. 3524).

5. Six-well clusters (Costar, cat. no. 3506).
6. Dulbecco's Modified Eagle's Medium (DMEM, Gibco-BRL, Gaithersburg, MD, cat. no. 11965-092).
7. DMEM without L-glutamine (Gibco-BRL, cat. no. 11960-044).
8. Bovine calf serum (HyClone, Logan, VT, cat. no. SH30072.03).
9. Fetal bovine serum, dialyzed (Gibco-BRL, cat. no. 26300-061).
10. Stock solution of L-glutamine (200 mM solution, Gibco-BRL, cat. no. 25030-081).
11. Stock solution of penicillin-streptomycin (contains 10,000 U/mL of penicillin and 10 mg/mL of streptomycin, Gibco-BRL, cat. no. 15140-122).
12. Stock ketamine solution: Dissolve 2.06 g of ketamine (Research Biochemicals International, Natick, MA, cat. no. K-101) in sterile 25 mL dH₂O (300 mM), and filter through a 0.22- μ m syringe filter. Divide into 0.6-mL aliquots, and store frozen at -70°C for up to 3 mo.
13. Stock solution of Geneticin (G418 sulfate, Gibco-BRL, cat. no. 11811-031) dissolved in DMEM at a concentration of 50 mg/mL active form.
14. Phosphate-buffered saline (PBS) (Gibco-BRL, cat. no. 10010-023): 137 mM NaCl, 2.7 mM KCl, 10 mM Na₂HPO₄, 1.7 mM KH₂PO₄, pH 7.4.
15. Phenol red (0.5%): Dissolve 0.5 g of phenol red (Sigma Chemical Co., St. Louis, MO, cat. no. P-4633) in 100 mL PBS, and filter through a 0.22- μ m filter system (Corning, Boston, MA, cat. no. 430767).
16. Trypsin/EDTA solution: Add 50 mL of 10X-trypsin/EDTA (Gibco-BRL, cat. no. 15400-054) and 2 mL of 0.5% sterile phenol red to 450 mL of PBS. Divide into 30-mL aliquots, and store frozen at -20°C for up to 6 mo.

2.2. Reagents and Supplies Used for Transfections

1. Twofold concentrated HEPES 42 mM HEPES-free acid (Calbiochem, La Jolla, CA, cat. no. 391338), 74 mM NaCl, pH to 7.10 \pm 0.05.
2. One hundred-fold concentrated phosphate buffer (100X PO₄): Mix 70 mM Na₂HPO₄ with 70 mM NaH₂PO₄ at 1:1 ratio.
3. 2 M CaCl₂: Dissolve 58.8 g CaCl₂ · 2H₂O in 200 mL dH₂O.
4. Solution A: Mix 0.5 mL of 2X HEPES and 10 μ L of 100X PO₄ in a 15-mL polypropylene tube.
5. Solution B: Mix 0.44 mL of dH₂O containing the specified amount of DNA and 60 μ L of 2 M CaCl₂ in a 15-mL polypropylene tube.

2.3. Intracellular Calcium ([Ca²⁺]_i) Measurements

1. HEPES-buffered saline (HBS): 20 mM HEPES, 125 mM NaCl, 5 mM KCl, 0.62 mM MgSO₄, 1.8 mM CaCl₂, 6 mM glucose, pH 7.4.
2. A solution of fluo-3-acetoxymethyl ester (fluo-3-AM) (Molecular Probes, Inc., Eugene, OR) prepared as follows: To a 50- μ g vial of fluo-3-AM, add 30 μ L dimethylsulfoxide (DMSO) and 15 μ L pluronic F127 (20% wt/vol in DMSO, Molecular Probes, Inc.). Dissolve this mixture in 4.4 mL of HBS, resulting in a final concentration of 10 μ M fluo-3-AM.

3. 96-Well microtiter plates ((Nalgene Nunc, cat. no. 25382-342) were coated with poly-D-lysine as follows: Pipet 50 μ L of stock poly-D-lysine solution into each well, and incubate for 30–60 min at room temperature. Remove the poly-D-lysine solution completely by aspiration, and wash twice with 100 μ L of sterile dH₂O. Remove the dH₂O, and dry the plates in a hood. Coated plastic plates can be stored at 4°C for up to 3 wk.

2.4. [¹²⁵I]-MK-801 Binding

1. Tris-EDTA buffer: 10 mM Tris-HCl containing 10 mM EDTA, pH 7.4, at 4°C.
2. Protein assay kit (Bio-Rad, Richmond, CA, cat. no. 500-0112).
3. Binding assay buffer: 20 mM HEPES containing 1.0 mM EDTA, pH 7.4.
4. [¹²⁵I]-MK-801 (DuPont NEN, Boston, MA, cat. no. NEX-265, 0.25 mCi/mL, SA 2200 Ci/mmol).
5. (+)-MK-801 hydrogen maleate (Research Biochemicals International, cat. no. M-107).
6. Whatman GF/C filters (Brandel, Gaithersburg, MD, cat. no. FPB-248).
7. Polyethylenimine (Sigma Chemical Co., St. Louis, MO, cat. no. P3143).
8. 96-Well deep-well plates (Beckman, Fullerton, CA, cat. no. 140504).

2.5. Equipment Used in Tissue Culture

1. Tissue-culture hood.
2. CO₂ incubator.
3. Inverted phase-contrast microscope.
4. Water bath.
5. Freezers (–70 and –20°C).

2.6. Equipment Used for Molecular Biology

1. Electrophoresis apparatus and power supply.
2. Polaroid camera equipped with an ethidium bromide filter.
3. Water bath.
4. Benchtop microcentrifuge and refrigerated ultracentrifuge.
5. Microwave oven.

2.7. Equipment for Intracellular Calcium ([Ca²⁺]_i) Measurements

A 96-well plate-reading fluorimeter (Cambridge Technical Instruments, Inc., Watertown, MA), equipped with an excitation filter with a bandpass of 485 \pm 20 nm and an emission filter with a bandpass of 530 \pm 20 nm.

2.8. Equipment Used for [¹²⁵I]-MK-801 Binding

1. Sorvall centrifuge with SS 34 rotor.
2. Benchtop centrifuge.
3. Cell harvester (Brandel).
4. Tight-fitting Teflon-glass homogenizer.
5. Polytron (Brinkman, Westbury, NJ).

6. γ -Radioactivity counter (or β -scintillation counter).
7. ELISA reader for protein assays.

3. Methods

3.1. Construction of Expression Vectors Encoding Human NMDAR Subunits

The cDNAs encoding the human NMDA receptor subunits were isolated as described elsewhere (8).

1. Construct the expression plasmids, pCMV-T7-2 and pCMV-T7-3, containing the constitutive CMV promoter by modification of pCMV β (Clontech, Palo Alto, CA, cat. no. 6177-1). More specifically, remove the *lacZ* gene, add the T7 RNA polymerase promoter, and expand the polylinker region.
2. Subclone the full-length hNMDAR1A cDNA as a 4.3-kb *EcoRI* fragment into the unique *EcoRI* site of pcDNA1 (Invitrogen, San Diego, CA, cat. no. V490-20). Construct the pCMV-T7-2-hNMDAR1A by ligating the 4.3-kb *EcoRI* fragment from pcDNA1-hNMDAR1A into the *EcoRI* site of pCMV-T7-2. Determine the orientation of hNMDAR1A in pCMV-T7-2 by restriction analysis, using the unique *BglII* site in the hNMDAR1A cDNA and the polylinker of pCMV-T7-2.
3. Construct the pCMV-T7-2-hNMDAR2A plasmid by ligating the 4.6-kb *XhoI/EcoRI* fragment containing the full-length hNMDAR2A cDNA into the *XhoI/EcoRI*-digested pCMV-T7-2 vector.
4. Construct the pCMV-T7-3-hNMDAR2B plasmid by ligating the 5.0-kb *EcoRI/EcoRV* fragment containing the full-length hNMDAR2B cDNA into the *EcoRI/EcoRV*-digested pCMV-T7-3 vector.

3.2. Transfection of the Host Cells

Cells were transfected with the cDNA vectors encoding hNMDAR1A and hNMDAR2A or hNMDAR1A and hNMDAR2B using the calcium phosphate coprecipitation method (12).

1. One day prior to the transfection, plate the HEK293 cells on poly-D-lysine-coated 10-cm² tissue-culture dishes at 1×10^6 cells/dish in DMEM containing 6% bovine calf serum, 100 U/mL penicillin G, and 100 μ g/mL streptomycin.
2. Prepare solution B. Dissolve the specified amounts of DNA (see Note 1) in sterile dH₂O to a total volume of 0.44 mL, and add 60 μ L of 2 M CaCl₂.
3. Prepare solution A. Add 10 μ L of 100X PO₄ to 0.5 mL of 2X HEPES.
4. Add solution B to solution A dropwise while continually mixing solution A to form the DNA/calcium precipitate. Allow the precipitate to form for 20 min at room temperature.
5. Add 300 μ M ketamine to each transfection plate (see Note 2).
6. Pipet the precipitate mixture up and down several times, and then add it dropwise to a plate of cells.
7. Swirl the plate to mix the precipitate and the medium, and incubate the cells at 37°C for 6 h.

8. Wash the cells twice with PBS, and culture the transfected HEK293 cells in DMEM culture medium supplemented with 10% dialyzed fetal bovine serum, 2 mM L-glutamine, 100 U/mL penicillin G, 100 µg/mL streptomycin, and 300 µM ketamine.
9. Two days after the transfection, split the transfected HEK293 cells at 1:3 ratio with DMEM supplemented with 10% dialyzed fetal bovine serum, 2 mM L-glutamine, 100 U/mL penicillin G, 100 µg/mL streptomycin, 0.5 mg/mL G418 sulfate, and 300 µM ketamine, and culture in poly-D-lysine-coated 10-cm² tissue-culture dishes. Change the selection medium every 2 d.
10. After 2 wk in culture, pick colonies of G418-resistant HEK293 cells. Place a cloning cylinder onto each colony. Detach the cells by pipeting up and down using a 200-µL pipetter, and transfer the detached cells into 24-well plates.
11. When the cells reach 80–100% confluence in the 24-well plate (approx 4–10 d), plate them on poly-D-lysine-coated 96-well assay plates and measure the [Ca²⁺]_i responses to 100 µM glutamate/30 µM glycine as described in **Subheading 3.3** (see **Note 3**).
12. Subclone the agonist-responsive clones through limiting dilution. Dilute the cells at 80 cells/20 mL medium, and distribute 200 µL/well in 96-well plates. Examine each well the following day, and mark each well that contains a single cell.
13. Change the selection medium every 3–4 d. After growth in culture for 2–3 wk, transfer the cells from 96-well plates to 24-well plates.
14. When the cells reach 80–100% confluence in the 24-well plate, plate them on poly-D-lysine-coated 96-well assay plates, and measure the [Ca²⁺]_i responses to 100 µM glutamate/30 µM glycine as described in **Subheading 3.3** (see **Notes 4** and **5**).

3.3. Screening of Transfected Cells for Functional Expression of hNMDAR1A/2A or hNMDAR1A/2B by Measurement of [Ca²⁺]_i

The functional expression of human NMDA receptors in transfected HEK293 cells was assessed by measurement of changes in [Ca²⁺]_i as described in detail elsewhere (**13,14**).

1. Plate the cells on poly-D-lysine-coated 96-well microtiter assay plates at a density of 2×10^5 cells/well.
2. Twenty-four hours after plating, aspirate the culture medium, and wash the cells twice with 250 µL HBS. Add 200 µL HBS containing 100 µM ketamine to each well, and record the background fluorescence (F_{bkg}).
3. Incubate cells at room temperature for 2 h.
4. Remove the buffer, and add 100 µL of 10 µM fluo-3-AM and 100 µM ketamine to the cells. Incubate for 1–2 h at 20°C.
5. Remove unincorporated dye from the cells by aspiration, and wash each well four times with 250 µL HBS.
6. Add 180 µL HBS to each well, and allow cells to recover for 2 min before testing (see **Note 6**).
7. Record 10 basal fluorescence readings (F_{b}) at 0.33-s intervals.
8. Add 20 µL of 1 mM glutamate/300 µM glycine in HBS containing 40 mM CaCl₂ to each well to give a final concentration of 100 and 30 µM, respectively. Record the response fluorescence (F_{res}) at 0.33-s intervals for 40–60 s.

9. At the end of the experiment, add 25 μL 1% Triton X-100 (v/v in H_2O) to give a final concentration of 0.20%. Mix the contents of the wells by pipeting up and down five times. Incubate approx 2–5 min to lyse the cells, and record the maximal fluorescence (F_{max}).
10. Add 25 μL of 100 mM MnCl_2 to a final concentration of 10 mM, and mix the contents of the wells. Incubate for 2 min, and record the fluorescence (F_{Mn}).
11. Calculate the $[\text{Ca}^{2+}]_i$ levels for each well according to Grynkiewicz et al. (15). First, subtract F_{bkg} from each of F_{res} , F_{Mn} , and F_{max} . Next, calculate $F_{\text{min}} = F_{\text{Mn}}/8$. Calculate $[\text{Ca}^{2+}]_i$ (in nM) = $K_d (F_{\text{res}} - F_{\text{min}})/(F_{\text{max}} - F_{\text{res}})$, where $K_d = 390$ nM for fluo-3.
12. Perform all fluorescence determinations in duplicate or quadruplicate wells.
13. Quantitate the receptor-mediated $[\text{Ca}^{2+}]_i$ responses by calculating the difference between peak $[\text{Ca}^{2+}]_i$ and basal $[\text{Ca}^{2+}]_i$.

3.4. Stability Studies

The stability of the expression of recombinant hNMDAR1A/2A and hNMDAR1A/2B was monitored by measurement of the magnitude of the agonist-induced $[\text{Ca}^{2+}]_i$ response over the course of 40 cell passages in culture (Figs. 1 and 2). The cells are subcultured every 3–4 d (twice per week) when they reach 80–100% confluence in a six-well plate.

1. Warm the culture medium (defined in **Subheading 3.2., step 9**) and trypsin to 37°C.
2. Remove the medium from cell plates by aspiration.
3. Rinse the cells with 1 mL PBS.
4. Add 0.5 mL trypsin. When the cells start detaching from the plate (approx 10 s), promptly remove the trypsin solution. Do not trypsinize excessively.
5. Add 1 mL medium to each six-well plate of cells, and pipet up and down gently to resuspend to single cells.
6. Transfer 0.25 mL from each well into a corresponding well in another six-well plate containing 3 mL of fresh medium in each well. This represents one cell passage at a 1:4 ratio.
7. Swirl each plate to distribute the cells evenly. Return the cells to CO_2 incubator.
8. Measure the $[\text{Ca}^{2+}]_i$ response to 100 μM glutamate/30 μM glycine as described in **Subheading 3.3., steps 1–13**.
9. Select the clonal cell line that displays the most stable $[\text{Ca}^{2+}]_i$ response and expand the cell line on 10-cm² dishes (see **Notes 7 and 8**).
10. The hNMDAR1A/2A-expressing HEK72-4 cell line (hNMDAR1A/2A/HEK72-4) and the hNMDAR1A/2B-expressing HEK4-3 cell line (hNMDAR1A/2B/HEK4-3) are subcultured at a 1:4 ratio on 10-cm² dishes approx every 3–4 d.

3.5. Pharmacological Characterization of HEK293 Cells Stably Expressing hNMDAR1A/2A and hNMDAR1A/2B

The validation of the cloned stable cell line expressing the hNMDAR1A/2A or hNMDAR1A/2B was performed by pharmacological characterization of the

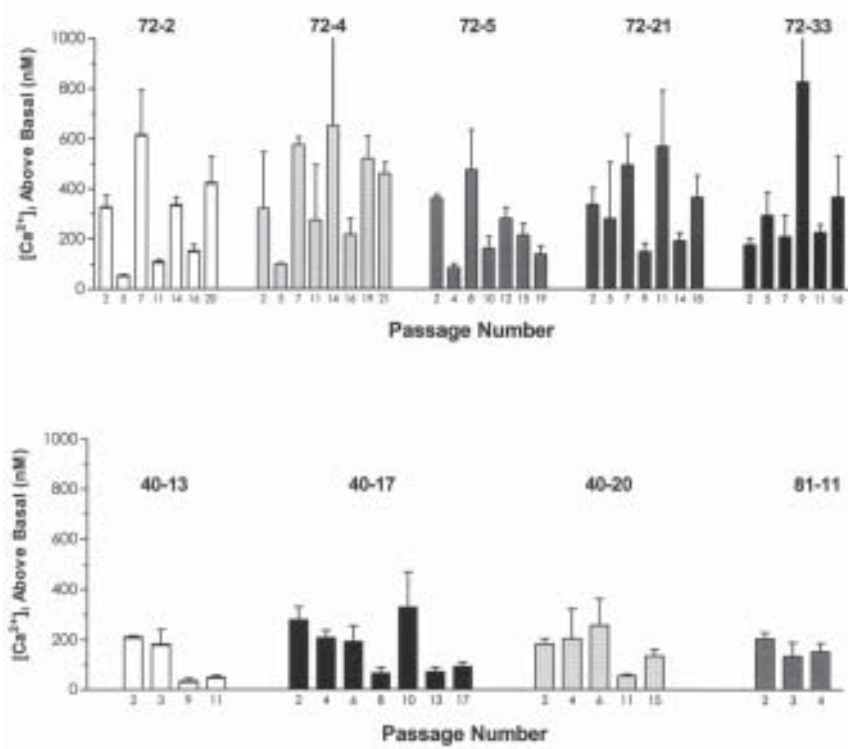


Fig. 1. Stability of hNMDAR1A/2A/HEK293 subclones. $[Ca^{2+}]_i$ signals were measured in response to $100 \mu M$ glutamate/ $30 \mu M$ glycine with increasing cell passage number. Data were analyzed as peak response above basal values and represent the mean \pm SD from quadruplicate wells.

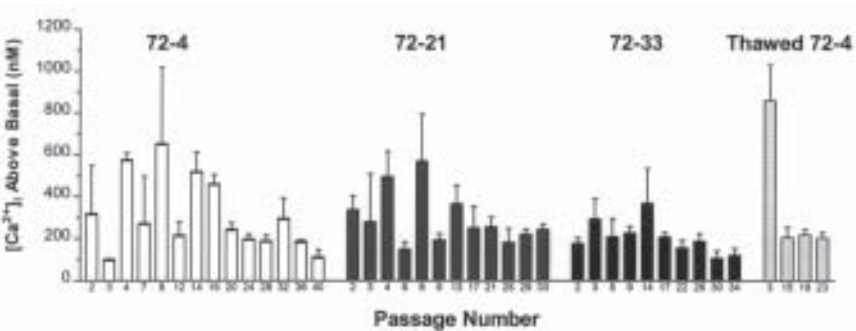


Fig. 2. Stability of hNMDAR1A/2A/HEK72 subclones. $[Ca^{2+}]_i$ signals were measured in response to $100 \mu M$ glutamate/ $30 \mu M$ glycine with increasing cell passage number. Data were analyzed as peak response above basal values and represent the mean \pm SD from quadruplicate wells.

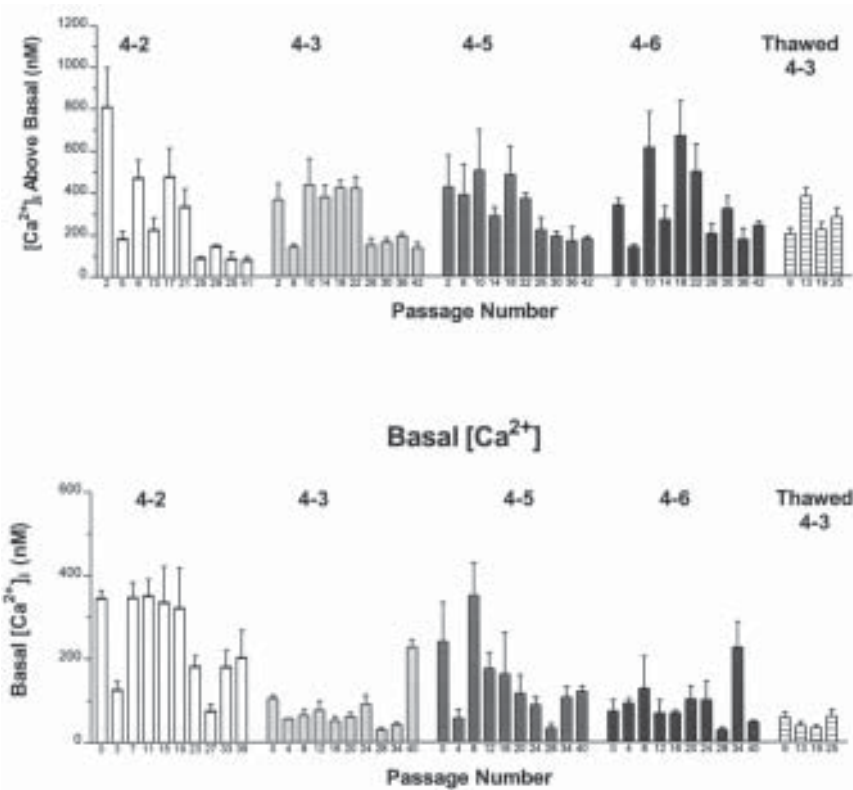


Fig. 3. Stability of hNMDAR1A/2B/HEK4 subclones. $[Ca^{2+}]_i$ signals were measured in response to $100 \mu M$ glutamate/ $30 \mu M$ glycine with increasing cell passage number. Data were analyzed as peak response above basal values and represent the mean \pm SD from quadruplicate wells.

$[Ca^{2+}]_i$ response using reference agonists and antagonists. As part of the pharmacological characterization, we measured the activation of the recombinant receptors as a function of increasing concentration of NMDA, a reference agonist, and inhibition of the glutamate/glycine-induced $[Ca^{2+}]_i$ response as a function of increasing concentration of MK-801, a channel blocker, or CGS19755, a competitive glutamate-site antagonist (**Fig. 3**).

1. The expanded clonal hNMDAR1A/2A/HEK72-4 and hNMDAR1A/2B/HEK4-3 cell lines were plated for $[Ca^{2+}]_i$ measurements as described in **Subheading 3.3**.
2. To measure the potency of NMDA as an agonist, the $[Ca^{2+}]_i$ response was measured as a function of increasing concentration of NMDA in duplicate wells. The $[Ca^{2+}]_i$ response was expressed as percent of normalized maximal response to NMDA,

and the curve was fitted to a four-parameter logistic equation $\{y = \text{bottom} + [\text{top} - \text{bottom}] / (1 + 10^{-(\log EC_{50} - x) \cdot \text{Hill slope}})\}$. The EC_{50} for NMDA, calculated from the curve fit, was 8 μM for hNMDAR1A/2A and 9 μM for hNMDAR1A/2B.

3. To determine the IC_{50} values for MK-801 and CGS19755, the antagonist was added to duplicate wells at the indicated final concentration and incubated for 2 min before 3 μM glutamate/30 μM glycine were added. The $[Ca^{2+}]_i$ response was measured as described in **Subheading 3.3** and plotted as a function of the antagonist concentration. The inhibition curves were fitted to a four-parameter logistic equation $\{y = \text{bottom} + [\text{top} - \text{bottom}] / (1 + 10^{-(\log IC_{50} - x) \cdot \text{Hill slope}})\}$. The IC_{50} was determined from the curve fit as 0.5 μM for MK-801 at both hNMDAR1A/2A and hNMDAR1A/2B receptors, and 6 and 9 μM for CGS19755 at hNMDAR1A/2A and hNMDAR1A/2B receptors, respectively.

3.6. Determination of the Number of Receptors per Cell

The total number of hNMDAR1A/2A or hNMDAR1A/2B expressed per cell was determined by measuring the specific binding of $[^{125}I]$ -MK-801 to total membranes prepared from these cells (*see Note 9*). The data were analyzed by the Scatchard method to determine the values of the binding dissociation constant (K_d) and binding capacity (B_{max}) (**Fig. 4**). Our analysis indicated that the B_{max} of the hNMDAR1A/2A/HEK72-4 cells was 701 fmol/mg protein, i.e., approx 42,000 receptors/cell, and the B_{max} of the hNMDAR1A/2B/HEK4-3 cells was 831 fmol/mg protein, i.e., approx 50,000 receptors/cell (*see Note 10*). The K_d for MK-801 binding was 3.4 nM in the hNMDAR1A/2A/HEK72-4 and 6.8 nM in the hNMDAR1A/2B/HEK4-3 cells, respectively.

3.6.1. Membrane Preparation

1. Remove the cells from 10 T-225-cm² flasks (approx 7×10^8 cells) using a cell scraper. Resuspend the cells from five flasks (approx 3.5×10^8 cells) in 50 mL PBS in a 50-mL conical tube, and centrifuge for 5 min at approx 800g.
2. Remove the supernatant, resuspend the cells in 50 mL PBS by gentle vortexing, and recentrifuge the tubes for 5 min at approx 800g.
3. Resuspend each cell pellet in 80 mL of 0.32 M sucrose at 4°C, and homogenize the cells in a glass-Teflon homogenizer using 10–20 strokes.
4. Transfer the suspension equally to four centrifuge tubes, and centrifuge the cell homogenates at 48,000g for 20 min at 4°C.
5. Discard the supernatants, and resuspend each pellet in 10 mL of Tris-EDTA buffer, homogenize the suspension using a Brinkman Polytron (setting 3, approx 30 s), and add 30 mL Tris-EDTA buffer to each tube.
6. Centrifuge the suspension at 48,000g for 20 min at 4°C.
7. Repeat **steps 5** and **6** three more times.
8. Resuspend the final pellets (each approx 20 mg) in 10 mL Tris-EDTA buffer. Prepare 1-mL aliquots, freeze the aliquots in a dry ice/ethanol mixture, and store

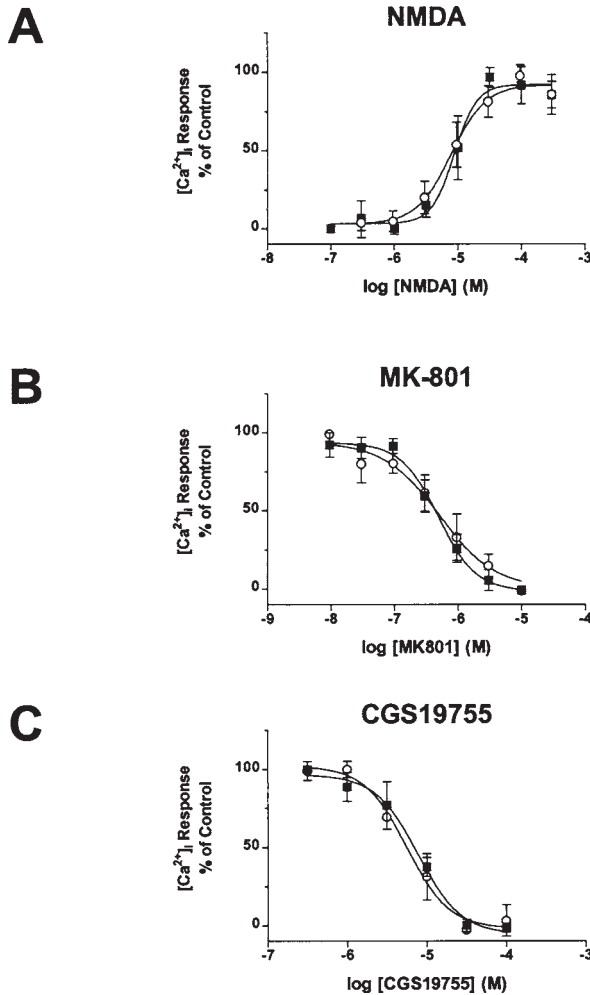


Fig. 4. Concentration-response curves to NMDA (A), and inhibition curves to MK-801 (B) and CGS19755 (C) were constructed from $[Ca^{2+}]_i$ measurements performed in HEK293 cells stably expressing hNMDAR1A/2A (clone HEK72-4) and hNMDAR1A/2B (clone HEK4-3). Data represent the mean \pm SEM from three to five separate experiments, each performed in replicates of four. For agonists, the data are normalized to the response elicited by 100 μ M glutamate/30 μ M glycine. For antagonist studies, data are normalized to the response elicited by 3 μ M glutamate/30 μ M glycine.

at -70° C. These membranes retain their ability to bind MK-801 for at least 6 mo when stored under these conditions.

- Reserve 0.5 mL of sample to determine the protein concentration using the Bio-Rad DC-Protein Assay Kit.

3.6.2. MK-801 Binding Assay

1. On the day of the assay, thaw the frozen membrane suspension, and dilute in assay buffer (20 mM HEPES containing 1.0 mM EDTA, pH 7.4) to approx 0.25 mg protein/mL.
2. Homogenize briefly for 20–30 s using a Polytron homogenizer at setting 3, and incubate at 37°C for 20 min.
3. Centrifuge the membrane suspension for 10 min at 48,000g at 4°C.
4. Discard the supernatants. Resuspend the pellets at 0.25 mg protein/mL by homogenization using a Polytron homogenizer for approx 30 s at setting 3.
5. Repeat **steps 3 and 4** three more times.
6. Resuspend the final washed pellet at 1.0 mg protein/mL in assay buffer using a Polytron homogenizer for 30 s at setting 3. Keep the membrane suspension on ice until use. Typically we use 100 or 150 μL /well in the binding assay.
7. The binding assays are performed in 96-well (deep-well) plates in triplicate.
8. Prepare 100-mM stocks of glutamate, glycine, and spermine tetrahydrochloride in water. Mix 80 μL of each stock, and add to 3760 μL assay buffer. Use 25 μL of this mixture (GGs mixture)/well to achieve a final concentration of 100 μM of each compound in the assay.
9. Dilute an aliquot of the stock [^{125}I]-MK-801 solution (114 nM) 76-fold to obtain a working concentration of 1.5 nM. We use 0.3-nM final concentration in the assay (approx 120,000 cpm/well) in a total assay volume of 500 μL (*see Note 11*).
10. Prepare a 5-mM stock solution of MK-801 in water, and prepare serial dilutions down to 0.5 nM. Since 100 μL of solution are used in a final assay volume of 500 μL , the final concentrations are diluted another fivefold.
11. To the total binding wells, add 100 μL of 1.5 nM [^{125}I]-MK-801 (0.3 nM final concentration), 100 μL membrane (100 μg /tube), 25 μL GGS mixture (*see step 8*), and 275 μL assay buffer.
12. To the nonspecific binding wells, add 100 μL of 1.5 nM [^{125}I]-MK-801 (0.3 nM final concentration), 100 μL membrane (100 μg /tube), 25 μL GGS mixture (*see step 8*), 100 μL MK-801 (10 μM final concentration), and 175 μL assay buffer.
13. To the sample binding wells, add 100 μL of 1.5 nM [^{125}I]-MK-801 (0.3 nM final concentration), 100 μL membrane (100 μg /tube), 25 μL GGS mixture (*see step 8*), 175 μL assay buffer, and 100 μL of unlabeled MK-801.
14. Incubate samples for 3 h at room temperature.
15. After setting up the incubation, presoak Whatman GF/C filters for 2–3 h at 4°C in 0.3% polyethylenimine prepared in ultrapure water.
16. Filter the assay mixture through the soaked GF/C filters using a 48-well Brandel cell harvester, and wash the filters four times with ice-cold assay buffer.
17. Cut the filters, and transfer them to test tubes.
18. Count the samples and an aliquot of the [^{125}I]-MK-801 in a γ -radioactivity counter for 1 min (**Note 12**).

3.7. Analysis of Results

1. Determine specific binding by subtracting nonspecific binding from the binding obtained with each sample.

2. Calculate the actual concentration of the label used in the experiment, based on the number of cpm, as follows: Concentration of [125]-MK-801, in mol/l = (total cpm/efficiency)/(SA in Ci/mol) \times (assay volume, in L) \times (2.22×10^{12}).
3. For each concentration of MK-801, calculate the free concentration, which is equal to the concentration of [125]-MK-801 plus the concentration of MK-801 added to the assay, expressed in mol/L (*see Note 13*).
4. Calculate the specific activity of the [125]-MK-801 at each data point as follows: SA of label (Ci/mol) \times 2.22×10^{12} to determine dpm/mol. Multiply this value by the concentration of [125]-MK-801 in mol/L (calculated in **step 2**), and divide this by the free concentration, in mol/L (obtained in **step 3**), to give the specific activity for each concentration of MK-801 in dpm/mol.
5. Calculate the amount of bound MK-801 by dividing the specific binding, in dpm (obtained in **step 1**) by the specific activity, in dpm/mol, and divide this number by the amount of membrane protein (g) used for each well. This will give the amount bound in mol/g protein, although we typically express this as fmol/mg protein.
6. Divide the bound (obtained in **step 5**) by free (obtained in **step 3**), to give the bound/free ratio.
7. To obtain K_d and B_{\max} values, plot bound (y-axis) vs free (x-axis), and fitting the data to a hyperbola using nonlinear regression, where $y = B_{\max} * x / (K_d + x)$, where B_{\max} is the maximal binding, and K_d is the concentration of ligand required to reach half-maximal binding. Additionally, a Scatchard plot can be made by plotting the B/F ratio (y-axis) vs bound (x-axis), and fitting the data by a straight line using the method of least squares (*see Note 14*). The intercept on the x-axis gives the B_{\max} , and $-1/\text{slope}$ of the fit gives the K_d .

4. Notes

1. Transfect HEK293 cells with the following amounts of plasmids: For cells expressing hNMDAR1A/2A, use 2 μg of pCMV-T7-2-hNMDAR1A, 8 μg of pCMV-T7-2-hNMDAR2A, and 1 μg of pSV2neo; for cells expressing hNMDAR1A/2B, use 2 μg of pCMV-T7-2-hNMDAR1A, 20 μg of pCMV-T7-2-hNMDAR2B, and 2 μg of pSV2neo. One milliliter of the DNA/calcium phosphate precipitate is used to transfect one 10-cm² plate of cells.
2. Ketamine is a noncompetitive antagonist of the NMDA receptor, and is included in the growth conditions to reduce the excitotoxicity mediated by activation of the NMDA receptor. Even under normal growth conditions, there are sufficient levels of glutamate to activate the NMDA receptor, resulting in death of the host cell. Ketamine rapidly dissociates from the receptor and therefore is preferred over MK-801, which is more difficult to remove.
3. Four clones of hNMDAR1A/2A-transfected HEK293 cells (HEK18, HEK40, HEK72, and HEK81) displayed [Ca^{2+}]_i signals of 150–300 nM to 100 μM glutamate/30 μM glycine. Among the G418-resistant hNMDAR1A/2B-transfected HEK293 cells, one colony, hNMDAR1A/2B/HEK4, exhibited [Ca^{2+}]_i responses of 290 nM above basal levels.

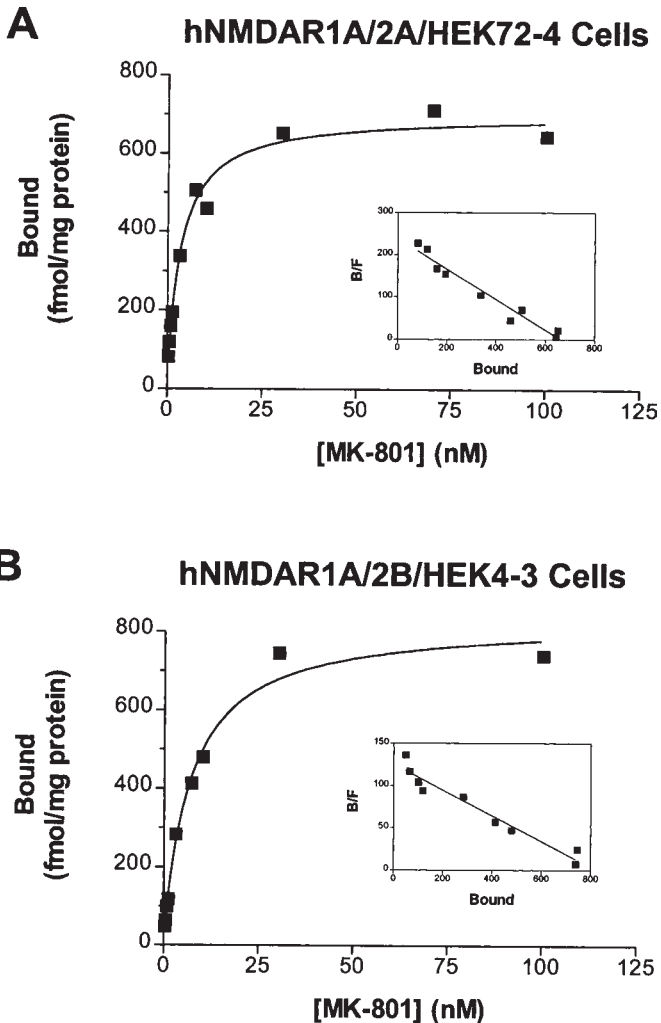


Fig. 5. Saturation analysis of specific [125 I]-MK-801 binding in membranes prepared from hNMDAR1A/2A/HEK72-4 (A) and hNMDAR1A/2B/HEK4-3 (B) cells. Scatchard transformation of the same data are shown in the insets. Data points represent the mean of triplicate values from a single experiment.

4. A total of 80 subclones derived from limiting dilution of hNMDAR1A/2A/HEK18, hNMDAR1A/2A/HEK40, and hNMDAR1A/2A/HEK72 cells were screened for $[Ca^{2+}]_i$ responses to 100 μ M glutamate/30 μ M glycine. An initial examination of the stability of these subclones through several passages in culture is shown in Fig. 5. Four subclones, hNMDAR1A/2A/HEK40-17, hNMDAR1A/2A/HEK72-2, hNMDAR1A/2A/HEK72-4, and hNMDAR1A/2A/HEK72-5

- exhibited $[Ca^{2+}]_i$ responses of 200–1000 nM above basal levels. We have observed that the amplitude of the $[Ca^{2+}]_i$ responses is variable over time in culture; however, the responses have consistently been >200 nM in several subclones.
- Thirteen subclones of the hNMDAR1A/2B/HEK4 cells were screened for $[Ca^{2+}]_i$ responses to 100 μM glutamate/30 μM glycine. Five of the subclones (hNMDAR1A/2B/HEK4-2, hNMDAR1A/2B/HEK4-3, hNMDAR1A/2B/HEK4-5, hNMDAR1A/2B/HEK4-6, and hNMDAR1A/2B/HEK4-11) displayed glutamate/glycine-evoked increases in $[Ca^{2+}]_i$ ranging between 300 and 800 nM above basal levels.
 - The recovery period between washing of unloaded dye and measurement of agonist-induced $[Ca^{2+}]_i$ response should be <10 min to minimize time-dependent extrusion of the dye from the cells.
 - The parental clone, hNMDAR1A/2A/HEK72 and three of its subclones, hNMDAR1A/2A/HEK72-4, hNMDAR1A/2A/HEK72-21, and hNMDAR1A/2A/HEK72-33, were monitored for more prolonged study of the stability of glutamate/glycine-evoked $[Ca^{2+}]_i$ responses (**Fig. 1**). We tested hNMDAR1A/2A/HEK72-4 cells after one cycle of freeze–thaw and observed that $[Ca^{2+}]_i$ responses were comparable to those obtained before freezing (**Fig. 1**). Based on these results, the hNMDAR1A/2A/HEK72-4 cells were selected for further pharmacological and electrophysiological characterization, and validated as a cell line for drug screening.
 - Four subclones derived from hNMDAR1A/2B/HEK4 cells were monitored for stability of glutamate/glycine-evoked $[Ca^{2+}]_i$ responses (**Fig. 2**). We also monitored the basal $[Ca^{2+}]_i$ and found that hNMDAR1A/2B/HEK4-3 cells consistently exhibited the lowest level of basal $[Ca^{2+}]_i$ (**Fig. 2**). We tested hNMDAR1A/2B/HEK4-3 cells following freeze–thawing and observed that $[Ca^{2+}]_i$ responses were comparable to those obtained before freezing (**Fig. 2**). These stability studies indicated that the hNMDAR1A/2B/HEK4-3 cell line displayed a robust and stable NMDA/glycine-induced $[Ca^{2+}]_i$ signal of ≥ 200 nM with a relatively low basal $[Ca^{2+}]_i$ of approx 50 nM over 40 passages in culture (**Fig. 2**). Based on these results, the hNMDAR1A/2B/HEK4-3 cells were selected for further pharmacological and electrophysiological characterization, and validated as a cell line for drug screening.
 - In these studies, we use a competition binding experiment to determine the K_d and B_{max} , rather than a full saturation curve. That is, we use a fixed concentration of label, and increase the concentration of unlabeled MK-801, rather than increasing the concentration of $[^{125}I]$ -MK-801 as in a saturation experiment. Competition binding experiments have the advantage that they require lower levels of radioactivity than saturation experiments. However, these measurements may be less sensitive in detecting a second, lower-affinity binding site, since $[^{125}I]$ -MK-801 will bind to only a small fraction of low-affinity sites at the relatively low concentration that it is used.
 - These estimates are derived from total cell membranes, and thus include receptors in both the plasma membrane as well as membranes from various intracellular organelles.

11. The [^3H]-MK-801 can also be used as the radiotracer for these binding studies, although it is less sensitive than [^{125}I]-MK-801 because of its lower specific activity.
12. Alternatively, scintillant can be added to the filters, which are then soaked overnight, and the radioactivity determined by liquid scintillation spectrometry using a β -counter. The counting efficiency of ^{125}I is approx 80–90% in a γ -counter, but may be significantly lower in a β -counter.
13. The free concentration of [^{125}I]-MK-801 need not be corrected for ligand depletion as long as the bound dpm does not exceed approx 10% of the total dpm added. Where possible, design experiments to avoid binding more than 10% of the label by using less membrane protein or increasing the volume of the assay without changing the amount of membranes.
14. Although Scatchard plots fitted by linear regression are very useful for visualizing the data, a better way to analyze the data is to use the hyperbola fitted by nonlinear regression. The fit using linear regression assumes equal error for all points, which is not true with the transformed data. The error can be particularly large around the x -intercept where the B_{max} is determined. This problem is minimized when the data are fit to a hyperbola. Furthermore, values from x (bound) are used to calculate values of y (bound/free), violating the assumptions of linear regression. Therefore, we use Scatchard plots to visualize data sets, but use the K_d and B_{max} values determined from nonlinear regression fits.

Acknowledgments

We especially thank Michael Harpold for his valuable input and continued support and encouragement throughout this work. In addition, we acknowledge Sandy Madigan for critical review of the manuscript and Karen Payne for assistance in document preparation.

References

1. Choi, D. W. (1988) Glutamate neurotoxicity and diseases of the nervous system. *Neuron* **1**, 623–634.
2. Meldrum, B. S. (1996) Update on the mechanism of action of antiepileptic drugs. *Epilepsia* **37**, Suppl. **6**, S4–11.
3. Yaksh, T. L., Chaplan, S. R., and Malmberg, A. B. (1995) Future directions in the pharmacological management of hyperalgesic and allodynic pain states: the NMDA receptor. *NIDA Res. Monogr.* **147**, 84–103.
4. Hollmann, M., and Heinemann, S. (1994) Cloned glutamate receptors. *Annu. Rev. Neurosci.* **17**, 31–108.
5. Buller, A. L., Larson, H. C., Schneider, B. E., Beaton, J. A., Morrisett, R. A., and Monaghan, D. T. (1994) The molecular basis of NMDA receptor subtypes: Native receptor diversity is predicted by subunit composition. *J. Neurosci.* **14**, 5471–5484.
6. Sucher, N. J., Awobuluyi, M., Choi, Y.-B., and Lipton, S. A. (1996) NMDA receptors: from genes to channels. *Trends Pharmacol. Sci.* **17**, 348–355.

7. US Patent 5,202,257, April 13, 1993 Isolated Nucleic Acids Encoding Glutamate Receptor Protein. Assigned to the Salk Institute for Biological Sciences.
8. Hess, S. D., Daggett, L. P., Crona, J., Deal, C., Lu, C.-C., Urrutia, A., et al. (1996) Cloning and functional characterization of human heteromeric *N*-methyl-D-aspartate receptors. *J. Pharmacol. Exp. Ther.* **278**, 808–816.
9. Hess, S. D., Daggett, L. P., Deal, C., Lu, C.-C., Johnson, E. C., and Veliçelebi, G. (1998) Functional characterization of human *N*-methyl-D-aspartate subtype 1A/2D receptors. *J. Neurochem.* **70**, 1269–1279.
10. Daggett, L. P., Lu, C.-C., Deal, C., Hess, S. D., Jachec, C., Varney, M. A., et al. (1998) The 2C subunit of the human *N*-methyl-D-aspartate receptor: Cloning of isoforms, distribution in human brain, and functional expression. *J. Neurochem.* in press.
11. Varney, M. A., Jachec, C., Deal, C., Hess, S. D., Daggett, L. P., Skvoretz, R., et al. (1996) Stable expression and characterization of recombinant human heteromeric *N*-methyl-D-aspartate receptor subtypes hNMDAR1A/2A and hNMDAR1A/2B in mammalian cells. *J. Pharmacol. Exp. Ther.* **279**, 367–378.
12. Kingston, R. E. (1996) Calcium phosphate transfections, in *Current Protocols in Molecular Biology* (Ausubel, F. M., Brent R., Kingston R. E., Moore, D. D., Seidman, J. G., Smith J. A., et al., eds.), John Wiley, New York, pp. 9.1.4–9.1.6.
13. US Patent 5,670,113, September 23, 1997. Automated Analysis Equipment and Assay Method for Detecting Cell Surface Protein and/or Cytoplasmic Receptor Function Using Same. Assigned to SIBIA Neurosciences, Inc.
14. Veliçelebi, G., Stauderman, K. A., Varney, M. A., Akong, M., Hess, S. D., and Johnson, E. C. (1998) Fluorescent techniques for measuring ion channel activity, in *Methods in Enzymology; Volume on Ion Channels*, Academic, San Diego, CA.
15. Grynkiewicz, G., Poenie, M., and Tsien, R. Y. (1985) A new generation of Ca^{2+} indicators with greatly improved fluorescence properties. *J. Biol. Chem.* **260**, 3440–3450.

Expression of Extracellular N-Terminal Domain of NMDA Receptor in Mammalian Cells

Erik A. Whitehorn, William J. Dower, and Min Li

1. Introduction

NMDA receptor is a ligand-gated ion channel receptor composed of multiple subunits encoded by at least five genes and their splice variants (1). Functional channels can be produced with only the NR1 subunit. These single-subunit channels, exhibit many of the key properties found in native channels including the direct permeability of calcium, voltage-dependent Mg^{2+} blockade of the ion channel, and binding sites for modulators, such as Zn^{2+} , glycine, and polyamines (2). The NR1 subunit consists of two functionally distinct regions: a large amino-terminal extracellular domain containing the putative agonist binding site and a hydrophobic core consisting of four transmembrane-spanning domains that participate in the formation of the ion-conducting pathway.

In an effort to discover new ligands to the NR1 subunit, we chose to express the amino-terminal 561 amino acid extracellular domain in a phosphoinositol peptidoglycan- (PIG) linked form in CHO cells using the plasmid vector a + KH (Fig. 1). This vector facilitates the expression of genes in a PIG-linked form by creating a fusion to the 3' signal sequence of the naturally occurring PIG-linked enzyme, Human Placental Alkaline Phosphatase (HPAP). Genes of this type are expressed, transported, and anchored to the cell surface via the PIG linkage (3). With this method of expression, it is possible to obtain a purified, immobilized form of the receptor. For screening recombinant peptide libraries, we have previously demonstrated that PIG-linked expression of a wide variety of type 1 transmembrane receptors is a robust and reliable method to identify peptide ligands to these receptors (4–7). Expression of NR1 by this process has allowed the isolation of novel, biologically active peptides through in vitro selection (8). This chapter describes the process of cloning, expression, and purification of the NR1 first extracellular domain.

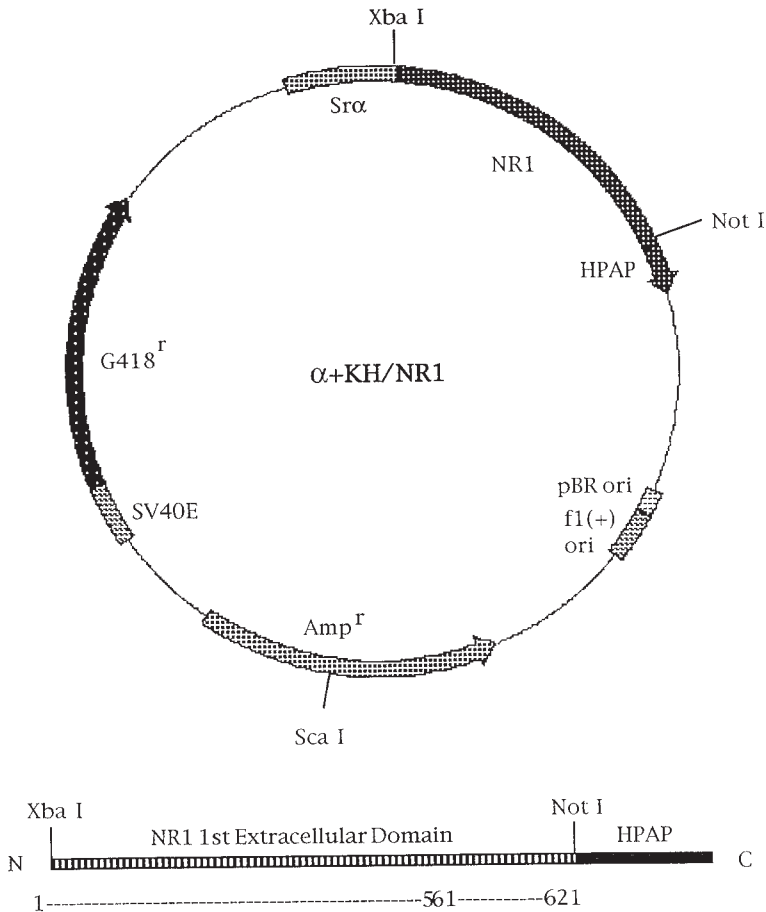


Fig. 1. Functional map of the $\alpha + KH$ vector with cloned NR1. The amino terminal 561 amino acids of NR1 are fused to the carboxy terminus of human placental alkaline phosphatase (HPAP) at the *NotI* site.

2. Materials

The majority of the equipment required is standard within a molecular biology laboratory and cell-culture facility.

2.1. Cloning

2.1.1. RNA Preparation

1. Rat.
2. TRIzol Reagent (Gibco-BRL, Gaithersburg, MD).
3. Isopropanol (100%).

2.1.2. cDNA Synthesis

1. 10X Reaction buffer: 0.5 M KCl, 100 mM Tris-HCl, pH 8.3 (25°C), 15 mM MgCl₂.
2. 25 mM dNTPs: Mix of equal parts of 100 mM dATP, dCTP, dGTP, and TTP (Pharmacia, Piscataway, NJ).
3. Superscript II M-MLV RNase H⁻ reverse transcriptase (Gibco-BRL).
4. Oligo dT₁₂₋₁₈ (0.5 μg/μL).
5. 3 M NaOAc (pH 5.4, 25°C).
6. TE buffer: 10 mM Tris-HCl, pH 7.5 (25°C), 1 mM EDTA.
7. Ethanol (100%).

2.1.3. PCR

1. 2.5 mM dNTPs.
2. 5'-PCR primer (20 μM) 5'-TAATCTAGAATGAGCACCATGCACCTGCTGACAT-3'.
3. 3'-PCR primer (20 μM) 5'-TTAGCGGCCGCTGTGCTCTGAAAAGGCTGCATAAAT-3'.
4. 9600 Thermal cycler (Perkin-Elmer, Norwalk, CT).
5. Thin-wall 100-μL PCR reaction tubes (Perkin-Elmer).
6. *Taq* DNA polymerase (Promega, Madison, WI).

2.1.4. Cloning

1. TAE Buffer: 40 mM Tris-AC (pH 7.8, 25°C)/1 mM EDTA.
2. Ethidium bromide (10 mg/mL in H₂O).
3. GeneClean (BIO 101, Vista, CA).
4. *Xba*I and *Not*I restriction enzymes and buffer (New England Biolabs, Beverly, MA).
5. T4 DNA ligase and buffer (New England Biolabs).
6. α + KH Vector (Affymax, Palo Alto, CA).
7. Electrocompetent *Escherichia coli*, DH10B (Gibco-BRL).
8. 0.1-cm Cuvet (Bio-Rad, Hercules, CA).
9. UV transilluminator (Fotodyne, Hartland, WI).
10. SOC bacterial medium.
11. LB/Amp⁵⁰ bacterial medium and plates.

2.2. Expression

2.2.1. Electroporation

1. *Sca*I restriction enzyme and buffer (New England Biolabs).
2. Gene Pulser (Bio-Rad).
3. 0.4-cm Cuvet (Bio-Rad).
4. GI medium (Gibco-BRL).
5. DMEM/F-12 (1:1) medium (Gibco-BRL).
6. Fetal bovine serum (Gibco-BRL).
7. Antibiotic/antimycotic (Gibco-BRL).
8. 225-cm² flasks.
9. G418 (200X stock in 25 mM HEPES, pH 7.2, 25°C).

2.2.2. Cell Sorting

1. FACS-STAR plus (Becton-Dickinson, Rutherford, NJ).
2. Ab179-FITC.
3. 96-Well tissue-culture plates.
4. DMEM/F-12 (1:1)/3% BSA.
5. Versene.

2.3. Purification

2.3.1. NR1 Receptor Harvest

1. T75 tissue-culture flask.
2. 100, 300, and 3000 mL spinner flasks (Bellco, Vineland, NJ).
3. PI-PLC (Calbiochem, La Jolla, CA, #524640-S).
4. DMEM/F-12 + 5% equine serum.
5. 0.2 μ m Cellulose acetate filters.
6. Endoglycosidase F/N-glycosidase F and buffer (Boehringer Mannheim, Mannheim, Germany, #8778 740).

2.3.2. 96-Well Plate Immobilization/ELISA

1. Immulon-4 microtiter plate (Dynatech, Chantilly, VA).
2. Binding buffer: 10 mM Tris-HCl, pH 8.1, 25°C, 100-mM NaCl, 1 mM EDTA.
3. Phosphate-buffered saline (PBS)/0.05% Tween 20.
4. Bovine serum albumin (BSA).
5. Ab179 (Affymax).
6. Mag.1.1 Phage containing the peptide sequence CDGLRHMWFC (Affymax).
7. Sheep anti-M13 Ab/HRP conjugate and detection kit (Pharmacia #27-9402-01).

3. Methods

3.1. Cloning of Rat NR1 ECD

The initial step in the cloning of the NR1 subunit first extracellular domain is preparation of cDNA from total RNA isolated from rat brain. Quickly remove the brain after the rat has been sacrificed and immediately dissect the tissue with a scalpel to generate a few pea-sized pieces. Two to three of these small pieces are pooled, weighed, and then suspended in TRIzol at 10 mg/mL. This process from euthanasia to suspension in TRIzol should take less than a minute. After following the manufacturer's recommended procedure, the RNA is quantified by absorbance measurement at 260 nm, and the concentration is adjusted to 1 μ g/ μ L in TE buffer.

cDNA is made from the total RNA prep using M-MLV SuperScript II RNase H⁻ reverse transcriptase in a 100- μ L reaction:

- 10 μ L 10X Reaction buffer.
- 2 μ L 25 mM dNTP.
- 10 μ L 0.5 μ g/ μ L Oligo dT₁₂₋₁₈.
- 5 μ L 1 μ g/ μ L RNA.

H₂O to 100 μ L

1 μ L SuperScript II RNase H⁻ reverse transcriptase (200 U).

The reaction is incubated at room temperature for 10 min and then at 42°C for 50 min. The cDNA is precipitated with 10 μ L 3 M NaOAc and 250 μ L ethanol at -70°C for 10 min. The precipitate is centrifuged at maximum speed in a tabletop microcentrifuge, dried briefly, and resuspended in 50 μ L H₂O.

Ten microliters are then amplified with the PCR using primers homologous to the 5'- and 3'-ends of the first ECD (9).

10 μ L cDNA.

10 μ L 10X Reaction buffer.

8 μ L 2.5 mM dNTPs.

5 μ L 5'-primer (20 μ M).

5 μ L 3'-primer (20 μ M).

H₂O to 100 μ L.

The assembled reaction mix is first heated at 95°C for 5', 2 μ L of *Taq* polymerase (5 U) are added, and the reaction is then cycled (30 \times : 95°C/1'-60°C/1'-72°C/5') in the Perkin-Elmer 9600 thermal cycler. After the PCR cycle is completed, the DNA is precipitated with NaOAc and ethanol as previously described, and the dried pellet, after suspension in 15 μ L TE buffer, is run on an agarose gel in 1X TAE buffer at 80 V (4.4 V/cm).

The a + KH vector is prepared for ligation to the edited NR1 cDNA by digestion of 1 μ g of plasmid DNA in 10 μ L buffer with 5 U each of *NotI* and *XbaI* at 37°C for 90 mins. The linear DNA is then run on the gel with the precipitated PCR reaction. The gel is stained with ethidium bromide (0.1 μ g/mL in H₂O) for 15 min, and the DNA visualized by exposure to UV light.

The predicted 1.6-kb cDNA and 7-kb linear a + KH bands are isolated from the gel by excision with a scalpel and placed in a microfuge tube. The DNA is then purified with GeneClean. The NR1 cDNA is then digested with the restriction enzymes *XbaI* and *NotI* in a 50- μ L reaction with 20 U of each enzyme at 37°C for 60 min. The DNA is again purified with GeneClean. Seven microliters of the purified cDNA are then ligated with 2 μ L (approx 100 ng) of the purified *XbaI-NotI*-digested a + KH vector in a 10- μ L reaction in ligase buffer using 1 μ L of added T4 DNA ligase. After 1 h at room temperature, 1 μ L of this ligation mix is then used to transform *E. coli* by electroporation. Selection for the transformants is by ampicillin at 50 μ g/mL.

The DNA sequence of the NR1 fusion gene from isolated plasmids is confirmed using standard DNA sequencing techniques.

3.2. Transfection of CHO Cells

Stable cell lines were obtained by transfection of CHO-K1 cells by electroporation in a 0.4-cm gap cuvet with 40 μ g DNA and 0.8 mL CHO-K1 cells

(8×10^6) in GI medium at 250 μ F/400 V in a Bio-Rad Gene Pulser. Electroporated cells are then transferred to a 225-cm² flask with 40 ml DMEM/F-12 (1:1)/10% fetal bovine serum/1X antibiotic-antimycotic, and maintained at 37°C/5%CO₂. After 36 h, selection is initiated with fresh medium containing 1 mg/mL of the eukaryotic antibiotic G418. This selection medium is replaced every 2–3 d for 10 d. At this time, several hundred colonies of selected cells should have developed in the flask.

3.3. FACS Analysis

Following G418 selection, cells are stained with FITC-MAb, labeled Ab179 and analyzed by FACS. Ab179 is a high-affinity monoclonal antibody, which recognizes the epitope, CLEPTYACD, within the HPAP-derived sequences of the PIG-linked NR1 receptor expression vector, α + KH/NR1(3). To stain, the cells are first removed from the flask with Versene (do **not** use trypsin) and then centrifuged (1000g/5' in a Beckman GS-6R centrifuge (Beckman, Fullerton, CA) with a GH-3.7 rotor). The cell pellet is resuspended in 1 mL DMEM/F-12 (1:1)/3% equine serum, and Ab179-FITC is added to 10 μ g/mL. The cell mixture is incubated on ice for 30' and then pelleted as above, washed once in fresh medium, and then run through the FACS. The brightest 5% of cells are then sorted as individual cells into wells of a 96-well plate. These cell clones are grown up and reanalyzed by FACS to confirm the level of receptor expression (**Fig. 2**).

3.4. NR1 Cell Harvest

The selected clone is then scaled up in a 3000-mL spinner flask in DMEM/F-12 (1:1) + 5% fetal bovine serum to a cell density of 10⁶/mL. The scale-up is done in three steps: the clone is transferred to a 75-cm² flask and grown to confluence, then the cells are transferred to a 100-mL suspension culture in a 300-mL spinner flask (all spinner suspensions are at 50g) until the cells reach 10⁶/mL, and then finally transferred to a 1000-mL vol in the 3000-mL spinner flask and grown to 10⁶cells/mL.

The NR1-HPAP receptor is harvested from the cell surface by cleavage with PI-PLC. The cells are prepared by pelleting at 1000g for 5 min as previously described. Wash the cells by resuspension in 1000 mL DMEM/F-12 + 5% equine serum, and pellet again. Resuspend the cells in 50 mL DMEM/F-12 without serum, supplemented with 1X antibiotic/antimycotic solution, in a 100-mL spinner flask. Add PI-PLC to 0.1 U/mL and incubate at 37°C for 1–2 h. The cells at this stage can be reanalyzed by FACS to show the extent of receptor removal by PI-PLC (**Fig. 2**). After PI-PLC treatment, pellet the cells at higher speed (3500g/5 min) and pass the clear supernatant through a 0.2- μ M cellulose acetate filter. The NR1 harvest is then stored at 4°C.

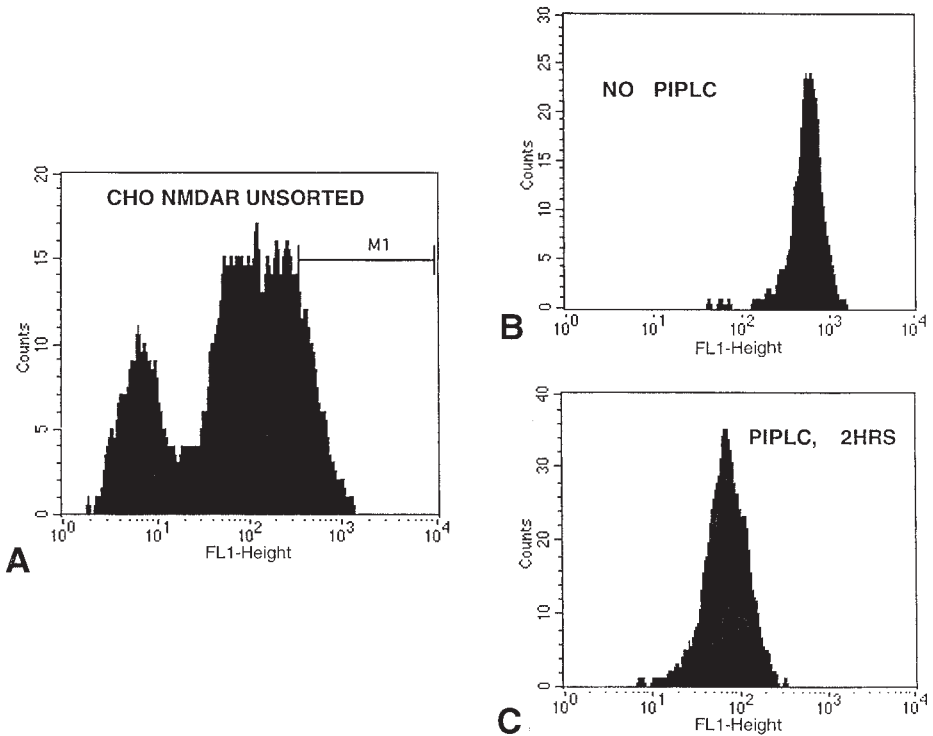


Fig. 2. FACS analysis of Ab 179-FITC-stained transfected CHO cells. (A) Staining of G418 selected CHO cells. The brightest 5% of the cell population, M1, is clone sorted into individual wells. (B) Staining of an individual clone, 2G8, prior to PI-PLC cleavage and (C) after PI-PLC cleavage of NR1 from the cells.

3.5. Characterization of NR1 Receptor Harvest

Endo F treatment of the receptor harvest will show a pattern of cleavage similar to that of the native receptor (10). Endo F cleavage is performed with 25- μ L harvest and 1 U enzyme in a 100- μ L reaction in the manufacturer-supplied buffer and 0.05% sodium dodecyl sulfate (SDS) for 4 h at 37°C. The proteins are separated by 10% SDS-polyacrylamide gel electrophoresis (PAGE) and transferred in a Western blot to nitrocellulose. The blot is then probed with Ab179 (Fig. 3). It is worth noting that the NR1 detected from the intact CHO cells yields two bands. The minor, higher-molecular-weight, band runs in the same position as that of the glycosylated NR1 harvest and the major, smaller-weight, band runs in an intermediate position relative to the Endo F-treated and untreated NR1. This probably represents material that was unglycosylated, retained within the cell, and not processed to create the PIG linkage. Processing to create the PIG

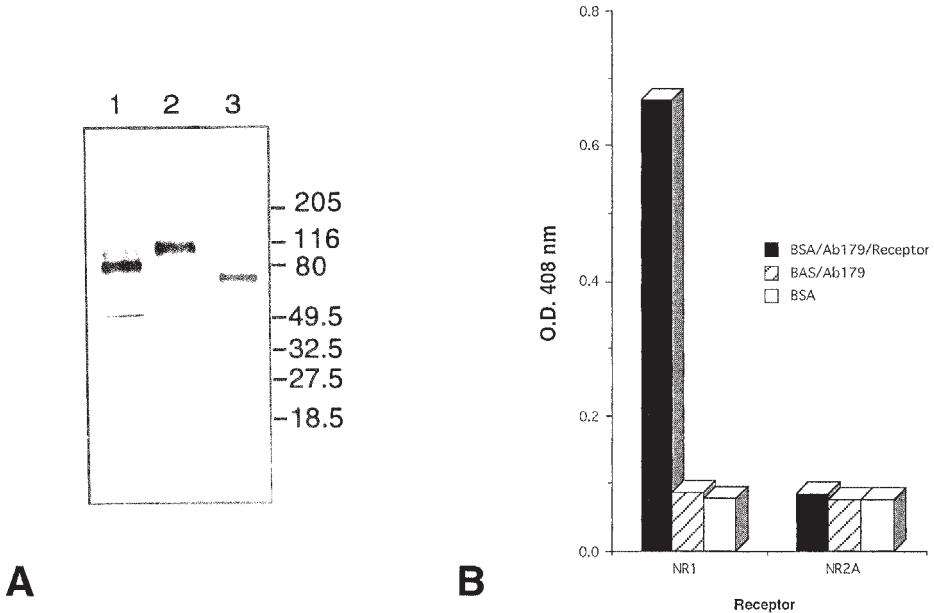


Fig. 3. Receptor characterization. (A) Endo F treatment of expressed NR1. Lane 1: total cell lysate; lane 2: surface NR1 after cleavage by PI-PLC; lane 3: PI-PLC-cleaved NR1 after digestion with Endo F. Prestained mol-wt markers (Bio-Rad) are indicated, (B) Mag-1 phage ELISA. Mag-1 phage binding to PIG-linked receptor harvests of NR1 and NR2A (another NMDA receptor subunit). Phage binding was detected by antiphage antibody as described.

linkage results in the removal of 29 amino acids from the carboxy-terminal portion of HPAP. It is not known why the majority of the expressed NR1 is not presented on the cell surface in the PIG-linked, PI-PLC-cleavable form.

To characterize further the NR1 harvest and prepare the receptor for panning experiments, the harvest is immobilized in microtiter wells, and a Mag1.1 Phage ELISA is performed.

The wells of a 96-well Immulon-4 microtiter plate (Dynatech) are precoated with 50 μ L Ab179 (100 μ g/mL) at 37°C for 60 min. The plate is then washed once with PBS, and then the wells are blocked for 1 h at 37°C by completely filling each well with 1% BSA in PBS. The plate is then washed again with PBS, 100 μ L of the NR1 harvest are added to each well, and the plate incubated at 4°C for 1 h. Receptor Harvest impurities are then removed by washing the wells once with PBS.

One hundred microliters of phage are added to the wells and incubated at room temperature for 1 h. The wells are then washed three times (5 min each wash) with PBS/0.05% Tween 20, and the anti-M13 phage-HRP-conjugated

antibody is added to the wells and again incubated at room temperature for 1 h. The wells are washed and developed with the ABTS reagents provided in the detection kit (**Fig. 3**).

4. Conclusion

Through screening of recombinant peptide libraries with the immobilized PIG-expressed NR1 first extracellular domain, novel peptides have been identified which confer modulatory activity on native NMDA receptors. Although the PIG linked form of the receptor does not create a functional ion channel, it is clear that many of the structural properties of the native receptor are retained. The broad applicability of this approach with type 1 receptors and this example with NR1 suggests that this strategy may be applicable to other ion channels and transporters.

5. Notes

1. Standard RNase precautions are required to obtain quality RNA. When the tissue is suspended in TRIzol, it is lysed by pipeting the tissue up and down in the TRIzol solution until the solution becomes viscous (approx 5 min). Add 0.2 mL chloroform/mL, vortex, and let stand at room temperature for 3 min. Spin in a 4°C microfuge for 15 min, and transfer the supernatant to a fresh, RNase-free tube. Precipitate the RNA with 0.5 vol isopropanol at room temperature for 10 min and the RNA is recovered by centrifugation at 4°C for 10 min in the microfuge. The RNA pellet is washed by vortexing with 75% Ethanol, spun for 5 min in the 4°C microfuge and the pellet is then dried for 10 min at room temperature (do **not** heat the pellet). Suspend the pellet in 10 µL water/mL original TRIzol solution. The yield should be approx 1 µg RNA/mg tissue. This reagent is also a useful tool for isolation of DNA and protein from the same sample. A detailed protocol is available from the manufacturer.
2. If you have access to the complete cDNA for NMDA R1, the PCR can be used to edit the sequence and add restriction sites in the same manner as is done with the RT-PCR method from total RNA described here. However, by starting the PCR with 1 µg of NR1 plasmid DNA, the PCR can be effective after only five cycles. The negligible mutagenesis caused by the PCR at this level of amplification will create an edited product without any unintended nucleotide changes. For optimum five cycle performance, include 10% glycerol in the PCR.

Ethidium bromide-stained TAE buffered agarose gels (0.1 µg/mL) are observed on a UV transilluminator, and the desired DNA band is excised with a scalpel and transferred to a clean microfuge tube. It is important to keep exposure of the gel to UV light at a minimum. Prolonged exposure will dramatically reduce the cloning efficiency of the DNA. To use the GeneClean purification kit, weigh the gel slice, and add approx 3 vol of the supplied NaI solution to the gel slice and incubate at 55°C with intermittent agitation until the gel slice has dissolved (approx 5'). Four microliters of the thoroughly mixed Glassmilk (BIO 101) sus-

pension are then added, vortexed briefly, and incubated for 5' at room temperature. The suspension is then centrifuged for 30 s in a microfuge to pellet the Glassmilk and adsorbed DNA. This pellet is washed three times by suspension in 0.5 mL of the NEW wash buffer and additional centrifugations. After the final wash spin, the tube is spun again, and the last traces of wash buffer are removed with a pipet tip. The DNA is then eluted from the Glassmilk by addition of 10 μ L H₂O, vortexing briefly, and incubation at 55°C for 3 min. The eluted DNA is recovered as supernatant after another spin in the microfuge. This step is repeated, and the 2 10 μ L fractions combined.

Geneclean is also used after restriction digestion of the gel-isolated PCR DNAs. Simply add 2.5 vol of the NaI solution directly to the restriction digest followed by addition of Glassmilk and the incubation, and wash/elution steps listed above.

3. Bacterial electroporation DH10B frozen electrocompetent cells are thawed on wet ice. Forty microliters of the cells are mixed with 1 μ L of the ligation in an ice-cold 0.1-cm gap electroporation cuvet and pulsed in the Gene Pulser at 1.8 kV. The cells are then suspended in 1 mL of SOC medium (2% tryptone /0.5% yeast extract /10 mM NaCl/2.5 mM KCl/10 mM MgSO₄ /20 mM glucose) and plated onto selective plates (Luria Bertani broth [LB]/2% agar with 50 μ g/mL ampicillin).

CHO cell electroporation Vector DNA containing the NR1 ECD is prepared by using a Qiagen Plasmid Midi Kit (#12143) (Qiagen, Inc., Hilden, Germany) from a 100 mL bacterial culture grown overnight at 37°C from a single colony. The DNA is linearized and sterilized prior to electroporation by digestion of 50 μ g DNA in 400 μ L *ScaI* buffer with 100 U enzyme at 37°C/120' followed by precipitation with NaOAc and EtOH as described. The vacuum-dried pellet is suspended in 50 μ L sterile water. The ethanol precipitation serves to sterilize the DNA. Digestion by *ScaI* linearizes the DNA by cutting within the bacterial ampicillin resistance gene. This serves to facilitate chromosomal integration of the DNA via the free *ScaI* ends of the plasmid and increase the proportion of transfected G418 selected cells which also express the receptor.

CHO-K1 cells should be rapidly growing and at approx 10⁶/mL. Spin down 10⁷ cells at 2000g/5 min and resuspend the pellet in 1 mL GI medium (without serum). Transfer the cells to the *ScaI*-digested DNA (50 μ L), mix gently, and incubate on ice for 10 min. Transfer 0.8 mL of the DNA/cell mix to an ice-chilled 0.4-cm cuvet and electroporate at 250 μ F/400 V. The time constant, τ , should be between 4.5 and 6.0 ms.

4. The analysis of CHO cells by FACS does not require any specialized techniques or additional reagents.
5. FITC labeling of Ab179 Adjust Ab179 (typically 20 mg at 4mg/mL or 5 mL) to 0.1 M carbonate buffer, pH 9.3, at 25°C by dialysis (against 4000 mL) or size exclusion with Sephadex G-25 (Pharmacia, St. Albans, UK). Check recovery of Ab179 by absorbance at A₂₈₀ nm. Transfer Ab179 to an amber vial and chill to 0°C for FITC reaction. Dissolve FITC (Molecular Probes, Eugene, OR, #F-1906) in DMSO to 4 mg/mL. Stirring rapidly, add FITC in 10 μ L aliquots to Ab179 at

50 µg FITC/mg Ab179, and then mix slowly for 2–3 h at 20°C. Remove uncoupled FITC by dialysis overnight at 4°C against three changes of 4000 mL PBS (pH 7.2)/0.1% NaAzide. Aliquot FITC-Ab179 into amber tubes and store at –80°C. An alternative to using an FITC-labeled Ab179 is to use a commercially available FITC-labeled antimouse IgG 1 detection step after staining the cells with Ab179.

Preparation of Mag. 1.1 phage from bacterial stock. Inoculate a single colony from a plate into 5 mL of LB containing:

- 25 µL of 50% K₂HPO₄.
- 25 µL of 20% MgSO₄.
- 25 µL of 20% glucose.
- 10 µL of 50 mg/mL ampicillin.

Grow at 37°C with vigorous shaking to A₆₀₀ = 0.2–0.4. Add 1–2 x 10¹⁰ tu₀ VCSm13 helper phage (Stratagene, La Jolla, CA, #200251). Incubate at 37°C for 30 min without shaking, and then add the following to the 5-mL culture: 50 µL 20% arabinose, and 5 µL 20 mg/mL kanamycin.

Grow at 37°C shaking vigorously overnight. Isolate phage particles by centrifugation of cell suspension in a microfuge, at maximum speed, for 15 min. Transfer the cleared supernatant to a new tube, and precipitate phage by adding 0.2 vol of 20% PEG / 2.5 M NaCl. Mix well, and let stand on ice for 1 h. Pellet phage by centrifugation again for 15 min. Remove as much of the supernatant as possible, and resuspend phage pellet in PBS. Heat the phage suspension to 70°C for 15 min to kill any residual bacteria. Phage stock suspension can be stored for up to 24 h at 4°C or indefinitely at –20°C.

Western blot we prefer to transfer proteins to nitrocellulose with a cold (4°C) phosphate buffer (10 mM NaH₂PO₄/10 mM Na₂HPO₄) in a Bio-Rad Mini Trans-blot cell (limit of 0.8 A, approx 40 V). After transfer, the blot is blocked with 3% nonfat dry milk in PBS for 30 min. Primary antibody, Ab179, is used at 0.5 µg/mL in 10 mL PBS/0.05% Tween 20 for 60 min. The blot is washed 3 times in 25 mL PBS/0.05% Tween 20 for 10 min each. Add peroxidase-conjugated secondary antibody (Tago #34017) at 1:5000 dilution in 10 mL PBS/0.05% Tween-20 for 1 h. Wash as before, and then visualize with the ECL reagent kit from Amersham (Arlington Heights, IL, #RPN 2209).

References:

1. Hollmann, M., and Heinemann, S. (1994) Cloned glutamate receptors. *Annu. Rev. Neurosci.* **17**, 31–108.
2. Nakanishi, S. (1992) Molecular diversity of glutamate receptors and implications for brain function. *Science* **258**, 597–603.
3. Whitehorn, E. A., Tate, E., Yanofsky, S.D., Kochersperger, L., Davis, A., Mortensen, R. B., et al. (1995) A generic method for expression and use of “tagged” soluble versions of cell surface receptors. *Bio/Technology* **13**, 1215–1219.
4. Cwirla, S. E., Peters, E. A., Barrett, R. W., and Dower, W. J. (1990) Peptides on phage: a vast library of peptides for identifying ligands. *Proc. Natl. Acad. Sci. USA* **87**, 6378–6382.

5. Yanofsky, S. D., Baldwin, D. N., Butler, J. H., Holden, F. R., Jacobs, J. W., Balasubramanian, P., et al. (1996) High affinity type I interleukin 1 receptor antagonists discovered by screening recombinant peptide libraries. *Proc. Natl. Acad. Sci. USA* **93**, 7381–7386.
6. Martens, C. L., Cwirla, S. E., Lee, R. Y.-W., Whitehorn, E., Chen, E. Y.-F., Bakker, A., et al. (1995) Peptides Which Bind to E-selectin and Block Neutrophil Adhesion. *J. Biol. Chem.* **270**, 21129–21136.
7. Wrighton, N. C., Farrell, F. X., Chang, R., Kashyap, A. K., Barbone, F. P., Mulcahy, L. S., et al. (1996) *Science* **273**, 458–463.
8. Li, M., Yu, W., Chen, C. -H., Cwirla, S., Whitehorn, E., Tate, E., et al. (1996) In vitro selection of peptides acting at a new site of NMDA glutamate receptors. *Nature Biotechnol.* **14**, 986–991.
9. Moriyoshi, K., Masu, M., Ishii, T., Shigemoto, R., Mizuno, N., and Nakanishi, S. (1991) Molecular cloning and characterization of the rat NMDA receptor. *Nature* **354**, 31–37.
10. Chazot, P. L., Cik, M., and Stephenson, F. A. (1992) Immunological detection of the NMDAR1 glutamate receptor subunit expressed in embryonic kidney 293 cells and in rat brain. *J. Neurochem.* **59**, 1176–1178.

Immunocytochemistry of NMDA Receptors

Ronald S. Petralia and Robert J. Wenthold

1. Introduction

This chapter covers the major immunocytochemical methods used in our laboratory for NMDA receptor localization. There are three methods: pre-embedding immunoperoxidase for light microscopy (LM), the same for electron microscopy (EM), and postembedding immunogold (1–5). General versions of these techniques, as well as related techniques (immunofluorescence, immunocytochemistry of cultures) have been discussed and compared for immunolabeling of all types of glutamate receptors in Petralia and Wenthold (6). Also, for more information on interpretation of immunolabeling data for glutamate receptors, *see* Petralia and Wenthold (7) and Petralia (8). Various modifications of these methods have been described briefly (9–17).

The major NMDA receptor antibodies available are listed in **Table 1** (*see* also tables in recent works [8,18]). Only the antibodies used in immunocytochemical studies of tissues or cultured neurons are included in this table. The monoclonal NR1 antibody made to the II–IV transmembrane region (19,20) labels a major band in immunoblots from cells transfected with NR1, but not NR2A. Lower-mol-wt bands seen in immunoblots from synaptic membranes and NR1-transfected cells (but not in monkey hippocampus) may be breakdown products of NR1 protein. The Wenthold NR1 antibody recognizes a band of 120 kDa in cells transfected with NR1, but not in cells transfected with GluR1-7 or KA1-2. A monoclonal antibody (MAb) made to human NR1 (21) recognizes a band of about 115 kDa in cells transfected with hNMDA1-1 and a slightly higher band in cells transfected with hNMDA1-2. By using a series of truncated fusion proteins and NR1 splice variants, this antibody was shown to recognize specifically the N-terminus insert encoded by exon 5. The Wenthold NR2A/B antibody recognizes a band of 172 kDa in cells transfected with

Table 1
Characterization of NMDA Receptor Antibodies Used in Immunocytochemical Studies^a

Antibody	Amino acids	Region, refs.	Transfected cells		Brain
			Type	Major band	
NR1 (MAb 54)	660–811	III–IV ^b (19,20)	HEK-293	116	116 (rat SM and monkey)
NR1 Bro	660–811	III–IV ^b (53)	HEK-293	116	116/97
NR1 Wen	909–938	C (10)	HEK-293	120	<120
NR1 Aoki	923–938	C (52)	COS-7	110	110
NR1 Jan	864–900	C-alt. splice (55,57)	—	—	120
NR1 Rema	195–357	N ^b (23)	HEK-293	—	116/100
NR1 Ting	Lys + 919-938	C (56,58)	HEK-293	120	120
NR1 Hug	19–38 + Cys	N (56)	—	—	120 (rat spinal cord)
Human NR1 MAb (mNMDA1a.1)	22–268	N ^b , exon 5 region (190–210) (21)	COS-7	~115 hNMDA1-1 >115 hNMDA1-2	~115 + >115 (rat and human)
NR2A/B Wen	1426–1445 (NR2A)	C (11)	HEK-293	172 (NR2A) 165/172 (NR2B)	172
NR2A (MAb 2F6.3D5)	886–1029	C ^b (22)	HEK-293	163	163
NR2B Hug	1463–1482	C (54)	QT-6 fibroblasts	—	180 (rat SM)
NR2D	1307–1323	C (NR2D-2) (59)	—	—	150

^aMAB, monoclonal antibody; all others are polyclonal antibodies. C, C-terminus; N, N-terminus; III–IV, transmembrane regions III–IV; SM, synaptic membranes. Antibody designations: Bro, Brose; Hart, Hartveit; Hug, Haganir; Wen, Wenthold; Jan, Liu et al. (**55**). For details, *see text*.

^bAntibody made from fusion protein; all other antibodies were made from peptides.

NR2A, but not in cells transfected with GluR1-7, KA1-2, or NR1, and recognizes two bands in cells transfected with NR2B (the lower-mol-wt band probably is the deglycosylated form of the protein); it also shows a slight recognition of NR2C and NR2D-2 in transfected cells (but no corresponding bands are seen in brain). An MAb to NR2A (22) immunolabels cells transfected with NR2A, but not those transfected with NR2B, NR2C, or NR2D. The Haganir NR2B antibody recognizes a band in cells transfected with NR2B, but not in cells transfected with NR2A.

In the pre-embedding immunoperoxidase method, immunolabeling is carried out before the tissue is embedded for EM observation (tissue sections used for LM are not embedded). There are several methods for immunoperoxidase labeling. We use a common method with four basic steps:

1. Primary antibody (e.g., NMDA receptor antibody made in a rabbit) binds to the antigenic site in the tissue.
2. Biotinylated secondary antibody binds to the primary antibody.
3. Avidin–biotin–peroxidase compound binds to the secondary antibody.
4. Peroxidase reacts with hydrogen peroxide in the presence of the chromogen, 3',3'-diaminobenzidine tetrahydrochloride (DAB).

The last step causes the precipitation of a reaction product that appears as a brown staining with LM and as a black and often granular material with EM.

Light-microscope pre-embedding immunoperoxidase (**Fig. 1**) can be used for identifying the distribution of NMDA receptors in neuron populations. Such studies are mainly qualitative comparisons of immunolabeling in different brain structures; typically we use “light,” “moderate,” “moderately dense,” and “dense” to describe this staining. Quantitation based on labeling density is possible (23), but such staining may not be very linear.

Electron-microscope pre-embedding immunoperoxidase can be used to localize NMDA receptors to synaptic vs nonsynaptic regions of a neuron (**Figs. 2** and **3**) or among synaptic populations. The tendency for immunoperoxidase reaction products to diffuse from the antigenic site can create problems in the interpretation of the specific localization of the immunolabeling, and this technique is not very useful for quantitative analysis, except in cases where there are large differences in immunolabeling (24). Immunolabeling typically extends only to about 5–10 μm below the surface of the tissue, owing to limitations in tissue penetration (unless done in conjunction with various permeabilization protocols that can cause artifacts; 6,8). This technique has produced some controversial staining patterns using glutamate receptor antibodies (6,8). Thus, in addition to the common presence of staining for NMDA receptors in the postsynaptic density/membrane and associated cytoplasm, presynaptic labeling has been described for at least five different NMDA

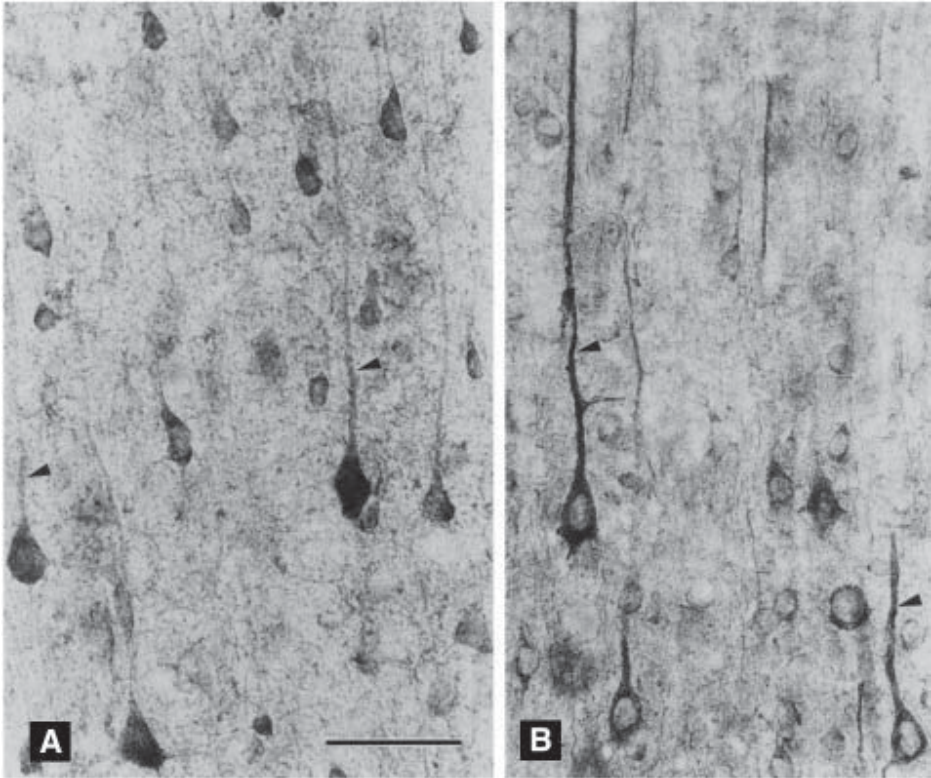


Fig. 1. Coronal sections of layer V of the hindlimb/parietal area of the cerebral cortex labeled with antibody to NR1 (**A**) and NR2A/B (**B**) (LM immunoperoxidase; both are polyclonal antibodies). Arrowheads, apical dendrites of pyramidal cells. Note denser staining with this NR1 antibody in the cell body compared to the apical dendrite of the pyramidal cell; in contrast, staining with the NR2A/B antibody is equally dense in the cell body and apical dendrite of the pyramidal cell. Line scale is 50 μ m. Modified from Petralia et al. (*11*).

receptor antibodies (**Fig. 3**; see discussions in **refs. 8,18**). Although there are a number of physiological/pharmacological studies that indicate the presence of functional presynaptic NMDA receptors at some kinds of synapses, it is possible that the antibodies may recognize another protein in some cases. For example, the pinceau, a highly specialized presynaptic structure formed from the cerebellar basket cell axon and associated with the Purkinje cell axon, labels with NR2A/B antibody (*11,25*). However, the amino acid sequence used to make this antibody shows many similarities to that of a potassium channel, which is found in high concentration in the pinceau (*26,27*), and it is possible

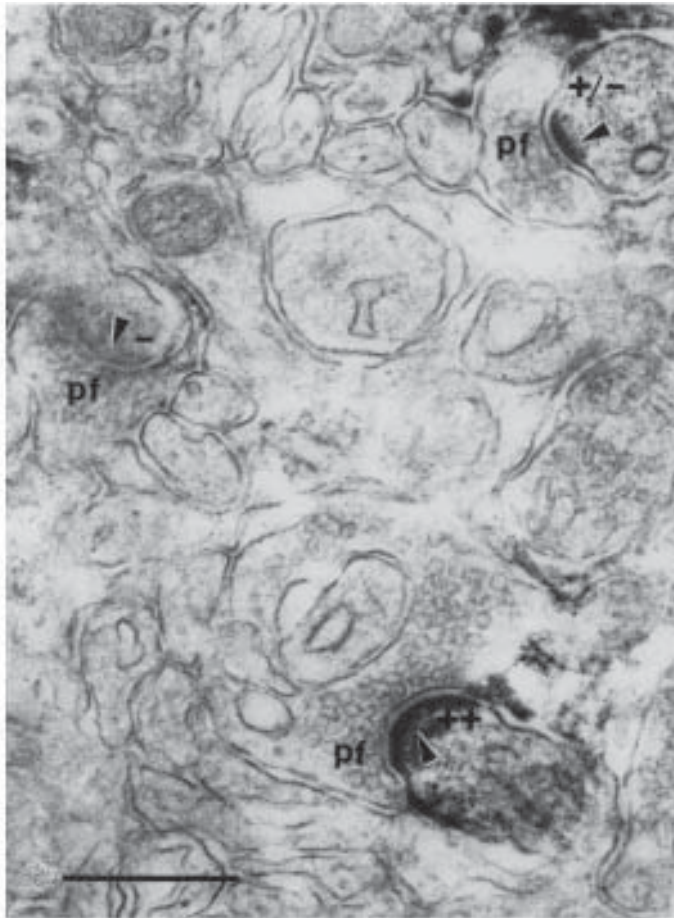


Fig. 2. Electron micrograph of the cerebellar molecular layer immunostained with antibody to NR1 (EM immunoperoxidase; polyclonal antibody). Staining is moderate (++) , light (\pm), and negative (-) in parallel fiber synapses (pf). Note the staining in the postsynaptic density and absence of staining in the synaptic cleft and presynaptic terminal. Line scale is 0.5 μ m. Modified from Zhao et al. (24).

that NR2A/B antibody is detecting the potassium channel protein. In such cases, the significance of labeling patterns may be tested by immunostaining with two or more antibodies made from different regions of the same NMDA receptor molecule (18,28,29). Another controversy involving NMDA receptor antibodies concerns the consistent pattern of postsynaptic staining, i.e., labeling of the postsynaptic density and membrane, but lack of labeling of the synaptic cleft (i.e., the space between the pre- and postsynaptic membranes). For

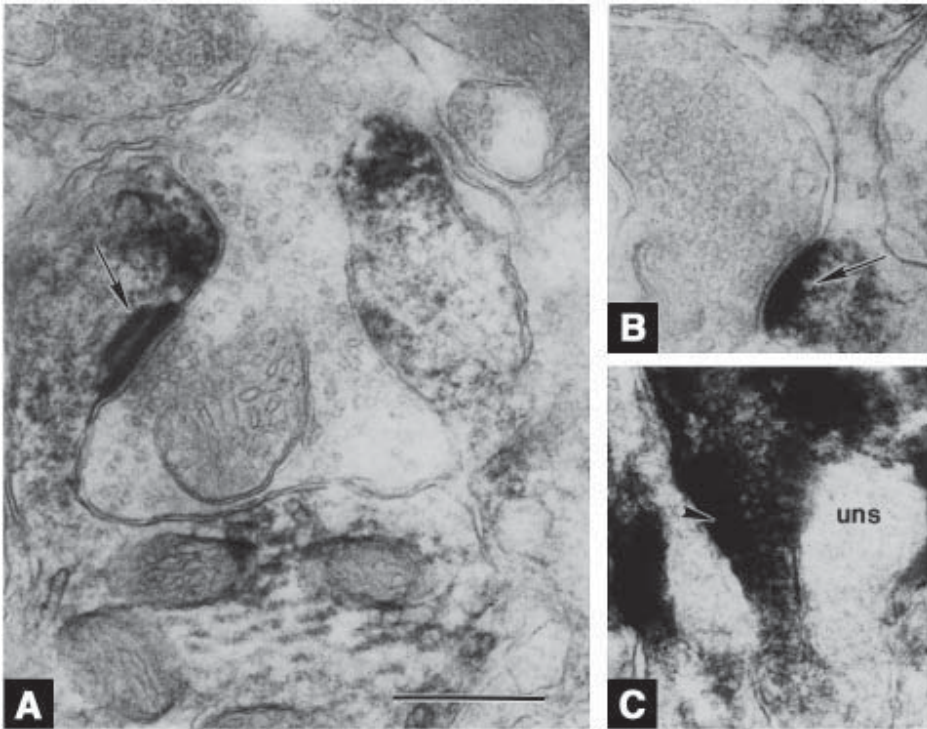


Fig. 3. Electron micrographs (EM immunoperoxidase) of the dorsal cochlear nucleus immunostained with antibodies to NR1 (A; MAb) and NR2A/B (B,C; polyclonal antibody). Note the staining in the postsynaptic density and absence of staining in the synaptic cleft and presynaptic terminal in A and B. In contrast, C illustrates staining in a presynaptic terminal and absence of any postsynaptic staining. Line scale is 0.5 μ m. Modified from Petralia et al. (12).

C-terminus antibodies (*see Table 1* and tables in recent works [8,18]), this pattern is consistent with the intracellular location of the C-terminus (*see review in ref. 30*), but the pattern does not fit for a monoclonal NR1 antibody presumably made to an extracellular loop (*see recent discussion in ref. 8*). In this case, one would expect to see staining in the synaptic cleft; its absence (**Fig. 3A**) suggests that the antigenic site on the extracellular loop of the membrane-incorporated NR1 molecule is blocked somehow (i.e., because of an associated protein or configurational phenomenon). Alternatively, the antigenic site is so close to the postsynaptic membrane that the immunoperoxidase reaction product does not spread into the cleft.

In postembedding immunogold (**Fig. 4**), the immunolabeling is performed after embedding the tissue in a hard material (usually an acrylic resin), and

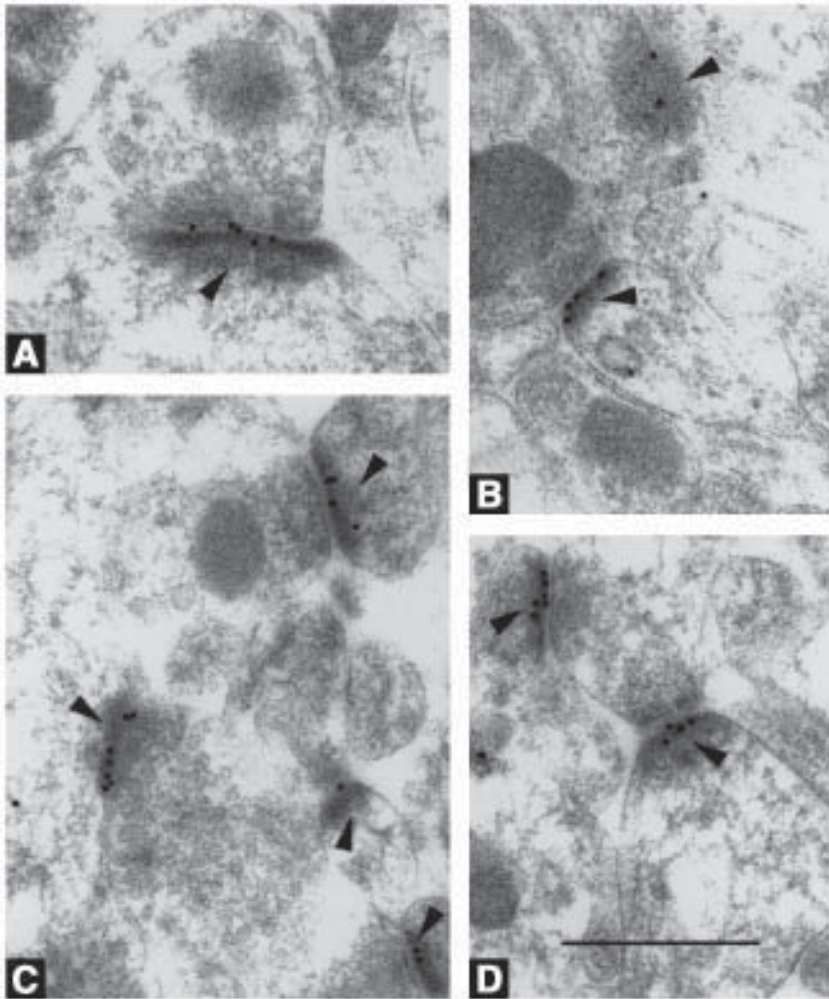


Fig. 4. Electron micrographs (postembedding immunogold) of the hippocampus (A,C,D, CA1-stratum oriens; B, CA3-stratum oriens) immunolabeled with polyclonal antibodies to NR1 (A,B: antibody made similarly to that in Petralia et al. [10]) and NR2A/B (C,D). Note the specific labeling of the postsynaptic membrane and density with 10-nm gold particles (arrowheads). Line scale is 0.5 μ m. Unpublished data of R. S. Petralia, Y.-X. Wang, and R. J. Wenthold.

detection is via protein-gold conjugates (usually attached to the secondary antibody) of standard sizes, most commonly 5, 10, and 15 nm; 1- or 1.4-nm gold particles also are used commonly, but normally must be silver-enhanced for detection. Postembedding immunogold is the most accurate method available

for localization of NMDA and other receptors at the synapse, whereas pre-embedding immunoperoxidase is the most sensitive (*see* recent discussions in **refs. 6,8**). Another advantage of postembedding immunogold is that the labeling is mainly on the surface of the section, so that penetration of labeling into the section is not as important for good labeling as it is when using pre-embedding techniques. Immunogold labeling is particularly useful for quantification because of the ease in counting gold particles, although the linearity of immunogold labeling for receptors has not been determined. However, the resolution is limited to about 15–30 nm (*see* review in **ref. 8**), so that the accuracy of the localization of the gold particles is limited, e.g., a gold particle in the cleft could represent an antigenic site in the postsynaptic membrane.

There are three major methods of postembedding immunogold used for immunolabeling of glutamate receptors. Those of the Weinberg laboratory (**31–33**) employ osmium-free epon embedding using tannic acid and other special additives. The other two methods (Somogyi laboratory method [**34–37**]; Ottersen laboratory method [**38,39**]) involve freeze-substitution and embedding in Lowicryl. Our method is a variation of the Ottersen laboratory method (**14,15,17,40**). In addition, pre-embedding immunogold techniques, usually involving silver enhancement of very small immunogold particles, also are used for localization of glutamate receptors (**34,35,37,41–43**).

2. Materials

2.1. Chemicals

2.1.1. General

1. PBS: We buy a 10X solution without added calcium or magnesium, pH 7.4 (Biofluids, Rockville, MD). The pH of the diluted solution is 7.3–7.4. All buffer working solutions and fixatives are stored at 4°C.
2. Phosphate buffer (PB): A 0.4 M stock solution is made by adding 15.9 g $\text{NaH}_2\text{PO}_4 \cdot \text{H}_2\text{O}$ and 40.5 g Na_2HPO_4 to a container, filling it to 1 L with deionized water, mixing, and adjusting the pH to 7.2. This stock solution is kept at room temperature. Working solutions (0.1 or 0.12 M) are adjusted to pH 7.3, filtered, and kept at 4°C.
3. Fixative: 4% paraformaldehyde, 0.1 or 0.5% glutaraldehyde is added for pre-embedding or postembedding EM procedures, respectively. The paraformaldehyde may be made up the night before the perfusions; glutaraldehyde is added just before the perfusions. To make paraformaldehyde solution, 40 g of paraformaldehyde are added to 300 mL of the 0.4 M PB stock solution (final result is 4% paraformaldehyde in 0.12 M PB; use 250 mL PB stock solution to make 4% paraformaldehyde in 0.1 M PB) and about 400 mL water. The solution is heated with stirring to 60°C, then two to three drops of 5 N NaOH are added, and it is allowed to cool while stirring. The solution is filtered and filled with

water to 1 L. Formaldehyde is a possible carcinogen, and should not be inhaled or allowed to contact skin. All work should be done in the hood. Waste formaldehyde should be treated as a hazardous chemical waste. As an added precaution, the formaldehyde can be mixed with Formalex (Sasco/S&S Company of Georgia, Albany, GA) to neutralize it.

4. Primary antibodies to NMDA receptor subunits: We store our antibodies at -80°C and do not thaw them more than four or five times. We keep aliquots of some antibodies at 4°C for long periods of time; sodium azide is added as a preservative (final solution is 0.01%).

2.1.2. Chemicals Used Specifically for Pre-Embedding Immunoperoxidase Methods

1. 1% Agarose is used to support some specimens for cutting sections with a Microslicer. Start with 2 g agarose, and fill the container to 200 mL with PBS; heat and stir to dissolve. Cool and keep refrigerated. Small amounts can be warmed in a microwave oven before use.
2. DAB (Polysciences, Warrington, PA; 10 mg/20 mL PBS plus 5 μL of 30% hydrogen peroxide). DAB should be made up just before use and kept sealed. Hydrogen peroxide is the last ingredient to be added, immediately before use. DAB is a carcinogen; gloves should be worn at all times and all steps should be done in the hood.
3. 1% Gelatin solution for mounting sections on slides: Start with 2 g gelatin, and fill the container to 150 mL with water. Warm and stir to dissolve, and then add 50 mL of ethanol while stirring (use caution). Refrigerate. It can be warmed in a microwave oven before use.
4. Slide Brite (Sasco/S&S Company of Georgia, Albany, GA) is used for mounting cover slips on slides. It is a substitute for xylene and is relatively nontoxic. The quality of the final slides is similar to that produced using xylene.
5. Permount: It is very toxic and should be used in the hood only. We keep the slides in the hood for several hours after the cover slips are attached to reduce inhalation of the vapors.
6. Propylene oxide (used as an intermediate step between ethanol and epon): It is toxic and will dissolve many plastics. Thus, we use it only in glass containers.
7. Osmium tetroxide: It is very toxic and must be used in the hood; gloves must be worn and the solution should be viewed behind the glass door of the hood (it can fix eyes and skin rapidly). A 1% solution is made from a 4% stock solution (various companies); combine 2.5 mL of the stock solution, 1 mL 10X PBS, and 6.5 mL water. Keep sealed at all times. Dispose of as a hazardous chemical waste.
8. Epon: We use a standard mix and formula (Polysciences): 21 mL Poly/BED 812, 13 mL dodecanyl succinic anhydride (DDSA), 11 mL NMA (nadic[®] methyl anhydride), and 0.7 mL DMP-30 (2,4,6-tri[*dimethylaminomethyl*] phenol). The first three ingredients are stirred together for 3 min, the DMP is added, and then the mix is stirred for 10 min; stirring should be slow to avoid bubble formation.

2.1.3. Chemicals Used Specifically for Postembedding Immunogold Methods

1. Lowicryl HM 20 (Polysciences): This is a nonpolar, hydrophobic acrylic resin, 2.98 g Crosslinker D are mixed with 17.02 g of Monomer E. This is mixed for 30 s by bubbling nitrogen gas through it (keep it covered as much as possible). Then 0.1 g of initiator C is added and nitrogen gas is bubbled for 3 min. Lowicryl has a very pungent odor, and all steps should be done in the hood (including weighing).
2. The methanol that we use for dehydration of tissue is bottled (by the company, Fluka, Ronkonkoma, NY) over a molecular sieve to reduce water absorption.
3. Uranyl acetate and lead citrate, used for the final EM staining, should be passed through a filter before being applied to grids. Both of these are toxic, and precautions should be enforced.
4. TBST buffer: Combine 100 mL of 0.05 M Tris, pH 7.4, with 900 mL of water and 1 g Triton X-100. Water used in any step in the immunogold-labeling procedure should be double-distilled or deionized and sterilized with UV light.
5. Sodium borohydride/glycine treatment. Combine 0.01 g sodium borohydride and 0.0375 g glycine (50 mM) with 10 mL TBST. This should be made up before use.
6. Polyethylene glycol: Mix 0.005 g polyethylene glycol (20,000 mol wt) in 1 mL 1% normal goat serum (or equivalent serum) in TBST. Refrigerate or keep on ice.

2.2. Apparatus

1. Leica EM CPC: Specimens are frozen in liquid propane at -184°C . The device maintains a constant temperature for uniform results. A small piece of double-stick tape is placed on the head of a small aluminum stub (bearing a straight slot in the middle of the head), and the tissue is placed on this with a fine brush. The brush then can be used to remove excess liquid. Then the specimen is plunge-frozen immediately. The frozen tissue on the stub is carried in liquid nitrogen to the Leica AFS.
2. Leica AFS (freeze-substitution device): Once in the AFS, the tissue and tape are removed from the stub, using a fine scalpel. Then the tape can be bent with a fine forceps while gently forcing the tissue off with a fine scalpel. It is crucial that the instruments are very cold (thin cotton gloves are recommended); otherwise, the tissue may thaw partially when touched with the instruments. The instruments can be cooled in the chamber for several minutes before touching the tissue. For faster cooling, the tips of the instruments can be placed for a few seconds in the small transport chamber that is filled with liquid nitrogen ("LN2 cooled cryo transfer container"). All of these steps are done within the AFS chamber, and the instruments are never allowed to move above the rim of the chamber. Also, the nitrogen gas flow control ("TF-regulator control for LN2 vaporizer") should be fully open during these procedures. Similarly, proper cooling of all chemicals used in the AFS is necessary. The sequence we use in the AFS (using instrument terminology) is: T1 = -90°C for 32 h, S1 = increase temperature by $4^{\circ}\text{C}/\text{h}$, T2 = -45°C for 50 h, S2 = increase temperature by $5^{\circ}\text{C}/\text{h}$, T3 = 0°C for 40 h.

3. Methods

3.1. Immunoperoxidase Studies

3.1.1. Fixation and Sectioning

1. Rats are anesthetized with a Ketaset/Rompun mixture (1:1; Ketaset [ketamine]—Aveco Co., Fort Dodge, IA; Rompun [xylazine]—Mobay Corp., Shawnee, KS) by injection into the biceps femoris muscle of the right hindleg (approx 0.1 mL/100 g body wt).
2. The heart is exposed and the right atrium is cut, and a large (for adults) perfusion needle is inserted through the left ventricle to the ascending aorta.
3. Rats are perfused with room-temperature buffer (0.12 M phosphate buffer [PB], pH 7.3) for about 1 min (until the fluid coming from the heart appears to be free from red blood cells).
4. Rats are perfused with cold 4% paraformaldehyde with/without 0.1% glutaraldehyde for electron microscopy/light microscopy, respectively (for about 10 min—less time for young animals) (*see Note 1*).
5. The brain is kept in the same fixative at 4°C for 1 h, and then washed in PBS, pH 7.3–7.4, three times (total time is 1 h). The brain may be stored in PBS for several days if necessary.
6. Fifty-micrometer sections are cut on a Microslicer™ (Pelco DTK-3000W; Ted Pella, Redding, CA). For this, the brain is glued onto the metal plate with a tissue adhesive (Permapond Industrial Grade 910; Electron Microscopy Sciences, Fort Washington, PA [EMS]), and sectioned at a slow speed and moderate frequency to minimize chatter artifacts (*see Note 2*).

3.1.2. Pre-Embedding Immunolabeling (*see Notes 3–7*)

1. Procedures are carried out in plastic 6-, 12-, or 24-well clusters (Costar, Cambridge, MA) using 1.5, 1, or 0.4–0.5 mL of antibody solution, respectively. Incubations are at room temperature unless stated otherwise.
2. For polyclonal antibodies, sections typically are incubated in 10% normal goat serum (the blocking serum should be from the same kind of animal as that used to make the secondary antibody; for mouse MAbs, we use the horse serum in the Vectastain kit and follow the instructions for its use) (*see Note 8*).
3. Sections are incubated in the primary antibody in PBS overnight at 4°C, and then washed three times in PBS over a 1-h period (*see Notes 9 and 10*).
4. Sections are incubated in biotinylated secondary antibody (Vectastain Kit; Vector Laboratories, Burlingame, CA) for 1 h, and then washed three times in PBS (three times over a 1-h period).
5. Sections are incubated in the avidin-biotin-peroxidase (ABC) reagent for 1 h, and then washed in PBS (three times over a 1-h period).
6. Sections are incubated in DAB solution for 1–2 min, and then washed three to four times over a 1-h period. Sections can be stored for a day or more in PBS at 4°C (*see Note 11*).

7. For LM, sections are mounted on slides with 1% gelatin in 25% ethanol (slides are leaned on the side of a shallow, plastic Petri dish and the sections are spread out on the slide with a fine brush) and dried overnight.
8. Slides are soaked in Slide Brite for several minutes, and a cover slip is applied (use a bent needle to lower the cover slip slowly) using 1–3 drops of Permount (Fisher, Pittsburgh, PA).

3.1.3. Further Processing for Electron Microscopy (Continues from the Previous **Step 6**)

1. DAB-treated and washed sections are incubated in 1% osmium tetroxide in PBS for 1 h and then washed 3 times over a 1-h period (*see Note 12*).
2. Sections are dehydrated with 10-min incubations in 50, 75, 95, and 3 × 100% ethanol (*see Note 13*).
3. Sections are placed in a glass vial with propylene oxide. After about 3 min, the propylene oxide is changed (3 min).
4. Sections are placed in a 1:1 mixture of propylene oxide and epon for 1 h, then in a 1:2 mixture for 1–2 h, and then in pure epon overnight.
5. Sections are placed in new epon in an aluminum weighing dish and polymerized for 24 h at 65°C; thus, the sections become embedded in a hardened block of epon.
6. Embedded sections are cut out of the block with a fine hand saw, trimmed, and mounted on an epon stub with tissue adhesive (Permapond Industrial Grade 910; EMS) (*see Note 14*).
7. Thin sections are cut with a diamond knife (Diatome, Fort Washington, PA or Delaware Diamond Knives, Wilmington, DE) on a Leica Reichert Ultracut S ultramicrotome; typically, sections are yellow (about 75 nm) and are collected on copper grids, and examined without EM stains (*see Note 15*).

3.2. Postembedding Immunogold

3.2.1. Tissue Preparation

1. Animals are perfused with 0.12 M PB, followed by 4% paraformaldehyde plus 0.5% glutaraldehyde in 0.12 M PB.
2. Brains are postfixed for 2 h at 4°C and washed three times over a 1-h period. Washing and sectioning (*see Subheading 3.1.1.*) are performed in 0.1 M PB with 4% glucose.
3. Sections are cut on the Microslicer at 200–300 µm.
4. Sections are cryoprotected in glycerol (30 min each in 10, 20, and 30%, and then overnight in 30%) in 0.1 M PB.
5. Sections are plunge-frozen in liquid propane at –184°C in a Leica EM CPC.
6. Frozen sections are immersed in 1.5% uranyl acetate in methanol at –90°C in a Leica AFS freeze-substitution unit (in flowthrough plastic capsules), then infiltrated with Lowicryl HM 20 resin at –45°C (Lowicryl/methanol at 1:1 and 2:1, each for 2 h, followed by pure Lowicryl for 2 h, and then the Lowicryl is changed and kept overnight). The Lowicryl is changed again the next day, and

the capsules with the specimens are moved to Lowicryl-filled gelatin capsules. The double capsules (plastic + gelatin) are transferred to new containers and suspended in 15 mL of ethanol (*see* manufacturer's instructions for more details), then polymerized with UV light (−45 to 0°C; total just under 3 d; *see* **Subheading 2.2.**).

3.2.2. Immunolabeling

1. Thin sections (silver to yellow range) are cut on an Ultramicrotome and placed on grids coated with Coat-quick "G" coating pen (EMS).
2. Grids are attached to Hiraoka support plates (EMS). New plates are used for each antibody (*see* **Note 16**).
3. Grids are incubated in 0.1% sodium borohydride + 50 mM glycine in Tris-buffered saline/0.1% Triton X-100 (TBST, 10 min).
4. Grids are placed in 10% normal goat serum in TBST (10 min).
5. Grids are incubated in primary antibody in 1% serum/TBST for 2 h.
6. Grids are washed in TBST (3 times quickly, then for 10 min, then 3 times quickly).
7. Grids are blocked in 1% serum/TBST for 10 min.
8. Grids are incubated in immunogold (1:20) in 1% serum/TBST + 0.5% polyethylene glycol (20,000 mol wt; to reduce aggregation of gold particles) for 1 h (*see* **Notes 17–19**).
9. Grids are washed in TBST (three times fast) and distilled water (six times fast), and dried.
10. Grids are stained in 1% uranyl acetate for 10 min, then washed three times fast, and dried.
11. Grids are stained in 0.3% lead citrate for 2 min, then washed three times fast, and dried.

4. Notes

1. Glutaraldehyde is excluded for general LM, because it tends to reduce the intensity of immunostaining and sometimes can increase the frequency of artifacts, such as nuclear staining.
2. Most brain structures do not require any supporting matrix. Among those that do need extra support (1% agarose solution in PBS) are the spinal cord, dorsal root ganglia, and pituitary and pineal glands.
3. Recently, we have added a freeze–thaw step to our general procedure for light microscope immunostaining. Immunostaining is enhanced in frozen–thawed sections, presumably because of increased permeability of cell membranes, and background staining is reduced. Usually, there seems to be little ultrastructural damage, but this method may not be reliable for EM. Sections are placed in 30% sucrose in PBS at 4°C for about 24 h, then frozen in dry-ice-cooled acetone (remove excess liquid and use freeze-resistant plastic tubes), and stored at −80°C. After thawing, sections are washed three times in PBS (over 1 h) prior to immunolabeling.
4. Farb et al. (28) compared the effects of three fixatives on glutamate receptor immunolabeling in the rat amygdala. For NMDA receptor antibodies, acrolein-

fixed (3% acrolein and 2% paraformaldehyde) tissue produced generally weaker staining (Wenthold NR1 antibody) or less extensive cytoplasmic staining (Brose NR1 antibody) than either 4% paraformaldehyde- or 4% paraformaldehyde/0.1% glutaraldehyde-fixed tissue.

5. Sodium borohydride treatment (typically 1% for 30 min, prior to serum blocking; **28**) is believed chemically to reduce Schiff bases created by glutaraldehyde-protein crosslinking, to neutralize excess aldehyde groups, to improve cell matrix permeability (**44**), and to reduce nonspecific staining (**45**); we have found sodium borohydride treatment excellent for reducing background staining and improving specific staining patterns when high glutaraldehyde ($\geq 0.5\%$) fixatives are used (unpublished data).
6. Triton X-100 is not used in most of our studies, because Triton X-100 and detergents in general are believed to alter membrane structure and to enhance artifactual diffusion of DAB reaction products (**46–48**). Johnson et al. (**18**) avoided Triton X-100 when using the Wenthold or Brose NR1 antibodies, because these antibodies were “highly sensitive to Triton,” while 0.05% Triton X-100 sometimes was used with the Jan NR1 antibody “to increase antibody penetration.”
7. Other special variations in the NMDA receptor immunoperoxidase staining procedure include silver intensification/gold chloride treatment, the TMB-T/Co-DAB reaction, and Histo blotting. The silver intensification/gold chloride treatment (**22**) produces a reaction product that resembles gold particles using EM. In this case, these particles (representing NR2A immunolabeling) were found in a very discrete location in the rat retina—postsynaptic in the specialized synapses between cone bipolar cells and ganglion cells. The method involves fixation in 4% paraformaldehyde plus 0.2% picric acid, cryoprotection and repeated freeze–thawing, primary and secondary antibody incubations, incubation in extravidin–peroxidase complex, DAB treatment, postfixing in 2.5% glutaraldehyde, silver intensification and treatment with 0.05% gold chloride, postfixing in 2% osmium tetroxide, dehydration and embedding in Epon 812, and staining of thin sections with uranyl acetate and lead citrate. The TMB-T/Co-DAB reaction is a substitute for DAB, and includes 3,3',5,5'-tetramethylbenzidine with ammonium tungstate, cobalt, and DAB (**18**). At the electron microscope level, it produces both a DAB-type reaction product and large crystals. Johnson et al. (**18**; Jan NR1 antibody immunostaining in visual cortex and hippocampus) note that the TMB-T/Co-DAB reaction is more sensitive than DAB at the light microscope level, and provides a clearer distinction between labeled and unlabeled synapses at the electron microscope level. Histo blotting is an adaptation of Western blotting techniques; brain sections are transferred to nitrocellulose membranes, and the resulting “Histo blots” are immunolabeled (NR2 antibodies [**49,50**]). This method may be useful for gross localization of labeling in brain regions, using antibodies that do not work well with conventional immunocytochemistry; the harsher treatment of Histo blotting may free antigenic sites that remain blocked in conventional immunocytochemistry.

8. Sera are not used for subsequent steps in our general immunoperoxidase procedure, although sera are utilized in several steps for certain special procedures. Actually, some serum is retained in the primary antibody solution following the blocking step, since there are no intervening washes between the blocking step and incubation with the primary antibody. However, use of large amounts of sera in many steps following blocking is avoided, because sometimes this has produced a distinctive reduction in apparent specific staining level.
9. The first wash after the primary antibody consists of a transfer of the sections to new wells. Crosscontamination in subsequent washes can be avoided by using separate pipets to remove waste fluids. During exchange of fluids, it is also very important not to let sections dry, which may lead to an artifactual darkening of the section following the final peroxidase/chromogen reaction. Conversely, it is equally important not to leave too much waste fluid in the well when exchanging it with secondary antibody or peroxidase compound, since this can lead to an unplanned dilution of the reagents.
10. Controls include "PBS controls" in which PBS is used in place of the primary antibody (these controls are used in every experiment) and preadsorption controls. Preadsorption control studies involve a comparison among four groups: primary antibody incubated with the peptide (usually conjugated to bovine serum albumin [BSA]; 50 $\mu\text{g}/\text{mL}$), primary antibody incubated with glutaraldehyde-treated BSA (50 $\mu\text{g}/\text{mL}$), primary antibody only, and PBS controls; all are incubated for 24 h and centrifuged before application to the sections.
11. Generally, 1–2 min incubation in DAB solution is required for adequate staining while maintaining clean control sections (i.e., low background staining). If the reaction product is very light after 2 min, longer times can be tried as long as the control remains clean. An alternative method is to incubate the sections in the DAB solutions minus the hydrogen peroxide, for about 10 min. This is followed by the aforementioned incubation in the DAB solution with hydrogen peroxide. This can enhance staining, but can sometimes produce a background staining in the section (evident in the control sections).
12. Spreading of the sections just before adding the osmium tetroxide will ensure that the sections will not harden (owing to osmication) in a folded position.
13. Dehydration times should be shortened when using thinner sections (e.g., 5 min for 30- μm sections) and lengthened when using thicker sections (M. E. Rubio, personal communication).
14. The epon stubs can be made by cutting off the pointed end of a Beem capsule (EMS) and capping the other end; this mold is filled with epon, which then is polymerized. Following rough trimming with handheld blades and with glass knives, 1- μm sections are cut with a HistoKnife (Diatome, Fort Washington, PA) and stained with Epoxy Tissue Stain (EMS) for light microscope observation. Sections are cut on their edge, perpendicular to the plane of vibratome sectioning.
15. Contrast is enhanced by using a small objective lens aperture (20 μm) and by printing negatives on high-contrast paper. However, the selection of print paper

varies with the contrast obtained in the negative. It is most important that the staining owing to the DAB reaction product (i.e., associated with the glutamate receptors) is distinguished readily from the background staining of the section.

16. Hiraoka plates are cleaned after every use by washing them (the plates are bent on a curved plate holder to open the grid slots) for 20–30 min in nitric acid solution (440 μ L/250 mL water), followed by two quick washes in water and one quick wash in ethanol.
17. We prefer 10 nm gold when using only one gold size, because 10 nm gold is small enough to yield a good labeling density (we usually have noticed an inverse relationship between gold size and density of gold labeling), yet large enough to be seen easily (negatives typically are taken at 20,000 \times).
18. For double labeling with antibodies made in two different animal species (e.g., rabbit and mouse), the primary antibodies can be incubated together, and the secondary antibodies can be incubated together. For double labeling with antibodies made in the same animal (e.g., rabbit), the first primary/secondary antibody procedure is completed, and then the dry sections are treated with formaldehyde vapors by sealing the grids in a container with 3 g of paraformaldehyde for 1 h at 80°C; finally, the second primary/secondary antibody procedure is completed, and the grids are stained (38,39,51). This second procedure can be delayed until the next day; we wash for 5 min in water, then 3 times quickly in water, then wash for 5 min in TBST, then 3 times quickly in TBST, then incubate in 1% serum/TBST for 10 min, then incubate with the primary antibody, and continue as in the first procedure.
19. The size difference between the large and small gold particle used for double labeling should be substantial, e.g., 5 + 15 nm, 10 + 25 nm, 10 + 30 nm, to avoid misidentification of gold particles of intermediate size.

Acknowledgments

We thank Y.-X. Wang, M. E. Rubio, and H.-M. Zhao for contributing to the development of many of these methods, O. P. Ottersen, A. S. Landsend, B. Riber, and K. M. Gujord for advice on immunogold techniques, and J. Fex and M. E. Rubio for reviewing the manuscript.

References

1. Sternberger, L. A. (1979) *Immunocytochemistry*, 2nd ed. John Wiley, New York.
2. Beltz, B. S. and Burd, G. D. (1989) *Immunocytochemical Techniques: Principles and Practice*. Blackwell Scientific, Cambridge, MA.
3. Polak, J. M. and Priestley, J. V. (eds.) (1992) *Electron Microscopic Immunocytochemistry: Principles and Practice*. Oxford University, New York.
4. Cuello, A. C. (ed.) (1993) *Immunohistochemistry II*. John Wiley, New York.
5. Hockfield, S., Carlson, S., Evans, C., Levitt, P., Pintar, J., and Silberstein, L. (1993) *Selected Methods for Antibody and Nucleic Acid Probes*, vol. 1. Cold Spring Harbor Laboratory, Plainview, NY.

6. Petralia, R. S. and Wenthold, R. J. (1998) Glutamate receptor antibodies: Production and immunocytochemistry, in *Receptor Localization: Laboratory Methods and Procedures* (Ariano, M. A., ed.), Wiley, New York, pp. 46–74.
7. Petralia, R. S. and Wenthold, R. J. (1996) Types of excitatory amino acid receptors and their localization in the nervous system and hypothalamus, in *Excitatory Amino Acids: Their Role in Neuroendocrine Function* (Brann, D. W. and Mahesh, V. B., eds.), CRC, Boca Raton, FL, pp. 55–101.
8. Petralia, R. S. (1997) Immunocytochemical localization of ionotropic glutamate receptors in neural circuits, in *The Ionotropic Glutamate Receptors* (Monaghan, D. T. and Wenthold, R. J., eds.), Humana Press, Totowa, NJ, pp. 219–263.
9. Petralia, R. S. and Wenthold, R. J. (1992) Light and electron immunocytochemical localization of AMPA-selective glutamate receptors in the rat brain. *J. Comp. Neurol.* **318**, 329–354.
10. Petralia, R. S., Yokotani, N., and Wenthold, R. J. (1994) Light and electron microscope distribution of the NMDA receptor subunit NMDAR1 in the rat nervous system using a selective anti-peptide antibody. *J. Neurosci.* **14**, 667–696.
11. Petralia, R. S., Wang, Y.-X., and Wenthold, R. J. (1994) The NMDA receptor subunits NR2A and NR2B show histological and ultrastructural localization patterns similar to those of NR1. *J. Neurosci.* **14**, 6102–6120.
12. Petralia, R. S., Wang, Y.-X., Zhao, H.-M., and Wenthold, R. J. (1996) Ionotropic and metabotropic glutamate receptors show unique postsynaptic, presynaptic and glial localizations in the dorsal cochlear nucleus. *J. Comp. Neurol.* **372**, 356–383.
13. Petralia, R. S., Wang, Y.-X., Singh, S., Wu, C., Shi, L., Wei, J., et al. (1997) A monoclonal antibody shows discrete cellular and subcellular localizations of mGluR1 α metabotropic glutamate receptors. *J. Chem. Neuroanat.* **13**, 77–93.
14. Petralia, R. S., Wang, Y.-X., Mayat, E., and Wenthold, R. J. (1997) Glutamate receptor subunit 2-selective antibody shows a differential distribution of calcium-impermeable AMPA receptors among populations of neurons. *J. Comp. Neurol.* **385**, 456–476.
15. Rubio, M. E. and Wenthold, R. J. (1997) Glutamate receptors are selectively targeted to postsynaptic sites in neurons. *Neuron* **18**, 939–950.
16. Wang, Y.-X., Wenthold, R. J., and Petralia, R. S. (1996) Distribution of glutamate receptor subunits associated with auditory nerve terminals in the anteroventral cochlear nucleus. *Assoc. Res. Otolaryngol. Abstr.* **19**, 168.
17. Wang, Y.-X., Wenthold, R. J., Ottersen, O. P., and Petralia, R. S. (1998) Endbulb synapses in the anteroventral cochlear nucleus express a specific subset of AMPA-type glutamate receptor subunits. *J. Neurosci.* **18**, 1148–1160.
18. Johnson, R. R., Jiang, X., and Burkhalter, A. (1996) Regional and laminar differences in synaptic localization of NMDA receptor subunit NR1 splice variants in rat visual cortex and hippocampus. *J. Comp. Neurol.* **368**, 335–355.
19. Sucher, N. J., Brose, N., Deitcher, D. L., Awobuluyi, M., Gasic, G. P., Bading, H., et al. (1993) Expression of endogenous NMDAR1 transcripts without receptor protein suggests post-transcriptional control in PC12 cells. *J. Biol. Chem.* **268**, 22,299–22,304.

20. Siegel, S. J., Brose, N., Janssen, W. G., Gasic, G. P., Jahn, R., Heinemann, S. F., et al. (1994) Regional, cellular, and ultrastructural distribution of *N*-methyl-D-aspartate receptor subunit 1 in monkey hippocampus. *Proc. Natl. Acad. Sci. USA* **91**, 564–568.
21. Nash, N. R., Heilman, C. J., Rees, H. D., and Levey, A. I. (1997) Cloning and localization of exon 5-containing isoforms of the NMDAR1 subunit in human and rat brains. *J. Neurochem.* **69**, 485–493.
22. Hartveit, E., Brandstätter, J. H., Sassoè-Pognetto, M., Laurie, D. J., Seeburg, P. H., and Wässle, H. (1994) Localization and developmental expression of the NMDA receptor subunit NR2A in the mammalian retina. *J. Comp. Neurol.* **348**, 570–582.
23. Rema, V. and Ebner, F. F. (1996) Postnatal changes in NMDAR1 subunit expression in the rat trigeminal pathway to barrel field cortex. *J. Comp. Neurol.* **368**, 165–184.
24. Zhao, H.-M., Wenthold, R. J., Wang, Y.-X., and Petralia, R. S. (1997) Delta glutamate receptors are differentially distributed at parallel and climbing fiber synapses on Purkinje cells. *J. Neurochem.* **68**, 1041–1052.
25. Schell, M. J., Brady, R. O., Jr., Molliver, M. E., and Snyder, S. H. (1997) D-Serine as a neuromodulator: Regional and developmental localizations in rat brain glia resemble NMDA receptors. *J. Neurosci.* **17**, 1604–1615.
26. Laube, G., Roper, J., Pitt, J. C., Sewing, S., Kistner, U., Garner, C. C., et al. (1996) Ultrastructural localization of Shaker-related potassium channel subunits and synapse-associated protein 90 to septate-like junctions in rat cerebellar Pinceaux. *Mol. Brain. Res.* **42**, 51–61.
27. McNamara, N. M., Averill, S., Wilkin, G. P., Dolly, J. O., and Priestley, J. V. (1996) Ultrastructural localization of a voltage-gated K⁺ channel alpha subunit (KV 1.2) in the rat cerebellum. *Eur. J. Neurosci.* **8**, 688–699.
28. Farb, C. R., Aoki, C., and LeDoux, J. E. (1995) Differential localization of NMDA and AMPA receptor subunits in the lateral and basal nuclei of the amygdala: A light and electron microscopic study. *J. Comp. Neurol.* **362**, 86–108.
29. Farb, C. R. and LeDoux, J. E. (1997) NMDA and AMPA receptors in the lateral nucleus of the amygdala are postsynaptic to auditory thalamic afferents. *Synapse* **27**, 106–121.
30. Hollmann, M. (1997) The topology of glutamate receptors, in *The Ionotropic Glutamate Receptors* (Monaghan, D. T. and Wenthold, R. J., eds.), Humana Press, Totowa, NJ, pp. 39–79.
31. Phend, K. D., Rustioni, A., and Weinberg, R. J. (1995) An osmium-free method of epon embedment that preserves both ultrastructure and antigenicity for post-embedding immunocytochemistry. *J. Histochem. Cytochem.* **43**, 283–292.
32. Kharazia, V. N., Phend, K. D., Rustioni, A., and Weinberg, R. J. (1996) EM colocalization of AMPA and NMDA receptor subunits at synapses in rat cerebral cortex. *Neurosci. Lett.* **210**, 37–40.
33. Popratiloff, A., Weinberg, R. J., and Rustioni, A. (1996) AMPA receptor subunits underlying terminals of fine-caliber primary afferent fibers. *J. Neurosci.* **16**, 3363–3372.

34. Baude, A., Nusser, Z., Roberts, J. D. B., Mulvihill, E., McIlhinney, R. A. J., and Somogyi, P. (1993) The metabotropic glutamate receptor (mGluR1a) is concentrated at perisynaptic membrane of neuronal subpopulations as detected by immunogold reaction. *Neuron* **11**, 771–787.
35. Baude, A., Nusser, Z., Molnár, E., McIlhinney, R. A. J., and Somogyi, P. (1995) High-resolution immunogold localization of AMPA type glutamate receptor subunits at synaptic and non-synaptic sites in rat hippocampus. *Neuroscience* **69**, 1031–1055.
36. Nusser, Z., Mulvihill, E., Streit, P., and Somogyi, P. (1994) Subsynaptic segregation of metabotropic and ionotropic glutamate receptors as revealed by immunogold localization. *Neuroscience* **61**, 421–427.
37. Luján, R., Nusser, Z., Roberts, J. D. B., Shigemoto, R., and Somogyi, P. (1996) Perisynaptic location of metabotropic glutamate receptors mGluR1 and mGluR5 on dendrites and dendritic spines in the rat hippocampus. *Eur. J. Neurosci.* **8**, 1488–1500.
38. Matsubara, A., Laake, J. H., Davanger, S., Usami, S., and Ottersen, O. P. (1996) Organization of AMPA receptor subunits at a glutamate synapse: A quantitative immunogold analysis of hair cell synapses in the rat organ of Corti. *J. Neurosci.* **16**, 4457–4467.
39. Landsend, A. S., Amiry-Moghaddam, M., Matsubara, A., Bergersen, L., Usami, S., Wenthold, R. J., et al. (1997) Differential localization of δ glutamate receptors in the rat cerebellum: Coexpression with AMPA receptors in parallel fiber-spine synapses and absence from climbing fiber-spine synapses. *J. Neurosci.* **17**, 834–842.
40. Zhao, H.-M., Wenthold, R. J., and Petralia, R. S. (1998) Glutamate receptor targeting to synaptic populations on Purkinje cells is developmentally regulated. *J. Neurosci.* **18**, 5517–5528.
41. Aoki, C., Rhee, J., Lubin, M., and Dawson, T. M. (1997) NMDA-R1 subunit of the cerebral cortex co-localizes with neuronal nitric oxide synthase at pre- and postsynaptic sites and in spines. *Brain Res.* **750**, 25–40.
42. Bernard, V., Somogyi, P., and Bolam, J. P. (1997) Cellular, subcellular, and subsynaptic distribution of AMPA-type glutamate receptor subunits in the neostriatum of the rat. *J. Neurosci.* **17**, 819–833 (correction in *J. Neurosci.* **17**, 7180).
43. Gracy, K. N. and Pickel, V. M. (1997) Ultrastructural localization and comparative distribution of nitric oxide synthase and *N*-methyl-D-aspartate receptors in the shell of the rat nucleus accumbens. *Brain Res.* **747**, 259–272.
44. Willingham, M. C. (1983) An alternative fixation-processing method for preembedding ultrastructural immunocytochemistry of cytoplasmic antigens: The GBS (glutaraldehyde-borohydride-saponin) procedure. *J. Histochem. Cytochem.* **31**, 791–798.
45. Kosaka, T., Nagatsu, I., Wu, J.-Y., and Hama, K. (1986) Use of high concentrations of glutaraldehyde for immunocytochemistry of transmitter-synthesizing enzymes in the central nervous system. *Neuroscience* **18**, 975–990.
46. Willingham, M. C. and Yamada, S. S. (1979) Development of a new primary fixative for electron microscopic immunocytochemical localization of intracellular antigens in cultured cells. *J. Histochem. Cytochem.* **27**, 947–960.

47. Courtoy, P. J., Picton, D. H., and Farquhar, M. G. (1983) Resolution and limitations of the immunoperoxidase procedure in the localization of extracellular matrix antigens. *J. Histochem. Cytochem.* **31**, 945–951.
48. Fang, S., Christensen, J., Conklin, J. L., Murray, J. A., and Clark, G. (1994) Roles of Triton X-100 in NADPH-diaphorase histochemistry. *J. Histochem. Cytochem.* **42**, 1519–1524.
49. Wenzel, A., Villa, M., Mohler, H., and Benke, D. (1996) Developmental and regional expression of NMDA receptor subtypes containing the NR2D subunit in rat brain. *J. Neurochem.* **66**, 1240–1248.
50. Wenzel, A., Fritschy, J. M., Mohler, H., and Benke, D. (1997) NMDA receptor heterogeneity during postnatal development of the rat brain: Differential expression of the NR2A, NR2B, and NR2C subunit proteins. *J. Neurochem.* **68**, 469–478.
51. Wang, B.-L. and Larsson, L.-I. (1985) Simultaneous demonstration of multiple antigens by indirect immunofluorescence or immunogold staining. Novel light and electron microscopical double and triple staining method employing primary antibodies from the same species. *Histochemistry* **83**, 47–56.
52. Aoki, C., Venkatesan, C., Go, C.-G., Mong, J. A., and Dawson, T. M. (1994) Cellular and subcellular localization of NMDA-R1 subunit immunoreactivity in the visual cortex of adult and neonatal rats. *J. Neurosci.* **14**, 5202–5222.
53. Brose, N., Gasic, G. P., Vetter, D. E., Sullivan, J. M., and Heinemann, S. F. (1993) Protein chemical characterization and immunocytochemical localization of the NMDA receptor subunit NMDA R1. *J. Biol. Chem.* **268**, 22,663–22,671.
54. Lau, L.-F. and Haganir, R. L. (1995) Differential tyrosine phosphorylation of *N*-methyl-D-aspartate receptor subunits. *J. Biol. Chem.* **270**, 20,036–20,041.
55. Liu, H., Wang, H., Sheng, M., Jan, L. Y., Jan, Y. N., and Basbaum, A. I. (1994) Evidence for presynaptic *N*-methyl-D-aspartate autoreceptors in the spinal cord dorsal horn. *Proc. Natl. Acad. Sci. USA* **91**, 8383–8387.
56. O'Brien, R. J., Mammen, A. L., Blackshaw, S., Ehlers, M. D., Rothstein, J. D., and Haganir, R. L. (1997) The development of excitatory synapses in cultured spinal neurons. *J. Neurosci.* **17**, 7339–7350.
57. Sheng, M., Cummings, J., Roldan, L. A., Jan, Y. N., and Jan, L. Y. (1994) Changing subunit composition of heteromeric NMDA receptors during development of rat cortex. *Nature* **368**, 144–147.
58. Tingley, W. G., Roche, K. W., Thompson, A. K., and Haganir, R. L. (1993) Regulation of NMDA receptor phosphorylation by alternative splicing of the C-terminal domain. *Nature* **364**, 70–73.
59. Wenzel, A., Benke, D., Mohler, H., and Fritschy, J.-M. (1997) *N*-methyl-D-aspartate receptors containing the NR2D subunit in the retina are selectively expressed in rod bipolar cells. *Neuroscience* **78**, 1105–1112.

The Use of Ligand Binding in Assays of NMDA Receptor Function

Ian J. Reynolds and Terre A. Sharma

1. Introduction

The quantification of drug interaction with NMDA receptors has been greatly facilitated by the use of ligand binding assays. The first assays for this receptor measured NMDA-sensitive [^3H]glutamate binding (*see 1* for review). However, [^3H]glutamate has relatively low affinity for the receptor, and is also a substrate for transport processes in brain membranes, which can make it difficult to isolate receptor binding from ligand sequestration. The recognition that dissociative anesthetics, such as phencyclidine and ketamine, were NMDA receptor antagonists (**2,3**) was an important pharmacological advance, because these drugs were more potent NMDA antagonists than others available at the time. However, phencyclidine also proved to be a difficult ligand to use because of nonspecific binding. The identification of MK801 (dizocilpine) and thienylphencyclidine (TCP) as highly potent and very selective inhibitors of NMDA receptor function (**4–6**) brought the possibility of ligand binding to NMDA receptors into the mainstream.

The NMDA receptor is pharmacologically complex. Activation of the receptor requires occupation of both the NMDA and glycine recognition sites by agonists (**7,8**), and the overall level of activation of the receptor is subject to modulation by numerous modulatory sites that may be occupied by endogenous or exogenous modulators. These include Mg^{2+} , Zn^{2+} , polyamines, reactive oxygen species, ifenprodil-like drugs, and some steroids (**9**). The complexity is compounded by the likelihood that native receptors exist in several heterodimeric or trimeric forms, which may have different pharmacological properties (**9**). Nevertheless, it has been possible to develop assay strategies that can adequately quantitate these modulatory effects in native receptors using a single ligand

binding assay, and recent studies suggest that the approach is effective in expressed recombinant receptors, too.

This approach exploits the properties of the binding of phencyclidine-like drugs to the receptor. Early studies with ketamine and subsequent studies with MK801 (3,10) demonstrated that phencyclidine-like drugs probably bind within the pore of the channel operated by NMDA. When applied to ligand binding assays, this gives the binding the interesting property of being sensitive to the state of activation of the channel, so that NMDA and glycine site agonists were found to increase [³H]MK801 and [³H]TCP binding to the receptor (6,11,12). Indeed, the properties of ligand binding to the phencyclidine site appeared to mimic closely the guarded receptor model previously proposed to account for local anesthetic blockade of voltage-sensitive Na⁺ channels (13,14). Subsequent studies determined that the main effect of NMDA and glycine site activation was to increase the rate of binding, without having much effect on equilibrium affinity of [³H]MK801 (15,16). The effects of agonist addition will only be evident if the [³H]MK801 assay is performed under nonequilibrium conditions. Using this approach, it became possible to assay agonist and antagonist activity at the NMDA and glycine sites, and generate results that accurately predict the effectiveness of pharmacological agents in physiological paradigms.

The assay of other modulatory effects is readily achieved, but is often harder to interpret mechanistically. Ligands that bind to the other modulatory sites may alter the activation properties of the receptor or may alter [³H]MK801 binding by allosterically modifying the binding site (Table 1). A number of noncompetitive antagonists, including Zn²⁺ and also pentamidine-like drugs (17), inhibit [³H]MK801 by restricting activation of the receptor, in accordance with their use- and voltage-independent, noncompetitive blockade of the receptor seen in functional preparations. The prominent effects of polyamine agonists and antagonists, on the other hand, appear to be mediated at least partly by an alteration of [³H]MK801 binding affinity (16). Under these circumstances of multiple drug binding sites, it can be difficult to determine whether drugs of unknown mechanisms of action are interacting competitively or noncompetitively with the [³H]MK801 binding site. Classically, a drug that alters the density of binding sites without altering [³H]MK801 affinity in a saturation binding experiment would be classified as a noncompetitive antagonist. However, in the case of [³H]MK801 binding, there are few modulators that have been shown to have this property. It is nevertheless inappropriate to assume that a drug that decreases the affinity of [³H]MK801 without altering binding site density is acting competitively at the phencyclidine site. Instead, an analysis of the influence of the unknown drug on the rate of dissociation of [³H]MK801 is likely to be more revealing. Drugs which compete with

Table 1
Effects of Modulators on [³H]MK801 Binding

Modulator	Effect of modulator on binding ^a			Notes
	Nonequilibrium	Saturation	Dissociation	
NMDA site				
Agonists	↑	No effect	↑	
Antagonists	↓	No effect	↓	For example, CPP, AP5
Glycine site				
Agonists	↑	No effect	↑	
Antagonists	↓	No effect	↓	For example, 7-Chlorokynureate
Channel blockers	↓	Decrease affinity	No effect	For example, Phencyclidine and MK801
Divalent cations				
Mg ²⁺ -like	↑ then ↓	Decrease affinity	↑	Cations include Ca ²⁺ , Sr ²⁺ , Ba ²⁺
Zn ²⁺ -like	↓	?	↓	Includes Hg ²⁺ and Cd ²⁺
Polyamines	↑ then ↓	Increase affinity	↓	Arcaïne blocks increase in binding
Protons	↓	No effect	↓	
Ifenprodil	↓	?	?	Selective inhibitor of NR2B receptors
Sulphydryl reduction	↑	?	?	For example, Dithiothreitol

^aThe change in binding or rate indicated by the arrows compares the effect to the properties of [³H]MK801 binding in the presence of low concentrations of glutamate and glycine.

[³H]MK801 do not alter dissociation rates, whereas allosteric interactions are reflected as a change in the dissociation rate (18).

There are a number of other ligands that can be used to label directly the other sites on the NMDA receptor. As noted above, [³H]glutamate has been used, as has [³H]glycine, to label the primary agonist sites. High-affinity antagonists for the NMDA and glycine site are also available, such as [³H]CGP 39653 and [³H]L-689560, respectively (19,20). Although these ligands are undoubtedly useful for direct assays of ligand binding to their respective sites, they cannot readily distinguish between agonists and antagonists, and the effects of allosteric modulators are generally less dramatic than is observed with [³H]MK801. For these reasons, the following methods will focus exclusively on [³H]MK801 and related drugs.

2. Materials

2.1. Sources of Receptors

All rodent brains provide membranes that have a relatively high density of NMDA receptors. The highest density of binding sites are found in the forebrain, so midbrain, cerebellum, and spinal cord can normally be discarded prior to preparation. Brains may be obtained fresh or frozen. The goal of the membrane preparation process is to minimize the contamination of membranes by factors that affect binding. Using rat brains, add 10 vol (about 10 mL) of 10 mM HEPES/NaOH pH 7.4 at 4°C to which 1 mM EDTA has been added, for each forebrain. Homogenize the brain thoroughly using a polytron. Centrifuge the homogenate at 40,000g for 15 min. Resuspend the pellet in fresh buffer using the polytron, and repeat the centrifugation step. This process should be repeated four additional times. The pellet can then be resuspended in 10 mM HEPES without EDTA in the original volume. The homogenate is then incubated at 37°C for 30 min, which is followed by three additional centrifugation steps in 10 mM HEPES without EDTA. Resuspending this pellet in the original volume should yield a stock suspension of membranes that contains about 3–5 mg membrane protein/mL of suspension. This can be frozen at –20°C until use and is stable for several months if kept frozen. Aliquots of this frozen stock should be thawed and used, but refreezing unused material is not recommended.

2.2. Binding Assay Supplies

Binding assays may be performed using any one of the several cell harvester systems that are currently available. We routinely use a Brandel 24-well cell harvester along with Schleicher and Schuell #32 glass fiber filter strips. However, [³H]MK801 is characterized by relatively little nonspecific binding to filters, so the make and model of the harvester or filters should not be critical.

It is not necessary to pretreat the filters to reduce nonspecific binding, although it is more convenient to use filters that have been dampened with buffer prior to use. Likewise, the choice of buffer for performing the assay or subsequent washes is not critical provided that a low-ionic strength is used (≤ 20 mM). We routinely use 10 mM HEPES (pH adjusted to 7.4 with NaOH), and Tris is equally effective. At the end of the assay incubation, the assay mixture is aspirated onto the filter strips and washed with 10–15 vol of buffer. [3 H]MK801 dissociates relatively slowly, so the wash duration does not have a marked effect on the level of binding observed, and the wash buffer can be kept at room temperature without adversely affecting binding. Filters need to be incubated in scintillant for ≥ 1 h prior to counting.

2.3. Ligands and Drugs

[3 H]MK801 is obtained from New England Nuclear (Boston, MA). Glutamate and glycine can be obtained from any source. Unlabeled MK801 is available from Research Biochemicals Inc. (Natick, MA), as are most of the other standard NMDA receptor ligands that may be used to characterize the assay. MK801 is soluble in aqueous solutions at 10 mM and is stable for months when kept frozen at -20°C between use, and can be thawed and refrozen.

3. Methods

3.1. Nonequilibrium Assays

1. For a 1-mL final assay volume, the incubation can conveniently contain 0.05 mL [3 H]MK801, 0.1 mL of the appropriate glutamate and glycine concentration (*see step 2*), 0.1 mL of the drug to be assayed, and 0.75 mL tissue. [3 H]MK801 should be at a concentration of 0.5–1 nM (about 50,000 cpm). The glutamate and glycine and assay drug can be prepared as 10X stock solutions, and the tissue should reach a final concentration of about 100 $\mu\text{g}/\text{mL}$. This represents a 40-fold dilution of the stock prepared as described above. All solutions should be prepared with the assay buffer of choice.
2. The final glutamate and glycine concentration will vary depending on experimental design. In practice, it is not possible to eliminate completely endogenous sources of these amino acids. To avoid the problem of variable low levels of glutamate and glycine, we supplement basal binding conditions with 30 nM glycine and 100 nM glutamate, to provide a low, but known concentration of these modulators. Thirty and 100 μM of glycine and glutamate, respectively, represent suprasaturating concentrations.
3. Nonspecific binding can be determined using 30 μM MK801 or 300 μM ketamine.
4. The incubation is initiated by the final addition of the tissue suspension. Assays are incubated at room temperature for 2 h. The binding reaction does not reach equilibrium under these conditions. Assays are terminated by filtration under vacuum onto prewetted glass fiber filter strips as described above. Filters are

washed with three 5-mL aliquots of assay buffer. Filters are then incubated in scintillant for ≥ 1 h prior to counting.

5. This procedure should yield about 400–800 cpm of binding with low glutamate and glycine concentrations, which should increase to about 1500–2000 cpm with the addition of saturating concentrations of the agonists. About 80% or more of the binding under the latter condition should be specific binding.

3.2. Saturation Assays

To measure saturation parameters accurately, it is necessary to modify the above conditions to ensure that equilibrium is reached. Under conditions of basal concentrations of glutamate and glycine, it has been estimated that ~ 24 h may be required to reach equilibrium (**15**). Tissue degradation may become a problem with this duration of incubation. Assays performed in the presence of saturating glycine and glutamate concentrations reach equilibrium in 4–6 h (**16**).

1. The above conditions should be modified to increase the incubation time to 6 h for saturation experiments provided that saturating glycine and glutamate concentrations are used.
2. It is necessary to reduce the concentration of [^3H]MK801 to about 0.2 nM, because the K_d for [^3H]MK801 is about 1 nM at equilibrium (**16**). The saturation curve can then be defined by adding increasing concentrations of unlabeled MK801, which is more cost-effective than changing the concentration of [^3H]MK801.
3. Decreasing the added radioactivity will decrease the signal in the assay, so it may be necessary to increase the volume of the assay to 2 or 3 mL. By increasing the tissue and total amount of radioactivity added, it is possible to increase the counts retrieved on the filter to a more manageable level.
4. This procedure should yield a K_d for [^3H]MK801 of about 1 nM.

3.3. Dissociation Assays

In order to measure dissociation rates, it is first necessary to generate a mixture of tissue and ligand that has reached equilibrium, and then to terminate effectively the association reaction so that the dissociation reaction can be measured. In the approach described below, the on reaction is terminated by a 120-fold dilution of the ligand. This reduces the association to a negligible rate, because this component is concentration-dependent and, thus, allows measurement of the off reaction.

1. Incubate tissue at a concentration of about 3 mg/mL protein with 10 nM [^3H]MK801, 1 μM glycine, and 3 μM glutamate for 2 h. At the higher ligand concentration, the mixture will reach equilibrium more quickly.
2. Nonspecific binding is determined by adding an aliquot of the ligand–tissue mixture to a tube containing 3 mL buffer and 30 μM MK801 immediately after the tissue and [^3H]MK801 have been mixed (i.e., prior to the 2-h incubation).

3. After the 2-h incubation, add 25 μL of the incubation mixture to 3 mL assay buffer that contains the drug to be assayed. Mix well by vortexing, and incubate for an appropriate additional time period. A range of incubation times between 1 and 180 min is usually sufficient to define the dissociation reaction. It is usually desirable to perform the dilutions at different time-points and then terminate the assay by filtration at the same time, although the reverse approach can also be used.
4. Vacuum filtration and radioactivity determination are exactly as described above.
5. This procedure should yield off rates of about $0.003\text{--}0.004\text{ min}^{-1}$ when the dissociation reaction is measured in the presence of saturating concentrations of glutamate and glycine.

3.4. Data Analysis

Data obtained from both saturation and dissociation experiments can be fit by standard software packages designed for analyzing ligand binding data, or by generic curve-fitting programs intended for nonlinear, least-squares analysis. This principles that should be applied to the analysis of nonequilibrium binding experiments, such as those described in **Subheading 3.1.**, have not been precisely established. However, empirically it appears that such data can be fitted by a standard four-parameter logistic equation as is found in packages like Prism (GraphPad Inc. San Diego, CA). Some of the conditions that will be assayed will generate binding curves that rise rather than fall (i.e., modulators that stimulate binding), and such curves are not always well tolerated by standard ligand binding analysis programs.

4. Notes

1. Variation may be encountered in the extent to which binding can be stimulated by NMDA, glycine, or polyamine site agonists. The extent of stimulation over basal levels is sensitive to contamination by endogenous amino acids or divalent cations, so that high basal levels of binding caused by endogenous glutamate and/or glycine will not be further stimulated by the addition of exogenous agonists. It is possible to measure the amino acid content of the membrane preparation (21). It is also possible to infer the concentration of contaminants by the sensitivity of binding to inhibition by site-specific antagonists. Thus, a glycine-contaminated preparation will show binding that is less sensitive to inhibition by 7-chlorokynurenate, for example.
2. [^{125}I]Iodo-MK801 can be used as the radioligand in these studies. It has similar properties to [^3H]MK801 (22), although iodination of the parent compound slightly alters the affinity for the receptor. It is also helpful to use filter strips pretreated with a 0.3% polyethyleneimine solution prior to filtration to decrease filter binding of the ligand. Typically, much lower concentrations of iodinated ligands are used owing to the higher specific activity, and this results in slowing of the association kinetics. As a consequence, receptor activation typically has

- proportionately larger effects on [125 I]Iodo-MK801 binding compared to the tritiated counterpart.
3. As noted in **Table 1**, [3 H]MK801 binding is sensitive to inhibition by protons. The pK_a of the pH-sensitive site is close to 7.4, which is the normal pH for the assay buffer. Thus, small variations in the pH of the assay buffer could have a substantial impact on the properties of [3 H]MK801 binding (**23**). Specifically, decreasing pH will slow association and dissociation, and result in a decrease in nonequilibrium binding.
 4. Although rodent brains provide an abundant source of NMDA receptors for binding assays, it may be preferable to use receptors of defined subunit composition transiently or stably expressed in cell lines. The expression approaches are described elsewhere in this volume. Studies thus far suggest that the properties of [3 H]MK801 or [125 I]MK801 binding in expressed receptors are similar to those encountered in native receptors (**24,25**) with the expected differences between the ifenprodil sensitivity of NR1/2A and NR1/2B combinations. Typically, a lower density of binding is found compared to forebrain membranes. However, in most cases the expressed receptors have not been characterized in the same pharmacological detail as the native receptors.
 5. Investigators have reported both monophasic and biphasic dissociation kinetics for [3 H]MK801. Adding noncompetitive inhibitors of [3 H]MK801 binding, such as Mg^{2+} , that greatly increase the dissociation rate almost inevitably reveals biphasic dissociation kinetics. This suggests that under control conditions, the existence of the two phases may be difficult to resolve because of a relative small fraction of the dissociation in one state or because of similarity in the rate constants.

References

1. Foster, A. C. and Fagg, G. E. (1984) Acidic amino acid binding sites in mammalian neuronal membranes: their characteristics and relationship to synaptic receptors. *Brain Res. Rev.* **7**, 103–164.
2. Anis, N. A., Berry, S. C., Burton, N. R., and Lodge, D. (1983) The dissociative anaesthetics, ketamine and phencyclidine, selectively reduce excitation of central mammalian neurones by *N*-methyl-aspartate. *Br. J. Pharmacol.* **79**, 565–575.
3. Honey, C. R., Miljkovic, Z., and MacDonald, J. F. (1985) Ketamine and phencyclidine cause a voltage-dependent block of responses to *L*-aspartic acid. *Neurosci. Lett.* **61**, 135–139.
4. Wong, E. H. F., Kemp, J. A., Priestley, T., Knight, A. R., Woodruff, G. N., and Iversen, L. L. (1986) The anticonvulsant MK 801 is a potent *N*-methyl-D-aspartate antagonist. *Proc. Natl. Acad. Sci. USA* **83**, 7104–7108.
5. Vignon, J., Chicheportiche, R., Chicheportiche, M., Kamenka, J. M., Geneste, P., and Lazdunski, M. (1983) [3 H]TCP: a new tool with high affinity for the PCP receptor in rat brain. *Brain Res.* **280**, 194–197.
6. Johnson, K. M., Snell, L. D., and Morter, R. S. (1988) *N*-methyl-D-aspartate enhanced 3 H-TCP binding to rat cortical membranes: effects of divalent cations and glycine, in *Sigma and Phencyclidine-like Compounds as Molecular Probes in*

- Biology* (Domino, E. F. and Kamenka, J. M., eds.). NPP Books, Ann Arbor, pp. 259–268.
7. Johnson, J. W. and Ascher, P. (1987) Glycine potentiates the NMDA response in cultured mouse brain neurons. *Nature* **325**, 529–531.
 8. Kleckner, N. W. and Dingledine, R. (1988) Requirement for glycine in activation of NMDA receptors expressed in *Xenopus* oocytes. *Science* **241**, 835–837.
 9. McBain, C. J. and Mayer, M. L. (1994) *N*-methyl-D-aspartic acid receptor structure and function. *Physiol. Rev.* **74**, 723–760.
 10. Huettner, J. E. and Bean, B. P. (1988) Block of NMDA-activated current by the anticonvulsant MK-801: selective binding to open channels. *Proc. Natl. Acad. Sci. USA* **85**, 1307–1311.
 11. Reynolds, I. J., Murphy, S. N., and Miller, R. J. (1987) ³H-labelled MK-801 binding to the excitatory amino acid receptor complex from rat brain is enhanced by glycine. *Proc. Natl. Acad. Sci. USA* **84**, 7744–7748.
 12. Foster, A. C. and Wong, E. H. F. (1987) The novel anticonvulsant MK801 binds to the activated state of the *N*-methyl-D-aspartate receptor in rat brain. *Br. J. Pharmacol.* **91**, 403–409.
 13. Bonhaus, D. W. and McNamara, J. O. (1988) *N*-methyl-D-aspartate receptor regulation of uncompetitive antagonist binding in rat brain membranes: kinetic analysis. *Mol. Pharmacol.* **34**, 250–255.
 14. Starmer, C. F., Packer, D. L., and Grant, A. O. (1987) Ligand binding to transiently accessible sites: mechanisms for varying apparent binding rates. *J. Theor. Biol.* **124**, 335–341.
 15. Kloog, Y., Haring, R., and Sokolovsky, M. (1988) Kinetic characterization of the phencyclidine *N*-methyl-D-aspartate receptor interaction: evidence for a steric blockade of the channel. *Biochemistry* **27**, 843–848.
 16. Reynolds, I. J. (1990) Arcaine uncovers dual interaction of polyamines with the *N*-methyl-D-aspartate receptor. *J. Pharmacol. Exp. Ther.* **255**, 1001–1007.
 17. Reynolds, I. J. and Aizenman, E. (1992) Pentamidine is an *N*-methyl-D-aspartate receptor antagonist and is neuroprotective in vitro. *J. Neurosci.* **12**, 970–975.
 18. Reynolds, I. J. and Miller, R. J. (1988) Multiple sites for the regulation of the *N*-methyl-D-aspartate receptor. *Mol. Pharmacol.* **33**, 581–584.
 19. Sills, M. A., Fagg, G., Pozza, M., Angst, C., Brundish, D. E., Hurt, S. D., et al. (1991) [³H]CGP 39653: A new *N*-methyl-D-aspartate antagonist radioligand with low nanomolar affinity in rat brain. *Eur. J. Pharmacol.* **192**, 19–24.
 20. Grimwood, S., Moseley, A. M., Carling, R. W., Leeson, P. D., and Foster, A. C. (1992) Characterization of the binding of [³H]L-689,560, an antagonist for the glycine site on the *N*-methyl-D-aspartate receptor, to rat brain membranes. *Mol. Pharmacol.* **41**, 923–930.
 21. Reynolds, I. J. and Palmer, A. M. (1991) Regional variations in [³H]MK801 binding to rat brain NMDA receptors. *J. Neurochem.* **56**, 1731–1740.
 22. Rajdev, S. and Reynolds, I. J. (1992) Effects of monovalent and divalent cations on 3-(+)[¹²⁵I]iododizocilpine binding to the *N*-methyl-D-aspartate receptor of rat brain membranes. *J. Neurochem.* **58**, 1469–1476.

23. Rajdev, S. and Reynolds, I. J. (1993) Effects of pH on the actions of dizocilpine at the *N*-methyl-D-aspartate receptor complex. *Br. J. Pharmacol.* **109**, 107–112.
24. Laurie, D. J. and Seeburg, P. H. (1994) Ligand affinities at recombinant *N*-methyl-D-aspartate receptors depend on subunit composition. *Eur. J. Pharmacol. Mol. Pharmacol.* **268**, 335–345.
25. Lynch, D. R., Anegawa, N. J., Verdoorn, T., and Pritchett, D. B. (1994) *N*-methyl-D-aspartate receptors: Different subunit requirements for binding of glutamate antagonists, glycine antagonists, and channel-blocking agents. *Mol. Pharmacol.* **45**, 540–545.

Calmodulin Modification of NMDA Receptors

Su Zhang and Richard L. Huganir

1. Introduction

Using approaches of molecular biology, biochemistry, and electrophysiology, we have recently discovered the interaction between calmodulin and NMDA receptor ion channels (*1*). We demonstrated that calmodulin specifically binds to two distinct sites (CBS1 and CBS2) localized in the C-terminus of the NR1 subunits, causing a fourfold decrease in the channel open probability (*1*). The CBS1 (K_d for calmodulin: 80 nM) covers most of the C-terminal region that is upstream to the C1 cassette, designated C0, and common to all NR1 splice variants (NR1a–h). The CBS2 (K_d for calmodulin: 4 nM) is downstream of the CBS1 and located in the C1 exon cassette, which is subject to alternative splicing. We further showed that calmodulin binding to the CBS1 is responsible for an important property of NMDA receptors, Ca²⁺-dependent inactivation (*2*). More studies are expected to clarify further the biological significance and molecular mechanisms of interaction between calmodulin and NMDA receptors. This chapter is a stepwise description of our laboratory protocols used in studying the modulation of NMDA receptors by calmodulin. We hope that the protocols will help people investigate the issue and evaluate the literature in this field.

2. Materials and Methods

2.1. Cell Culture

The physiological role of calmodulin binding to specific sites of the NR1 subunit can be investigated using recombinant NMDA receptors. There are many cell lines to choose for expressing recombinant NMDA receptors on cell membranes. We prefer using human embryonic kidney (HEK) 293 cells,

because they have few interfering endogenous ion channels and a clean membrane surface, which facilitates formation of a tight seal with a patch pipet.

1. HEK 293 cells can be purchased from American Type Culture Collection (ATCC CRL 1573, ATCC, Manassas, VA). Frozen stocks of HEK 293 cells should be stored in a liquid-nitrogen freezer.
2. Thaw frozen cells quickly at 37°C. As soon as the cells are thawed, transfer them (usually in 1 mL frozen medium) into a 100 × 20 mm tissue-culture dish (Falcon 3003), and add 9 mL culture medium (*see ref. 3* for the ingredients). After 6–8 h, newly thawed HEK 293 cells should settle down on the bottom of dish. Change the culture medium to get rid of the frozen medium completely.
3. Grow HEK 293 cells in the minimum essential medium (MEM) containing 10% fetal bovine serum (FBS, not necessary to use one that is heat-inactivated), 2 mM L-glutamine, 1 mM sodium pyruvate, 100 U/mL penicillin, and 100 µg/mL streptomycin in an incubator set at 37°C and 5% CO₂. The culture medium should be kept at 4°C and used within a month. Only take the necessary amount of the culture medium to warm up to 37°C before use in order to preserve freshness of the remaining medium.
4. Split the cells every 3–4 d when 70–80% cell confluence is reached. Aspirate out the culture medium, rinse the cells with warm (37°C) phosphate-buffered saline (PBS) once (5 mL/100 × 20 mm dish), and aspirate out the PBS. Use 1 mL/100 × 20 mm dish of 0.05% Trypsin-0.53 mM EDTA (Gibco-BRL, Gaithersburg, MD) at 37°C for 5 min to detach the cells from the bottom of the dish. Add in warm culture medium (5 mL/100 × 20 mm dish) to stop trypsin. The culture medium contains inhibitors of trypsin.
5. Plate HEK293 at 0.5–1 × 10⁵ cells/mL. After four passages from thawing, cells are usually fully recovered and ready for transfection. Discard cells after 35 passages, because they usually have very low transfection efficiency.
6. The laboratory supply of frozen HEK 293 cells should be monitored and periodically regenerated to prevent depletion. To make frozen medium, add dimethyl sulfoxide (DMSO) and FBS into the culture medium to the level of 10 and 50%, respectively. At 75% cell confluence of the 4th passage, use 4 mL of the frozen medium to wash down cells in a 100 × 20 mm culture dish and stock at 1 mL cells/vial in 1.8-mL Cryo tube vials (Nalgene Nunc International, Milwaukee, WI). Freeze the cells in two steps: first at –80°C overnight and then transfer to a liquid-nitrogen freezer for long-term storage.
7. For the purpose of patch recording, HEK 293 cells should be plated on a sterilized glass cover slip a day before transfection. To sterilize the glass cover slip, first dip glass cover slips in 100% ethanol for 15 min and then flame them in a tissue-culture hood.
8. For excising membrane patches from cultured HEK 293 cells, a strong adherence of the cells to glass cover slips is essential. To this end, the sterilized glass cover slips should be coated by immersion into poly-L-lysine (10 µg/mL in H₂O) for 1 h at room temperature and rinsed off with sterilized water to remove excessive unbound poly-L-lysine, which is toxic to cells.

2.2. Transfection

Transfection should be carried out 1 d after splitting cells for best transfection efficiency. Although HEK 293 cells could be transfected with many other methods, we prefer the following calcium phosphate-based method (3).

1. 0.1X TE: 1 mM Tris and 0.1 mM EDTA.
2. 2X BES: 50 mM BES (*N,N*-bis[2-Hydroxyethyl]-2-aminoethanesulfonic acid), 280 mM NaCl, and 1.5 mM Na₂HPO₄. Adjust the pH to 6.96, which is very critical. Inaccuracy in the determination of the pH could greatly reduce the transfection efficiency.
3. 2.5 M CaCl₂.
4. Keep these three solutions at 4°C.
5. To express functional recombinant NMDA receptors in HEK 293 cells, the cDNA cocktail should contain both NR1 and NR2 subunit cDNA constructs. Start with the quantity ratio of NR1 and NR2 as 1:1. The ratio may be adjusted according to relative expression levels or other experimental purposes.
6. Dilute 20 µg cDNA in 450 µL 0.1X TE in a 1.5-mL centrifuge tube, and mix thoroughly by pipeting up and down. Note: The quantities of transfection reagents given here are for transfecting HEK293 cells in a 100 × 20 mm tissue-culture dish having 10 mL culture medium and should be adjusted proportionally for transfecting cells cultured in different-sized dishes.
7. Add 50 µL 2.5 M CaCl₂, and mix thoroughly.
8. Add 500 µL 2X BES drop by drop, and mix thoroughly. Let it sit at room temperature for 30 min. In the meantime, place the dish of cells to be transfected in an incubator of 3% CO₂ and 35°C for 30 min. This conditioning will enhance transfection efficiency.
9. Pipeting the DNA mixture a few times, and slowly add it into the dish. Then gently shake the dish. At this time you should be able to see numerous small black calcium precipitates in the dish under a microscope.
10. Keep the cells in the incubator of 3% CO₂ and 35°C for 6–8 h to complete transfection.
11. Aspirate the transfection medium, and wash the cells with PBS (10 mL/100-cm dish) for 30 min at 37°C. Replace the PBS with a fresh culture medium.
12. Add 500 µM DL-2-amino-5-phosphonovaleric acid (APV), an NMDA receptor antagonist, into the culture medium to protect transfected cells from NMDA receptor-mediated excitotoxicity.
13. The transfected cells express functional recombinant NMDA receptors during 40–90 h after the completion of transfection. This is the time frame for carrying out physiology experiments.
14. For visual identification of positively transfected cells, include cDNA encoding the cell-surface antigen CD8 in the cDNA mixture at 1/10 of total cDNAs. CD8 is a cell-surface antigen. The transfected cells can be labeled and identified by anti-CD8 antibody-coated beads.

2.3. Single-Channel Recording from Inside-Out Membrane Patches

The calmodulin binding sites are localized in intracellular C-terminus of NR1 subunit. Inside-out membrane patches are used to gain access to these sites for administration of calmodulin. The effect of calmodulin binding to these sites on NMDA receptor functions can be evaluated by analyzing changes in single-channel currents.

1. Use a patch-clamp setup, including a PCM VCR tape recorder or equivalent, an air-table, an inverted light microscope with DIC optics, a 20× lens, a glass-bottomed recording chamber, and other necessary electrophysiology equipment.
2. Before experiments, add anti-CD8 antibody-coated microspheres (Dynabeads M-450, Dynal Inc., Lake Success, NY) into the culture dish at a concentration of 1 μL beads/mL culture medium to label transfected cells. Gently shake for 5 min (1 Hz).
3. Break the glass cover slip with a glass cutter into several pieces to fit the recording chamber. Transfer one of them at a time to the recording chamber, which contains the Ca^{2+} -free solution described in **Table 1**. Put the rest of them back to the CO_2 incubator for later use.
4. Include a low concentration of glutamate or NMDA (1–2 μM) with 10 μM glycine in Ca^{2+} -free solution as the pipet solution to achieve a steady-state activation of NMDA receptors on the membrane patches.
5. Use thick-wall glass capillaries (e.g., Corning 7052 glass, 1.5 mm od, 0.75 mm id, Warner Instrument Corp., Hamden, CT) to pull pipet electrodes.
6. Coat the pipets from the shoulder to 100 μm above the tip with Sylgard 184 silicone (Dow Corning Corp., Midland, MI). Cure the Sylgard by rotating the pipet inside a hot coil.
7. Fire-polish the pipet tip down to 1.5/m od with a microforger. The impedance of the pipet electrodes filled with the Ca^{2+} -free solution should be about 4–8 $\text{M}\Omega$.
8. Apply a small positive pressure to the pipet by pumping 0.1 cc air into the pipet holder with a 1-cc syringe to keep the pipet tip clean. Choose a clean surface area of a bead-decorated cell to land the pipet. Gently press the pipet onto the cell until a small dimple appears around the tip of the pipet.
9. Release the positive pressure inside the pipet. Usually a tight seal of 10 $\text{G}\Omega$ or greater will be formed between the rim of the pipet tip and the cell membrane in a few seconds. If not, apply a small negative pressure to the pipet to promote sealing and release it as soon as an ideal seal is formed.
10. Under this cell-attached mode, seeing unitary channel opening events indicates that the membrane patch contains NMDA receptors. Gently pull back the pipet (axially if the micromanipulator allows; otherwise straight upward) to excise an inside-out membrane patch.
11. Sometimes the edge of the excised membrane patch reseals by itself, forming a vesicle. A sign of a resealed vesicle is the disappearance of the unitary events

Table 1
Ca²⁺-Free Solution for Single-Channel Recording^a

Chemicals	Conc., mM	Formula Weight	g/L
NaCl	145	58.44	8.47
EGTA	1	380.40	0.38
HEPES	10	238.30	2.38

^aTitrate to pH 7.3–7.35 with NaOH. Filter before use. The osmolarity should be close to 300 mmol/kg. Store at 4°C.

detected under the cell-attached mode. Lift the pipet tip into the air briefly (a few seconds) to break the vesicle.

12. Voltage-clamp the inside-out membrane patch with the command voltage set at 60 mV, corresponding to a –60 mV transmembrane potential with the intracellular side being more negative.
13. The extracellular side of the membrane patch is continuously exposed to the agonists inside the pipet to achieve a steady-state activation of the NMDA receptors. Upward unitary deflections are “inward” (from the extracellular side to the intracellular side) currents through individual NMDA receptor ion channels during their opening (see **Fig. 1**).
14. Tape and compare the properties of single-channel NMDA currents under the following three conditions.
 - a. Perfuse the inside-out membrane patch with the Ca²⁺-free solution (see **Table 1**) as control (**Fig. 1A**).
 - b. Switch the perfusion solution to calmodulin (2–100 nM) in 50 μM Ca²⁺ solution (see **Table 2**) (**Fig. 1B**).
 - c. Switch back to the Ca²⁺-free solution to see if the change is reversible (**Fig. 1C**).
15. In the presence of Ca²⁺, calmodulin reduces the frequency and duration of channel opening of NMDA receptors without affecting the single-channel conductance (**I**).

2.4. Whole-Cell Recording and Concentration Clamp

The excised membrane patch imposes some nonphysiological conditions on NMDA receptors, such as stretching and losing some interactive cytoplasmic factors, just to name a few. Furthermore, since NMDA receptors are highly Ca²⁺-permeable, the NMDA receptor-mediated Ca²⁺-influx might play a role in calmodulin-induced inactivation of NMDA receptors. Thus, calmodulin modulation of NMDA receptors can be further evaluated under the whole-cell, patch-clamp configuration, which preserves a relatively intact intracellular environment and allows us to explore the biological significance of interaction between calmodulin and NMDA receptors.

1. The internal and external buffer solutions (Mg-free) for whole-cell patch recordings are described in **Tables 3–5**.

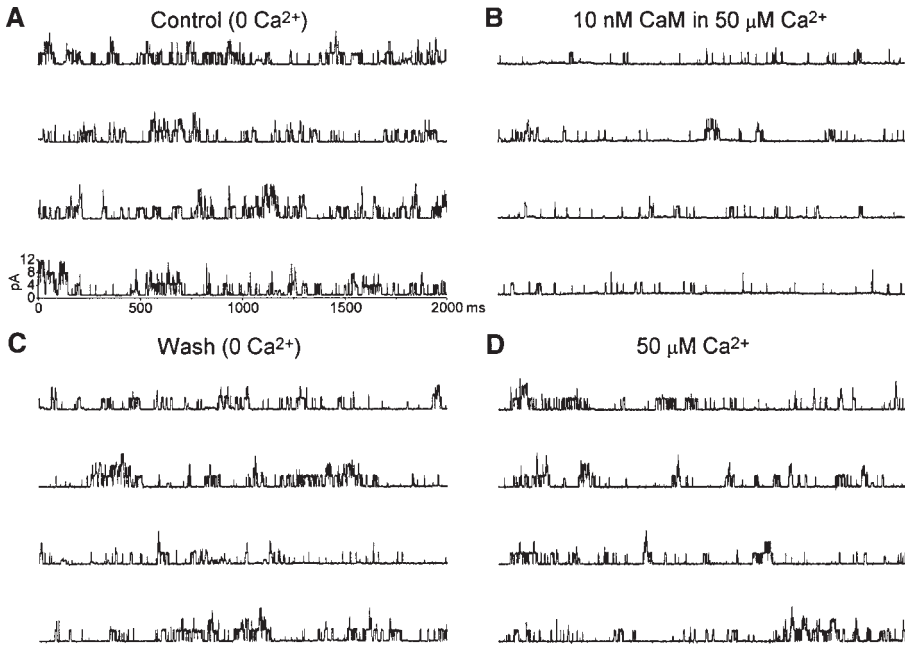


Fig. 1. Calmodulin inactivates NMDA receptor ion channels. (A–D) represent portions of a recording of NMDA channel currents (upward events; $V_c = 60$ mV) from a single inside-out membrane patch excised from an HEK 293 cell transfected with cDNAs encoding NR1a and NR2A subunits. Different experimental conditions are shown sequentially in each panel. The time and amplitude scales shown in (A) also apply to (B–D). (A) Continuous 8-s recording of NMDA channel currents under control where the cytoplasmic side of the patch was perfused with a Ca^{2+} -free buffer containing 1 mM EGTA. The baseline and primary conductance levels are indicated by dotted line. (B) The frequency and duration of channel opening were greatly reduced when 10 nM calmodulin in 50 μM Ca^{2+} was perfused onto the cytoplasmic face of the patch. (C) The inhibitory effect was reversed by washing with Ca^{2+} -free buffer containing 1 mM EGTA. (D) The inhibitory effect was not the result of Ca^{2+} ions alone, since perfusion with 50 μM without calmodulin did not inhibit channel activity. This figure is adapted from Fig. 5 of the **ref.** (1).

2. The internal solution (**Table 3**) contains ATP and should be kept on ice before use.
3. Use a piezoelectric instant solution exchanger (e.g., Burleigh LSS-3100, Burleigh Instruments Inc., Fishers, NY) to achieve a sudden concentration clamp by sweeping the liquid interface of two jet streams, containing the control solution and glutamate, respectively, across a cell.
4. To avoid mechanical coupling from the piezo device to the recording pipet through the air table, use a heavy stand for the piezo device, and stuff a foam pad between the stand and the air table.

Table 2
50 μ M Ca^{2+} Solution for Single-Channel Recording^a

Chemicals	Conc., mM	Formula Weight	g/L
NaCl	145.0	58.44	8.47
$\text{CaCl}_2(2\text{H}_2\text{O})$	0.7	147.00	8.47
Nitrilotriacetic acid	2.0	191.10	0.38
HEPES	10.0	238.30	2.38

^aTitrate to pH 7.3–7.35 with NaOH. Filter before use. The osmolarity should be close to 300 mmol/kg. Store at 4°C.

Table 3
Pipet Solution for Whole-Cell Recording^a

Chemicals	Conc., mM	Formula Weight	g/100 mL
CsCl	140	168.36	2.35
EGTA	10	380.40	0.38
HEPES	15	238.30	0.36
MgATP	4	507.20	0.20

^aTitrate to pH 7.3–7.35 with CsOH. Filter before use. The osmolarity should be close to 300 mmol/kg. Store at –20°C.

Table 4
Extracellular Solution of 0 mM Ca^{2+} ^a

Chemicals	Conc., mM	Formula Weight	g/L
NaCl	135.0	58.44	7.89
KCl	5.4	74.56	0.405
EGTA	1.0	380.40	0.38
HEPES	15.0	238.30	3.58
Glucose	15.0	180.20	2.703

^aTitrate to pH 7.3–7.35 with NaOH. Filter before use. The osmolarity should be close to 300 mmol/kg. Store at 4°C.

Table 5
Extracellular Solution of 1.8 mM Ca^{2+} Solution^a

Chemicals	Conc., mM	Formula Weight	g/22L
NaCl	135.0	58.44	7.89
KCl	5.4	74.56	0.41
$\text{CaCl}_2(2\text{H}_2\text{O})$	1.8	147.00	0.265
HEPES	15.0	238.30	3.58
Glucose	15.0	108.20	2.70

^aTitrate to pH 7.3–7.35 with NaOH. Filter before use. The osmolarity should be close to 300 mmol/kg. Store at 4°C.

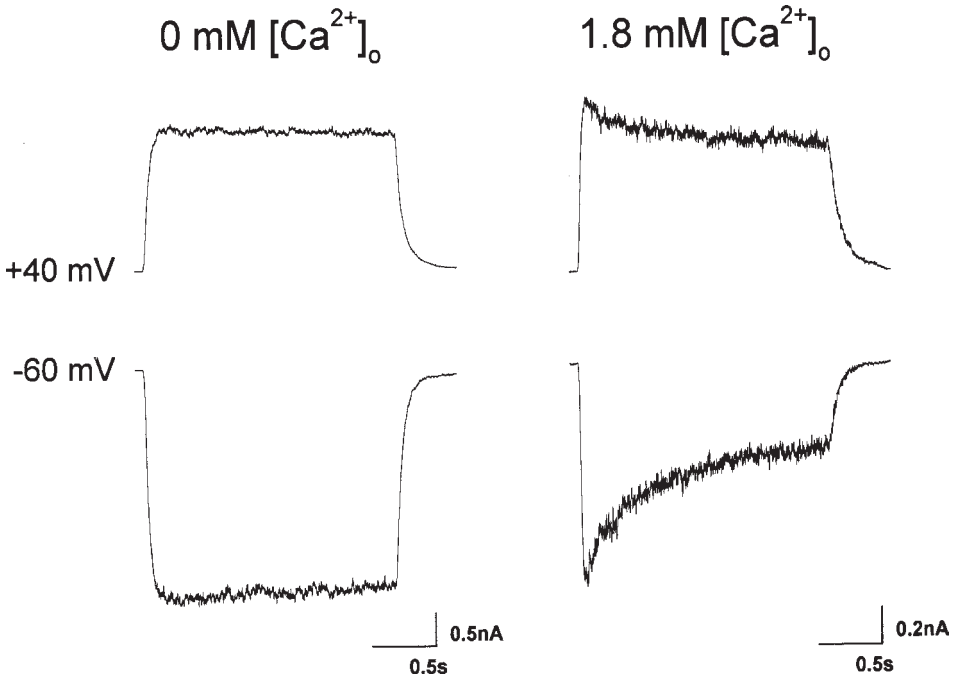


Fig. 2. Ca^{2+} -dependent inactivation of recombinant NMDA receptors. Whole-cell currents in response to a 2-s glutamate pulse ($10 \mu\text{M}$ glutamate and $10 \mu\text{M}$ glycine) were recorded from an HEK 293 cell transfected with NR1c/NR2A. The cell was voltage-clamped at $+40 \text{ mV}$ (upper panels) or -60 mV (lower panels) and bathed in the Ca^{2+} -free (left panels) or the 1.8 mM Ca^{2+} buffer. Without extracellular Ca^{2+} , NMDA currents are nondesensitized (left panels). With a physiologically normal level of extracellular Ca^{2+} , NMDA responses are smaller, probably because of a smaller Ca^{2+} conductance through NMDA channels, and decay during the glutamate application, as a result of Ca^{2+} -influx. This Ca^{2+} -dependent inactivation is much smaller when the cell is depolarized (the upper right panel), owing to a reduced electrical driving force for Ca^{2+} -influx.

5. Use a double-channel syringe pump (e.g., WPI sp210iw, WPI, Sarasota, FL) to drive two jet streams of extracellular solutions out of a θ tubing (with an inner diameter of 500 μm at each semicircle opening) at a constant flow rate (about 0.2 mL/min). Adjust the flow rate to strike a balance between a sharp liquid interface and mechanical stability.
6. The tip of the θ tubing should be kept away from the bottom of the recording chamber at least 3 mm to avoid a bouncing turbulence.
7. To measure the solution exchange time, a liquid-junction current waveform can be recorded with an open tip recording pipet using two solutions with different

concentrations of salt. Adjust the position of the pipet until a clean rectangular waveform is seen with a 10–90% rise time of about 2 ms. Use the coordinates of the pipet tip position in reference to the θ tubing as a start point for experiments. Using whole-cell current responses to fine-tune the pipet tip position and flow rate is often needed.

8. Use the same procedures to label transfected cells and break the cover slip as described in **steps 2 and 3 of Subheading 2.3.**
9. Use thin-wall glass capillaries (e.g., Corning 7052 glass, 1.65 mm od, 1.2 mm id, A-M Systems, Inc., Carlsborg, WA) to pull pipet electrodes. Fire-polish the pipet tip down to 2 μ m od with a microforger. The impedance of the pipet electrodes filled with the internal solution (**Table 3**) should be about 2–3 M Ω .
10. For whole-cell, patch-clamp experiments, choose a visually solitary CD8 positive cell to patch, because connected HEK 293 cells are electrically coupled through gap junctions. Follow **steps 8, 9, and 10 in Subheading 2.3.** to form a tight cell-attached seal.
11. To form a whole-cell, patch-clamp configuration, gently apply a negative pressure to the pipet to break the membrane patch under the pipet. Simultaneously using electrical pulses (the ZAP function in some patch-clamp amplifier) can also facilitate the “break-in.”
12. Keep the negative pressure on until lifting the cell from the cover slip. Bring the lifted cell to the predetermined position under the θ tubing. Voltage-clamp the cell at –60 mV.
13. Turn on the syringe pump. The cell should be bathed in the jet stream containing the control solution near the interface with the jet stream containing glutamate. Apply a voltage pulse to the piezo crystal to move back and forth the glutamate stream across the cell.
14. The kinetics of NMDA receptor-mediated, whole-cell currents is sensitive to extracellular Ca²⁺ and holding potentials (*see Fig. 2*) owing to a mechanism called Ca²⁺-dependent inactivation (CDI).
15. The involvement of calmodulin in CDI can be evaluated by mutating the calmodulin binding sites in the NR1 subunit and intracellular infusion or dialysis of calmodulin inhibitors.

References

1. Ehlers, M. D., Zhang, S., Bernhart, J. P., and Huganir, R. L. (1996) Inactivation of NMDA receptors by direct interaction of calmodulin with the NR1 subunit. *Cell* **84**, 745–755.
2. Zhang, S., Ehlers, M. D., Bernhardt, J. P., Su, C. T., and Huganir, R. L. (1998) Calmodulin mediates calcium-dependent inactivation of N-methyl-D-aspartate receptors. *Neuron* **21**, 443–453.
3. Chen, C. and Okayama, H. (1987) High-efficiency transformation of mammalian cells by plasmid DNA. *Mol. Cell. Biol.* **7**, 2745–2752.

Detergent Solubilization and Immunoprecipitation of Native NMDA Receptors

Robert J. Wenthold, Jaroslav Blahos II,
Kyung-Hye Huh, and Ronald S. Petralia

1. Introduction

The *N*-methyl-D-aspartate (NMDA) subtype of ionotropic glutamate receptor plays a major role in excitatory neurotransmission in the mammalian central nervous system (1,2). It is widely distributed and is found at the postsynaptic membrane of many synapses where it is thought to be anchored to the postsynaptic density (PSD) through a family of PDZ domain-containing proteins (3). Although NMDA receptors are concentrated at the postsynaptic membrane, an intracellular pool, probably representing receptors being transported to and from the synapse, is also present (4,5). Molecular cloning studies have identified five subunits, NR1 and NR2A–D, which can assemble and form functional receptor complexes in oocytes or transfected cell expression systems (2). The receptor complex is believed to be either a tetramer or pentamer comprised of NR1 and NR2 subunits (6,7). The number and composition of subunits in native receptors remain uncertain, but in expression systems, NR1 subunits are required for a functional receptor. Eight different splice variants of NR1, with distinct functional properties, have been identified (2). The NR2 subunits and NR1 splice variants are differentially distributed in the central nervous system indicating that a wide range of functionally distinct receptor complexes may be selectively expressed in different brain regions and neuronal cell types. The nature of these complexes can be explored with antibodies selective for the different forms of the receptor (4–6).

Detergent solubilization of intact receptor complexes is an important initial step in the molecular characterization of native receptors. The NMDA receptor complex historically has been difficult to solubilize with detergents, with few

reports in the literature of solubilized receptors, which have retained their ligand binding capability. We found that the NMDA receptor complex from brain can be effectively solubilized with sodium deoxycholate and still retain its subunit interactions, based on coimmunoprecipitation analysis (6). The NMDA receptor can be solubilized nearly completely with sodium dodecyl sulfate (SDS), and may retain associations between subunits and with some interacting proteins if the samples are not boiled (8). Both intact and denatured receptor complexes can be immunoprecipitated with subunit-specific antibodies. A number of antibodies to NMDA receptor subunits, many of which can immunoprecipitate or be used for Western blot analysis, have been developed, and some are now commercially available (Table 1). The detergent solubilization and immunoprecipitation methods can be applied to whole-brain tissue (such as dissected areas of the brain), brain subfractions, or primary cultures.

2. Materials

2.1. Chemicals

1. Protein A agarose and protein G agarose are from Pierce (Rockford, IL) (ImmunoPure Immobilized Protein A, no. 20334; ImmunoPure Immobilized Protein G, no. 20398).
2. Detergents: Triton X-100 is from Sigma, sodium deoxycholate is from Calbiochem (La Jolla, CA), and SDS is from Bio-Rad (Richmond, CA). A stock solution of 10% (w/v) Triton X-100 is prepared in water and stored at 4°C. Sodium deoxycholate solutions are made fresh before use.
3. Protease inhibitors: Pepstatin and leupeptin are from Boehringer Mannheim (Mannheim, Germany), and phenylmethylsulfonyl fluoride (PMSF) is from Gibco-BRL (Gaithersburg, MD).

2.2. Antibodies

Several antibodies, selective for NMDA receptor subunits and splice variants, have been reported to be useful for immunoprecipitation and Western blot analysis. Some of these and their properties are listed in Table 1. Antibodies are usually stored in aliquots (undiluted) at -70 to -80°C, although frequently used antibodies can be stored for several weeks at 4°C with 0.02% sodium azide. Diluted primary antibodies in Western blot solution containing 0.02% sodium azide are stored at 4°C and can be reused multiple times over several months. Our Western blot solution contains 50 mM Tris-HCl, pH 7.5, 150 mM NaCl, and 0.05% Tween 20. Usually blocking agents, such as bovine serum albumin (BSA) or nonfat dry milk, are not included in the primary antibody solution.

Table 1
NMDA Receptor Antibodies for Immunoprecipitation and Western Blotting^a

Subunit/splice variant	Epitope	Monoclonal/ polyclonal	Immuno- precipitation	Commercial Source	Reference
NR1 pan	660-811	Monoclonal—mouse	Yes	PharMingen, San Diego, CA	7
NR1 N1	N1 cassette	Polyclonal—rabbit	Yes	No	6
NR1 C2	909-938	Polyclonal—rabbit	Yes	Chemicon, El Segundo, CA	4
NR1 C2	909-938	Monoclonal—mouse	Yes	Chemicon,	
NR1 C2'	C2' cassette	Polyclonal—rabbit	Yes	No	6
NR2A/B	1426-1445	Polyclonal—rabbit	Yes	Chemicon, Temecula, CA	5
	(2A)				
NR2B	892-1051	Monoclonal—mouse	No	Transduction Laboratories, Lexington, KY	
NR2A	934-1203	Polyclonal—rabbit	Yes	No ^b	9
NR2B	935-1456	Polyclonal—rabbit	Yes	No ^b	10

^aWe find all these antibodies to be satisfactory for Western blotting.

^bSimilar antibodies are available from Chemicon, but these were not tested by the authors.

3. Methods

3.1. Detergent Solubilization of Intact Receptor Complexes

1. Homogenize tissue with a polytron (Brinkman, Westbury, NJ, #6 setting) at 4–8 mg protein/mL until homogenous in cold 50 mM Tris-HCl, pH 9.0. Protein concentration of brain tissue is estimated to be 10% wet wt of the tissue. Brain subfractions are prepared similarly.
2. Add protease inhibitors PMSF, ethylenediaminetetraacetic acid (EDTA), leupeptin, and pepstatin to final concentrations of 0.5 mM, 2.5 mM, 1 µg/mL, and 1 µg/mL, respectively.
3. Add sodium deoxycholate (10% w/v stock solution) to a final concentration of 1% w/v. Incubate 37°C with mixing for 1 h.
4. Centrifuge 100,000g for 1 h at 4°C.
5. Recover supernatant and add Triton X-100 to 0.1% (w/v). Dialyze overnight at 4°C against 50 vol of 50 mM Tris-HCl, pH 7.5, containing 0.1% Triton X-100.
6. Centrifuge at 100,000g for 1 h. Supernatants can be used immediately for immunoprecipitation or frozen on dry ice and stored indefinitely at –75°C. Repeat centrifugation if a precipitate is present after the freeze/thawing.

3.2. Detergent Solubilization and Denaturation of Receptor Complexes

1. **Steps 1 and 2** are carried out as for detergent solubilization of intact receptor complexes (**Subheading 3.1.**).
2. Add SDS (10% w/v stock solution) to a final concentration of 1 or 2% and NaCl to a final concentration of 200 mM. Incubate at 37°C for 30 min or boil for 5 min (*see Notes*).
3. Centrifuge 100,000g for 1 h at 4°C.
4. To supernatant, add Triton X-100 to a final concentration of 1 or 2% to match or exceed the concentration of the SDS. Alternatively, the supernatant can be diluted 10-fold with buffer containing 0.1% Triton X-100.
5. Centrifuge if precipitate is present. Use supernatants immediately or freeze on dry ice, and store indefinitely at –75°C.

3.3. Immunoprecipitation of NMDA Receptor Subunits

1. Attach antibodies to protein A-agarose or protein G-agarose. Use 25 µL of resin (packed resin volume) and 1–10 µg of antibody in 750 µL of phosphate-buffered saline (PBS), pH 7.5, containing 0.1% Triton X-100. Incubate in a microfuge tube with mixing on a platform rocker at 4°C for 2–12 h.
2. Centrifuge antibody/resin briefly (5–10 s) in a microfuge. Remove supernatant. Wash resin by resuspending in 750 µL of Tris-HCl, pH 7.5, containing 0.1% Triton X-100. Centrifuge briefly and remove supernatant.
3. Add 0.5–1 mL of detergent-solubilized brain extract to resin. Incubate with mixing on a platform rocker at 4°C for 2–12 h.

4. Centrifuge briefly. Add supernatant to fresh antibody/resin for second round of immunoprecipitation, if necessary. Incubate with mixing at 4°C for 2–12 h. Centrifuge briefly, and retain supernatants and pellets from both immunoprecipitations.
5. Resin pellets from **step 4** are washed three times by resuspending in 750 μL of cold 50 mM Tris-HCl, pH 7.5, containing 0.1% Triton X-100, followed by brief centrifugation. Pellets from first and second immunoprecipitations may be combined.
6. Analyze supernatants for unbound subunits. Mix supernatant with an equal volume of 2X SDS-polyacrylamide gel electrophoresis (SDS-PAGE) dissolving solution. With the exception of resin-bound samples, we usually do not boil tissue samples for SDS-PAGE analysis, because this appears to increase aggregation, particularly of NMDA receptors. Samples of brain regions or membranes are prepared with the protease inhibitors noted above.
7. Bound receptor is eluted from resin by adding 2X SDS-PAGE dissolving solution to resin (usually 75 μL is added to 25 μL resin) and boiling for 3 min. Resin is removed by brief centrifugation.

4. Notes

4.1. Detergent Solubilization of Intact Receptor Complexes

About 35% of the total NMDA receptor complex is solubilized with 1% deoxycholate at 37°C. Although solubilization at 37°C for 1 h is optimal, intact receptor complexes are also obtained with solubilization at 4°C and/or incubation for 30 min, but the efficiency of solubilization is lower. Solubilization can also be carried out at pH 7.5 instead of pH 9.0, but with lower efficiency. Triton X-100 is not an effective solubilizing agent for obtaining an NR1/NR2 complex, although it may selectively solubilize the NR1 subunit reflecting either a homomeric pool of this subunit or disruption of the receptor complex (**II**). Increasing ionic strength during solubilization disrupts the receptor complex. Thus, we keep the ionic strength of our buffers low when attempting to isolate intact NMDA receptor complexes.

Immunoprecipitation can be done directly on the 1% deoxycholate-soluble fraction, although we have found that addition of Triton X-100 and dialysis yields more reproducible results. Alternatively, the sample can be diluted with buffer containing 0.1% Triton X-100 to reduce the deoxycholate concentration. We have found that high concentrations of deoxycholate may adversely affect immunoprecipitation.

4.2. Detergent Solubilization and Denaturation of Receptor Complexes

NMDA receptor subunits from brain are nearly completely solubilized with 1 or 2% SDS. The ionic strength of the buffer is not critical, although 200 mM

NaCl is used routinely. It has been reported that boiling in SDS should be used to disrupt interactions with PDZ-containing proteins, such as PSD-95 (8). Solubilization in SDS at room temperature or 37°C can be used to demonstrate coimmunoprecipitation of NMDA receptors with interacting proteins (8).

4.3. Immunoprecipitation of NMDA Receptor Subunits

We routinely preattach antibodies to protein A- or protein G-agarose beads, although it is equally effective to incubate antibodies with the solubilized fraction first and then add the resin. We find that preattaching antibodies somewhat decreases the amount of antibody present in the unbound fraction, and this may be especially important if this fraction is analyzed with antibodies from the same species as used in the immunoprecipitation. For analysis of both bound and unbound fractions using Western blots, regardless of how the antibodies are attached to the resin, it is preferable to use antibodies made in a species different from that used for immunoprecipitation to decrease intense staining of heavy and light antibody chains. For example, we often immunoprecipitate with polyclonal rabbit antibodies and then analyze with Western blots using monoclonal mouse antibodies. Even with this approach, secondary antibody recognition of heavy and light chains can occur. The degree of recognition varies with commercial sources of the secondary antibody.

Using two rounds of immunoprecipitation, we obtain nearly complete (>90%) immunoprecipitation of deoxycholate-solubilized brain NMDA receptors. If the bound fraction is analyzed, the beads obtained from each round are combined. For quantitative analyses, however, we favor analyses of unbound fractions. Two rounds of immunoprecipitation are not necessary for routine, nonquantitative coimmunoprecipitation studies.

Immunoprecipitated proteins attached to protein A-agarose can be eluted and immunoprecipitated with a second antibody for sequential immunoprecipitation. In this case, boil the resin in 2% SDS without a reducing agent. Add Triton X-100 to a final concentration of at least 2%, and repeat immunoprecipitation steps. We have not attempted quantitative analyses with this approach.

References

1. Monaghan, D. T., Bridges, R. J., and Cotman, C. W. (1989) The excitatory amino acid receptors: their classes, pharmacology, and distinct properties in the function of the central nervous system. *Annu. Rev. Pharmacol. Toxicol.* **29**, 365–402.
2. Hollmann, M. and Heinemann, S. (1994) Cloned glutamate receptors. *Ann. Rev. Neurosci.* **17**, 31–108.
3. Gomperts, S. N. (1996) Clustering membrane proteins: it's all coming together with the PSD95/SAP90 protein family. *Cell* **84**, 659–662.

4. Petralia, R. S., Yokotani, N., and Wenthold, R. J. (1994) Light and electron microscope distribution of the NMDA receptor subunit NMDAR1 in the rat nervous system using a selective anti-peptide antibody. *J. Neurosci.* **14**, 667–696.
5. Petralia, R. S., Wang, Y.-X., and Wenthold, R. J. (1994) The NMDA receptor subunits NR2A and NR2B show histological and ultrastructural localization patterns similar to those of NR1. *J. Neurosci.* **14**, 6102–6120.
6. Blahos, J. II and Wenthold, R. J. (1996) Relationship between *N*-methyl-D-aspartate receptor NR1 splice variants and NR2 subunits. *J. Biol. Chem.* **271**, 15,669–15,674.
7. Siegel, S. J., Brose, N., Janssen, W. G., Gasic, G. P., Jahn, R., Heinemann, S. F., et al. (1994) Regional, cellular, and ultrastructural distribution of *N*-methyl-D-aspartate receptor subunit 1 in monkey hippocampus. *Proc. Natl. Acad. Sci. USA* **91**, 564–568.
8. Lau, L.-F., Mammen, A., Ehlers, M. D., Kindler, S., Chung, W. J., Garner, C. C., et al. (1996) Interaction of the *N*-methyl-D-aspartate receptor complex with a novel synapse-associated protein, SAP102. *J. Biol. Chem.* **271**, 21,622–21,628.
9. Leonard, A. S. and Hell, J. W. (1997) Cyclic AMP-dependent protein kinase and protein kinase C phosphorylate *N*-methyl-D-aspartate receptors at different sites. *J. Biol. Chem.* **272**, 12,107–12,115.
10. Wang, Y.-H., Bosy, T. Z., Yasuda, R. P., Grayson, D. R., Vicini, S., Pizzorusso, T., et al. (1995) Characterization of NMDA receptor subunit-specific antibodies: distribution of NR2A and NR2B receptor subunit in rat brain and ontogenic profile in cerebellum. *J. Neurochem.* **65**, 176–183.
11. Chazot, P. L. and Stephenson, F. A. (1997) Biochemical evidence for the existence of a pool of unassembled C2 exon-containing NR1 subunits of the mammalian forebrain NMDA receptor. *J. Neurochem.* **68**, 507–516.

Redox Sensitivity of NMDA Receptors

Stuart A. Lipton

1. Introduction

The redox modulatory sites of the NMDA receptor consist of critical cysteine residues, which when chemically reduced, increase the magnitude of NMDA-evoked responses. In contrast, after oxidation, NMDA-evoked responses are decreased in size. In recent years, as endogenous sources of oxidizing and reducing agents have been discovered, redox modulation of protein function has been recognized to be an important physiologic, as well as pathologic mechanism for many cell types. For our purposes, I will confine this review of redox modulation to covalent modification of sulfhydryl (thiol) groups on protein cysteine residues of native NMDA receptors. Of note, considerable recent work has focused on the use of recombinant NMDA receptor subunits and site-directed mutagenesis to identify the critical cysteine residues involved in this redox modulation, but these recombinant methods will not be reviewed here. For a recent summary of the molecular data, *see* **ref. 1**. If the cysteine sulfhydryls possess a sufficient redox potential, oxidizing agents can react to form adducts on single thiol groups, or if two free sulfhydryl groups are vicinal (in close proximity), disulfide bonds may possibly be formed. Reducing agents can regenerate free sulfhydryl (—SH) groups by donating electron(s). Considering endogenous redox agents, in addition to the usual suspects, including glutathione, lipoic acid, and reactive oxygen species, nitric oxide and its redox-related species have recently come to the fore. This has occurred largely because of the rediscovery and application to biological systems of work from the early part of this century showing the organic synthesis of nitrosothiols (RS-NO) (reviewed by **refs. 1–3**). NO group donors represent different redox-related species of the NO group, each with its own distinctive chemistry, which lead to entirely different biological effects. NO-related species include nitric

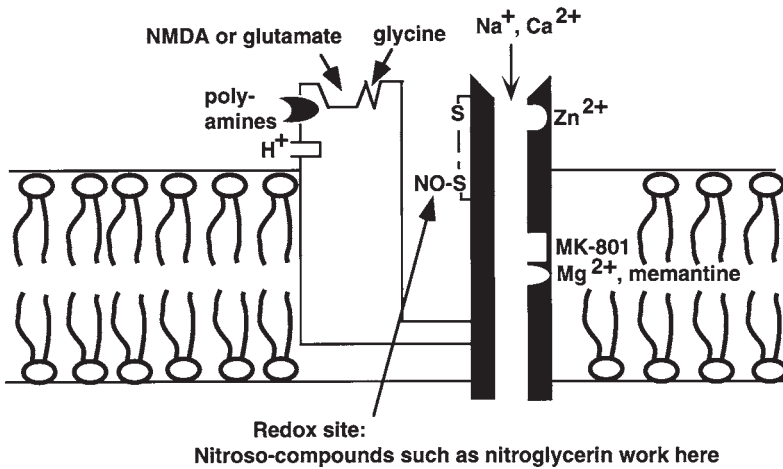


Fig. 1. *S*-Nitrosylation of critical thiol group(s) of the NMDA receptor's redox modulatory site by *S*-nitrosocysteine, a more general example of which is RS-NO, a nitrosylated protein. The redox modulatory site of the NMDA receptor is trans-nitrosylated by transferring the NO group (in the NO⁺ form) from RS-NO to cysteine sulfhydryl group(s) on the NMDA receptor-channel complex. This results in a decreased frequency of channel opening and, therefore, decreased NMDA receptor activity.

oxide (NO[•]), but also the other redox-related forms of the NO group: with one less electron (NO⁺ or nitrosonium ion) or one additional electron (NO⁻ or nitroxyl anion) (2). Recent evidence suggests that all three of these redox-related forms, if not in free form, then their functional equivalents, are important pharmacologically and physiologically, participating in distinctive chemical reactions. NO⁺ can be transferred from either endogenous or exogenous donors to thiol (a reaction termed *S*-nitrosylation) to form nitrosothiols on the NMDA receptor (NRS-NO), and the singlet (or high-energy state) of NO⁻ can also react with thiol groups. The reaction of the NO group with NMDA receptor thiol decreases NMDA-evoked responses similar to an oxidizing agent (Fig. 1). A consensus motif of amino acids comprised of nucleophilic residues surrounding a critical cysteine, which increase the cysteine sulfhydryl's susceptibility to *S*-nitrosylation by NO⁺ donors, has been proposed; NMDA receptor subunits contain typical consensus motifs for *S*-nitrosylation (1).

2. Materials

1. The sulfhydryl reducing agent dithiothreitol (DTT) is obtained from Boehringer-Mannheim, Mannheim, Germany, or Calbiochem, La Jolla, CA.
2. Endogenous reducing agents active at the NMDA receptor include dihydrolipoic acid (0.5–5 mM), available from Sigma, St. Louis, MO.

3. The strong oxidizing agent 5,5'-dithio-*bis*-2-nitrobenzoic acid (DTNB) is obtained from Boehringer-Mannheim or Calbiochem.
4. Endogenous oxidizing agents include oxidized glutathione (GSSG, 5–10 mM), lipoic acid (LA, 1–5 mM, in *R*- and *S*-enantiomers), and NO compounds (such as *S*-nitrosylated glutathione and *S*-nitrosocysteine, 100 μM to 1 mM) that donate or transfer NO⁺ equivalents to sulfhydryl groups of cysteine residues in proteins, including the NMDA receptor. *S*-nitroso-glutathione is commercially available (from CYCLO₃PSS Biochemical Corp., Salt Lake City, UT, and other companies), and *S*-nitrosocysteine can be synthesized from L-cysteine (Sigma, cat. no. C7755) and sodium nitrite (NaNO₂; Aldrich, Milwaukee, WI, cat. no. 23,721-3) with HCl (Chempure, cat. no. 831-088). Pyrroloquinoline quinone (PQQ, 10–100 μM) is another endogenous redox agent.
5. Exogenous NO compounds that function as oxidants and donate NO⁺ or NO⁺-like equivalents include nitroglycerin (NTG) and sodium nitroprusside (SNP). Exogenous NO⁻-generating drugs, include sodium trioxodinitrate, also known as Angeli's salt (Oxi-NO), *N*-nitrosohydroxylamine-*N*-sulfonate/ammonium salt (Sulfi-NO), and benzenesulfohydroxamic acid (Piloty's acid) (3).
6. *N*-ethylmaleimide (NEM, 1–5 mM) irreversibly alkylates thiol groups.
7. For chelation of NO to abrogate its effects, one can use hemoglobin (Hb [bovine, crystallized, mol wt ~64,500]; Sigma cat. no. H2500), prepared as described below, or the newer agent, Carboxy-PTIO (Alexis Corp.).
8. A pregnant Sprague-Dawley rat, at 15 or 16 d of gestation, is used to generate fetal cerebrocortical cultures to monitor NMDA-evoked responses and to test the effects of redox agents.

3. Methods

1. Cell culture: Cortical cultures are derived from embryonic Sprague-Dawley rats (4,5). Briefly, following dissociation in 0.027% trypsin, cerebrocortical cells are plated at a density of 4.5×10^5 /35-mm dish containing poly-L-lysine-coated glass cover slips in Dulbecco's Modified Eagle's Medium with Ham's F12, and heat-inactivated horse serum (HyClone) at a ratio of 8:1:1. After 15 d in culture (when the astrocyte layer had become confluent), the cultures are treated with cytosine arabinoside for 72 h. The culture medium is then partially replenished at weekly intervals. Cultures are incubated at 36°C in a 5% CO₂/95% air humidified atmosphere. The cultures are used for experiments at room temperature (21–24°C) 3–4 wk after plating. Neurons can be reliably identified by morphological criteria under phase-contrast optics, as later confirmed by patch-clamp recording.
2. The sulfhydryl reducing agent dithiothreitol (DTT, 0.5–10 mM) is dissolved in extracellular solution, generally Hanks' balanced salt solution, for use in mammalian neuronal cultures or slice preparations. DTT is used to effect chemical reduction, which increases NMDA- (50 μM) evoked responses. Generally, DTT is administered by superfusion into the bath. Addition of 0.5–10 mM for 2 min is generally used, but effects can be seen within seconds and continue to increase with time of addition. The increase in NMDA-evoked responses usually outlasts

the addition of DTT, because the reaction of DTT is covalent, producing free sulfhydryl groups on critical cysteine residues in the NMDA receptor's so-called redox sites. The same is true for the other reducing agents effective at the NMDA receptor, e.g., dihydrolipoic acid.

3. The strong oxidizing agent DTNB, which oxidizes available sulfhydryl groups to form thiobenzoate protein and may form disulfide bonds from paired thiol groups, decreases NMDA receptor function. Generally, 0.5 mM DTNB is superfused for 2 min to see these effects. For GSSG, generally 5–10 mM are used for 2 min, and for lipoic acid, 1–5 mM for 2 min.
4. Preparation of *S*-nitrosocysteine as a reagent that transfers NO⁺ to cysteine sulfhydryls of the NMDA receptor's redox modulator site(s): On ice, L-cysteine and sodium nitrite (NaNO₂) solid are combined in equimolar amounts and dissolved in double-distilled water by vortexing for ~20 s. To this solution, 10 N HCl are added to a final normality of 0.5 N and a final *S*-nitrosocysteine concentration of 100 mM; addition of the HCl results in a color change of the solution from clear colorless to clear red. For all experiments, this concentrated solution of *S*-nitrosocysteine is kept on wet ice and used in ≤2 h. The concentrated *S*-nitrosocysteine is diluted 1000-fold (5 μL into 5 mL Hanks' saline solution) such that the final concentration bathing the cells was 100 μM. No change in pH is noted on addition of the *S*-nitrosocysteine owing to the large volume of saline solution used. The solutions are mixed by inversion and by gentle trituration. The solution bathing the cells is then removed, and 1 mL of the 100 μM *S*-nitrosocysteine solution is added by Pasteur pipet every 30 s and removed, for a total of 5–10 applications, after which experimental measurements are obtained. Alternatively, the *S*-nitrosocysteine solution is administered continuously for 3–5 min to the cells by local superfusion, via a large bore microcapillary tube, with identical results. As a control, the following experiment is performed. After the passage of several hours at room temperature, the NO dissipates from the *S*-nitrosocysteine solution, but the resulting disulfide, cystine, is still present. This solution, then, can serve as a control, and it should exhibit no effect on NMDA-evoked responses.
5. Three donors of NO⁻ (Oxi-NO, Sulfi-NO, and Piloty's acid, 1–5 mM for 2 min) all exhibit qualitatively similar effects in decreasing NMDA-evoked responses. At 1–5 mM concentrations, these donors generate approximately low-micromolar levels of NO⁻. However, Piloty's acid, consistent with recent reports that it is a better NO[•] than NO⁻ donor at physiological pH, exhibits less of an effect.
6. NEM (1–5 mM) is superfused for 2 min. NEM, which irreversibly alkylates thiol groups of the NMDA receptor, thus prevents the inhibition of NMDA-evoked responses by other redox-active reagents. For example, following treatment with NEM, NMDA responses are not altered by DTNB, Oxi-NO, Piloty's acid, NTG, or lipoic acid in our hands.
7. Recording solutions: To permit physiology experiments (calcium imaging or patch-clamping) under normal room air conditions, just prior to a recording session, the culture medium is exchanged for a solution based on Hanks' balanced

salts. The Hanks' saline consists of (in mM): NaCl, 137.6; NaHCO₃, 1; Na₂HPO₄, 0.34; KCl, 5.36; KH₂PO₄, 0.44; CaCl₂, 1.25–2.5; HEPES, 5; dextrose, 22.2; adjusted to pH 7.2 with 0.3 M NaOH. To enhance physiological responses to NMDA, the saline is nominally magnesium-free and contains 1 μM glycine, a coagonist required for NMDA receptor activation. Tetrodotoxin (TTX; 1 μM) is added to block action potentials and ensuing neurotransmitter release from other neurons onto the cell of interest. The presence of intact neurotransmission would obfuscate the results, if, for example, high K⁺, kainate, or NMDA caused the release of a substance from one neuron, which in turn acted on the cell being monitored.

8. To maximize the effects of the NO compounds, in many but not all of our physiology experiments, DTT is added prior to the addition of a nitroso-compound. However, qualitatively similar effects of NTG, nitroxyl-generating compounds, S-nitrosocysteine, and other oxidizing agents mentioned above have been observed under physiological conditions in native neurons that have never been treated with DTT. The procedure of exposing the cells to DTT first is followed in cases in which one wishes to quantify the effects under standardized conditions, beginning from the state of maximal chemical reduction.
9. Digital Ca²⁺ imaging: Neuronal intracellular free Ca²⁺ concentration ([Ca²⁺]_i) is analyzed with fura-2 acetoxymethyl ester (AM; Molecular Probes) using a protocol for digital calcium imaging that has been detailed previously by this laboratory (4,5).
10. Patch-clamp recordings: Patch-clamp recordings are performed in the whole-cell configuration using standard procedures (4,5). Patch pipets typically contain (in mM): 140 KCl, 2 MgCl₂, 1 CaCl₂, 2.25 EGTA, 10 HEPES-NaOH; pH 7.2.
11. All redox reagents, including DTT (2 mM), DTNB (0.5 mM), NEM (1 mM), NTG (100 μM to 1 mM), and the NO⁻-generating drugs (1–5 mM), are typically superfused for 2 min, washed away with nominally Mg²⁺-free Hanks' buffered saline solution for 3–4 min, and then the NMDA-elicited [Ca²⁺]_i responses or electrical responses are monitored. The redox agents used here, either during incubation or after thorough washout, do not alter basal [Ca²⁺]_i.

In practice, prior to testing a putative reducing agent, DTNB can be administered so that the reducing agent will manifest a maximal effect. Prior to testing a putative oxidizing agent, DTT can be administered so that the oxidizing reagent will manifest a maximal effect. Application of NEM prior to a putative redox agent should permanently block its effect. However, there are some caveats (see **Notes 12–14**) to this paradigm since not all cysteine residues of the NMDA receptor may be equally accessible to various redox reagents, and NMDA receptors of varying subunit composition may have somewhat varying cysteines contributing to their redox-sensitive sites. Also, potential interaction of a putative redox reagent with other sites on the NMDA receptor must be rigorously tested.

12. Preparation of reduced Hb to complex NO: Hb is often used to bind to NO and thus block its effects on other proteins, such as the NMDA receptor. For this purpose, Hb must be in the reduced form and prepared in the following manner

(but there are caveats to this technique—see **Note 15**). Commercially available bovine Hb is diluted to a concentration of 1 mM in double-distilled water and chemically reduced, using a 10-fold molar excess of sodium dithionite ($\text{Na}_2\text{S}_2\text{O}_4$ [mol wt 174.1]; Sigma cat. no. 1256). On addition of sodium dithionite, the solution changes color from brown to bright red, signifying the presence of Hb in its reduced state. To remove the $\text{Na}_2\text{S}_2\text{O}_4$, the solution is extensively dialyzed against a 100-fold excess of double-distilled water at 4°C using rinsed dialysis tubing with a mol wt cutoff of 12,000–14,000 (Spectra/Por 2, cat. no. 132676). The dialysate is replaced twice with fresh double-distilled water at 6–12-h intervals. A solution of 10 mM $\text{Na}_2\text{S}_2\text{O}_4$, prepared and dialyzed in exactly the same fashion, is used as a control. The final concentration of $\text{Na}_2\text{S}_2\text{O}_4$ is calculated to be ~10 nM. During preparation and usage, exposure of the Hb to light is minimized. The reduced Hb is utilized immediately following preparation, and after the initial addition of $\text{Na}_2\text{S}_2\text{O}_4$, no significant color change is noted prior to use in the experiments, as monitored spectrophotometrically.

4. Notes

1. Redox reactions are both time- and concentration-dependent, so exposure to a low concentration of a redox reagent for a longer time period will manifest similar effects to high concentrations for a short time.
2. Care should be taken not to mix DTT with DTNB in the recording chamber, since they will annihilate each other's effect (this problem can be detected, because the two together form a yellowish solution).
3. Phenol red and DMSO should be avoided in solutions during redox experiments, because they can function as redox agents.
4. NO donors, such as NTG, can migrate into polyvinyl chloride plastic tubing, causing a loss in NO donor concentration. Some plastic syringes (e.g., from Becton Dickinson) generate free radicals and can therefore scavenge NO donors. These plastic materials should thus be avoided.
5. At near-millimolar concentrations, DTNB can also be an NMDA open-channel blocker. Care can be taken to distinguish this effect by recognizing that it is voltage-dependent, and therefore the block is relieved at depolarized potentials, but the redox effect of DTNB is not voltage-dependent.
6. As a control for the effects of the NO group donated by NTG, the diluent that NTG is commercially available in (and keeps it from being explosive) must be used. The diluent usually consists of polyethylene glycol and ethanol. For a more appropriate control solution, glycerol can be added to this diluent in an amount equimolar to the concentration of NTG used in the experiments, because NTG has a glycerol backbone with three ONO_2 groups attached to it that generate NO_x (with $x = 1$ or 2). Since ethanol can block NMDA receptor activity, the diluent must be applied and washed out on the same time scale as NTG itself. Since NTG is redox-active, its effects are long-lasting (covalent reaction), whereas the ethanol effect seen with the diluent is transient and effectively is eliminated after

washout, but the NTG effect persists after washout for some time (the exact time varies from preparation to preparation).

7. Under our conditions, $\text{NO}\cdot$ donors alone (in contrast to NO^+ -or NO^- -generating agents) do not affect NMDA-evoked responses. Free endogenous nitrosonium (NO^+) exists only at low pH. However, functional equivalents of NO^+ can be transferred to thiol or, more properly, thiolate anion (RS^-), at physiological pH. The reaction is pH-dependent as are many redox reactions, so care must be taken in holding the pH constant for all redox experiments. *S*-nitrosocysteine is less stable (homolytically breaks down to $\text{NO}\cdot + \text{Cys}\cdot$) at higher pH and temperature, so preparation and storage at low pH and low temperature is preferable. In the presence of a cysteine residue surrounded by an optimal motif, rather than breaking down homolytically, *S*-nitrosocysteine can undergo facile transfer of its NO^+ group to another peptide cysteine sulfhydryl, and this occurs for critical cysteines in the redox modulatory sites of the NMDA receptor. Such transfer of the NO^+ group from one RS-NO to another is termed transnitrosation or transnitrosylation.
8. The enantiomer of lipoic acid (LA) appears to be critical. (*S*)-LA works as an oxidizing agent at the NMDA receptor, but not (*R*)-LA. Thus, the stereospecificity of the redox effects of LA appear important on the NMDA receptor.
9. SNP is a complicated NO -generating agent, since it also produces redox-active pentocyanoferrate, which obfuscates the result. Therefore, SNP is generally to be avoided as an NO donor that reacts with the NMDA receptor redox modulatory sites, since SNP effects are difficult to interpret.
10. The NO^- donors also generate $\text{NO}\cdot$, although in very small amounts vis-à-vis their production of NO^- . Therefore, to ensure that the effects of NO^- donors are not owing to their production of $\text{NO}\cdot$, we have previously performed control experiments using the more specific $\text{NO}\cdot$ donors, diethylamine- NO (DEA/ NO) and spermine/ NO (SPER/ NO). With the use of a specific $\text{NO}\cdot$ -sensing electrode (WPI, Inc., Sarasota, FL), we calibrated the concentrations of these $\text{NO}\cdot$ donors to generate similar or slightly greater amounts of $\text{NO}\cdot$ over a 2-min period compared to the NO^- donors. At these concentrations, neither DEA/ NO nor SPER/ NO influenced the NMDA-evoked responses, consistent with our previous findings that $\text{NO}\cdot$ itself does not downregulate NMDA receptor activity under our conditions. Thus, transfer of NO^+ or singlet NO^- , but not $\text{NO}\cdot$ appears to be responsible for the inhibitory effect on the NMDA receptor-channel complex described here.
11. PQQ has been reported to be an endogenous redox reagent active at the NMDA receptor redox modulatory site, but this is probably not true under physiological conditions, since PQQ (the oxidized form) prefers to scavenge superoxide anion ($\text{O}_2^{\cdot-}$). In contrast, in the presence of ascorbate, rather than oxidize the NMDA receptor's redox site, PQQ itself becomes reduced (and may actually redox cycle between the oxidized and reduced states). Reduced PQQ ($\text{PQQ}\cdot\text{H}_2$) reacts readily to form superoxide. These reactions generally take preference over PQQ reaction with cysteine sulfhydryls at the NMDA receptor, so it is unlikely that PQQ directly affects the NMDA receptor redox state under physiological conditions according to experiments in our laboratory.

12. The transfer of NO^+ may possibly involve thiolate anion (R-S^-) as opposed to thiol (R-SH) and is therefore pH-dependent. NO^+ transfer reactions may also depend on catalytic amounts of transition metals. In particular, metals can facilitate nitrosation reactions involving $\text{NO}\cdot$ (2). Controversy over $\text{NO}\cdot$ interactions with the NMDA receptor is best understood by appreciating that nitrosation of the redox site is facilitated by oxygen, transition metals, and perhaps $\text{O}_2^{\cdot-}$ (superoxide anion) (3,6). The common event in every case is transfer of an NO^+ equivalent to form an RS-NO . In the case of vicinal thiols, *S*-nitrosylation may promote disulfide formation (3). That EDTA has been reported to interfere with the effects of $\text{NO}\cdot$ on NMDA receptor activity supports rather than contradicts the involvement of nitrosative chemistry on cysteine residues of the NMDA receptor/channel complex. In fact, several (possibly as many as seven) cysteine residues on NMDA receptor subunits appear to react with the NO group, and work on recombinant receptors to prove exactly which cysteine residues are involved is currently in progress. Other effects of NO are of course not ruled out by these findings. It is also true that the effects of Zn^{2+} on the NMDA receptor and that of redox agents can be confused, because some reducing agents (such as DTT) bind Zn^{2+} , because EDTA chelates Zn^{2+} , and because Zn^{2+} may also be coordinated, at least in part, by cysteine residues.
13. In theory, NEM will irreversibly alkylate thiol groups and prevent the effects of redox reagents. Although NEM at millimolar concentrations is not perfectly specific for cysteine residues, in conjunction with the effects of DTT and DTNB, the only reasonable explanation for the effects of all three of these drugs on NMDA-evoked responses is via interaction with thiol groups on the receptor. In practice, reaction with NEM depends on several important variables. First, NEM must have access to the particular sulfhydryl of interest in its thiolate anion form. This reaction can therefore be hindered for steric, kinetic, pH, redox, or charge-related reasons. The same argument holds true for the oxidizing agent DTNB and for NO donors. It follows that NEM or DTNB may not have access to thiols that react with NO -related species (which are much smaller in size), that not all NO donors will react with the NMDA receptor, and that these differences in reactivities are likely to be markedly influenced by assay conditions. Undoubtedly, some of the conflicting reports in this area reflect the different experimental conditions (6).

Under our conditions in primary cultures of cerebrocortical neurons, a rapid, but slight decrement in NMDA responses (in both whole-cell recording and in Ca^{2+} -imaging experiments) is observed following adequate NEM treatment. If the decrease in NMDA-evoked responses is not seen following NEM, then additional NEM must be added to ensure adequate alkylation of cysteine sulfhydryls. Importantly, once adequate NEM is added, NO -related species and other redox agents are no longer effective at modulating NMDA-evoked responses via the receptor's redox sites (4). Others have reported analogous results on a variety of channel proteins. Notwithstanding the lack of specificity of NEM at high concentrations and with prolonged exposures, it may require up to 60 min to alkylate protein thiols. Even so, it is not known if all thiols on the NMDA receptor are

accessible. As a further complicating matter, the priming of the NMDA receptor with DTT to produce free thiol, which is requisite for NEM reaction, can be transient in some preparations. NEM may therefore not have sufficient time to react. In sum, many pitfalls can affect the interpretation of experiments with NEM, and for this reason, negative experiments in which NEM fails to prevent subsequent redox reactions are much less meaningful than positive results. Under our conditions, it is unequivocal that NEM modulates NMDA channel activity and prevents the effect of NO donors in both patch-clamp and calcium-imaging experiments (4,5).

14. It is important to compare work on the NMDA receptor's redox modulatory site(s) in primary neurons to that on recombinant NMDA receptor subunits. However, the limitations of our work on recombinant NMDA receptor's redox site(s) (7) must be understood. First, we do not yet definitively know the stoichiometry of subunits in the NMDA receptor, and additional subunits are still being cloned. Indeed, during the course of our work on the redox site of the NMDA receptor using recombinant subunits, we discovered a new NMDA receptor subunit (8). Since the characteristics of redox modulation are dependent on subunit composition (7,9), it has not yet been possible to identify all of the redox site(s) of primary neurons. Using recombinant subunits, transient effects of chemical reduction with DTT occur only with NMDAR1/NMDAR2A subunit composition; recently, this was attributed to DTT chelation of Zn^{2+} , but a true transient redox effect also appears to be present in our experiments even after accounting for Zn^{2+} effects. The fact that different heteromers of NMDA receptor subunits display disparate redox properties may also contribute to the disagreement among laboratories working on primary neurons regarding the effects of NEM, NO donors, or other redox reagents; NMDA receptors of distinct neurons may have different redox properties because they are composed of different subunits. The study of various combinations of NMDA receptor subunit heteromers may well reveal additional redox sites.
15. The standard procedure for preventing the effects of NO is to bind this molecule to reduced Hb, as prepared in **step 12**. However, this is a problem in short-term physiology experiments, because reduced Hb by itself increases $[Ca^{2+}]_i$ for up to several minutes in the calcium-imaging experiments; during whole-cell recording, reduced Hb also generates an inward ionic current that lasts for several minutes when cells were voltage-clamped at -60 mV. In longer-term experiments, such as in neurotoxicity paradigms, these effects of Hb do not represent as much of a problem, because they reverse within minutes and do not influence neuronal survival. These effects of Hb, however, obfuscate the interpretation of short-term physiology experiments employing Hb. We do not have definitive information if other chelators of NO, such as myoglobin or carboxy-PTIO, display these or other confounding effects.

References

1. Stamler, J. S., Toone, E. J., Lipton, S. A., and Sucher, N. J. (1997) (S)NO signals: Translocation, regulation, and a consensus motif. *Neuron* **18**, 691–696.

2. Stamler, J. S., Singel, D. J., and Loscalzo, J. (1992) Biochemistry of nitric oxide and its redox activated forms. *Science* **258**, 1898–1902.
3. Feelisch, M. and Stamler, J. S. (eds.) (1996) *Methods in Nitric Oxide Research*, Wiley, Chichester, England, p. 712.
4. Lei, S. Z., Pan, Z.-H., Aggarwal, S. K., Chen, H.-S. V., Hartman, J., Sucher, N. J., et al. (1992) Effect of nitric oxide production on the redox modulatory site of the NMDA receptor-channel complex. *Neuron* **8**, 1087–1099.
5. Lipton, S. A., Choi, Y.-B., Pan, Z.-H., Lei, S. Z., Chen, H.-S. V., Sucher, N. J., et al. (1993) A redox-based mechanism for the neuroprotective and neurodestructive effects of nitric oxide and related nitroso-compounds. *Nature* **364**, 626–632.
6. Lipton, S. A., Choi, Y.-B., Sucher, N. J., Pan, Z.-H., and Stamler, J. S. (1996) Redox state, NMDA receptors, and NO-related species. *Trends Pharmacol. Sci.* **17**, 186–187.
7. Sullivan, J. M., Traynelis, S. F., Chen, H.-S. V., Escobar, W., Heinemann, S. F., and Lipton, S. A. (1994) Identification of two cysteine residues that are required for redox modulation of the NMDA subtype of glutamate receptor. *Neuron* **13**, 929–936.
8. Sucher, N. J., Schahram, A., Chi, C. L., Leclerc, C. L., Awobuluyi, M., Deitcher, D. L., et al. (1995) Developmental and regional expression pattern of a novel NMDA receptor-like subunit (NMDAR-L) in the rodent brain. *J. Neurosci.* **15**, 6509–6520.
9. Kohr, G., Eckardt, S., Lüddens, H., Monyer, H., and Seeburg, P. H. (1994) NMDA receptor channels: subunit-specific potentiation by reducing agents. *Neuron* **12**, 1031–1040.

In Vitro Selection of Peptides Acting on NMDA Receptors

Steven E. Cwirla, William J. Dower, and Min Li

1. Introduction

Phage-displayed random peptide libraries have been used to identify novel agonists and antagonists to a wide variety of receptors. Among these are a family of peptides that bind to the NMDA receptor subunit NR1 and non-competitively inhibit receptor channel activity (1). The peptide libraries used to identify these ligands were constructed by cloning a collection of random oligonucleotides into the phagemid vector p8V2 (Fig. 1). Peptides encoded by the cloned oligonucleotides are displayed on the surface of phage particles fused to the N-terminus of the major coat protein pVIII. The expression of gene VIII in p8V2 is under the control of the inducible P_{BAD} promoter (2), which allows one to produce phage particles with few or many copies of peptide-bearing pVIII relative to wild-type pVIII. Libraries were affinity-selected against a soluble form of the extracellular amino-terminal domain of NR1 produced by the method described in Chapter 5 in this volume (3). Individual isolates from the enriched pools were then characterized by a phage ELISA to identify clones that bound specifically to NR1. The sequence of peptides displayed by phage that bound to receptor was deduced by sequencing the cloned oligonucleotide contained in the virion. By this method, several peptide families were rapidly identified that specifically recognize the extracellular amino-terminal domain of the NR1 subunit. In this chapter, we describe methods for the construction of random peptide libraries in the phagemid vector p8V2, affinity selection of libraries against immobilized NR1, and the characterization of recovered phage clones.

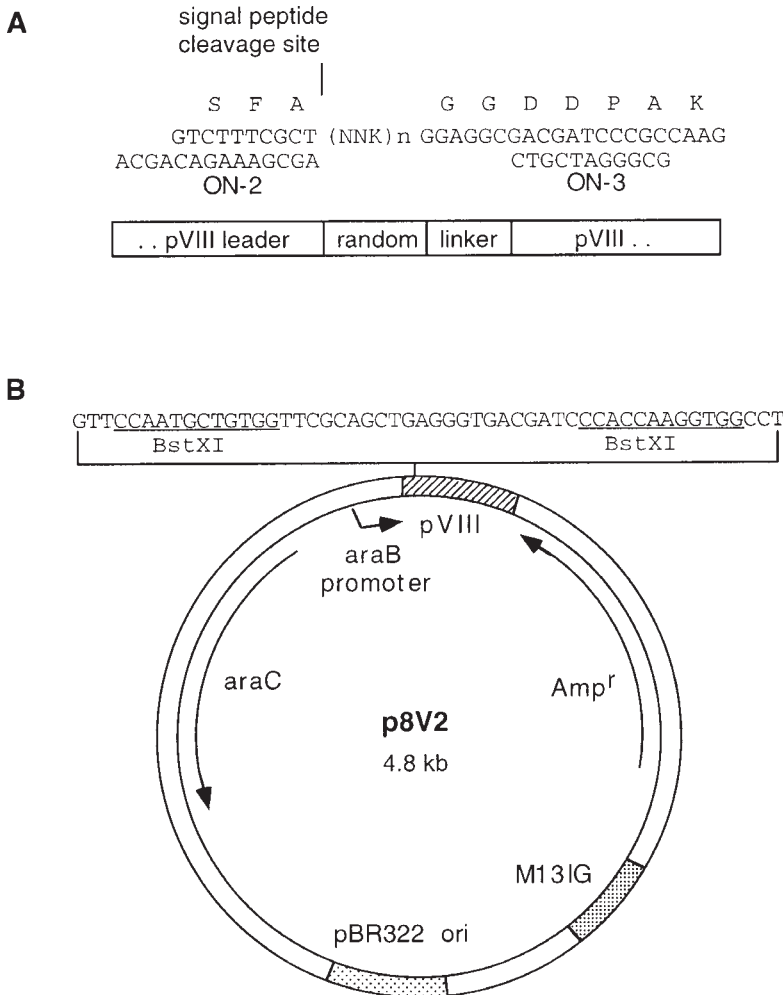


Fig. 1. Cloning scheme for constructing random peptide libraries in p8V2. (A) Structure of the oligonucleotide insert. The random codon containing oligonucleotide is annealed with two half-site oligonucleotides (ON-2, ON-3) to create a fragment with ends complementary to the two *Bst*XI sites in p8V2. The signal peptide cleavage site is located immediately upstream of the random region, and therefore, peptides are displayed fused to the amino-terminus of pVIII. (B) Map of the phagemid vector p8V2. Two noncomplementary *Bst*XI sites in the amino-terminus of gene VIII allow directional cloning of oligonucleotide inserts. The expression of gene VIII is under control of the P_{BAD} promoter, which is positively and negatively regulated by the *araC* gene. The M13 intergenic region contains the replication origin used for (+) strand DNA synthesis, which occurs in the presence of gene products supplied by the helper phage.

2. Materials

2.1. Library Construction

2.1.1. Preparation of p8V2 Vector

1. LB medium: 1% Bacto-tryptone, 0.5% Bacto-yeast extract (Difco, Detroit, MI), 0.5% NaCl.
2. LB-amp medium: LB-medium, 100 $\mu\text{g}/\text{mL}$ ampicillin.
3. MC1061 p8V2 (Affymax Research Institute, Palo Alto, CA).
4. Qiagen Plasmid Maxi Kit (Qiagen Inc., Valencia, CA).
5. 10X NE Buffer 3: 0.5 M Tris-HCl, pH 7.9, at 25°C, 1 M NaCl, 100 mM MgCl_2 , 10 mM DTT.
6. *Bst*XI (New England Biolabs, Beverly, MA).
7. Phenol/chloroform (1:1).
8. 13 \times 55 mm Polyallomer ultracentrifuge tubes (Beckman, Fullerton, CA)
9. Potassium acetate solutions: 10, 15, 20, and 25% w/v in 2 mM EDTA, 1 $\mu\text{g}/\text{mL}$ ethidium bromide.
10. 3 M NaOAc, pH 5.4, at 25°C.
11. Ethanol (70%, 100%).
12. TE: 10 mM Tris-HCl, 1 mM EDTA, pH 8.0.

2.1.2. Preparation of Insert Oligonucleotide

1. TBE: 0.089 M Tris-HCl, 0.089 M boric acid, 2 mM EDTA, pH 8.3.
2. 8% polyacrylamide/7 M urea/ TBE gel.
3. 2X Prep TBE-urea sample buffer (Novex, San Diego, CA).
4. Fluorescent aluminum oxide TLC plate (J. T. Baker, Phillipsburg, NJ).
5. Microspin Sephadex G-25 columns (Pharmacia, Piscataway, NJ).
6. T4 kinase (New England Biolabs).
7. 10X kinase buffer: 1 M Tris-HCl, pH 7.5, 100 mM MgCl_2 , 50 mM DTT.
8. 10 mM ATP.

2.1.3. Ligation of p8V2 with Insert Oligonucleotides

1. 10X annealing buffer: 200 mM Tris-HCl, pH 7.5, 20 mM MgCl_2 , 500 mM NaCl.
2. 10X ligation buffer: 100 mM Tris-HCl, pH 7.5, 50 mM MgCl_2 , 20 mM DTT, 10 mM ATP.
3. T4 DNA ligase (Boehringer Mannheim, Indianapolis, IN).
4. 25 mM dNTP (Pharmacia)
5. Sequenase 2.0 (Amersham, Arlington Heights, IL).

2.1.4. Electrotransformation and Amplification of the Library

1. Electro-competent *Escherichia coli* MC1061 F⁺.
2. 0.2-cm Electroporation cuvetts (Bio-Rad Laboratories, Richmond, CA)
3. LB-amp agar plates (LB-amp medium, 15 g/L Bacto-agar)
4. SOC medium: 2% Bacto-tryptone, 0.5% Bacto-yeast extract, 10 mM NaCl, 2.5 mM KCl, 10 mM MgCl_2 , 10 mM MgSO_4 , 20 mM glucose, pH 7.0 with NaOH.

5. SOP-amp/glu medium: 2% Bacto-tryptone, 1% Bacto-yeast extract (Difco), 100 mM NaCl, 15 mM K_2HPO_4 , 5 mM $MgSO_4$ pH 7.2, with NaOH, 100 μ g/mL ampicillin, 0.1 % glucose.
6. VCSM13 helper phage (Stratagene, La Jolla, CA).
7. 20% Arabinose (w/v) 0.2 μ m filter.
8. 20 mg/mL kanamycin (store at $-20^\circ C$).
9. 20% Polyethelene glycol (PEG, average mol wt 8000)/2.5 M NaCl.
10. PBS: 0.137 M NaCl, 4.3 mM Na_2HPO_4 , 1.4 mM KH_2PO_4 , 2.7 mM KCl, pH 7.4 at $25^\circ C$.
11. PBS/0.1% BSA (w/v) 0.2 μ m filter.

2.2. Peptide Library Screening

2.2.1. Immobilization of PIG-Linked NR1 Receptor Extracellular Domain

1. MAb 179 (Affymax).
2. PIG-linked NR1 receptor harvest (**Chapter 5**, this volume).
3. PBS/1% BSA (0.2- μ m filter).

2.2.2. Affinity Selection

1. MAb 179 blocking peptide (H_2N -AACLEPYTACDA-COOH, disulfide-linked cyclic form).
2. Elution buffer: 0.1 M HCl, pH 2.2 with glycine, 0.1% BSA.
3. 2 M Tris base (pH unadjusted).

2.2.3. Amplification of Selected Phage

1. *E. coli* ARI 292 (Affymax Research Institute).

2.3. Characterization of Recovered Clones

2.3.1. Phage ELISA

1. HRP-conjugated anti-M13 antibody (Pharmacia).
2. ABTS development buffer (Pharmacia).

2.3.2. Filter Lifts Probed with Mab 179/NR1 Receptor Complex

1. LB-amp/kan/glu/ara plates (LB-amp medium, 20 μ g/mL kanamycin, 0.1% glucose, 0.2 % arabinose, 15 g/L Bacto-agar).
2. Nitrocellulose filter circles (Bio-Rad Laboratories).
3. PBST: PBS, 0.05% Tween-20.
4. PBST/0.1% BSA.
5. Alkaline phosphatase-conjugated goat anti-mouse IgG (Gibco-BRL, Gaithersburg, MD).
6. NBT/BCIP (Gibco-BRL).
7. Substrate buffer: 0.1 M Tris-HCl, pH 9.5, 0.1 M NaCl, 50 mM $MgCl_2$. Immediately prior to use add 44 μ L NBT and 33 μ L BCIP/10 mL of substrate buffer.

3. Methods

3.1. Library Construction

3.1.1. Preparation of p8V2 Vector

1. Inoculate 5 mL of LB-amp medium with a single colony of MC1061 p8V2 and grow at 37°C for 6–8 h. Add culture to a 2.8-L Fernbach flask containing 1 L LB-amp medium, and grow at 37°C shaking vigorously overnight.
2. Isolate double-stranded phagemid DNA using Qiagen Plasmid Maxi columns according to the manufacturer's directions. The expected yield of double-stranded p8V2 DNA is approx 1 mg.
3. Combine 200 µg p8V2 DNA in TE with 40 µL 10X NE Buffer 3 and 20 µL *Bst*XI (200 U) in a total vol of 400 µL. Incubate the restriction digest overnight at 55°C.
4. Extract the reaction mixture twice with an equal vol of phenol/chloroform and once with chloroform.
5. Precipitate the DNA by adding 40 µL 3 M sodium acetate and 880 µL absolute ethanol. Spin in a microcentrifuge for 10 min at room temperature. Carefully remove the solution and resuspend the DNA pellet in 200 µL TE.
6. Slowly layer 1 mL of each potassium acetate solution, in order of decreasing density, into a 13 × 55 mm polyallomer ultracentrifuge tube. Layer 200 µL *Bst*XI digested p8V2 on top of the step gradient and ultracentrifuge in a SW50.1 rotor at 280,000g at 20°C for 3 h.
7. Visualize the broad band of linearized DNA contained in the lower half of the tube with a longwave handheld UV lamp. Carefully remove the band with a 23-gage needle attached to a 3-mL syringe, and extract the solution several times with an equal vol of water-saturated butanol to remove the ethidium bromide.
8. Precipitate the DNA by adding 0.1 vol 3 M sodium acetate and 2 vol ethanol. Spin in a microcentrifuge for 10 min at room temperature. Wash pellet with 70% ethanol, and resuspend in TE. Determine the DNA concentration by measuring absorbance at 260 nm.

3.1.2. Preparation of Insert Oligonucleotide

1. Synthesize oligonucleotides with the following sequences: ON-1: 5'-GTCTTTCGCT (N N K) *n* G G A G G C G G G G G T A G C G G C G G T G G G G G A AGTGGGGGAGGTGGCTCCCGACGATCCCGCCAAG-3' (N = A,C,G,T [equimolar]; K = G,T [equimolar]; *n* = the desired number of random codons; underlined sequence encodes [Gly₄Ser]₃ spacer) ON-2: 5'-AGCGAAAGACAGCA-3' ON-3: 5'-GCGGGATCGTC-3'.
2. Deprotect oligonucleotides in NH₄OH overnight at 55°C. Dry the samples in a Speed Vac and resuspend in 400 µL water.
3. Add 500 µg crude deprotected ON-1 to an equal vol of 2X Prep TBE-urea sample buffer, and load into a single 2-cm well of an 8% polyacrylamide/7 M urea/TBE gel (24 × 15 cm, 1.5-mm spacers). Load one well with sample buffer only that contains the tracking dyes bromophenol blue and xylene cyanol. Run at 500 V until the xylene cyanol tracking dye reaches the bottom of the gel.

4. Following electrophoresis, place the gel on plastic wrap on top of a fluorescent TLC plate (aluminum oxide IB-F, J.T. Baker, Phillipsburg, NJ). Visualize the full-length oligonucleotide band by briefly shadowing with a shortwave handheld UV lamp. Cut out the band, transfer to a microfuge tube, and crush into small pieces. Add 1 mL dH₂O, and elute the DNA overnight at room temperature.
5. Centrifuge briefly to pellet the polyacrylamide gel fragments. Transfer solution to a new microfuge tube, and reduce the vol to ~200 μ L by evaporation in a Speed Vac.
6. Desalt all three oligonucleotides by loading onto Microspin Sephadex G-25 spin columns. Collect the flowthrough, dry down each sample in a Speed Vac, and resuspend the pellets in water. Measure the absorbance at 260 nm to estimate the DNA concentration.
7. Kinase 5 μ g of each oligonucleotide by adding 2 μ L 10X kinase buffer, 2 μ L 10 mM ATP, and 2 μ L T4 kinase in a total reaction vol of 20 μ L. Incubate at 37°C for 90 min. Stop the reaction by heating to 70°C for 10 min, and store kinased oligonucleotides at -20°C.

3.1.3. Ligation of p8V2 with Insert Oligonucleotides

1. Combine 40 μ g purified *Bst*XI-digested p8V2, 1 μ g ON-1, 150 ng ON-2, 150 ng ON-3, and 40 μ L 10X annealing buffer in a total vol of 400 μ L. Incubate at 70°C for 5 min, and then slowly cool to room temperature.
2. Add 45 μ L 10X ligation buffer, 5 μ L T4 DNA ligase (5 U) and incubate at 14°C overnight.
3. Add 5 μ L 25mM dNTP solution, 1 μ L Sequenase 2.0, and incubate at 37°C for 90 min.
4. Precipitate the ligated DNA by adding 0.1 vol 3 M sodium acetate and 2 vol ethanol. Spin in a microcentrifuge for 10 min at room temperature. Wash pellet with 70% ethanol, and resuspend in 40 μ L TE.

3.1.4. Electrotransformation and Amplification of the Library

1. Prepare eight electrotransformations by combining 5 μ L ligated DNA with 100 μ L of electrocompetent *E. coli* MC1061 F' cells in each 0.2-cm cuvet, and pulse at 2.5 kV. Following the pulse, immediately transfer the cells from the cuvet to a culture tube containing 2 mL SOC medium, and incubate at 37°C for 1 h.
2. Combine the cultures, and prepare 10-fold serial dilutions from a small aliquot. Plate 100 μ L of the 10⁻⁴, 10⁻⁵, and 10⁻⁶ dilutions on LB-amp plates to assess the efficiency of transformation. Add the culture to a 2.8-L Fernbach flask containing 500 mL SOP-amp/glu medium, and grow at 37°C with shaking to A₆₀₀ = 0.8.
3. Transfer 100 mL to a sterile flask, and add VCSM13 helper phage (5 \times 10¹¹ PFU). Incubate at 37°C for 30 min without shaking.
4. Harvest the remainder of the cells by centrifugation at 12,000g for 15 min, resuspend in 10 mL LB medium/15% glycerol, and store in 2-mL aliquots at -70°C for future library amplifications.

5. Add helper phage-infected cells to a 2.8-L Fernbach flask containing 500 mL SOP-amp/glu medium. Add 6 mL 20% arabinose, 0.6 mL 20 mg/mL kanamycin, and grow at 37°C shaking vigorously overnight.
6. Centrifuge the 600-mL culture at 12,000g for 15 min, transfer supernatant to new bottles, and repeat the spin.
7. Transfer cleared supernatant to new bottles, and add 0.2 vol 20% PEG/2.5 M NaCl. Mix well, and keep on ice for 1 h.
8. Pellet phage by centrifugation at 12,000g for 15 min. Remove the supernatant, and resuspend the phage pellets in 10 mL PBS/0.1% BSA. Titer the phage stock and store aliquots at -20°C.

3.1.5. Notes: Library Construction

1. Complete removal of the 34-bp stuffer fragment following *Bst*XI digestion of p8V2 is important for achieving high cloning efficiency. The recovery of linearized vector DNA from the potassium acetate step gradient is typically only 50%; however, the large capacity of these gradients allows one to purify sufficient amounts of digested vector for constructing several libraries.
2. The insert is prepared as a complex of three oligonucleotides. The variable oligocodon-containing oligonucleotide (ON-1) is annealed to two half-site oligonucleotides (ON-2, ON-3) to create a fragment with ends complementary to the two *Bst*XI sites in p8V2 (**Fig. 1**). Once ligated, the single-stranded gap is filled in with Sequenase 2.0 prior to transformation of the DNA. Libraries in which this fill-in step was omitted contained a significant number of aberrant sequences (deletions, and so forth).
3. The quality of electrocompetent cells used to transform the ligated DNA is perhaps the most important factor in producing large libraries. *E. coli* MC1061 F⁺ cells are grown in a rich medium, such as Superbroth (3.5% Bacto-tryptone, 2% Bacto-yeast extract, 0.5% NaCl, pH 7.5, with NaOH), and harvested at A₆₀₀ = 0.5. Electrocompetent cells are then prepared as described in Dower et al. (**4**). Each preparation should be tested for transforming efficiency before committing the library DNA. Typical efficiencies are 2–5 × 10¹⁰ transformants/mg of pUC DNA and 5 × 10⁹/μg of uncut p8V2. Transformation of the ligated DNA usually results in 10⁷–10⁸ transformants/μg of p8V2.
4. Amplification of the large-scale transformation is a two-step process. The purpose of the first step is to amplify the number of transformed cells to provide stocks for future phage production. In the absence of helper phage, cells transformed with phagemid do not have the necessary phage gene products to produce phage particles. The pVIII peptide fusion is not made during this time, since the P_{BAD} promoter is strongly repressed in the presence of glucose. Following infection with helper phage and induction of the P_{BAD} promoter by the addition of arabinose, phage particles are produced that incorporate both wild-type and peptide-bearing pVIII molecules. The level of induction used in this procedure produces a population of phage particles with an average of ~100 copies of peptide-bearing pVIII/particle.

5. The titer of the phage stock obtained following amplification should be approx 10^{13} transducing unit (tu)/mL. Freeze aliquots of ~ 1000 “library equivalents” at -20°C or -70°C for long-term storage. One library equivalent is defined as the number of phage particles equal to the number of transformants that constitute the library.

3.2. Peptide Library Screening

3.2.1. Immobilization of PIG-Linked NR1 Receptor Extracellular Domain

1. Dilute MAb 179 to $100\ \mu\text{g}/\text{mL}$ in PBS and add $50\ \mu\text{L}$ to 6 wells of a 96-well microtiter plate. Cover the plate and incubate at 37°C for 1 h.
2. Wash wells three times with PBS, and then fill completely with PBS/1% BSA. Cover the plate, and incubate at 37°C for 1 h.
3. Wash plate with PBS, and add $100\ \mu\text{L}$ of PIG-linked NR1 receptor harvest to each well. Incubate plate at room temperature for 1 h. Receptor-coated plate may be stored up to 24 h at 4°C .

3.2.2. Affinity Selection

1. Wash receptor-coated wells three times with PBS. Add $50\ \mu\text{L}$ of a $100\text{-}\mu\text{M}$ solution of MAb 179 blocking peptide to each well, and incubate at 4°C for 30 min.
2. Dilute the peptide library ($\sim 10^{12}$ tu) in PBS/0.1% BSA to a final vol of $600\ \mu\text{L}$, and add $100\ \mu\text{L}$ to each receptor coated well. Incubate the plate at 4°C for 2 h.
3. Wash the wells five times with cold PBS. Completely fill wells with PBS, and incubate at 4°C for 30 min. Repeat PBS wash.
4. Add $100\ \mu\text{L}$ of elution buffer to each well, and incubate at room temperature for 10 min. Transfer eluates to a microfuge tube, and immediately neutralize with $35\ \mu\text{L}$ $2\ \text{M}$ Tris base (pH unadjusted).

3.2.3. Amplification of Selected Phage

1. Inoculate 5 mL of LB medium with a single colony of ARI 292, and grow at 37°C with shaking overnight. Add 1 mL of the overnight culture to a flask containing 20 mL LB and grow with shaking to $A_{600} = 0.4$. Pellet cells by centrifugation, and resuspend in 2 mL LB.
2. Add $600\ \mu\text{L}$ of eluate to $600\ \mu\text{L}$ concentrated ARI 292 cells, and incubate at 37°C for 20 min without shaking. Add the phage-infected cells to a flask containing 10 mL SOP-amp/glu medium, and grow at 37°C with shaking to $A_{600} = 0.2\text{--}0.4$.
3. Add VCSM13 helper phage (5×10^{10} pfu) to the culture, and incubate at 37°C for 30 min without shaking. Add $110\ \mu\text{L}$ 20% arabinose, $11\ \mu\text{L}$ 20 mg/mL kanamycin, and grow at 37°C shaking vigorously overnight.
4. Centrifuge culture at $12,000g$ for 15 min to pellet cells. Transfer cleared supernatant to a new tube, and add 0.2 vol 20% PEG/2 M NaCl. Mix well, and keep on ice for 1 h.
5. Pellet phage by centrifugation at $12,000g$ for 15 min, remove supernatant, and resuspend phage in 1 mL PBS/0.1% BSA.

3.2.4. Notes: Library Screening

1. A high-density array of immobilized receptor encourages multivalent attachment of specific binding phage. Since pVIII libraries display many copies of peptide per phage particle, it is possible to isolate peptide ligands with binding affinities as low as 500 μM . The sequences of these clones may then serve as the starting point for the construction of secondary libraries displaying variants of the original sequence, which can be selected for higher-affinity ligands.
2. Blocking peptide is included during the panning step to prevent the enrichment of phage-displaying peptide ligands to MAb 179-combining sites not occupied by receptor.
3. Multiple rounds of affinity selection and amplification are required to enrich specific receptor binding phage adequately. The number of phage recovered from the first and second rounds is normally between 10^{-4} and 10^{-6} of input. An increase in the number of recovered phage should be observed starting in round three. The maximum number of phage recovered will usually not exceed 10^{-2} of input. Following multiple rounds of affinity selection, individual clones are tested for specific binding to the target receptor by ELISA or filter lifts.
4. Washes in the first two rounds are done using cold PBS to minimize dissociation of captured phage from immobilized receptor. Room temperature washes and extended incubation times can be done in later rounds to increase the selection stringency.

3.3. Characterization of Recovered Clones

3.3.1. Phage Titering

1. Inoculate 10 mL of LB medium with a single colony of ARI 292 and grow at 37°C with shaking to $A_{600} = 0.5$.
2. Prepare 10-fold serial dilutions of the phage stock in PBS. Combine 10 μL diluted phage with 100 μL ARI 292 cells in sterile microfuge tubes. Incubate at 37°C for 20 min.
3. Plate infected cells on LB-amp plates, and incubate at 37°C overnight.
4. Multiply the number of colonies on each plate x dilution factor x 10 to determine the total number of phage/mL (usually expressed as tu/mL).

3.3.2. Phage ELISA

1. Inoculate 5 mL of SOP-amp/glu medium with a single colony from a titer plate, and grow at 37°C with shaking to $A_{600} = 0.5$.
2. Add VCSM13 helper phage (1×10^9 pfu), and incubate at 37°C for 30 min without shaking.
3. Add 50 μL 20% arabinose, 5 μL 20 mg/mL kanamycin, and grow at 37°C overnight.
4. Pellet cells by centrifugation at 4500g (Beckman J-6B) for 15 min, and transfer supernatant to a new tube.
5. Immobilize NR1 receptor with MAb 179 in a 96-well microtiter plate as previously described. Add 50 μL PBS/0.1% BSA and 50 μL phage supernatant to each well. Cover plate, and incubate at 4°C for 2 h.

6. Wash wells five times with PBS, and add 50 μL HRP-conjugated anti-M13 antibody diluted 1:5000 in PBS/0.1% BSA. Incubate at 4°C for 1 h.
7. Wash wells five times with PBS, and add 100 μL ABTS development buffer to each well. Measure the absorbance at 405 nm with a plate reader.

3.3.3. Filter Lifts Probed with MAb 179/NR1 Receptor Complex

1. Approx 200 colonies/100-mm plate or 5000 colonies/150-mm plate are screened by filter lifts. Add 10 μL of phage stock diluted in PBS to 100 μL log-phase ARI 292 cells. Incubate at 37°C for 15 min. (The titer of phage plated on LB-amp/kan/glu/ara plates is often lower than the titer obtained by plating on LB-amp medium. Therefore, several dilutions should be plated to obtain the appropriate number of colonies per plate.)
2. Add VCSM13 helper phage (1×10^9 PFU), and incubate an additional 15 min at 37°C.
3. Plate infected cells on LB-amp/kan/glu/ara plates, and incubate at 37°C overnight. Chill plates at 4°C for at least 1 h prior to doing lifts.
4. Mix 10 μg of MAb 179 with 0.5 mL of NR1 receptor harvest, and store at 4°C for 2 h to overnight.
5. Place a nitrocellulose circle on the plate, make orientation marks on the filter with a syringe needle, and carefully remove it after 1 min. Immediately wash the filter with PBS to remove any bacterial colonies that have adhered, and block the filter in PBST/1% BSA at 4°C for 1 h. Return the plate to 37°C for 4–6 h to allow the colonies to regenerate.
6. Wash filter three times for 5 min each with PBST. Dilute the MAb 179/NR1 receptor mixture in 10 mL PBST/0.1% BSA, and incubate with filter at 4°C for 1 h to overnight on a rotating platform.
7. Wash filter three times for 5 min each with cold PBST. Add 5 μL alkaline phosphatase-conjugated goat anti-mouse IgG to 10 mL PBST/0.1% BSA, and incubate with filter at 4°C for 1 h on a rotating platform.
8. Wash filter three times for 5 min each with cold PBST and then add 3 mL of substrate buffer. Incubate at room temperature until color develops, and stop reaction by rinsing filter in water.
9. Align orientation marks on the filter with those on the corresponding plate, and pick colonies that produced the darkest-intensity spots. Replate and screen again at low density to isolate pure clones if necessary.

3.3.4. Notes: Recovered Clones

1. A phage ELISA is one of the most sensitive methods for characterizing the binding specificity of clones isolated after multiple rounds of affinity selection. Phage added to wells coated with MAb 179 and blocked with BSA, and wells blocked only with BSA should be included as negative controls. An important point to remember is that the signal intensity in a phage ELISA does not necessarily correlate with the affinity of the displayed peptide. Multivalent binding, and differences in expression level and protease susceptibility among different peptides can all influence the signal intensity.

2. Filter lifts are used to screen a large number of clones when the level of enrichment is low, and are also used to discriminate peptides on the basis of affinity for the receptor. However, as with the phage ELISA, expression level and protease susceptibility factor into the signal intensity, and therefore, one should confirm that peptides identified in this manner are indeed higher affinity by testing the chemically synthesized peptide in a binding assay.
3. The phagemid DNA is sequenced to deduce the sequence of the displayed peptide of positive phage clones identified by ELISA or filter lift. Double-stranded DNA is isolated with the Qiagen Plasmid Mini Kit and sequenced by the dideoxy method using Sequenase 2.0.

References

1. Li, M., Yu, W., Chen, C.-H., Cwirla, S., Whitehorn, E., and Tate, E. (1996) In vitro selection of peptides acting at a new site of NMDA glutamate receptors. *Nature Biotechnol.* **14**, 986–991.
2. Guzman, L.-M., Belin, D., Carson, M.J., and Beckwith, J. (1995) Tight regulation, modulation, and high-level expression by vectors containing the arabinose P_{BAD} promoter. *J. Bacteriol.* **177**, 4121–4130.
3. Whitehorn, E.A., Tate, E., Yanofsky, S.D., Kochersperger, L., Davis, A., and Mortensen, R.B. (1995) A generic method for expression and use of “tagged” soluble versions of cell surface receptors. *Biotechnology* **13**, 1215–1219.
4. Dower, W.J., Miller, J.F., and Ragsdale, C.W. (1988) High efficiency transformation of *E. coli* by high voltage electroporation. *Nucleic Acids Res.* **16**, 6127–6145.

NMDA Receptor Pharmacology and Analysis of Patch-Clamp Recordings

Jerry M. Wright and Robert W. Peoples

Introduction

1. Comparison of Whole-Cell and Single-Channel Analysis

There are two approaches to evaluation of the effects of drugs on steady-state ligand-gated receptor function: (1) concentration–response curves derived from whole-cell recordings and (2) analysis of single-channel recordings. Whole-cell currents are the average response of a large population of channels, whereas single-channel recordings document the gating behavior of a single protein. Analysis of single-channel recordings details the effects of modulators and agonists on channel kinetics at the molecular level. Whole-cell concentration–response analysis is a standardized protocol for classification and interpretation of a mechanism that permits quantitative comparisons with other modulators. Quantitation of charge at the single-channel level can be used as a basis for comparison with whole-cell concentration–response curves. This procedure allows the investigator to compare the effects of a variety of drugs at the molecular level using a well-established set of tools developed for analysis of macroscopic responses.

1.2. Principles of Whole-Cell Response Data Analysis

The interaction between drugs or agonists and receptors is the fundamental concept of pharmacology. Correct interpretation of experimental results of studies of NMDA receptor-channel function, therefore, depends on a correct understanding of this interaction. The primary kinetic model underlying interpretation and analysis is the occupation theory of drug–receptor interaction, where channel openings occur as discrete events to a single conductance level

with an exponentially distributed mean open time (1,2). The model described below is highly simplified; additional kinetic states are known to exist for the NMDA receptor channel.



In this model, A represents agonist or drug concentration, R is receptor concentration, and AR is concentration of the drug–receptor complex. The subscripts C and O designate the closed and open states of the receptor-ion channel, and k_1 , k_{-1} , α , and β are the microscopic rate constants for the transitions into the different states. The left side of the model represents drug or agonist binding to the receptor, and the right side represents channel gating or efficacy. Binding affinity is commonly measured using the macroscopic dissociation constant, K_d , which is equal to k_{-1}/k_1 , and efficacy is measured using the term ϵ , which is equal to β/α .

1.3. Principles of Single-Channel Data Analysis

The principles of charge quantitation data analysis are derived from Ohm's law, which states that current (I) is directly proportional to voltage (V) and inversely proportional to resistance (R). The equation is usually restated for conductors, such as ion channels, by substituting the term conductance (γ) for the inverse of resistance. The driving potential (V) is the difference between the Nernst potential (V_r) and membrane potential (V_m). Unlike conductors, channels are not open all the time. Therefore, the current is proportional to the fraction of time the channel is in the open state, which is a product of the mean open time (τ_o) and frequency of opening (f_o)

$$I = (V_m - V_r) * \gamma * \tau_o * f_o \quad (2)$$

Analysis consists of measuring the total charge at several drug concentrations to produce a concentration–response curve in both whole-cell and single-channel configurations. Ideally, the difference in charge measurements between whole-cell and single-channel recordings would be owing to the greater number of channels in the whole-cell membrane. Because the driving potential is held constant, there are only three variables to be evaluated for more detailed analysis: conductance, mean open time, and frequency of opening.

1.4. Logistic Equation

Concentration–response curves are usually sigmoidal when displayed on a logarithmic scale. Concentration–response data are modeled using an equation, such as the four-parameter logistic equation:

$$y = [E_{\max} - E_{\min}/1 + (x/EC_{50})^{-n}] + E_{\min} \quad (3)$$

Where x and y are concentration and response, respectively, n is slope factor, ED_{50} is the concentration of drug producing 50% of maximal effect, and E_{\min} and E_{\max} are minimal and maximal effect, respectively (3).

Typically, analysis involves fitting each concentration–response curve separately, then comparing the slope, E_{\max} , and EC_{50} values of the curves. In studies of structure–function relationships where a series of related drugs are assayed, it is expected that the curves will share common parameters and can be analyzed simultaneously. In situations where some curves in a set may not span the full response range, simultaneous fitting may permit an investigator to proceed with analysis without repeating laborious experiments.

1.5. Relationship Between Single-Channel and Whole-Cell Observations

The link between the classical kinetic model and the single-channel model is that in both systems, the measured parameter is the current flow through the open channel. By measuring channel opening and closing kinetics, single-channel recordings inherently are measuring agonist efficacy (**Eq. 1**). There is no space for a full discussion of the underlying relationships between the classical and single-channel receptor models; for such detailed information, the reader is referred to **ref. (4)**.

Competitive antagonists interact with the agonist binding site. At the whole-cell level competitive antagonism is indicated by a rightward shift in the concentration–response curve without a reduction in E_{\max} (**Fig. 1A**). A molecular modification that changes receptor affinity without changing efficacy will also produce a parallel shift in the agonist concentration–response curve. When antagonist–receptor equilibrium time is faster than the channel closing rate, the effects of a competitive antagonist are not distinguishable from a reduction in agonist concentration (5). Therefore, at the single-channel level, competitive inhibition is characterized by a decrease in frequency of opening with no change in channel conductance or mean open time.

Uncompetitive antagonists act only on the open channel with the result that the efficacy is reduced, whereas affinity (K_d) is unchanged in the whole-cell response (**Fig. 1B**). Interpretation of single-channel recordings is a more complex problem, because the observed response depends on the frequency response of the recording system (2). Open-channel block is characterized by a decrease in mean open time, unless the duration of block is much shorter than the time resolution of the recording system. In that case, the open-channel response will be noisier, and average channel amplitude will decrease. A special case exists with low concentrations of some open-channel antagonists in the “local anesthetic model” (2). In this situation, whole-cell currents are not reduced, but there usually is a reduction in the amplitude of Gaussian noise

owing to filtering of new high-frequency components in the response. At the single-channel level, mean open-channel lifetime is reduced but total charge is not reduced, because frequency of channel opening increases.

Noncompetitive inhibitors act at a site other than the agonist site, and can interact with closed or open channels, resulting in a reduction in E_{\max} and often a rightward shift in the response curve (**Fig. 1 C**). There are no specific predictions for noncompetitive inhibitors at the single-channel level, and the response may be complex with changes in multiple parameters.

2. Materials

1. In whole-cell experiments, it is often adequate to acquire data using only a chart recorder connected to a patch-clamp amplifier, provided the response time of the recorder is sufficiently rapid (e.g., 10 ms rise time for a full-scale pen deflection) and that the only variable of interest is the current amplitude.
2. Because of the large amount of data generated, single-channel experiments should first be stored at high resolution in digital format on videocassettes that hold 2–6 h of data (VR 10-El Instrutech, 475 Northern Blvd., Suite 3,1 Great Neck, NY 11021-4802). The recorder has a separate audio track, which can be used to record voice notes during an experiment. Use of a headset microphone leaves both hands free during an experiment.
3. The RC Electronics ISC-16 A/D board and Channel Analysis Program (CAP) software (RC Electronics, 6464 Hollister Ave, Goleta, CA 93117-3110) are used to bring single-channel data into the computer for analysis.
4. For single-channel analysis, data are acquired by replaying selected portions of the tape, refiltering the analog signal using an eight-pole Bessel filter (model 900C9L8L, Frequency Devices, Haverhill), and sampling at five times the labeled filter cutoff frequency.
5. Analysis is done using two software packages: CAP and ALLFIT (3). ALLFIT is in the public domain and available with an accompanying manual from the Technical Assistance and Support Center, Center for Information Technology, National Institutes of Health, 12 South Dr. MSC 5605, Bethesda, MD 20892-5605.
6. The recommended minimum computer system is an 80486DX, 33 MHz, with 1 GB hard drive, VGA monitor, 8-MB RAM, DOS 3.3 or higher, and HP-compatible laser printer. The CAP and ALLFIT programs operate in DOS or in a DOS window under either Windows 3.1 or Windows 95.
7. CAP output was originally to a Hewlett Packard six-pen plotter. If a plotter is not available there are several utility programs that translate six-pen plotter output files to Hewlett Packard laser printer input: LP.EXE is often found in electrophysiology labs as part of the Axon Instrument Clampex program suite; LASER.EXE is available from J.M.W. CAP also has capability of saving figure data in ASCII files for export to other graphing programs such as Origin.
8. A large-capacity data backup system, such as an 800-MB tape or writeable CD, is recommended because of the large amounts of data generated in resampling the high-resolution, single-channel recordings.

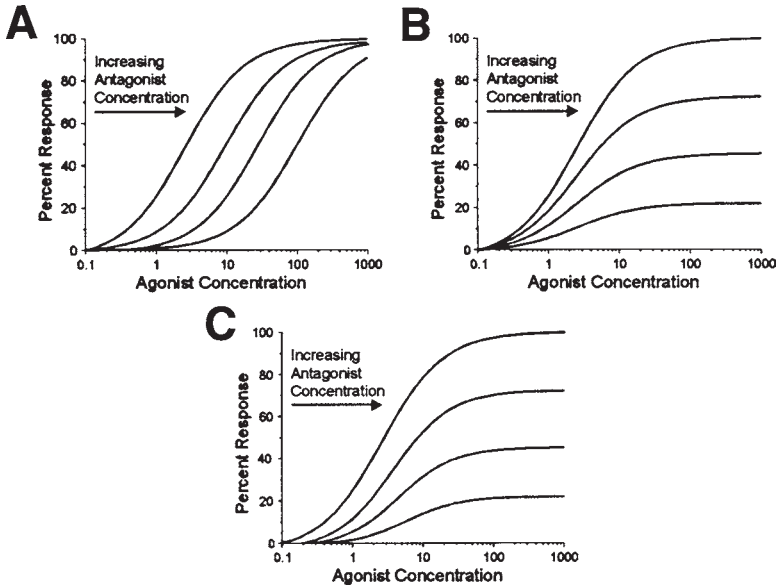


Fig. 1. Idealized concentration–response curves for an agonist in the presence of increasing concentrations of hypothetical antagonists with different mechanisms of inhibition. Competitive antagonists (**A**) shift the agonist concentration–response curve to the right in a parallel manner, increasing the agonist EC_{50} without changing its E_{max} ; uncompetitive (**B**) antagonists decrease the E_{max} without changing the EC_{50} ; and non-competitive antagonists (**C**) primarily decrease the E_{max} , and slightly increase the EC_{50} .

3. Methods

3.1. Construction of Whole-Cell Concentration–Response Curves

1. At least five to six concentrations are required to construct an adequate concentration–response curve, and more are preferable. These concentrations should span the range of the response, so that the lowest concentration gives little or no response, and the highest concentration gives a response that is clearly maximal (**Figs. 1** and **2**).
2. Plotting the drug or agonist concentrations on a log scale is essential, so that a sigmoidal curve is obtained. This allows visual comparison of the affinity, efficacy, and apparent Hill slope to be made among multiple curves (**Figs. 1** and **2B**).
3. Drug application order should be determined using a random number generator or table of random numbers.
4. An adequate number of cells (usually 4–6) must be tested to average out normal variations in response.
5. Drugs must be applied long enough for the response to reach steady state before measuring the current. Since the single-channel data are recorded at steady-state, the whole-cell data response should also be measured at steady state for a valid comparison.

3.2. Single Channel

1. The protocol for determination of drug concentrations and sequence of application is the same as described for the whole-cell trials.
2. Record single-channel responses at each concentration over periods of 40 s or longer, and if possible, records should contain at least several hundred openings.
3. The optimal filter setting produces a square-wave signal with the RMS noise level $< 1/6$ the open channel amplitude (6) (Fig. 2A). A 2-kHz or lower filter cutoff is usually adequate for analysis of the NMDA receptor channel at -60 mV. All data should be filtered at the same final setting for each set of curves. There may be a temptation to go into great detail with precise filter settings. Because this analysis procedure is concerned only with the mean open time, filter settings are usually not critical unless the signal approaches the limits of resolution. Alternate protocols for small amplitude channels are described in the notes **Subheading 4**.
4. Acquire raw data traces by setting the digital sampling frequency to be at least five times the filter cutoff frequency. The minimum requirement for square-wave signal reconstruction is that at least one sample occur during the detectable pulse interval (7). A point often confused in data acquisition is that the filter is calibrated for 50% reduction in amplitude of a sine-wave input. Square waves are not attenuated to the 50% threshold at the labeled settings.
5. Capture events in the data traces using 50% of the open-channel amplitude as the threshold criteria (Fig. 2A). Time spent above threshold is considered an event, whereas time below threshold is considered a closed state. The 50% of open-channel amplitude is a convenient point, since this provides an unbiased estimate of dwell time in either state. Default threshold in the program is 50% and can be adjusted from 25 to 75% of opening to accommodate special circumstances, such as small amplitude channel openings which are better acquired at higher thresholds (6).
6. Create a charge density histogram (Fig. 2) from the captured events file. All points above the 50% threshold in a recording are used to make amplitude density histograms, which represents the probability density of open channels. Histograms are normalized to 1-min periods, and the total charge determined by integration. Total charge is reported as picoCoulombs per minute (pC/min).
7. Determine open-channel amplitude from the peak of the charge density histogram (Fig. 2A).
8. Generate an open time table, and use a single exponential fitting to determine the mean open time adjusted for filter cutoff effects.
9. Determine frequency of opening at each drug concentration. This is the number of events divided by the file length in seconds.

3.3. Comparison of Concentration–Response Curves.

1. First determine if the individual concentration–response curves are acceptable for analysis. Using ALLFIT, curves are fit without any constraints (no shared or constant parameters) to obtain initial values of E_{\max} , E_{\min} , EC_{50} , and n .

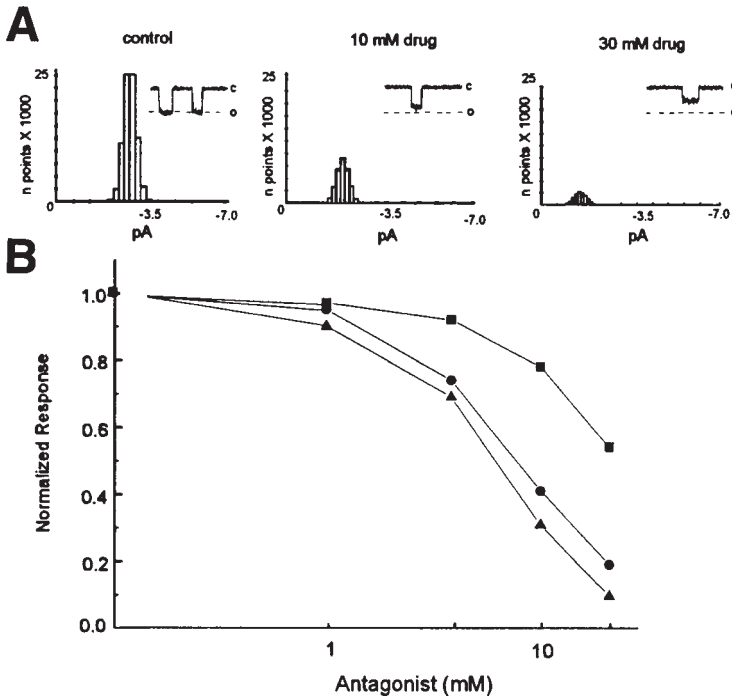


Fig 2. Concentration–response curves for a hypothetical antagonist similar to tetraethylammonium with multiple modes of inhibition. The antagonist reduced the frequency of opening with a K_d of 7 mM and reduced the open channel amplitude with a K_d of 35 mM; both mechanisms had a Hill coefficient of 1.0. A kinetic modeling program was used to generate raw data traces used in analysis. The histograms (A) are a set of all points above the 50% open-channel conductance. All histograms are normalized to 1 min recording times and are shown at the same scale. Decreases in probability of opening appear as a reduction in area of the histogram. Decreases in open-channel amplitude appear as a leftward shift in the histogram peak. Insets show examples from raw data traces used in analysis; (C) indicates the closed state. Concentration–response curves (B) of changes in open-channel amplitude (squares), frequency of opening (circles), and total charge (triangles) are shown on a semilog scale. Y-axis data are normalized to the response in the absence of drug. The resulting concentration–response curve for total charge inhibition was fit with an EC_{50} of 5 mM and a Hill coefficient of 1.4.

2. If a set of well-fitted curves is obtained, significant differences in a parameter (such as EC_{50}) are tested by refitting the curves and specifying that parameter as shared. Significant differences will be reflected in the P value given in the “F” column of the summary table.

4. Notes

4.1. Equipment

1. In whole-cell experiments, it is often useful to also acquire data on a computer, either directly during an experiment or from data stored on a PCM-VCR recording system. Data are usually filtered at 1–2 kHz with an eight-pole Bessel filter and acquired at two to three times the filter cutoff. The system we have used for several years uses the DigiData 1200A A/D interface with the AxoTape software (Axon Instruments, Foster City, CA).
2. A variety of A/D boards and software combinations may be used for acquiring single-channel data if the files can be created in or converted to a format compatible with the analysis software. CAP data file format specifications are available from the corresponding author if the user wishes to write a custom data acquisition or data translation utility.
3. An eight-pole Bessel filter is a close approximation of a Gaussian filter which has many properties appropriate for single-channel analysis, such as well-defined output with repeated filtering, high signal-to-noise ratio, and absence of overshoot or ringing for square wave transitions (6). The output cutoff frequency response of a signal repeatedly filtered in a cascade is determined by the formula:

$$1/f_c^2 = 1/f_1^2 + 1/f_2^2 \quad (4)$$

4. Some filters, such as the Ithaco model 4302, are designed and labeled for use with square-wave pulses, and the front panel setting reflects the 50% reduction in pulse amplitude.
5. The dead time of a recording system is defined by the minimal event duration required to reach the detection threshold after filtering. Pulses shorter than the dead time cannot be detected. The effect of the absence of events shorter than the dead time on the mean open time is accounted for in the single exponential fitting process.

4.2. Logistic Curve Creation

6. A primary consideration in whole-cell concentration–response experiments is whether to use peak or steady-state current amplitude. Although peak current is often used, steady-state current is preferable under certain conditions. Measurement of peak current may underestimate the effect of drugs that have a slow onset of action or drugs that influence receptor desensitization.
7. To facilitate comparisons with other drugs, experiments should be conducted at the agonist EC_{50} when antagonists are being tested. Agonist EC_{50} varies slightly among preparations and should be confirmed with any new culture protocol or after a mutation.
8. Drug application must be in random order to exclude systematic errors in the response. If drugs or agonists are applied in sequence, any time-dependent changes in channel activity (such as response rundown) could be confounded with drug effects, resulting in systematic errors.

4.3. Data Interpretation

9. Antagonists may have multiple sites of action and simultaneously exhibit properties of competitive, noncompetitive, and uncompetitive antagonists. Zinc (**8**) and tetraethylammonium (**9**) each have voltage-dependent actions, which affect open-channel amplitude and an additional voltage-independent effect of reduction in the frequency of opening.
10. The terms “affinity” and “efficacy” should not be used interchangeably. Changes in affinity are marked by parallel shifts in the concentration–response curve along the x -axis, whereas changes in efficacy are marked by changes in E_{\max} . Under conditions where efficacy is very high (greater than 95%), changes in efficacy may be confused with changes in affinity (**10**).
11. Although a voltage-dependent inhibition usually identifies an antagonist as an open-channel blocker, voltage dependence is not a requirement of uncompetitive antagonism. Bicuculline, and its degradation product bicucine, block the NMDA receptor channel in a voltage-independent manner (**11**). Bicuculline is often used to block chloride currents and can be especially troublesome as a contaminant, because at low concentrations, it affects NMDA channel kinetics at the single-channel level with little observable effect on the whole-cell response (**11**).
12. Allosteric modulators can act by reducing agonist affinity. In this case, they can be separated from true competitive antagonists at the whole-cell level, because an allosteric modulator will not produce an additional shift to the right of the agonist concentration–response curve when its site of action is saturated (**12**).
13. HA-966 and *D*-cycloserine are partial agonists that act at the glycine coagonist site of the NMDA receptor channel (**13**). Partial agonists shift concentration–response curves to the right and increase the E_{\min} . Because they displace the agonist and activate the receptor channel with lower efficacy, they may appear to be competitive antagonists if full whole-cell concentration–response curves are not constructed. Partial agonists can be identified by their ability to generate a response in the absence of agonist and by their failure to produce complete block of the agonist response even at high concentrations. At the single-channel level, partial agonists decrease the mean open time reflecting their reduced efficacy.

4.4. Difficult to Analyze Patches

14. The single-channel analysis program will handle up to three levels of opening, so patches with multiple active channels can be analyzed. The event capture procedure locates the start and end of openings without distinguishing the number of levels of opening. The second stage of processing produces an events table by randomly assigning closings to active channels, which results in an unbiased estimate of the mean open time (**14**). Data on channel-closed times are difficult to interpret when multiple active channels are present and are usually considered unreliable for kinetic modeling.
15. Patches with more than three levels of channel opening can be used in total charge concentration–response curves. In this situation, a histogram is constructed from all points in the record. The baseline is ignored and the total charge calculated

from all points above the 50% level of the first open state. Open time and frequency of opening data cannot be derived.

16. NMDA single-channel activity in a patch often varies over a period of 30–60 s. If onset and recovery from drug effects are sufficiently rapid, short application periods may be alternated with short recovery periods and the responses to each condition averaged to minimize the effects of variation in single-channel activity (15).
17. Low driving potentials or mutations that decrease open-channel conductance may make it difficult to resolve openings. Again, a histogram is constructed from all points in the record instead of capturing events. The baseline without channel activity is tested for a symmetrical Gaussian noise distribution. The baseline is then subtracted to reveal low-amplitude currents that otherwise cannot be distinguished (16). Only total charge information and possibly channel amplitude can be determined by this method.

4.5. Fitting Concentration–Response Curves

18. ALLFIT data files may be written using any ASCII text editor, as long as the editor used does not insert additional coded information (e.g., formatting information in a file header) into the file. One pair of concentration–response data is entered per line and concentrations must be in ascending order. Because of the analysis procedure employed, means can be used in place of raw data.
19. In some cases, it may be necessary to constrain one or two parameters to constant values in order to obtain an adequate fit. For example, if concentrations of an inhibitor high enough to approach the E_{\max} cannot be attained, the fitting will often yield an unreasonably high value for this parameter (i.e., greater than 100% inhibition). It would then be necessary to constrain the E_{\max} to 100% inhibition and repeat the curve fitting.

References

1. del Castillo, J., and Katz, B. (1956) Interaction at end-plate receptors between different choline derivatives. *Proc. R. Soc. Lond. (Biol.)* **146**, 369–381.
2. Hille, B. (1984) *Ionic Channels of Excitable Membranes*. Sinauer Associates, Sunderland, MA.
3. De Lean, A., Munson, P. J., and Rodbard, D. (1978) Simultaneous analysis of families of sigmoidal curves: application to bioassay, radioligand assay, and physiological dose–response curves. *Am. J. Physiol.* **235**, E97–E102.
4. Pallotta, B. S. (1991) Single ion channel's view of classical receptor theory. *FASEB J.* **5**, 2035–2043.
5. Rang, H. P. (1981) Drugs and ionic channels: mechanisms and implications. *Postgrad. Med. J.* **57** (Suppl. 1), 89–97.
6. Colquhoun, D., and Sigworth, F. J. (1995) Fitting and statistical analysis of single-channel records, in *Single-Channel Recording* (Sakmann, B., and Neher, E. eds.), Plenum, New York, pp. 483–587.

7. McManus, O. B., Blatz, A. L., and Magleby, K. L. (1987) Sampling, log binning, fitting and plotting durations of open and shut intervals from single channels and the effects of noise. *Pflügers Arch.* **410**, 530–553.
8. Legendre, P., and Westbrook, G. L. (1990) The inhibition of single *N*-methyl-*D*-aspartate-activated channels by zinc ions on cultured rat neurones. *J. Physiol. (Lond.)* **429**, 429–449.
9. Wright, J. M., Kline, P. A., and Nowak, L. M. (1991) Multiple effects of tetraethylammonium on *N*-methyl-*D*-aspartate receptor-channels in mouse brain neurons in cell culture. *J. Physiol. (Lond.)* **439**, 579–604.
10. Colquhoun, D., and Farrant, M. (1993) The binding issue. *Nature* **366**, 510–511.
11. Wright, J. M., and Nowak, L. M. (1992) Effects of low doses of bicuculline on *N*-methyl-*D*-aspartate single channel kinetics are not evident in whole cell currents. *Mol. Pharmacol.* **41**, 900–907.
12. Li, C., Peoples, R. W., and Weight, F. F. (1997) Mg^{2+} inhibition of ATP-activated current in rat nodose ganglion neurons: evidence that Mg^{2+} decreases the agonist affinity of the receptor. *J. Neurophysiol.* **77**, 3391–3395.
13. Henderson, G., Johnson, J. W., and Ascher, P. (1990) Competitive antagonists and partial agonists at the glycine modulatory site of the mouse NMDA receptor. *J. Physiol. (Lond.)* **430**, 189–212.
14. Jackson, M. B. (1985) Stochastic behavior of a many-channel membrane system. *Biophys. J.* **47**, 129–137.
15. Wright, J. M., Peoples, R. W., and Weight, F. F. (1996) Whole-cell and single-channel analysis of ethanol inhibition of NMDA-activated currents in cultured mouse cortical and hippocampal neurons. *Brain Res.* **738**, 249–256.
16. Wright, J. M., and Li, C. (1995) Zn^{2+} potentiates steady-state ATP activated currents in rat nodose ganglion neurons by increasing the burst duration of a 35 pS channel. *Neurosci. Lett.* **193**, 177–180.

Determination of Membrane Topology of Glutamate Receptors

Hendrika M. A. VanDongen and Antonius M. J. VanDongen

1. Introduction

Glutamate receptors are large integral membrane proteins that belong to the class of ligand-gated ion channels. They constitute a family of receptors that are activated by binding of the neurotransmitter L-glutamate. Functional receptors are formed by assembly of several subunits around a central ion-conducting pore. Each subunit is thought to contain multiple membrane-spanning domains. A reliable membrane topology model, which defines the number of transmembrane segments and their orientation, is critical for understanding the relationship between the structure of these receptors and their function. This chapter describes some of the technical considerations of an approach that we and others have used to determine experimentally aspects of the membrane topology of ionotropic glutamate receptors (1–7). This strategy uses the fact that glycosylation of asparagine residues only occurs in extracellular domains, owing to the fact that the glycosyl transferases are localized to the lumen of the endoplasmic reticulum. Demonstration of functional *N*-linked glycosylation therefore provides a definitive measure of extracellular localization. Alternative approaches that do not rely on alteration of *N*-glycosylation status have also provided information on membrane topology of glutamate receptors (7–9), but a detailed discussion of these methods is outside the scope of this chapter.

1.1. Hydrophobicity Analysis

An important first step in building a membrane topology model is the construction of a hydrophobicity profile from the linear amino acid sequence. First, the individual amino acids are assigned a hydrophobicity score according to one of the available scales. A popular hydrophathy scale is the one published by

Kyte and Doolittle in 1982 (**10**). In order to reduce the noise present in the hydropathy graph, a moving average is usually employed in which the average hydrophobicity score is calculated in a window of consecutive amino acids. The window is moved along the sequence, and the average is graphed against the position of the central amino acid. Increasing the size of the window will reduce the noise, but also limit the spatial resolution. Typically, window widths between 11 and 21 amino acids are useful. Hydrophobicity profiles can be generated by commercially available software packages for analyzing proteins. Alternatively, you can submit your amino acid sequence to a number of computational servers on the World Wide Web, which will return the hydrophobicity profile and estimates for the number, location, and orientation of the transmembrane segments. Links to several useful servers (TMpred, TMAP and SOSUI) can be found on the ExpASy site, on the Analysis Tools page: <http://expasy.hcuge.ch/www/tools.html>.

Putative transmembrane segments are found in the hydropathy plot as regions of approx 20 amino acids for which the average hydrophobicity exceeds a critical value (1.0 in the Kyte and Doolittle scale). The orientation of the transmembrane segments can sometimes be inferred from the distribution of charged residues that flank them, although the rules for such assignment are still being investigated (**11**). Additional clues can be obtained from the presence of a signal peptide at the N-terminus of the protein, which suggests an extracellular localization of this domain. The SignalP prediction server on the World Wide Web (<http://www.cbs.dtu.dk/services/>) uses neural network technology to help you decide whether your protein has a signal peptide and to predict where it will be cleaved by proteases. Typically, initial topology models are generated by assuming that all hydrophobic segments of sufficient length (~20 amino acids) cross the membrane once as an α -helix. Assignment of the N-terminus to either the cytoplasm or extracellular space then determines the orientation of all the subsequent transmembrane segments. Although this strategy has resulted in topology models that have held up to experimental scrutiny for many integral membrane proteins, recent results obtained for glutamate receptors have shown that hydrophobicity profiles should be interpreted with care.

Hydrophobicity profiles of all ligand-gated ion channels show a similar pattern (**Fig. 1**). The N-terminus starts with a signal peptide, suggesting it is externally localized. Furthermore, all profiles show four hydrophobic domains (M1–M4), the first three of which are closely spaced. Following cloning of the first member of this class, the α -subunit of the nicotinic acetylcholine receptor (nAChR) of *Torpedo californica* (**12**), the membrane topology model shown in **Fig. 2A** was proposed by making the standard assumptions. This model is still favored today for the superfamily of ligand receptors, which includes the nACh,

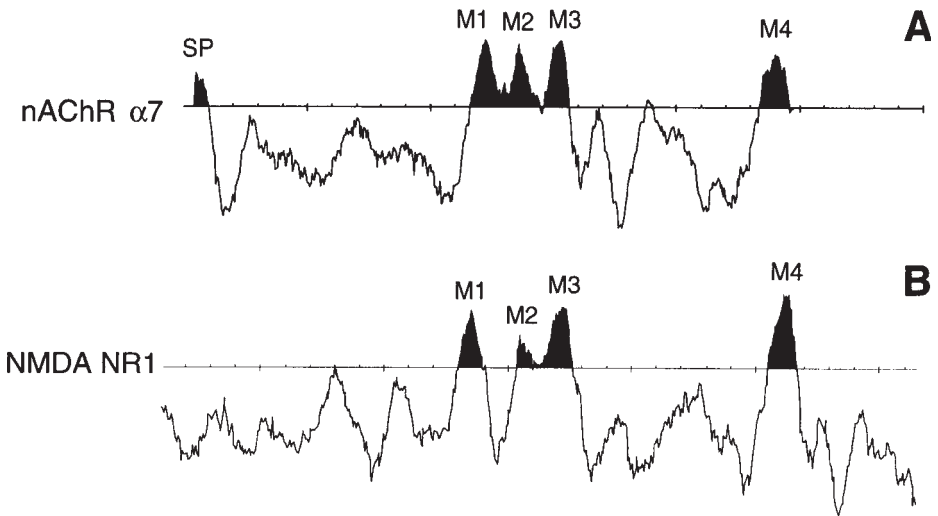


Fig. 1. Conserved hydrophobicity profiles in ligand-gated ion channels. Hydrophobicity profiles were generated by the computational server TMpred (*see text*). The first part of the N-terminus of the NMDA receptor NR1 subunit is not shown. Because of this truncation, the NR1 signal peptide is not visible. SP indicates signal peptide; M1–M4 are hydrophobic domains.

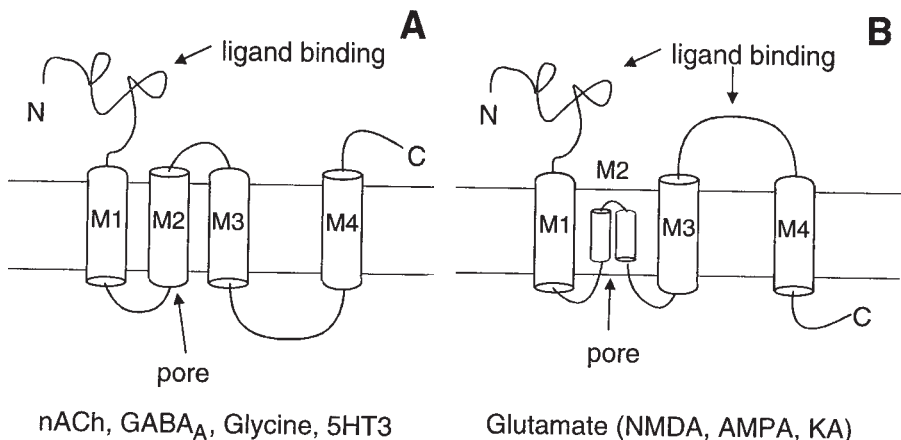


Fig. 2. Divergent membrane topologies in ligand-gated ion channels. Current membrane topology models for ligand-gated ion channels. The four hydrophobic M-segments are thought each to cross the membrane once in the superfamily of nicotinic acetylcholine, GABA_A, glycine, and serotonin 5HT3 receptors (**A**). The pore-forming M2 segment is proposed to be a re-entrant hairpin loop for the glutamate receptor family, which reverses the orientation of M3 and M4 (**B**).

GABA_A, glycine, and serotonin 5HT₃ receptors. Although glutamate receptors form a distinct family with virtually no amino acid homology to members of the superfamily, their hydrophobicity profile is conserved (**Fig. 1B**). The membrane topology initially proposed for glutamate receptors was therefore the same as the nACh receptor model, with all four M-segments crossing the membrane once (**Fig. 2A**). However, experimental results accumulated over the last several years have challenged this four-transmembrane domain (4-TMD) model for the glutamate receptor family. It was shown that the M2 segment does not cross the membrane, but forms a re-entrant hairpin loop, but the long hydrophilic M3–M4 linker is extracellular instead of cytoplasmic. To explain these data, the 3-TMD model shown in **Fig. 2B** was proposed (3–5,8,9).

1.2. Determination of Membrane Topology

Establishing the correct membrane topology of an integral membrane protein requires that all transmembrane domains are identified and their orientation determined. The putative transmembrane domains suggested by an analysis of the hydrophobicity profile provide a good starting point. The transmembrane domains themselves are usually not very amenable to experimental manipulation. An exception is the amphipathic M2 segment that lines the channel pore, which has been subjected to cysteine-scanning mutagenesis and chemical modification for both nicotinic ACh and glutamate receptors (13,14). However, the surface accessibility profiles resulting from these studies do not by themselves allow a definitive conclusion regarding the membrane orientation of the M2 segments.

Whether or not a hydrophobic domain spans the membrane can be determined by localizing the hydrophilic regions that flank it to opposite sites of the membrane. This will also define the orientation. Several approaches can be used to map hydrophilic regions to either the cytoplasm or the extracellular space. A generic method that works for both cytoplasmic and extracellular domains is epitope mapping using antibodies raised against peptides corresponding to the hydrophilic domains to be localized. Bound antibodies are visualized by immuno-electron microscopy. This approach has been most extensively used for the nACh receptor. Results obtained were often incompatible with the model shown in **Fig. 2A** and suggested the existence of extra-transmembrane domains not predicted from the hydrophobicity profile (15–17). An extensive discussion of the technical aspects and possible pitfalls associated with this approach can be found in Pedersen et al. (15). An alternative to raising anti-peptide antibodies is the introduction of small epitopes for which monoclonal antibodies (MAbs) are commercially available, using site-directed mutagenesis. Suitable epitopes include FLAG (DYKDDDDK), HA (YPYDVP DYA), Glu-Glu (EEEEYMPME), AU1 (DTYRYI), and AU5 (TDFYLK).

A second generic approach that can be used on both sides of the membrane is the introduction of novel sites that can be cleaved by specific proteases (*18–20*). Proteases and the sequences they recognize include factor Xa (IEGR), thrombin (GVRGPR), and enterokinase (DDDDK). Proteases will not cross the membrane, so they can be applied selectively on one side of the membrane. Successful cleavage can be monitored using Western analysis or electrophysiology (if cleavage causes a functional effect).

There are also several methods that use either cytoplasmic or extracellular markers. Phosphorylation of serine (S), threonine (T), or tyrosine (Y) residues provides a reliable cytoplasmic marker. Many receptors contain functional phosphorylation sites. Localization of these sites together with demonstration of functional phosphorylation (in vivo) helps to pinpoint aspects of membrane topology. Evidence of functional phosphorylation in the M3–M4 linker of the nicotinic receptor (*21*) and the C-terminus of the NMDA receptor NR1 subunit (*22*) lended support for the models shown in **Fig. 2**. However, functional phosphorylation sites in the M3–M4 linker of glutamate receptors (*1,23–26*) are inconsistent with the model in **Fig. 2B**, which is supported by results obtained using *N*-glycosylation tagging, as well as ligand binding site mapping. This controversy still remains unresolved.

Instead of relying on existing phosphorylation sites, it may be possible to create novel phosphorylatable sites by introducing the proper consensus sequence. The cAMP-dependent protein kinase A (PKA) is particularly suitable for this purpose, because its consensus sequence (Arg-Arg-Xxx-Ser/Thr) is well studied. The enzyme is abundant and can be easily activated using membrane-permeable analogs of cAMP. We have attempted to introduce a novel PKA site in the center of the M3–M4 linker of the NMDA receptor NR1 subunit by mutating amino acids 710–714 (NYSESA → RRASL). This mutation failed to produce a novel PKA site, but inadvertently affected the glycine binding pocket (*7*).

Identification of amino acid residues that contribute to the ligand binding site infers an extracellular localization. Mutations that affect the agonist or antagonist sensitivity of a receptor have therefore been used to infer external localization of the mutated residue. However, when a point mutation results in a shift of the agonist dose–response curve, it cannot be concluded that the mutated amino acid makes a critical contribution to the ligand binding site. The reason for this is that mutations can also affect the dose–response curve by altering the transduction process that couples ligand binding to channel opening (*7,27*). The structural basis for this transduction process is currently not known, so it is conceivable that residues that are localized to the cytoplasm or are in the membrane affect agonist sensitivity because they are part of the transduction machinery.

Finally, functional *N*-glycosylation is a reliable measure of external localization. Manipulation of *N*-glycosylation status has played a critical role in identifying extracellular domains in glutamate receptors (3–6). Mutagenesis is used to introduce or destroy a consensus sequence for *N*-glycosylation: Asn-Xxx-Ser/Thr, where Xxx is any amino acid except proline. If the mutation results in an alteration of glycosylation status, then this should result in a small change in apparent molecular weight as visualized on a Western blot. The change in molecular weight resulting from the addition or deletion of a sugar moiety depends on the complexity of the sugar, which is subject to processing. The first modification results in the addition of a high-mannose sugar, which adds only 2.6 kD to the molecular weight. Since the expected shifts are this small, it is important to show that the shift did not result from an altered secondary structure caused by the mutation. This can be checked by demonstrating that the wild-type and mutant proteins run at the same molecular weight, following removal of the sugars using endoglycosidase-H, as described below (5). Alternatively, glycosylation can be prevented by treating the cells that are producing the recombinant proteins with tunicamycin (4). Unfortunately, when introduction of an NxS consensus sequence fails to result in a detectable increase in molecular weight, it cannot be concluded that the domain is cytoplasmic, since many other factors can be responsible for failed glycosylation. One important limitation of this approach is the requirement that the asparagine that accepts the sugar is at least 10 amino acids away from the nearest transmembrane segment (28). This method can therefore only be used for long external loops (28). Many integral membrane proteins contain hydrophilic domains linking putative transmembrane segments that are too short to support *N*-glycosylation. New methods will need to be developed to map these short linkers.

Another potential problem results from the fact that successful introduction of a novel glycosylation site may in fact alter the membrane topology and cause misfolding (29). To guard against this possibility, it is desirable to demonstrate uncompromised function of *N*-glycosylation mutants (5,7), since misfolding is unlikely to have occurred there.

The rest of this chapter describes in detail the methods we have used to isolate integral membrane proteins exogenously expressed in *Xenopus* oocytes and how to perform the deglycosylation experiments. The membrane preparation uses a sucrose fractionation step to remove the majority of the yolk proteins. The resulting membrane preparation can be used for further biochemical manipulations. In addition to deglycosylation experiments described here, this membrane preparation has been successfully used for immunoprecipitation experiments and Western blot analysis.

2. Materials

1. Oocyte homogenization buffer: 83 mM NaCl, 1 mM MgCl₂, 10 mM HEPES, 5 mM EDTA, Adjust pH to 7.9 using NaOH. Autoclave.
2. Sucrose solution: 15% Sucrose in oocyte homogenization buffer. Sucrose should be ultrapure and ultracentrifuge grade. Make this solution fresh for every experiment.
3. Protease inhibitor cocktail (from Higgins and Casey [30]): The compounds used are extremely toxic, so appropriate care should be taken. Solution 1: 0.16 g of TPCK (Sigma, St. Louis, MO, no. T4376) and 0.16 g of TLCK (Sigma no. T7254) dissolved in 5 mL of DMSO. Solution 2: 10 mL of 0.2 M PMSF (Sigma no. P7626) in isopropanol. Mix the two solutions and aliquot out in 500- μ L samples. Store at -20°C . Mixture is 1000X (see Note 3).
4. Ultraclear centrifuge tubes: 13 \times 51 mm Tubes for use in ultracentrifuge (Beckman, Palo Alto, CA, no. 344057).
5. Swinging bucket rotor: SW50.I 50.000 g (Beckman).
6. Resuspension solution: 20 mM Tris/HCl, 1 mM EGTA, 1 mM EDTA. Adjust pH to 7.5 using HCl. Add Triton X-100 to a final concentration of 0.1–1%. Add NaCl to final concentration of 150–500 mM (see Note 4).
7. 4X Tris-HCl: 6.05 g Tris-HCl/100 mL, adjust pH to 6.8 using HCl. Filter-sterilize. Add 0.4 g SDS. Store at 4°C .
8. 6% SDS-loading buffer: 3.6 g SDS, 0.93 g DTT, 1.2 mg bromophenol blue, 3 mL glycerol. Add 4X Tris-HCl to a total of 10 mL. Dissolve by vigorously vortexing and heating to 65°C . Aliquot out and store at -20°C (see Note 4).
9. Endoglycosidase-H: New England Biolabs, cat. no. 702 S (Beverly, MA).
10. 4 M Urea: Prepare a 4-M urea stock in autoclaved H₂O.

3. Methods

3.1. Membrane Preparation of *Xenopus laevis* Oocytes (See Note 1)

1. Prechill a Dounce homogenizer (10 mL) (VWR, Atlanta, GA) cat. no. KT 885450-0021, and place oocyte homogenization buffer plus protease inhibitors on ice.
2. Add 800 μ L oocyte homogenization buffer to the homogenizer, and transfer 20 oocytes into the solution. Homogenize until homogeneous mixture.
3. Transfer to an autoclaved test tube, and spin at 800g for 10 min at 4°C . This will pellet the nuclear material.
4. Transfer the supernatant to a fresh autoclaved tube. Keep on ice.
5. Prepare the sucrose solution, and add protease inhibitors. Chill on ice.
6. Aliquot 150 μ L of sucrose solution into ultraclear centrifuge tube.
7. Carefully overlay the sucrose solution with the supernatant of **step 4**. Extreme care should be taken not to mix the two layers.
8. Spin in an ultracentrifuge at 36,000g at 4°C for 1 h. The pellet will contain the membrane fraction.
9. Prechill the resuspension solution plus protease inhibitors.

10. Decant the tube and keep it inverted. Wipe out the inside of the tube with a Kimwipe to remove all the sucrose. It is important to remove as much as possible, since sucrose will interfere with the protein gel.
11. Keep the pellet on ice, and dissolve in 50 μL of the resuspension solution. Leave at 4°C for 1 h to overnight for solubilization of the protein. At this point, you can use the sample for SDS-PAGE and Western analysis or for further experiments.

3.2. Deglycosylation of Membrane Proteins

1. Add 25 μL of 4 M urea to 50 μL membrane prep.
2. Add 5 μL of 10X denaturation buffer (supplied by the manufacturer of Endo-H).
3. Incubate at 67°C for 10 min (*see Note 4*).
4. Add 5.5 μL of 10X Endo-H buffer (supplied by the manufacturer of Endo-H).
5. Add 2 μL Endo-H (400,000 U/mg).
6. Incubate at 37° for 1 h.
7. Add 1/6 vol of 6% SDS buffer.
8. Incubate at 67°C for 10 min, and separate by SDS-PAGE.

4. Notes

1. Yolk proteins constitute a major component of *Xenopus* oocytes. On an SDS-PAGE gel, they will follow the following pattern: Lipovittelin-I runs as a very strong band at ~120 kDa, Phosvitin at ~35 kDa, Lipovittelin-II at ~30 kDa, and Phosvettes at 15–21 kDa (**31**). Regular membrane preparations as described for cultured cells or brain tissue will not remove these yolk proteins. Proteins running at a molecular weight similar to one of the yolk proteins will therefore be poorly resolved on SDS-PAGE. This results in smearing or masking of the band of interest when probed by Western analysis. Yolk proteins can also interfere with immunoprecipitations by nonspecific binding to antibodies. Even if the protein of interest does not run close to a yolk protein, it is advisable to remove the yolk because their presence may result in overloading the gel. A method for removing yolk proteins from cytosolic samples that involves a freon extraction has been described elsewhere (**32**). This method is unsuitable for analyzing integral membrane proteins, however. We have therefore developed the sucrose fractionation procedure described in **Subheading 3**.
2. The number of oocytes per preparation has to be determined empirically. When expression levels are high, as checked by two-electrode voltage-clamp experiments, membranes prepared from 20 oocytes/lane were found to be sufficient for detection by Western analysis.
3. Oocytes contain a very large amount of proteases. It is eminent to keep protease inhibitors present during the whole procedure and even supplement them in the case of long incubation times. All of the solutions used are either autoclaved or filter-sterilized to remove proteases.
4. Methods for solubilization of integral membrane proteins vary significantly between different proteins. Solubilization conditions therefore have to be optimized empirically for each protein tested. Parameters to vary include:

- a. The amount of NaCl in the resuspension solution: concentrations between 150 and 500 mM are useful.
 - b. The type and amount of detergent used; alternatives for Triton X-100 are NP40 and Tween.
 - c. The addition of urea up to a final concentration of 4 M.
5. Some protocols advise that you boil the sample before loading on SDS-PAGE. However, for certain integral membrane proteins, it may be advisable to lower the temperature to 67°C, since boiling can produce formation of large aggregates, which fail to enter into the stacking gel. One way to test for this is to include the stacking gel when a Coomassie or silver stain is performed. When performing a Western blot, also leave the stacking gel on and probe the entire gel. The incubation temperature will once again vary between the different proteins. Some proteins need to be incubated overnight at room temperature (H. M. A. VanDongen, unpublished observations). The use of a very high percentage SDS in the sample buffer aids in preventing aggregates.
6. It is important that your protein standards contain the same detergents and sample buffer as your samples. Loading all empty lanes with the same solution will also greatly improve the quality of your SDS-PAGE gel.
7. Experiments that test alteration of glycosylation status require the detection of minor differences in molecular weight on an SDS-PAGE gel. During glycosylation, the first modification of an asparagine is addition of a high-mannose moiety, which contains two *n*-acetylglucosamines, nine mannoses, and three glucoses. This gives rise to an increase in molecular weight of only 2.6 kDa. Modifications to enhance resolution include the following.
- a. Optimize the percentage of the gel.
 - b. Increase the electrophoresis time in order to run your protein to the bottom of the gel (most protocols tell you to run the Coomassie blue dye to the bottom). Multicolored protein standards are extremely helpful in this case, because they show exactly where the protein of interest is running. For larger proteins, it is common to run the gel up to three times longer to obtain optimal resolution. For accurate estimation of the molecular weight, it is advisable to run unstained standards (for Coomassie or silver stain) or biotinylated standards (for Western blot) on the same gel.
 - c. Lower the temperature during gel electrophoresis. Gels run at 4° in a cold room generally result in a more compact banding pattern of the proteins, which will allow better interpretation of minor shifts.
 - d. Prerun the gel. Prerunning of the gel allows the impurities in the acrylamide/*bis*-acrylamide mixture to run out of the gel. Inclusion of cytochrome-c at 5 mg/mL during the prerun lowers the background of the Western blot.
8. There are several enzymes that can be used to remove sugar moieties from proteins. In the case where an N-linked glycosylation site is altered, Endoglycosidase-H or PNGase-F are the suitable choices, because they both cleave in the high-mannose core. When the native glycosylation status of a protein is investigated, other enzymes may be more appropriate.

References

1. Taverna, F. A., Wang, L. Y., MacDonald, J. F., and Hampson, D. R. (1994) A transmembrane model for an ionotropic glutamate receptor predicted on the basis of the location of asparagine-linked oligosaccharides. *J. Biol. Chem.* **269**, 14,159–14,164.
2. Roche, K. W., Raymond, L. A., Blackstone, C., and Huganir, R. L. (1994) Transmembrane topology of the glutamate receptor subunit GluR6. *J. Biol. Chem.* **269**, 11,679–11,682.
3. Wo, Z. G. and Oswald, R. E. (1994) Transmembrane topology of two kainate receptor subunits revealed by N-glycosylation. *Proc. Natl. Acad. Sci. USA* **91**, 7154–7158.
4. Hollmann, M., Maron, C., and Heinemann, S. F. (1994) N-glycosylation site tagging suggests a three transmembrane domain topology for the glutamate receptor GluR1. *Neuron* **13**, 1331–1343.
5. Wood, M. W., VanDongen, H. M. A., and VanDongen, A. M. J. (1995) Structural conservation of ion conduction pathways in K channels and glutamate receptors. *Proc. Natl. Acad. Sci. USA* **92**, 4882–4886.
6. Wo, Z. G. and Oswald, R. E. (1995) A topological analysis of goldfish kainate receptors predicts three transmembrane segments. *J. Biol. Chem.* **270**, 2000–2009.
7. Wood, M. W., VanDongen, H. M. A., and VanDongen, A. M. J. (1997) An alanine residue in the M3-M4 linker lines the glycine binding pocket of the N-Methyl-D-Aspartate receptor. *J. Biol. Chem.* **272**, 3532–3537.
8. Stern-Bach, Y., Bettler, B., Hartley, M., Sheppard, P. O., O'Hara, P. J., and Heinemann, S. F. (1994) Agonist selectivity of glutamate receptors is specified by two domains structurally related to bacterial amino acid-binding proteins. *Neuron* **13**, 1345–1357.
9. Bennett, J. A. and Dingledine, R. (1995) Topology profile for a glutamate receptor: three transmembrane domains and a channel-lining re-entrant membrane loop. *Neuron* **14**, 373–384.
10. Kyte, J. and Doolittle, R. F. (1982) A simple method for displaying the hydrophobic character of a protein. *J. Mol. Biol.* **157**, 105–132.
11. Gafvelin, G., Sakaguchi, M., Andersson, H., and Von Heijne, G. (1997) Topological rules for membrane protein assembly in eukaryotic cells. *J. Biol. Chem.* **272**, 6119–6127.
12. Noda, M., Takahashi, H., Tanabe, T., Toyosato, M., Furutani, Y., Hirose, T., et al. (1982) Primary structure of alpha-subunit precursor of Torpedo californica acetylcholine receptor deduced from cDNA sequence. *Nature* **299**, 793–797.
13. Akabas, M. H., Kaufmann, C., Archdeacon, P., and Karlin, A. (1994) Identification of acetylcholine receptor channel-lining residues in the entire M2 segment of the alpha subunit. *Neuron* **13**, 919–927.
14. Kuner, T., Wollmuth, L. P., Karlin, A., Seeburg, P. H., and Sakmann, B. (1996) Structure of the NMDA receptor channel M2 segment inferred from the accessibility of substituted cysteines. *Neuron* **17**, 343–352.

15. Pedersen, S. E., Bridgman, P. C., Sharp, S. D., and Cohen, J. B. (1990) Identification of a cytoplasmic region of the *Torpedo* nicotinic acetylcholine receptor α -subunit by epitope mapping. *J. Biol. Chem.* **265**, 569–581.
16. Ratnam, M., Nguyen, D. L., Rivier, J., Sargent, P. B., and Lindstrom, J. (1986) Transmembrane topography of nicotinic acetylcholine receptor: immunochemical tests contradict theoretical predictions based on hydrophobicity profiles. *Biochemistry* **25**, 2633–2643.
17. Criado, M., Hochschwender, S., Sarin, V., Fox, J. L., and Lindstrom, J. (1985) Evidence for unpredicted transmembrane domains in acetylcholine receptor subunits. *Proc. Natl. Acad. Sci. USA* **82**, 2004–2008.
18. Wilkinson, B. M., Critchley, A. J., and Stirling, C. J. (1996) Determination of the transmembrane topology of yeast Sec61p, an essential component of the endoplasmic reticulum translocation complex. *J. Biol. Chem.* **271**, 25,590–25,597.
19. Wang, C. C., Schultz, D. E., and Nicholas, R. A. (1996) Localization of a putative second membrane association site in penicillin-binding protein 1B of *Escherichia coli*. *Biochem. J.* **316**, 149–156.
20. Zen, K. H., Consler, T. G., and Kaback, H. R. (1995) Insertion of the polytopic membrane protein lactose permease occurs by multiple mechanisms. *Biochemistry* **34**, 3430–3437.
21. Haganir, R. L. and Miles, K. (1989) Protein phosphorylation of nicotinic acetylcholine receptors. *Crit. Rev. Biochem. Mol. Biol.* **24**, 183–215.
22. Tingley, W. G., Roche, K. W., Thompson, A. K., and Haganir, R. L. (1993) Regulation of NMDA receptor phosphorylation by alternative splicing of the C-terminal domain. *Nature* **364**, 70–73.
23. McGlade-McCulloh, E., Yamamoto, H., Tan, S., Brickey, D., and Soderling, T. (1993) Phosphorylation and regulation of glutamate receptors by calcium/calmodulin protein kinase II. *Nature* **362**, 640–642.
24. Wang, L.-Y., Taverna, F. A., Huang, X.-P., MacDonald, J. F., and Hampson, D. R. (1993) Phosphorylation and modulation of a kainate receptor (GluR6) by cAMP-dependent protein kinase. *Science* **259**, 1173–1175.
25. Nakazawa, K., Mikawa, S., Hashikawa, T., and Ito, M. (1995) Transient and persistent phosphorylation of AMPA-type glutamate receptor subunits in cerebellar Purkinje cells. *Neuron* **15**, 697–709.
26. Yakel, J., Vissavajhala, P., Derkach, V., Brickey, D., and Soderling, T. (1995) Identification of a Ca^{2+} /calmodulin-dependent protein kinase II regulatory phosphorylation site in non-*N*-methyl-D-aspartate glutamate receptors. *Proc. Natl. Acad. Sci. USA* **92**, 1376–1380.
27. Colquhoun, D. and Farrant, M. (1993) Molecular pharmacology. The binding issue. *Nature* **366**, 510–511.
28. Landolt-Martcorena, C. and Reithmeier, R. A. F. (1994) Asparagine-linked oligosaccharides are localized to single extracytosolic segments in multi-span membrane glycoproteins. *Biochem. J.* **302**, 253–260.
29. Gafvelin, G. and Von Heijne, G. (1994) Topological “frustration” in multi-spanning *E. coli* inner membrane proteins. *Cell* **77**, 401–412.

30. Higgins, J. B. and Casey, P. J. (1994) In vitro processing of recombinant G protein gamma subunits. Requirements for assembly of an active beta gamma complex. *J. Biol. Chem.* **269**, 9067–9073.
31. Wiley, H. S. and Wallace, R. A. (1981) The structure of vitellogenin. Multiple vitellogenins in *Xenopus* eggs give rise to multiple forms of the yolk protein. *J. Biol. Chem.* **256**, 8626–8634.
32. Evans, J. P. and Kay, B. K. (1991) Biochemical fractionations of oocytes. *Methods Cell Biol.* **36**, 133–148.

Engineering the NMDA Receptor Channel Lining

Antonio V. Ferrer-Montiel and Mauricio Montal

1. Introduction

Neurotransmitter-gated channels, such as the NMDA receptor, are oligomeric membrane proteins assembled from multiple homologous subunits organized around a central ion-conducting pore (1,2). A major effort is directed toward understanding the structural features that determine their function. However, the absence of an atomic resolution structure for even a single ligand-gated ion channel remains a serious deficiency to accomplish this goal. There has been little success in the preparation of high-quality three-dimensional crystals of these membrane proteins, and the determination of their structures in solution by multidimensional NMR spectroscopy has been hampered by the large size and multiplicity of their subunits as well as the requirement of a lipid environment to maintain the native folded conformation. These significant limitations in the conventional methods of structural biology have prompted the development of indirect strategies to identify and characterize those segments of these proteins that contribute directly to the formation of the channel lining. In this context, a biomimicry-based strategy founded on the tenet that a specific functional feature may be transferred to a receptor lacking it by implanting the structural determinants that define the property is contributing considerable diagnostic information. The uniqueness of the biomimicry-based strategy resides in the notion of achieving a “gain of function” in contrast with the classical mutagenesis approach that randomly aims for a “loss of function.” This approach has successfully led to changing the ion selectivity of the neuronal $\alpha 7$ acetylcholine receptor from cationic to anionic (3), to transfer a scorpion toxin binding site to an insensitive potassium channel (4), and to engineer an NMDA receptor-like pore on a glutamate receptor (5). These results represent significant progress in identifying structural components of

the pore-lining structure of ion channel proteins and are beginning to delineate guidelines to engineer new proteins with desired specifications.

Here, we concentrate on glutamate receptors and describe the experimental strategy used to restructure the permeation pathway of a non-NMDA receptor subunit, GluR1, to mimic that of the NMDA receptor. NMDA receptors, but not non-NMDA receptors, exhibit high Ca^{2+} -permeability and sensitivity to block by psychotropic drugs, such as phencyclidine (PCP) and dizolcipine (MK-801), that act as uncompetitive NMDA antagonists (5). These are small molecules that enter the open channel and transiently occlude it by presumably interacting with residues exposed to the channel lumen (6), thus making them good probes of the accessibility of pore-lining residues. Because of their preferential blockade of activated NMDA receptors, these sorts of drugs are considered candidates for drug development in the area of neuroprotectants (7). Accordingly, a great deal of attention is being paid to unraveling the molecular determinants of the blocker binding pocket. We approach the problem focusing on function and aiming to design homomeric glutamate receptors that would imitate the pore blockade and ionic selectivity properties of the heteromeric NMDA receptor.

2. Materials

1. cDNA encoding the protein to be engineered kept at -20°C .
2. PCR primer oligonucleotide specifying the designed mutations.
3. Sequencing (Sequenase) and cRNA in vitro transcription (mMessage mMachine) kits (Ambion, Austin, TX).
4. *Xenopus laevis* frogs (Nasco, Fort Atkinson, WI or *Xenopus* I) are maintained in animal facilities with a 12-h light–dark cycle, constant temperature, and ion-balanced clean water. Frogs should be fed twice per week, followed by the cleaning of the tanks and supply of fresh water.
5. Frog oocytes should be extracted as needed and may be kept in the follicles at 4°C in oocyte buffer for 2–3 d. Change buffer daily.
6. Defolliculation buffer: 82.5 mM NaCl, 2.5 mM KCl, 1 mM MgCl_2 , 5 mM HEPES, pH 7.0, 2 mg/mL Collagenase Type IA (Sigma, St. Louis, MO). Collagenase is added immediately before defolliculation. Defolliculated oocytes should be kept at 17°C and injected within 24 h.
7. Oocyte buffer: 100 mM NaCl, 2 mM KCl, 1.8 mM CaCl_2 , 1 mM MgCl_2 , 5 mM HEPES, pH 7.0, 0.55 g/L Napyruvate, 50 $\mu\text{g}/\text{mL}$ gentamicin. This buffer should be stored at 4°C .
8. Ba^{2+} -Ringer's medium: 120 mM NaCl, 2.8 mM KCl, 1.8 mM BaCl_2 , 10 mM HEPES, pH 7.4.
9. Niflumic and/or flufenamic acids: A solution 100 mM is prepared dissolving 280 mg of either acid in bidistilled water and slowly raising the pH until all the powder is dissolved. Store the solution at 4°C protected from light and discard after 1 wk.

10. Extraction buffer: 20 mM Tris-HCl, pH 7.4, 150 mM NaCl, 1% Nonidet P-40, 0.25% deoxycholate, 1 mM EGTA, 1 mM NaF, 1 mM Na₃VO₄, 1 μg/mL pepstatin, A, 1 μg/mL leupeptin, 1 μg/mL aprotinin, 1 mM phenylmethylsulfonyl-fluoride, and 5 mM iodoacetamide.
11. Oocyte nanoinjector (Drummond microdispenser. Drummond Scientific, Broomall, PA).
12. Two-microelectrode voltage-clamp amplifier with dedicated computer: We use the Turbo TEC amplifier from NPI (Turbo TEC O1C; NPI Electronics, Tamm, Germany) interfaced to a PC computer through 12-bit acquisition board from Axon (Axon Instruments, Foster City, CA). The software for data acquisition is pClamp6.0 (Axon Instruments).

3. Methods

3.1. Sequence Alignment:

Identification of Molecular Determinants of Pore Function

Since our goal is to engineer an NMDAR-like permeation pathway on a non-NMDA receptor, GluR1, we constrained the search to the M2 transmembrane segment, considered an essential component of the ionic pore of this superfamily of ligand-gated ion channels (*1,5,8–17*). As a first strategy, it may be considered to create chimeric receptor by replacing the original M2 transmembrane segment of GluR1 by that of the NMDA receptor. The structural disruption imposed on the protein by this domain swapping was incompatible with channel function (*5*). An alternative strategy is the identification and stepwise replacement of specific residues, facilitated by considering amino acid conservation as an index of functional relevance. We now turn to highlight the important steps in the process.

1. Align the amino acid sequences of the M2 transmembrane segment for all NMDA receptor subunits (**Fig. 1**), and search for absolute amino acid conservation among the NMDA receptor subunits. Notice that ¹²W (corresponding to ⁵⁹³W in NR1) and ¹⁷N (corresponding to ⁵⁹⁸N in NR1) in the M2 segment are absolutely conserved among all the NMDA receptor subunits.
2. Locate the corresponding amino acids on the non-NMDA receptors (GluRs) by aligning their amino acid sequences with that of the NMDA receptor (**Fig. 1**). Clearly, these residues in the M2 of GluRs are ¹²L and ¹⁷Q (corresponding to ⁵⁷⁷L and ⁵⁸²Q in M2 of GluR1). Note that ³T and ⁹W are conserved among NMDA and several GluR receptor subunits.

3.2. Engineering the GluR1 M2 Transmembrane Segment

The stepwise replacement of amino acids in the M2 transmembrane segment of the GluR1 is carried out by PCR amplification with mutagenic oligonucleotides and subcloning the PCR fragments into the cDNA (*5*). The important steps in the protocol are:

	1	2	3	4	5	6	7	8	9	10	11	12	13	14	15	16	17	18	19	20	21	22
GluR1	E	F	G	I	F	N	S	L	W	F	S	L	G	A	F	M	Q	Q	G	-	C	D
GluR2	E	F	G	I	F	N	S	L	W	F	S	L	G	A	F	M	<u>K</u>	Q	G	-	C	D
GluR3	E	F	G	I	F	N	S	L	W	F	S	L	G	A	F	M	Q	Q	G	-	C	D
GluR4	E	F	G	I	F	N	S	L	W	F	S	L	G	A	F	M	Q	Q	G	-	C	D
GluR5	N	F	T	L	L	N	S	F	W	F	G	V	G	A	L	M	Q	Q	G	-	S	E
GluR6	N	F	T	L	L	N	S	F	W	F	G	V	G	A	L	M	Q	Q	G	-	S	E
GluR7	N	F	T	L	L	N	S	F	W	F	G	V	G	A	L	M	Q	Q	G	-	S	E
KA1	Q	Y	S	L	G	N	S	L	W	F	P	V	G	G	F	M	Q	Q	G	-	S	T
KA2	Q	Y	T	L	G	N	S	L	W	F	P	V	G	G	F	M	Q	Q	G	-	S	E
NR1	A	L	I	L	S	S	A	M	<u>W</u>	<u>F</u>	<u>S</u>	<u>W</u>	<u>G</u>	V	L	L	<u>N</u>	<u>S</u>	<u>G</u>	I	G	E
NR2A	S	<u>F</u>	<u>I</u>	I	G	K	A	I	<u>W</u>	L	L	<u>W</u>	<u>G</u>	L	V	F	<u>N</u>	<u>S</u>	<u>S</u>	V	P	V
NR2B	S	<u>F</u>	<u>I</u>	I	G	K	A	I	<u>W</u>	L	L	<u>W</u>	<u>G</u>	L	V	F	<u>N</u>	<u>S</u>	<u>S</u>	V	P	V
NR2C	S	<u>F</u>	<u>I</u>	I	G	K	<u>S</u>	V	<u>W</u>	L	L	<u>W</u>	A	L	V	F	<u>N</u>	<u>S</u>	<u>S</u>	V	P	V
NR2D	T	<u>F</u>	<u>I</u>	I	G	K	<u>S</u>	I	<u>W</u>	L	L	<u>W</u>	A	L	V	F	<u>N</u>	<u>S</u>	<u>S</u>	V	P	V

Fig. 1. Amino acid sequence alignment of the M2 segments of AMPA and kainate (KA) receptor subunits GluR1-7, KA binding proteins KA1-2, and all of the NMDA receptor subunits (**10,11**). Residues underlined indicate conservation among the NMDA receptor subunits. For GluR2, the edited version is displayed. Shaded residues signify conservation with respect to GluR1.

1. Design and synthesize the sense and antisense mutagenic primers for PCR amplification.
2. Run the PCR, isolate, purify the amplified fragments, and subclone them into the corresponding coding region of GluR1.
3. Sequence the mutated region and the restriction sites used for subcloning (*see Note 1*).
4. Purify the mutated cDNA by CsCl gradient centrifugation.
5. Linearize the cDNA with a restriction enzyme that cuts downstream of the 3'-end after the coding region (**18**). Linear cDNA is extracted with phenol/chloroform and precipitated with 1/10 vol of 5 M ammonium acetate and 2 vol of isopropanol or ethanol at -20°C for 20 min, and washed with 80% ethanol. The concentration of cDNA is estimated from $\text{OD}_{260\text{ nm}}$ values using the following equivalence: $1 \text{ OD}_{260} = 50 \mu\text{g/mL}$.
6. One microgram of linear cDNA is used as a template for in vitro transcription of cRNA using the mMESSAGE mMACHINE from Ambion following the manufacturer's instructions (*see Note 2*).
7. cRNA transcripts are alcohol-precipitated and dissolved in DEPC-treated water (**step 5**). The concentration of cRNA is estimated from the $\text{OD}_{260\text{ nm}}$ using the relationship $1 \text{ OD}_{260} = 40 \mu\text{g/mL}$ cRNA. The quality of the synthesized transcripts may be qualitatively assessed from the ratio $\text{OD}_{260}/\text{OD}_{280}$, which should be in the range of 1.8–2.0. It is advisable to analyze the size of the in vitro transcribed cRNA by agarose or polyacrylamide gel electrophoresis.
8. Small aliquots ($\sim 3 \mu\text{L}$) of cRNA at 10–100 $\mu\text{g/mL}$ should be stored at -80°C .

3.3. Functional Expression of Engineered GluR1 Channels

The procedures used in our laboratory concerning harvesting and defolliculation of oocytes were described in detail in a methodological paper (18). No significant refinements that warrant detailed description have been implemented. Thus, we next just list the major steps of the process and refer the reader to **ref. 18**.

1. Oocytes are harvested from anesthetized, adult female *X. laevis* frogs and placed in defolliculation buffer for 2 h at room temperature under vigorous shaking.
2. Oocytes are extensively washed (six to seven times) with collagenase-free defolliculation buffer and incubated in this buffer for 2 h. Thereafter, undamaged oocytes are transferred to oocyte buffer and kept at 18°C. Oocytes are now ready for injection of cRNA.
3. For cRNA injection, pipets are pulled in a pipet puller, and the tip cut with fine scissors to an opening diameter of 10–50 μm . Pipets should be decontaminated of RNases by baking them for ≥ 3 h at 180°C.
4. Thaw a cRNA aliquot, incubate it at 37°C for 10 min, and load it into the pipet.
5. Inject 25–50 nL/oocyte in the vegetal pole (18). Place oocytes into a 48-well tissue culture plate (1 oocyte/well), and maintain them with oocyte buffer at 18°C until assayed for functional expression. Alternatively, you may group the injected oocytes and keep them together in 60-mm dishes. In this case, remove dead oocytes, and change buffer daily.

3.4. Functional Characterization of Engineered GluR1 Channels

All functional measurements are performed using the two-microelectrode voltage-clamp technique as described (18). We focus here on the characterization of the functional properties of the restructured GluR1 channels. These properties include the efficacy and potency of channel blockade by uncompetitive NMDA antagonists, the voltage- and use-dependence of the blockade activity, and the ionic selectivity (**Table 1**).

3.4.1. Sensitivity of GluR1 Mutants to Open-Channel Blockers of the NMDA Receptor

1. Injected oocytes are transferred to the recording chamber and impaled with the current and potential electrodes. The holding potential is held at -80 mV and oocytes are continuously perfused with Ba^{2+} -Ringer's solution supplemented with 100 μM niflumic and/or flufenamic acids.
2. Ionic currents are activated by perfusing with a saturating concentration of agonist, prepared in Ba^{2+} -Ringer's/flufenamic (*see Note 3*). For GluR1, we used 500 μM kainate, and for NMDAR, we used 100 μM L-glutamate along with 20 μM glycine.
3. Open-channel blockers are prepared at various concentrations in the agonist solution. Since these drugs require channel opening to access their binding site,

Table 1
Pore Properties of Restructured GluR1 and NMDA Receptors

	GluR1		NMDAR
	L577W/Q582N	L577W/Q582T	NR1:NR2A
Permeation ^a			
Monovalent cations	1.3	1.1	1.2
Divalent cations	5.0	4.5	7.0
Channel blockade ^b			
PCP	10 ⁻⁶ M	10 ⁻⁷ M	10 ⁻⁸ M
MK-801	10 ⁻⁶ M	10 ⁻⁶ M	10 ⁻⁸ M
Memantine	10 ⁻⁵ M	10 ⁻⁶ M	10 ⁻⁷ M
Amantadine	10 ⁻³ M	10 ⁻⁴ M	10 ⁻⁵ M
Ketamine	10 ⁻⁵ M	10 ⁻⁶ M	10 ⁻⁷ M
Dextrorphan	10 ⁻⁵ M	10 ⁻⁶ M	10 ⁻⁸ M
Dextromethorphan	10 ⁻⁵ M	10 ⁻⁶ M	10 ⁻⁷ M
Extracellular Ca ²⁺	10 ⁻³ M	10 ⁻³ M	10 ⁻⁴ M
Extracellular Mg ²⁺	10 ⁻³ M	10 ⁻³ M	10 ⁻⁵ M
Subunit stoichiometry	Pentameric ^c	Pentameric ^c	Pentameric ^d
Oligomeric structure	Homomeric	Homomeric	Heteromeric

^aRelative permeabilities to monovalent (P_K/P_{Na}) and divalent (P_{Ca}/P_{Na}) cations, taken from (8).

^bConcentration at which the drug and/or cations inhibited half of the maximal agonist-activated current (19).

^cValue taken from (20).

^dValue taken from (21).

the experimental paradigm consists of the activation of the channel by perfusing agonist solution followed by application of agonist supplemented with the open-channel blocker.

4. Receptor block is terminated by washing out the blocker with agonist. Thereafter, the agonist is removed to cease the functional response. This paradigm should be repeated for each blocker concentration tested in at least three oocytes of two different batches.
5. The unblocked response is calculated as the ratio $I_{\text{blocker}}/I_{\text{agonist}}$ and plotted as a function of the drug concentration to build up a dose-response curve.
6. The experimental data are fitted to the logistic equation $I_{\text{blocker}}/I_{\text{agonist}} = 1/[1 + (\text{blocker}/IC_{50})^n]$, where IC_{50} denotes the concentration of blocker to inhibit half-maximal of the agonist response, and n represents the Hill coefficient of the blocker. The IC_{50} values may be taken as an index of the fidelity of the design (5) (Table 1).
7. The voltage dependence of channel blockade is analyzed at concentrations of blocker $\leq IC_{50}$, because higher concentrations may obscure it owing to excessive blockade. Experimentally, two protocols may be used: (1) a voltage-step protocol where the voltage is changed in discrete voltage steps from -80 – 0 mV; and

- (2) a continuous membrane potential change using a computer-controlled voltage-ramp protocol. Leak currents, obtained by running the voltage-ramp protocol without agonist, are subtracted from agonist-elicited responses (*see Note 5*).
8. The use dependence of channel blockade is determined by repetitive activation of the receptor channel in the presence of the blocker. This is accomplished by applying 5–10 s agonist or/and agonist blocker pulses interspersed by 60-s wash periods. After blocker application, recovery of receptor channel activity may be investigated. The agonist-elicited responses are plotted as a function of the number of pulses. Use-dependent blockade is readily recognized as a continuous increase in channel blockade that does not recover after the blocker is washed out (5). Rundown of agonist-operated responses is evaluated performing the paradigm with agonist alone.

3.4.2. Ionic Selectivity of Restructured GluR1 Channels

The hallmark of the NMDA receptor is its high permeability to Ca^{2+} (12,22). Thus, the Ca^{2+} permeability of mutated GluR1 receptors provides a test of the validity of the design (Table 1).

1. Determine the reversal potential of the agonist-activated currents at different external ionic concentrations. To avoid changes in the ionic strength of the external solution, alterations in the concentration of a particular ion must be compensated with addition or removal of a nonpermeant ion. For example, the Na^+ concentration may be varied from 0 to 120 mM by substituting it with *N*-methylglucamine (8).
2. Calculate the ionic activity of your external solution using the relation $a_x = [X] \gamma_x$, where a_x is the activity of the ion *X*, $[X]$ denotes the concentration in mol/L, and γ_x refers to the activity coefficient (8,22).
3. Plot the reversal potentials as a function of the ionic activities, and fit the experimental data to the Goldman-Hodging-Katz (GHK) equation (8,22,23). The outcome of the fit will be the relative ionic permeabilities of the permeant ions (Table 1).

3.4.3. Specificity of the Engineered Properties on GluR1 Channels

To determine the specificity of the engineered receptor phenotype, functional properties not specified by the implemented molecular determinants should be evaluated. This is a critical requirement since site-directed mutagenesis may alter the global fold of the protein leading to unspecific functional changes. The functional properties to measure are sensitivity to several agonists (for GluR1, L-glutamate, kainate, domoate, and AMPA) and level of protein expression.

1. Obtain the concentration of agonist that activates half-maximal response, EC_{50} , and the maximal response (I_{max}) from dose–response curves. These values must be obtained for all mutant receptors. Changes in these parameters may indicate perturbations of the global fold of the protein introduced by the mutations.

2. The amount of expressed protein:
 - a. Homogenize oocytes in 0.1 mL of extraction buffer, sonicate for 20 s, incubate on ice for 30 min, and then sediment in a microfuge for 20 min at 4°C.
 - b. Carefully remove the supernatant avoiding as much as possible contamination of the yolk protein phase that appears as a dense layer on top of the supernatant.
 - c. The supernatants are subjected to SDS-PAGE.
 - d. Proteins are electrotransferred onto nitrocellulose or poly(vinylidene difluoride) membranes.
 - e. Probe the membranes with a specific primary antibody, followed by incubation with a secondary antibody conjugated to horseradish peroxidase, alkaline phosphatase, or [¹²⁵I]protein A (or G).
 - f. Develop immunoblots. This process depends on the design of the secondary antibody used. For horseradish peroxidase, the enhanced chemiluminescence method works very well. If a radioactive secondary antibody is used, the membrane is directly exposed to Kodak X-Omat AR X-ray film. The relative amount of protein may be quantified by image analysis of digitized films.

4. Notes

4.1. Technical Notes

1. Always confirm the nucleotide sequence of the site mutated, as well as that of the restriction sites used for subcloning if the PCR-based method was used. This precaution helps to minimize the appearance of stray mutations arising from polymerase mistakes during DNA synthesis and manipulation.
2. Special care must be taken when preparing cRNA *in vitro* to avoid contamination with RNases. *In vitro* transcription should be carried out in a dedicated, clean space, and all aqueous solutions should be prepared with DEPC-treated water and autoclaved.
3. Use a saturating concentration of agonist to obtain the dose–response curve for an uncompetitive antagonist. This ensures that small variations in the concentration, as a result of adding increasing amounts of blocker, will not affect the size of the agonist-evoked current. Agonist concentrations around the EC₅₀ will produce large changes in the agonist-elicited response that will lead to an overestimation of the blocker efficacy and potency. For competitive antagonists, however, the concentration should be near the EC₅₀ to avoid application of excessive antagonists to displace the agonist from its binding site.
4. Oocytes express endogenous ion channels that may contaminate the agonist-operated responses of the channel under study. This is especially important for the NMDA receptor or GluR1 restructured to mimic the permeation properties of the NMDA receptor, because the high Ca²⁺ influx through these channels may activate the notorious Ca²⁺-activated, voltage-dependent Cl⁻ channel (24). It is advisable to include in the buffers specific inhibitors of Cl⁻ channels, such as niflumic and flufenamic acids. Furthermore, Ca²⁺ should be substituted by Ba²⁺, which is a weaker activator of these chloride channels. If Ca²⁺ must be used,

then EGTA or BAPTA may be injected into the oocytes to a final concentration of 10 mM.

5. For voltage-dependent blockade of channel activity, the blocker affinity increases as the membrane is hyperpolarized, indicating that the blocker moves into the pore electric field. The fraction of unblocked response is a function of the concentration of blocker and the applied voltage (23). Considering a single binding site within the pore electric field, the IC_{50} of a molecule with valence z is described by the Woodhull model (25), represented by the equation: $IC_{50}(V_m) = IC_{50}(0 \text{ mV}) \times \exp(z\delta V_m F/RT)$. δ Denotes the location of the energy barrier for block expressed as a fraction of the electric field gradient sensed by the blocker binding site. Analysis of the voltage dependence of channel blockade was used to locate the blocking site deep ($\delta \sim 0.6$) into the pore electric field of both the NMDA receptor and the restructured GluR1.
6. Determination of the amount of expressed protein is important to ensure that mutations do not significantly affect protein expression. Expression levels around that observed for wild-type channels should be obtained. Much larger or lower levels may indicate significant effects on the global protein conformation.

4.2. The Scope of the Strategy

7. It should be highlighted that the biomimicry-based approach relies on a stepwise mutational strategy. First, single mutants are obtained and analyzed, followed by the double mutants. The functional properties of the receptor mutants are compared to those characteristic of the receptor to be emulated (Table 1). If the full complement of functional properties were not reproduced on transfer of the identified determinants, substitutions of neighboring residues should be explored. If the disparity remains, then attention should be shifted to investigating contributions of other transmembrane segments, starting with the most conserved. For example, to endow GluR1 channels with high sensitivity to dizolcipine, it was necessary to mutate residue ³¹⁰Ser in the M3 transmembrane segment to Ala (5).
8. The design may be refined by a close examination of the chemical properties of the implanted residues. For example, the interaction of open channel blockers with the NMDA receptor pore structure is governed by the formation of hydrogen bonds between the ⁵⁹⁸Asn and the blockers. One option is to explore the effect of introducing a hydroxyl-containing group, such as threonine, in the corresponding position in M2 of GluR1, ⁵⁸²Gln. The rationale considers that the higher hydrogen bonding energy of the hydroxyl group may increase the binding energy and, therefore, enhance the blocker affinity (Table 1).
9. The generation of an array of mutant receptors may be useful to gain information about the biology of these membrane proteins. A case in point is the unknown subunit stoichiometry of GluRs. We used a functional assay based on the blockade of two GluR1 mutant subunits engineered to exhibit differential sensitivity to the open-channel blocker PCP. Specifically, we used the single mutant L577W of GluR1 that is weakly sensitive to these drugs and the double mutant L577W/Q582T that is highly sensitive. Coinjection into *Xenopus* oocytes of cRNAs for

L577W with L577W/Q582T subunits produced heteromeric receptors with mixed blocker sensitivities. Increasing the fraction of L577W/Q582T subunits augmented the proportion of blocker-sensitive receptors. Analyzing the blockade efficacy of heteromeric GluR1 receptor composed of different ratios of these engineered mutant subunits using a model based on random aggregation, we determined a pentameric subunit stoichiometry for GluR1 (**Table 1**) (20). Similar results were obtained for the NMDA receptor (**Table 1**) (21), substantiating the notion that a pentameric subunit organization underlies the structure of ionotropic glutamate receptors.

10. Our results suggest that the homomeric GluR1 double mutants, L577W/Q582N and L577W/Q582T, fairly approximate the permeation properties of the heteromeric NMDA receptor. Two key observations are noteworthy. First, the permeation properties of ionotropic glutamate receptors appear to be defined by the *N/Q/R-site* (5,8,12–17), and the recently identified *W/L-site* in the M2 transmembrane segment (**Table 1**) (5,8). Second, the M2 segment is a key structural component of the permeation pathway, and the M3 segment plays a thus far unknown role in modulating aspects of pore function (5).
11. Our findings argue in favor of the reliability of a biomimicry-based design strategy that involves the identification of pore-forming structures and demonstration of the attributed functions, and leads to the incorporation of newly recognized functional determinants into the structure of otherwise intact proteins with the consequent retrieval of novel functions. For ionotropic glutamate receptor channels, the M2 segment in the context of the protein subunit within a functional oligomer appears to be mostly helical (9). Selective replacement of residues guided by a helical structure confers new properties on mutant receptors: the restructured receptors mimic the drug binding and ionic selectivity properties of the receptors they were designed to emulate (**Table 1**). The selectively engineered properties of the restructured receptors have been successfully used to determine the thus far unknown stoichiometry of neuronal glutamate receptor channels (**Table 1**) (20). Restructuring of channel proteins with the generation of new functional attributes implies the ability to control, which comes with the acquisition of knowledge of their structure. Availability of a structure of the M2 pore-lining segment, together with a detailed map of the binding pocket for open-channel blockers, would provide unprecedented guidelines for the development of the next generation of drugs targeted against neurodegeneration and stroke.

Acknowledgment

This work was supported by a grant from NIH (GM-49711) (M. M.).

References

1. Sutcliffe, M., Wo, G. Z., and Oswald, R. E. (1996) Three-dimensional models of non-NMDA glutamate receptors. *Biophys. J.* **70**, 1575–1589.
2. Montal, M. (1995) Design of molecular function: channels of communication. *Annu. Rev. Biophys. Biomol. Struct.* **24**, 31–57.

3. Galzi, J. L., Devillers-Thiery, A., Hussy, N., Bertrand, S., Changeaux, J. P., and Bertrand, D. (1992) Mutations in the channel domain of a neuronal nicotinic receptor convert ion selectivity from cationic to anionic. *Nature* **359**, 500–505.
4. Gross, A., Abramson, T., and MacKinnon, R. (1994) Transfer of the scorpion toxin receptor to an insensitive potassium channel. *Neuron* **13**, 961–966.
5. Ferrer-Montiel, A. V., Sun, W., and Montal, M. (1995) Molecular design of the *N*-methyl-D-aspartate receptor binding site for phencyclidine and dizolcipine. *Proc. Natl. Acad. Sci. USA* **92**, 8021–8025.
6. Zarei, M. M. and Dani, J. A. (1995) Structural basis for explaining open-channel blockade of the NMDA receptor. *J. Neurosci.* **15**, 1446–1454.
7. McBurney, R. W. (1997) Development of the NMDA ion-channel blocker, aptiganel hydrochloride, as a neuroprotective agent for acute CNS injury. *Int. Rev. Neurobiol.* **40**, 173–195.
8. Ferrer-Montiel, A. V., Sun, W., and Montal, M. (1996) A single tryptophan on M2 of glutamate receptor channels confers high permeability to divalent cations. *Biophys. J.* **71**, 749–758.
9. Kuner, T., Wollmuth, L. P., Karlin, A., Seeburg, P. H., and Sackman, B. (1996) Structure of the NMDA receptor channel M2 segment inferred from the accessibility of substituted cysteines. *Neuron* **17**, 343–352.
10. Nakanishi, S. and Masu, M. (1994) Molecular diversity and functions of glutamate receptors. *Annu. Rev. Biophys. Biomol. Struct.* **23**, 319–348.
11. Hollman, M. and Heinemann, S. F. (1994). Cloned glutamate receptors. *Annu. Rev. Neurosci.* **17**, 31–108.
12. Burnashev, N., Schoepfer, R., Monyer, H., Ruppersberg, J. P., Gunther, W., Seeburg, P. H., et al. (1992) Control by asparagine residues of calcium permeability and magnesium blockade in the NMDA receptor. *Science* **257**, 1415–1419.
13. Burnashev, N., Monyer, H., Seeburg, P. H., and Sakmann, B. (1992) Divalent ion permeability of AMPA receptor channels is dominated by the edited form of a single subunit. *Neuron* **8**, 189–198.
14. Dingledine, R., Hume, R. I., and Heinemann, S. F. (1992) Structural determinants of barium permeation and rectification in non-NMDA receptor channels. *J. Neurosci.* **12**, 4080–4087.
15. Sakurada, K., Masu, M., and Nakanishi (1993) Alteration of Ca²⁺ permeability and sensitivity to Mg²⁺ and channel blockers by a single amino acid substitution in the *N*-methyl-D-aspartate receptor. *J. Biol. Chem.* **268**, 410–415.
16. Verdoorn, T. A., Burnashev, N., Monyer, H., Seeburg, P. H., and Sakman, B. (1991) Structural determinants of ion flow through recombinant glutamate receptor channels. *Science* **252**, 1715–1718.
17. Egebjerg, J. and Heinemann, S. F. (1993) Ca²⁺ permeability of unedited and edited versions of the kainate selective glutamate receptor GluR6. *Proc. Natl. Acad. Sci. USA* **90**, 755–759.
18. Ferrer-Montiel, A. V. and Montal, M. (1994) Structure-function relations in ligand-gated ion channels: reconstitution in lipid bilayers and heterologous expression in *Xenopus* oocytes. *Methods: Companion Methods Enzymol.* **6**, 60–69.

19. Ferrer-Montiel, A. V., Merino, J. M., Planells-Cases, R., Sun, W., and Montel, M. (1998) Structural determinants of the blocker binding site in glutamate and NMDA receptor channels. *Neuropharmacology* **37**, 139–147.
20. Ferrer-Montiel, A. V. and Montal, M. (1996) Pentameric subunit stoichiometry of a neuronal glutamate receptor. *Proc. Natl. Acad. Sci. USA* **93**, 2741–2744.
21. Premkumar, L. S. and Auerbach, A. (1996) Stoichiometry of recombinant NMDA receptor channels. *Soc. Neurosci. Abstracts* **22**, 593; Abstract no. 237.8.
22. Mayer, M. L. and Westbrook, G. L. (1987) Permeation and block of *N*-methyl-D-aspartic acid receptor channels by divalent cations in mouse cultured central neurons. *J. Physiol. (Lond.)* **286**, 417–445.
23. Hille, B. (1992) *Ion Channels of Excitable Cells*, 2nd ed., Sinauer Assoc., Sunderland, MA.
24. Miledi, R. and Parker, I. (1984) Chloride current induced by injection of calcium into *Xenopus* oocytes. *J. Physiol. (Lond.)* **357**, 173–188.
25. Woodhull, A. M. (1973) Ionic blockage of sodium channels in nerve. *J. Gen Physiol.* **61**, 687–708.

High-Throughput Functional Detection of NMDA Receptor Activity

Martin Donal Cunningham and Sara Mary Cunningham

1. Introduction

A prominent current paradigm in the discovery of potential drugs directed toward therapeutic targets relies on the combination of brute force and specificity. The increasing number of entities in pharmaceutical company compound libraries, frequently surpassing 10^6 , dictates the use of a high-throughput screening (HTS) process. In practice, large numbers of individual compounds are quickly tested for their ability to interact with, and affect a change in, a previously identified and validated target protein. The heterologous expression of cloned receptor proteins in defined cell lines provides the specificity of the interaction.

HTS is a relative phrase, but currently is considered to be the ability to test between 10^4 and 10^5 compounds/day for interactions with targets. Medium-sized laboratories are typically being asked to screen between 50 and 100 targets/yr using library subsets that range between $1-5 \times 10^5$ compounds. Therefore, it is important that the screening methodology used is fast, accurate, quantitative, inexpensive, easy to perform, and amenable to automation. Furthermore, the method chosen must have a large dynamic range, a good signal-to-noise ratio (SNR), be universally adaptable to different targets, and have low rates of false-positive and false-negative signals.

HTS processes have several sequential phases. The initial or primary screen has historically taken the form of a radioligand binding displacement assay on isolated plasma membrane fractions. Plasma membranes may be batch-prepared and frozen for future use, and provide a low-maintenance source of biological material on which to test compounds. A secondary, confirmational binding assay is frequently used to eliminate false-positive

“hits.” This is followed by potency and selectivity profiling, and then functional assays. Receptor-mediated functional assays measure changes in second messenger production, ion flux, or enzyme activity, and ensure that there is a physiologically relevant consequence to the ligand–receptor interaction detected in binding assays.

Although it is possible to conduct most functional assays on plasma membranes, whole-cell systems are increasingly considered to be one of the better environments in which to screen for potential drugs. Functional, cell-based primary screens have the advantage of being able to detect compounds that activate, inactivate, or modulate receptor targets, and are also able to identify compounds that interact with novel sites for which no known ligand exists. However, cultured cells are less convenient than membranes to handle and, until recently, have not made their way into HTS environments.

An important advance in the HTS and drug discovery process has been the development of a commercially available imaging fluorometer with an integrated liquid delivery system capable of cell-based fluorescence detection using 96- or 384-well microplates. This Fluorescent Imaging Plate Reader system (FLIPR®; Molecular Devices Corp., Sunnyvale, CA) measures kinetic changes in dye or reporter fluorescence by simultaneously delivering argon laser excitation and capturing emission light images with a cooled CCD camera as fast as 800 ms/frame, while controlling fluid delivery from an integrated 96- or 384-tip pipetter. The pipetter can be programmed to make three separate additions from microplates containing reagents to be tested, which we hereafter refer to as “compound addition plates” to microplates containing a monolayer of cultured cells that express the receptor of interest, which we call “cell plates.” This allows FLIPR to be used in assays designed to screen for receptor/antagonists, as well as those assays designed to examine receptor desensitization. FLIPR provides precise heating control, permitting assays to be run at physiological temperature. The design of FLIPR optics restricts the field of measurement to the cell monolayer, which reduces background fluorescence and results in a robust SNR, comparable in many cases to fluorescent confocal microscopy assays. The optical detection scheme is sensitive enough to measure luminescence from cells expressing firefly and *Renilla* luciferase (1,2).

Many fluorescent dyes capable of excitation with the discrete spectral lines of an argon laser have been developed and include those that change emission characteristics in response to changes in calcium concentration as well as pH and membrane potential. Because of the instrument sensitivity and flexibility, an increasing number of laboratories use FLIPR as a primary screening tool to quantify the functional consequence of receptor activation. The protocol described in this chapter is designed for kinetic measurements of NMDA receptor-mediated calcium flux using FLIPR.

The importance of NMDA receptors in normal and pathological processes has been well-documented. Functional NMDA receptor activity is generally assessed by electrophysiological recordings or $[Ca^{2+}]_i$ measurements, the latter being amenable to microplate-based assays for screening large numbers of drug candidates. Using this format, mGluR and NMDA receptor responses have been successfully measured in continuous cell lines (3–5) and primary cell cultures (6) using endogenous and heterologous receptors expressed constitutively, transiently, or under regulatable control (7,8).

This chapter is not intended to be a comprehensive treatment of all issues surrounding the functional detection of NMDA receptors. Rather, it is intended as a starting point for those using FLIPR as an HTS tool for the detection of active compounds directed against NMDA receptors. We will identify the major points of consideration with suggestions on the direction to take for assay optimization. Discussion will be limited to situations involving a pre-existing, stable cell culture expressing functionally active NMDA receptors that form ligand-gated ion channels (*see Note 1 and ref. 7*). It is further assumed that the investigator will be adequately familiar with technical aspects of the instrument.

To summarize briefly the protocol described, CHO cells expressing functional NMDA receptors are grown to confluence in 96-well microplates (cell plates), are washed with fresh balanced salt solution, and incubated in the presence of the Ca^{2+} -sensitive dye Fluo-3. After incubation, the extracellular dye is rinsed away, and the cell plate and the compound addition plate(s) are placed on the instrument. The optical gain, dispensing parameters, and timing are adjusted, and the plate is read.

As an example of the time-course of the response, NMDAR1 and NMDAR2A subunits were simultaneously expressed in a CHO cell line using the bidirectional tetracycline expression system (submitted; 9). **Figure 1** shows that in response to NMDA and 10 μM glycine, there is a rapid, dose-dependent, transient rise in fluorescent counts followed by a slow, monophasic return toward the baseline. Each trace in **Fig. 1** is from a single well of cells. In 8 h, it is possible to assay up to 150 plates or >14,000 kinetic determinations. This number increases by a factor of 4 when 384-well plates are used.

2. Materials

1. It is anticipated that the investigator will already possess a cell line expressing the receptor subunit combination of interest and that there is sufficient prior evidence of functionality (*see Note 2 and Chapters 3 and 4, in this vol.*).
2. Black-walled, clear-bottom, 96-well polystyrene microplates; that are tissue-culture treated and sterile (Corning, Corning, NY/Costar, Cambridge, MA, no. 3606 or Packard Instruments, Downers Grove, IL, no. 6005182) (*see Note 3*).
3. Black 250- μL capacity tips, nonsterile, 96-tip racks (Robbins, Sunnyvale, CA, no. 1043-24-0) (*see Note 4*).

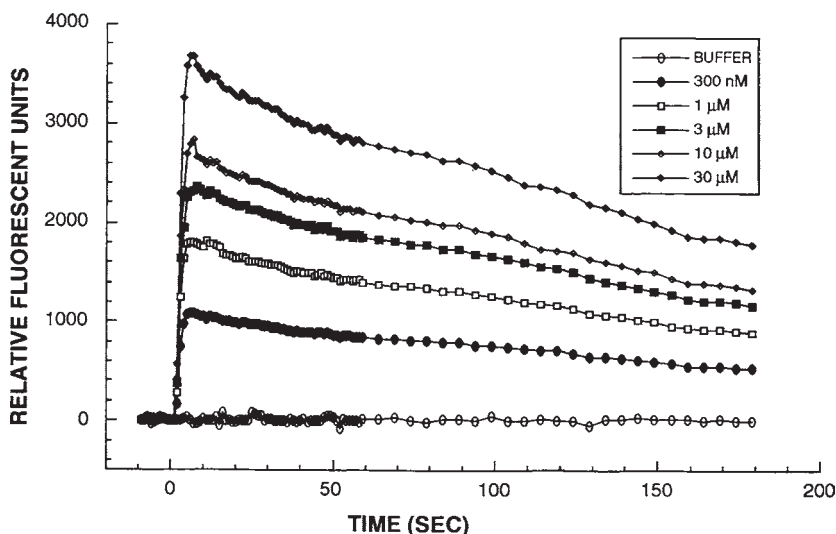


Fig. 1. Functional expression of NMDAR1 and NMDAR2A in CHO-K1 cells stably transfected with the tetracycline-responsive bidirectional plasmid containing genes for each protein and the pTet-On regulator plasmid (Clontech) was monitored using FLIPR. Forty-eight hours after gene induction, confluent cell cultures were washed three times with fresh Hank's balanced salt solution (HBSS) containing a 1% final concentration of bovine serum albumin and 1.0 ng/mL doxycycline (running buffer), and then replaced with running buffer containing 2 μ M Fluo-3. After 30 min incubation at room temperature the extracellular dye was rinsed away, and the cell plate and the compound addition plate were placed on the instrument. Running buffer containing 20 μ M glycine and twice the indicated concentrations of NMDA were added at time = zero. Images were acquired every second for the first minute and then every 10 s for the duration of the assay.

4. Fluo-3-AM ester (Molecular Probes, Eugene, OR, no. F-1241) (*see Note 5*).
5. 4-Bromo-A23187 (Molecular Probes no. B1494).
6. Pluronic F-127 (Molecular Probes no. P-6867).
7. Anhydrous DMSO (Sigma, St. Louis, MO, no. D-2650).
8. Eight- or 12-channel, 200- μ L capacity pipetter with tips and basin.
9. Microplate washer (Denley Cellwash [now Lab Systems], Helsinki, Finland, no. CW018B/p) (*see Note 6*).
10. HEPES 1 X buffer (Irvine Scientific, Irvine, CA, no. 9319).
11. HBSS, 10X concentrate (Gibco-BRL, Gaithersburg, MD, no. 14065-056).
12. Bovine serum albumin (BSA) (Sigma no. A-8412).
13. 10-mM stock solutions of glycine and NMDA receptor agonists/antagonists in the appropriate diluent.
14. Samples of diluent used for mixing stock solutions of test compounds to use as controls.

15. Solution for incubation of cells with Fluo-3 (*see Note 7*): 1X HBBS containing 20 mM HEPES and 1 mg/mL BSA, pH 7.4 (H/H/BSA).
16. Assay buffer: 125 mM NaCl, 5 mM KCl, 1.8 mM CaCl₂, 20 mM HEPES, 10 mM D-glucose, pH 7.4 (approx 100 mL will be required to prepare a single compound addition plate, and wash a cell plate a total of four times using 200 μ L/wash).
17. Round-bottom, 96-well polypropylene microplates for compound addition (Nalgene Nunc, Rochester, NY, no. 442587).

3. Methods

1. Plate cells in clear-bottom, black-walled microtiter plates at a sufficient density to achieve a confluent monolayer at the time of the assay (*see Note 1*). Leave at least one well free of cells in order to measure background fluorescence associated with the polystyrene plate.
2. Prepare Fluo-3 in H/H/BSA. The following quantity is sufficient for a single 96-well microtiter plate and may be scaled according to the number of plates to be run:
 - a. Dissolve Fluo-3 powder in anhydrous DMSO (4-mM stock) and mix. Appropriately sized aliquots may be stored at -20°C . Spontaneous hydrolysis will occur slowly in aqueous solutions.
 - b. Just prior to the assay, add 20 μ L of 20% pluronic acid (w/v in DMSO) to an equal volume of dye stock, mix well, and add to 10 mL of H/H/BSA. Mix well, keep out of direct light, and use this 8 μ M dye solution within 8 h of preparation.
 - c. Using the plate washer, rinse growth media from cells using two to three washes of 200 μ L of H/H/BSA, leaving exactly 100 μ L of H/H/BSA remaining in each well (*see Note 8*).
 - d. Add 100 μ L of the 8 μ M dye solution (**step 2.b**) to each well using a multi-channel pipetter (*see Note 9*).
3. Incubate for 60 min at room temperature (*see Note 10*).
4. Prepare compound addition plate(s) using assay buffer as diluent, making sure to include 10 μ M A23187 in at least one well as a positive control (*see Note 11*).
5. Program FLIPR software so that the pipetter delivers a specific volume from the compound addition plate(s) to the cell plate (*see Notes 12 and 13*) and so that FLIPR acquires one image of the bottom of the cell plate per second for a total of 3 min (*see Fig. 1*). Adjust software so that the pipetter will dispense compounds after acquiring 5–10 baseline images.
6. Remove residual extracellular dye from all wells of the cell plate using the plate washer and assay buffer (*see Note 6*), and place cell plate and compound addition plate(s) in FLIPR.
7. Adjust the laser voltage, CCD camera exposure length, and aperture setting so that the fluorescence associated with wells that contain cells is approx 5–10K fluorescence counts above the background fluorescence from empty wells (*see Note 14*).
8. Replace pipetter tips with clean ones and begin assay.
9. Repeat **steps 6 and 8** if multiple plates are to be tested.

4. Notes

1. Responses with this imaging system have been successfully obtained with a wide variety of cell types and clonal cell lines. Clonal cell lines expressing only specific NMDA receptor subunits will eliminate ambiguity arising from EAAR subtype crossreactivity. Cell types that adhere tightly to the polystyrene microplates and grow to confluent monolayers are used preferentially, since this eliminates the concern of disrupting the cell layer during vigorous microplate washing techniques. We recommend the CHO cell line as host for the NMDA receptor. This selection is based entirely on the tight adherence properties of the cell to the microplate matrix.

If there is no option, and if the cell line of choice tends to detach easily, then there are several alternatives. First, the cell plate may be coated with compounds, such as poly-D-lysine, laminin, fibronectin, or gelatin, to improve adherence of the cell. Alternatively, a cell suspension that has been loaded with dye and washed with centrifugation and resuspension steps may be dispensed into microplate wells and centrifuged at 200g for 5 min. A high concentration of cells (e.g., 3×10^5 cells/well of HEK-293 cells) handled in this manner will yield a packed monolayer. This methodology may also be employed for almost any cell type provided that the cells are detached from the culture flask without enzyme treatment, which may disrupt receptor function.

It is difficult and unnecessary to obtain confluent primary neuronal cultures for use on FLIPR. We have observed that plating a moderate quantity (1×10^5) of hippocampal cells prior to chemical selection results in a density of neuronal cells sufficient to see robust NMDA receptor-mediated signals.

2. When two heteromeric NMDA receptor subunits must be expressed for receptor functionality, particularly if prolonged overexpression of such a combination results in toxic effects to the cell (8), we have found that the tetracycline-controlled gene expression system (9,10) is ideal. This system has been found to lack the pleiotropic effects of other inducible systems, while allowing reversible, tightly regulated gene expression (7).
3. These two plates differ slightly in their tissue-culture treatments. We recommend that the investigator try each plate to determine which has the best adherence and cell growth properties for the particular cell line.
4. Since kinetic measurements of intracellular calcium flux are relatively fast compared to the speed of the pipetter movement, the pipet tips are programmed to remain inside the microplate wells after compound delivery and during data collection. Therefore, in order to minimize light-scattering effects owing to the presence of pipet tips, we recommend the use of black-colored tips.
5. We have observed that some host cell lines have preferences for the Ca^{2+} -indicator dye that is taken up into the cell. As a starting point, we recommend the plasma membrane-permeant acetoxymethyl (-AM) form of Fluo-3 (cat. no. F-1241; Molecular Probes). Fluo-3 has a large change in emission intensity (4–5 \times) for a given change in calcium concentration compared to some alternative dyes. It is estimated that this dye has sensitivity to detect changes in calcium concentration

on the order of 10 nM. Alternative dyes to consider are: calcium green-1 (Molecular Probes no. C-3010), calcium green-2 (Molecular Probes no. C-3730), or Oregon green 488 BAPTA-1 (Molecular Probes no. O-6806). All of these dyes have been successfully employed with many different cell lines expressing voltage-dependent and ligand-gated ion channels.

6. One of the more important aspects of using cell-based high-throughput screening assays with fluorescent dyes is the need for consistency during the microplate washing process. Rinsing with assay buffer to remove extracellular dye ensures that the baseline fluorescence and the receptor-mediated signal are proportional to total intracellular volume. We have had experience with several plate washers and recommend the Denley Cell Washer as an all-purpose machine. It has the capability of gently washing cell lines that are only loosely adherent (i.e., HEK-293 or IMP-32) or those that are normally nonadherent (i.e., THP-1 or Jurkat) without disturbing the cell monolayer. On the downside, the Denley is a strip washer and is not as fast as whole-plate washers.
7. Several cell types express different forms of the organic anionic transporter, which cause a rapid efflux of the hydrolyzed form of fluorescent dyes (**11**), or the *p*-glycoprotein (Multidrug resistant [MDR] pump), which acts on nonhydrolyzed -AM forms (**12**). The net result of these extrusion processes is a rapid movement of fluorescent dye into the extracellular space that becomes apparent as a “dilution artifact” or a large drop in baseline fluorescence on addition of compounds to the cell plate. Inhibition of these activities results in increased dye influx and decreased dye efflux. For HTS assays against NMDA receptors, a 1% final concentration of BSA or human serum albumin (HSA) in the loading and assay buffers is recommended. These carrier proteins appear to block extrusion of dye from cells and have the added benefit of facilitating dye loading by acting as a dispersing agent for the -AM dyes. The mechanism of this inhibition has not yet been determined.

Several alternatives to BSA or HSA in these assays include probenecid (Sigma no. P8761) and (\pm) sulfinpyrazone (Sigma no. S9509) to inhibit the anionic transporter, and (\pm) verapamil (Sigma no. V4629) and cyclosporin A as inhibitors of *p*-glycoprotein activity. Unfortunately, these compounds may have multiple cellular and signal transduction effects at the concentrations used to inhibit transport activity (**13–15**). To date, we have no firm evidence that the use of probenecid or sulfinpyrazone interferes with known NMDA receptor-mediated signal transduction. Whether or not to employ drugs or carrier proteins to block dye efflux depends largely on the SNR. Those responses to weak, but potentially selective lead compounds must have an SNR that permits unambiguous identification of true-positive responses and elimination of false negatives. Inhibition of artifacts by one of these methods may be necessary in systems with a modest SNR (<5).

8. Primary and secondary amino groups from amino acid-containing buffers may cleave the -AM esters and prevent passage of dye into the cell. Similarly, nonspecific esterases from serum-containing media may hydrolyze the -AM esters. Therefore, it is generally recommended that you remove the serum-

containing growth media from cell cultures prior to the addition of fluorescent dye. However, some cell types (primary cortical neurons) appear to require fresh growth media and serum to take up these dyes efficiently; this must be determined empirically.

9. Fluorescent dyes are eventually toxic to cells; exactly when this will happen is cell-type dependent. However, we observed no significant loss of NMDA receptor-mediated calcium flux when the assay was performed within 3 h after the introduction of dye. With this in mind, it is possible to load multiple plates with dye and sequentially wash the plates prior to assay within the aforementioned time constraints.
10. Anecdotal information regarding incubation conditions for dye loading raises the possibility that incubation at 37°C for 60 min may contribute to dye sequestration within intracellular organelles, resulting in an increase in background fluorescence. Room temperature incubation is adequate for most cell types and does not affect cell viability, provided that pH buffering conditions are altered to account for the absence of CO₂.
11. The pipetter on FLIPR is accurate and precise (CVs from 2–5% at 50 µL). However, do not count on the pipetter to pick up the remaining 30 µL from the polypropylene compound addition plate. That is, leave that addition quantity in each well as dead volume.

Individual components of compound libraries are typically dissolved in DMSO. Frequently, this dictates that the concentration of DMSO in the compound addition plate exceeds 1%. As a general rule, we have not observed significant effects on NMDA receptor-mediated changes in Ca²⁺ flux by concentrations of DMSO <1%. However, this should be tested against each cell type and receptor construct.

12. The volume of compound to be tested, which is added to the cell plate, is dictated by the concentration of the compound and by the experimental paradigm employed. The NMDA receptor-mediated response is fast (*see Fig. 1*). To avoid incomplete or slow mixing of the liquids, it is suggested that 2X concentrations be added when possible. These concentrations should not exceed 5X. The situation is more complex when preincubation with one compound (e.g., a potential antagonist is required prior to stimulation by an agonist). Since receptor on- and off-rates for potential antagonists are unknown, it is desirable to preincubate with a 2X antagonist (i.e., the final concentration in the well is 1X), followed by stimulation with a mixture of 2X agonist and 1X antagonist (i.e., both compounds are at a final 1 X concentration).

If there is little concern for the effective concentration of antagonist, for instance, during initial screening, a volume of 4X antagonist may be preincubated with cells (i.e., 25 µL into 75 µL), followed by 2X agonist (i.e., 100 µL into 100 µL). The difference between these two scenarios and the benefit of this latter method is that antagonist need not be added to the agonist-containing plate.

13. The height from which the pipetter dispenses fluid in relation to the bottom of the inside of the cell plate wells, as well as the dispensing force or speed, can

be controlled with the FLIPR software. The pipetter dispense height should not be too close to the cells, since the cell layer may be disrupted by the force of the liquid stream. Set the dispense height to be 25 μL less than the total volume in each well after compound is delivered (i.e., set to 175 μL if 100 μL is dispensed into 100 μL). This ensures that no liquid will remain adhered to the outside of the pipet tips. As a general rule, 20 $\mu\text{L/s}$ dispensing speed is slow and 100 $\mu\text{L/s}$ is fast. For CHO cells, we recommend 80 $\mu\text{L/s}$.

14. Starting points are as follows: laser power 400 mW; camera exposure 0.4 s; camera lens aperture F/2. As the laser power increases by a factor of two, the baseline fluorescence also increases by a factor of two. The same relationship applies to the camera exposure length and baseline fluorescence. As the camera aperture is closed from F/2 to the next position, F/2.8, the amount of light going through the CCD camera lens is reduced by half.

References

1. Cunningham, S. M., Cunningham, M. D., Zhu, L., and Kain, S. (1997) Determination and correlation of expression levels of luciferase and EGFP using the tetracycline-controlled gene expression system and FLIPR. *Abstr. Soc. Neurosci.* **23**, 467.
2. Wada, G., Neagle, B., and Schroeder, K., (1997) Luminescence assays using the FLIPR high throughput system. *Abstract Soc. Biomol. Screen* **3**, 267.
3. Daggett, L. P., Saccaan, A. I., Akong, M., Rao, S. P., Hess, S. D., Liaw, C., et al. (1995) Molecular and functional characterization of recombinant human metabotropic glutamate receptor subtype 5. *Neuropharmacology* **34**, 871–886.
4. Lin, F. F., Varney, M., Saccaan, A. I., Jachec, C., Daggett, L. P., Rao, S., et al. (1997) Cloning and stable expression of the mGluR1 b subtype of human metabotropic receptors and pharmacological comparison with the mGluR5a subtype. *Neuropharmacology* **36**, 917–931.
5. Varney, M. A., Jachec, C., Deal, C., Hess, S. D., Daggett, L. P., Skvoretz, R., et al. (1996) Stable expression and characterization of recombinant human heteromeric *N*-methyl-D-aspartate receptor subtypes NMDAR1/2A in mammalian cells. *J. Pharm. Exp. Ther.* **279**, 367–378.
6. Rock, D. M. (1996) Monitoring voltage- and ligand-gated ion channels, in *Cultured Neurons Using FLIPR*. Abstract Symposium on Microphysiometry and Fluorometric Cellular Screening, Paris.
7. Besnard, F., Renard, S., Partiseti, M., Drouet-Petre, C., Langer, S. Z., and Graham, D. (1997) An inducible NMDA receptor stable cell line with an intracellular calcium reporter. *Abstract Soc. Neurosci.* **23**, 920.
8. Cik, M., Chazot, P. L., and Stephenson, F. A. (1994) Expression of NMDAR1-1a (N598Q)/NMDAR2A receptors results in decreased cell mortality. *Eur. J. Pharmacol.* **266**, R1–R3.
9. Baron, U., Freundlieb, S., Gossen, M., and Bujard, H. (1995) Co-regulation of two gene activities by tetracycline via a bidirectional promoter. *Nucleic Acids Res.* **23**, 3605–3606.

10. Gossen, M. and Bujard, H. (1992) Tight control of gene expression in mammalian cells by tetracycline-responsive promoters. *Proc. Natl. Acad. Sci. USA* **89**, 5547–5551.
11. Cao, C., Steinberg, T. H., Neu, H. C., Cohen, D., Horwitz, S. B., Hickman, S., et al. (1993) Probenecid-resistant J774 cell expression of enhanced organic anion transport by a mechanism distinct from multidrug resistance. *Infect. Agents Dis.* **2**, 193–200.
12. Gollapudi, S., Kim, C. H., Tran, B. N., Sanga, S., and Gupta, S. (1997) Probenecid reverses multidrug resistance in multidrug resistance-associated protein-overexpressing HL60/AR and H69/AR cells but not *p*-glycoprotein-overexpressing HUTax and P388/ADR cells. *Cancer Chemother. Pharmacol.* **40**, 150–158.
13. Packham, M. A., Rand, M. L., Perry, D. W., Ruben, D. H., and Kinlough-Rathbone, R. L. (1996) Probenecid inhibits platelet responses to aggregating agents in vitro and has a synergistic effect with penicillin G. *Thromb. Haemost.* **76**, 239–244.
14. Amrani, Y., Da-Silva, A., Kassel, O., and Bonner, C. (1994) Biphasic increase in cytosolic free calcium induced by bradykinin and histamine in cultured tracheal smooth muscle cells: is the sustained phase artifactual? *Naunyn-Schmiedebergs Arch. Pharmacol.* **350**, 662–669.
15. Di Virgilio F., Steinberg, T. H., and Silverstein, S. C. (1989) Organic ion transport inhibitors to facilitate measurement of cytosolic free Ca^{+2} with fura-2. *Metab. Cell Biol.* **31**, 453–462.

Index

A

- Adenoassociated virus vector,
 - glutamate receptor protein expression, 19, 20
- Adenovirus vector, glutamate receptor protein expression, 19, 20

B

- Baculovirus-Sf9 expression system,
 - amplification of recombinant virus, 24
 - cloning receptor channel subunit cDNAs into transfer vectors, 23, 29
 - cotransfection of viral and transfer vector DNAs using lipofectin, 23, 24
 - expression vector construction, 19
 - insect cell infection and expression, 24, 25, 29
 - materials, 22, 23
 - plaque assay for recombinant virus purification, 24
 - transfer vectors, 20
- Biomimicry, examples of protein engineering, 167, 168, 175

C

- Calcium flux,
 - Fluorescent Imaging Plate Reader screening for *N*-methyl-D aspartate receptor, cell lines for study, 181, 184
 - expression systems, 181, 183

- Fluo-3 detection,
 - cell loading and toxicity, 183, 185, 186
 - comparison to other dyes, 184, 185
 - data acquisition, 183, 186, 187
 - materials, 181–185
 - microplate washing, 185
 - overview, 180, 181
- HEK 293 cell measurements,
 - stable transfectants,
 - antagonist screening, 49, 51, 52
 - functional receptor screening, 48, 49
 - materials, 45, 46
 - transient transfectants, 37, 38
 - redox studies of *N*-methyl-D-aspartate receptor, 125, 129

Calmodulin,

- binding sites on *N*-methyl-D-aspartate receptor, 103
- electrophysiological analysis of modified *N*-methyl-D-aspartate receptors,
 - HEK 293 cell culture, 103, 104
 - single-channel recording from inside-out patches, 106, 107
 - solutions, 109
 - transfection, 105
 - whole-cell recording and concentration clamp, 107, 108, 110, 111
- modulation of calcium-dependent inactivation on receptors, 103

D

- Detergent solubilization, *N*-methyl-D-aspartate receptor,
detergents, 113, 114
intact receptor complexes,
116, 117
solubilization and denaturation, 116,
118
- 5,5'-Dithio-*bis*-2-nitrobenzoic acid
(DTNB), *N*-methyl-D-aspartate
receptor modification,
123–126, 128
- Dithiothreitol (DTT), *N*-methyl-D-
aspartate receptor modification,
122–125
- DTNB, *see* 5,5'-Dithio-*bis*-2-nitrobenzoic
acid
- DTT, *see* Dithiothreitol

E

- Electrophysiology, *N*-methyl-D-aspartate
receptor,
calmodulin-modified receptors,
HEK 293 cell culture,
103, 104
single-channel recording from
inside-out patches,
106, 107
solutions, 109
transfection, 105
whole-cell recording and
concentration clamp, 107,
108, 110, 111
concentration, response curve,
comparison of curves, 148, 149
curve fitting, 152
data interpretation, 151
difficult to analyze patches, 151,
152
equipment, 146, 150
inhibitor effects, 145, 146, 151

- logistic equation for
concentration–response
data, 144, 145, 150
single-channel recordings, 148
whole-cell recordings, 147, 150
- GluR1 engineered for *N*-methyl-D-
aspartate receptor properties,
172, 173
- redox studies, 124, 125
- single-channel data analysis, 144
- transient expression system
measurements, 37, 38
- whole-cell response data analysis,
143, 144
- whole-cell versus single-channel
analysis,
overview, 143
relationships in data analysis, 145,
146
- Xenopus* oocyte expression
cloning system
measurements,
apparatus, 5–7
electrode pulling and preparation,
12
perfusion, 12
two-electrode voltage clamp, 12,
14–16
- ELISA, *see* Enzyme-linked
immunosorbent assay
- Endo-F, digestion of NR1
extracellular N-terminal domain,
66, 67
- Endo-H, glycosylation
characterization of *N*-methyl-D-
aspartate receptor membrane
topology, 162–163
- Enzyme-linked immunosorbent assay
(ELISA),
NR1 extracellular N-terminal
domain ligand screening,
64, 68

- phage enzyme-linked immunosorbent assay for ligand screening, 134, 139, 140
 - Epitope mapping, membrane topology determination, 158, 159
 - N*-Ethylmaleimide (NEM), *N*-methyl-D-aspartate receptor modification, 123–125, 128, 129
- F**
- FACS, *see* Fluorescence-activated cell sorting
 - FLIPR, *see* Fluorescent Imaging Plate Reader
 - Fluo-3, *see* Calcium flux
 - Fluorescence-activated cell sorting (FACS), NR1 extracellular N-terminal domain expression on Chinese hamster ovary cells, 64, 66, 70, 71
 - Fluorescent Imaging Plate Reader (FLIPR), *see* High-throughput screening
- G**
- GluR1, engineering for *N*-methyl-D-aspartate receptor properties, expression in *Xenopus* oocytes, 171
 - functional characterization, agonist sensitivity, 173
 - ion permeability, 168, 173–175
 - open-channel blocker sensitivity, 171–176
 - psychotropic drug blockade, 168
 - M2 transmembrane segment engineering, 169, 170, 174, 176
 - materials, 168, 169
 - quantification of expressed protein, 174
 - sequence alignment of pore residues, 169
 - Glutamate, radioligand binding to *N*-methyl-D-aspartate receptor, 93, 96
 - G-protein-coupled receptor, *Xenopus* oocyte expression cloning, 13, 14
- H**
- HEK 293 stable expression system, calcium flux measurements, antagonist screening, 49, 51, 52
 - functional receptor screening, 48, 49
 - materials, 45, 46
 - expression vectors, 44, 47
 - materials, 44–47
 - N*-methyl-D-aspartate receptor, number per cell, determination, calculations, 54, 55, 58
 - membrane preparation, 52, 53, 57
 - MK-801 binding, 46, 47, 54, 58
 - screening for ligands, 43, 49, 51, 52
 - stability of expression, 49, 57
 - tissue culture, 44–46
 - transfection, 45, 47, 48, 55–57
 - HEK 293 transient expression system, cells, culture, 34
 - harvesting, 35
 - cytotoxicity, assay following transfection, 36, 37
 - protectants, 37
 - materials, 34
 - N*-methyl-D-aspartate receptor, calmodulin modification system, 103–105

- characterization of receptors,
 - electrophysiology and calcium flux, 37, 38
 - quantification, 39, 40
 - radioligand binding, 37, 39
 - glycosylation role in surface expression, 40, 41
 - mutant analysis, 33, 34
 - multiple clone expression, 36
 - transfection, 35–37, 105
 - vector preparation, 36
- Hemoglobin, nitric oxide scavenging, 125, 126, 129
- Herpes simplex virus-1 expression system,
 - advantages, 20, 21
 - materials, 22
 - stocks, preparation, 27
 - superinfection, 27
 - transfection, 26, 27
 - vectors,
 - amplicon plasmid construction, 25, 26
 - amplification of recombinant-defective vector, 27
 - preparation of recombinant-defective vector solution, 27
 - types, 21, 22
- Vero cell expression and analysis of *N*-methyl-D-aspartate receptor subunits, 27–29
- High-throughput screening (HTS),
 - criteria, 179
 - definition, 179
 - Fluorescent Imaging Plate Reader screening for *N*-methyl-D-aspartate receptor,
 - cell lines for study, 181, 184
 - expression systems, 181, 183
 - Fluo-3 detection,
 - cell loading and toxicity, 183, 185, 186
 - comparison to other dyes, 184, 185
 - data acquisition, 183, 186, 187
 - materials, 181–185
 - microplate washing, 185
 - overview, 180, 181
 - phases, 179, 180
 - HTS, *see* High-throughput screening
 - Hydrophobicity analysis, ligand-gated channels, 155–158
- I**
 - Immunocytochemistry, *N*-methyl-D-aspartate receptor,
 - antibody,
 - postsynaptic versus synaptic cleft staining, 77, 78
 - specificity, 75–77
 - types, 73–75
 - postembedding immunogold,
 - apparatus, 82
 - chemicals, 80–82
 - immunolabeling, 85, 88
 - overview, 78–80
 - resolution, 80
 - specificity, 79, 80
 - tissue preparation, 84, 85
 - pre-embedding immunoperoxidase,
 - antibody incubations and washings, 83, 85–87
 - apparatus, 82
 - chemicals, 80, 81
 - electron microscopy, 75, 84, 87, 88
 - fixation and sectioning, 83, 85
 - light microscopy, 75, 84
 - overview of steps, 75
 - sensitivity, 80
 - Immunoprecipitation, *N*-methyl-D-aspartate receptor,
 - antibody types, 114, 115, 118
 - efficiency, 118

incubation and washings, 116–118

L

Lipoic acid, *N*-methyl-D-aspartate
receptor modification, 122, 123,
125, 127

M

Membrane topology,
epitope mapping, 158, 159
glycosylation characterization of *N*-
methyl-D-aspartate receptor,
deglycosylation with Endo-H,
162, 163
extracellular domain marker, 155,
160
gel electrophoresis, 163
limitations, 160
materials, 161
membrane preparation of *Xenopus*
oocytes, 161, 162
hydrophobicity analysis of ligand-
gated channels, 155–158
ligand-binding site identification,
159
phosphorylation markers, 159
N-Methyl-D-aspartate receptor,
anchoring proteins, 113
calmodulin interactions, *see*
Calmodulin
clone isolation by expression
screening, *see Xenopus* oocyte
expression cloning
complexity of activation, 93
high-throughput detection of activity,
see High-throughput screening
immunocytochemistry, *see*
Immunocytochemistry
immunoprecipitation, *see*
Immunoprecipitation
ligand binding assays, *see* MK-801

peptide ligands, *see* NR1 extracellular
N-terminal domain; Phage
display
physiological functions, 33, 43
protein engineering, *see* GluR1
redox modulation,
cysteine, 121, 122
modification studies, 123–129
subunit composition effects, 129
solubilization, *see* Detergent
solubilization
stable expression, *see* HEK 293 stable
expression system
subunit expression,
NR1 extracellular N-terminal
domain, *see* NR1
extracellular N-terminal
domain,
viral vectors, *see* Baculovirus-Sf9
expression system; Herpes
simplex virus-1 expression
system
subunit genes and types, 33, 43, 61,
113
three-dimensional structure
determination, 167
topology, *see* Membrane topology
transient expression, *see* HEK 293
transient expression system
MK-801,
assays of other ligand binding to *N*-
methyl-D-aspartate receptor,
data analysis, 99
dissociation assays, 98–100
effects of modulators on binding,
94, 95
ligands and drugs, 96, 97
nonequilibrium assays, 97, 98
principle, 94, 96
radiolabels, 99, 100
receptor sources, 96, 100
saturation assays, 98
supplies, 96, 97

- binding site on *N*-methyl-D-aspartate receptor, 93, 94
 - GluR1 engineering for *N*-methyl-D-aspartate receptor sensitivity, 171–176
 - HEK 293 transient expression system, binding assay, 37, 39
 - proton inhibition of receptor binding, 100
 - receptors per cell, binding assay, 46–47, 54, 58
- N**
- NEM, *see N*-Ethylmaleimide
 - Nitric oxide (NO),
 - hemoglobin modification, 125–126, 129
 - S*-nitrosylation of *N*-methyl-D-aspartate receptor, 122–128
 - redox-related forms, 121–122
 - S*-Nitrosocysteine, *N*-methyl-D-aspartate receptor modification, 123–125
 - S*-Nitrosogluthathione, *N*-methyl-D-aspartate receptor modification, 123, 125
 - NMDA receptor, *see N*-Methyl-D-aspartate receptor
 - NO, *see* Nitric oxide
 - NR1 extracellular N-terminal domain,
 - agonist binding site, 61
 - expression in Chinese hamster ovary cells,
 - cloning,
 - cDNA synthesis, 63–65
 - ligation, 63, 65, 69–70
 - polymerase chain reaction, 63, 65, 69
 - RNA preparation, 62, 64, 69
 - electroporation, 63, 70
 - Endo-F digestion, 66–67
 - enzyme-linked immunosorbent assay, 64, 68
 - fluorescence-activated cell sorting, 64, 66, 70–71
 - harvesting of cells, 64, 66
 - materials, 62–64
 - screening of recombinant peptide libraries, 61, 68–69
 - transfection, 65–66
 - vector construction, 61
 - filter lift probing of ligands with antibody/NR1 complex, 134, 140–141
 - immobilization, 134, 138–139
 - phage enzyme-linked immunosorbent assay of ligands, 134, 139–140
- P**
- Patch-clamp recording, *see* Electrophysiology
 - Phage display, *N*-methyl-D-aspartate receptor ligands,
 - characterization of recovered clones,
 - filter lift probing with antibody/NR1 complex, 134, 140–141
 - phage enzyme-linked immunosorbent assay, 134, 139–140
 - phage titering, 139
 - sequencing, 141
 - random peptide library
 - construction,
 - cloning scheme, 131–132
 - electrotransformation and amplification, 133–134, 136–137

- insert oligonucleotide
 - preparation, 133, 135–137
- materials, 133–134
- p8V2 vector preparation, 133, 135
- quantification, 138
- vector ligation, 133, 136
- random peptide library screening,
 - affinity selection, 134, 138, 139
 - amplification of selected phage, 138, 139
 - materials, 134
 - NR1 extracellular N-terminal domain immobilization, 134, 138, 139
- PQQ, *N*-methyl-D-aspartate receptor modification, 127
- R**
- Random peptide library, *see* Phage display
- Redox modulation, *N*-methyl-D-aspartate receptors,
 - cysteine, 121, 122
 - modification studies, 123–129
 - subunit composition effects, 129
- S**
- Sequence alignment, pore residues, 169
- Single-channel recording, *see* Electrophysiology
- Solubilization, *see* Detergent solubilization
- T**
- Topology, *see* Membrane topology
- Two-electrode voltage clamp, *see* Electrophysiology
- V**
- Voltage clamp, *see* Electrophysiology
- W**
- Western blot,
 - antibodies for *N*-methyl-D-aspartate receptor, 114, 115
 - deglycosylated receptors, 163
- Whole-cell recording, *see* Electrophysiology
- X**
- Xenopus* oocyte expression cloning,
 - advantages, 1
 - applications, 1, 13
 - buffers for oocytes,
 - collagenase solution, 5
 - culture solution, 4
 - dissection and washing medium, 5
 - cDNA library,
 - construction,
 - materials, 2, 3
 - synthesis, 8
 - sibling selection, 8, 9, 14
 - disadvantages, 2
 - electrophysiology,
 - apparatus, 5–7
 - electrode pulling and preparation, 12
 - perfusion, 12
 - two-electrode voltage clamp, 12, 14–16
 - frogs,
 - maintenance, 10
 - sources, 4
 - G-protein-coupled receptor analysis, 13, 14
 - N*-methyl-D-aspartate receptor analysis, 1, 13
 - oocyte separation, 10, 11
 - RNA injection, 11, 14–16
 - RNA preparation,

materials, 2, 3
size fractionation, 7, 14
surgery,
anesthesia and ovary excision, 10
apparatus, 4

transcription, in vitro,
cDNA template preparation, 9
materials, 2, 3, 9
product analysis, 10
reaction conditions, 9

NMDA Receptor Protocols

Edited by

Min Li*Johns Hopkins School of Medicine, Baltimore, MD*

In *NMDA Receptor Protocols*, Min Li and a panel of hands-on experimentalists detail state-of-the-art molecular techniques for studying NMDA ligand-gated ion channels and developing assays for nontherapeutic lead selection. The topics range from cDNA cloning to in vitro and in vivo investigation of the channel complex in the mammalian brain. Additional topics include the biochemical analysis of the channel protein and the construction of various heterologous systems for both basic research and high throughput screens (HTS) for pharmaceutical chemicals. Although the focus is on NMDA receptors, the methods are applicable to other ligand-gated ion channels and with some modification may be extended to related membrane receptors or signaling systems.

NMDA Receptor Protocols provides today's scientists at all skill levels a diverse collection of highly reproducible molecular techniques for ion channel research and biotherapeutic development. Eminently practical and reproducible, these techniques offer powerful methods for basic research on NMDA receptor structure and function, as well as enormous opportunities for clinical investigation toward the development of novel bioactive compounds.

FEATURES

- Offers detailed protocols ranging from basic procedures to the most advanced technologies
- Shows how to integrate molecular approaches into standard ion channel assays such as electrophysiological recording
- Prepared by leading scientists from both basic research laboratories and innovative biotech companies
- Requires little previous experience to successfully carry out each technique

CONTENTS

Isolation of Receptor Clones by Expression Screening in *Xenopus* Oocytes. Expression of NMDA Receptor Channel Subunit Proteins Using Baculovirus and Herpesvirus Vectors. Transient Expression of Functional NMDA Receptors in Mammalian Cells. Stable Expression of Human NMDA Receptors in Cultured Mammalian Cells. Expression of Extracellular N-Terminal Domain of NMDA Receptor in Mammalian Cells. The Use of Ligand Binding in Assays of NMDA Receptor Function. Calmodulin Modification of NMDA Receptors. Detergent Solubilization and Immunoprecipitation of Native NMDA

Receptors. Redox Sensitivity of NMDA Receptors. In Vitro Selection of Peptides Acting on NMDA Receptors. NMDA Receptor Pharmacology and Analysis of Patch-Clamp Receptors. Determination of Membrane Topology of Glutamate Receptors. Engineering the NMDA Receptor Channel Lining. High-Throughput Functional Detection of NMDA Receptor Activity. Index.

